Mineralogical Association of Canada

Working with Migmatites

Editors:
Edward W. Sawyer &
Michael Brown

Short Course Series
Volume

38

QUEBEC CITY, QUEBEC, 2008
Series Editor
Robert Raeside

WORKING WITH MIGMATITES

Mineralogical Association of Canada
Short Course Series Volume 38

Edited by

Edward W. Sawyer
Department of Applied Science
Université du Québec à Chicoutimi
Chicoutimi, Québec, G7H 2B1

Short Course delivered in association with the annual meeting of the Geological Association of Canada and the Mineralogical Association of Canada, Quebec City, Quebec, 24-25 May, 2008.

TABLE OF CONTENTS

DETAILED LIST OF CONTENTS

WORKING WITH MIGMATITES
PREFACE

Migmatites occur widely in cratons and orogenic belts throughout the world. Much of the published work on migmatites has concentrated on the petrological processes that have changed relatively homogeneous sedimentary, igneous and metamorphic protoliths into migmatites that are much more heterogeneous in appearance. From their location in metamorphic terrains between amphibolite-facies metamorphic rocks and bodies of granite, migmatites and the study of them have also played a significant part in the long-lived debate over the formation of granites and the related problem of how the continental crust differentiated into a more felsic upper part, and a more mafic lower part. Currently, interest in migmatites has expanded into geodynamics and the role that their partially melted precursors may play as very weak rocks or zones in the tectonic evolution of orogens and plateaus. This interest from the geodynamics community in the changes in rheology with melting and the effects of the transfer of mass and heat in orogens will surely increase in the coming years.

Most migmatites are striking-looking rocks, with very complex morphologies that result from the interplay of both petrological and structural processes. Unfortunately, these same characteristics which fascinate a few geologists enough to make a career out of studying migmatites have the opposite affect on the majority of geologists. One of the most common comments one hears on field trips is “migmatite are too complex, I don't know where to start”. Much of the background material that a geologist new to the study of migmatites requires to begin working in migmatites is not directly available in the current research literature. Principally, this is because this material is considered to be “common knowledge” by authors, reviewers and editors alike. Moreover, a geologist new to migmatites cannot go to textbooks to obtain this background information because there are none more recent Mehnert’s (1968) highly influential book or Ashworth’s (1985) volume, and much has changed in our understanding of processes in migmatites since these volumes were published.

This short course volume, therefore, is intended to fill the "information gap" that has developed between those who have a long term interest in migmatites and those wanting to begin working with migmatites. Most geological studies begin with the documentation and understanding of the small-scale relationships in rocks, commonly at the outcrop-scale, even if the overall scope of the work is regional in scale. This is especially true for migmatites. For this reason we emphasize the field, petrographic and petrological aspects of migmatites. This is the basic information a geologist needs to have a better understanding of how to describe the constituent parts of a migmatite to decide by what processes a migmatite formed and to learn what meaning may be ascribed to the migmatite terrain under investigation.

The volume starts (Sawyer chapter 1) with an outline of the terminology that is used to describe migmatites. This is followed by an outline of the constituent parts and the principal morphologies of migmatites which are defined using a genetic nomenclature based on the understanding that migmatites are produced by partial melting. A two-tier classification scheme for the morphologies of migmatites is proposed and the various types described.

Migmatites are heterogeneous rocks, therefore what can be depicted on a map depends largely on the scale of observation. In chapter 2 Sawyer proposes that mapping migmatites at the outcrop scale is concerned principally with the recognition of the various parts of the migmatites, and is a pre-requisite to sampling. However, for regional- and terrain-scale maps details of lithology, type of migmatite and the relationship between these different migmatites and other rocks, most notably the lower-grade non-melted rocks, are important considerations.

Most migmatites have cooled slowly and the microstructural relationships and mineral compositions in them have been modified with time. In chapter 3, Cesare examines the micro-structures and mineral relationships in melt-bearing pelitic rocks that were brought rapidly to the surface as enclaves in volcanic eruptions. These partially melted rocks have cooled so quickly that the melt in them quenched to glass, and the features that formed during partial melting are preserved without resetting. These rocks, therefore, provide a test for many of our ideas on partial melting.

The presence of glass is definitive evidence for the former presence of melt. However, most migmatites cooled slowly so that the melt has crystallized rather than quenched. Holness shows in chapter 4 that microstructures formed during partial melting and during crystallization of the anatectic melt are preserved in some migmatites. The microstructures in rocks adjusts to changes in the conditions that the rocks experience, and consequently understanding the microstructure in migmatites has the potential to reveal much new information. Holness describes how the microstructure and range of dihedral angles in the pockets of former melt can be used extract information, such as cooling rates, from migmatite terrains.

Petrogenetic modeling has become a wide-spread tool in the understanding of metamorphic rocks. In chapter 5, White demonstrates some of the applications of petrogenetic modeling to understanding processes in migmatites. Examples are given of how this approach can provide significant insights into understanding the evolution of mineral assemblages, mineral compositions and microstructures in migmatites.

The broad-scale implications of the movement of melt within the partially melted regions of the crust have been known for some time. In chapter 6, Brown outlines the outcrop-scale evidence for the segregation, extraction and ascent of melt from the source to the upper crust. This contribution makes clear the connection between the small-scale features, such as the networks of leucosomes, that can be mapped in an outcrop of migmatites, to medium-scale features, such as shear zones and dykes that transport melt longer distances. These connections may enable distinction among the mechanisms proposed for the large-scale movement of anatectic melt through the continental crust.

Most migmatites were forming at the same time as the rocks were deforming. Solar, in chapter 7, describes the effect that deformation has on the morphology of migmatites. He stresses that migmatites cannot be properly interpreted without understanding the structure and lithologies in the nearby unmelted rocks on the low-grade side of the "melt-in" isograd. Context is important in understanding tectonics and migmatites. Changes in the morphology of migmatites and the amount of melt it may have contained may indicate differences among structural domains and may allow the identification of regions of net gain of melt and net loss of melt, in migmatite terranes.

We thank The Mineralogical Association of Canada for sponsoring the workshop, the reviewers of the individual chapters for their advice and Rob Raeside, the MAC short course editor, for his thorough and helpful editorial work in making this volume a reality.

REREFENCES

ASHWORTH, J.R. (1985): *Migmatites*. Ashworth, J. R. (editor). Blackie, Glasgow. 302 pp.

MEHNERT, K.R. (1968): *Migmatites and the origin of granitic rocks.* Developments in Petrology **1.** Elsevier, Amsterdam. 393 pp.

Ed Sawyer
Department of Applied Science
Université du Québec à Chicoutimi
Chicoutimi, Québec, G7H 2B1, Canada

Mike Brown: University of Maryland.
Laboratory for Crustal Petrology,
Department of Geology,
University of Maryland,
College Park, MD 20742-4211, USA

April 2008

Cover: Steeply east-dipping sheets of granite in stromatic migmatite, Tumbledown anatectic domain, Central Maine belt, west-central Maine. Sheets are concordant to weakly discordant with respect to migmatite structure and host rock (biotite-sillimanite) foliation implying control by the fabric anisotropy on sheet geometry. The largest sheet (at left) has magmatic foliation defined by multiple sheeting and biotite schlieren that are sub-parallel to sheet margins. (Photo courtesy of Gary Solar).

Distribution

Copies of Volume 38 and preceding volumes are obtainable from:

Mineralogical Association of Canada/Association Minéralogique du Canada
c/o INRS-ETE
490, rue de la Couronne
Québec (Québec) G1K 9A9
Tel. 418-654-2606 Fax: 418-654-2525

e-mail: office@mineralogicalassociation.ca
www.mineralogicalassociation.ca

Series Coordinator: R. Raeside
Department of Earth and Environmental Science
Acadia University
Wolfville, Nova Scotia
Canada, B4P 2R6

Fax: +1 902-585-1816
e-mail: rob.raeside@acadiau.ca

ISBN 978-0-92129-446-7

CHAPTER 1: WORKING WITH MIGMATITES: NOMENCLATURE FOR THE CONSTITUENT PARTS

E.W. Sawyer
Department of Applied Science,
Université du Québec à Chicoutimi,
Chicoutimi, Quebec, G7H 2B1, Canada
ewsawyer@uqac.ca

INTRODUCTION

This contribution is on the nomenclature and the terminology that is used to describe migmatites. Two sets of terms are required. One, for the identification and naming of the constituent parts of a migmatite, is based firmly on the petrological processes associated with partial melting. The other, used to describe the overall morphology of a particular migmatite, includes consideration of other factors such as the nature of the protolith and whether or not deformation accompanied partial melting.

What is a migmatite?

Sederholm (1907) introduced the term **migmatite** for the new rocks formed where an older foliated granite was intruded by the younger Hango granite in Finland. In his detailed description of the changes that had occurred to the older granite, Sederholm used terms such as "reborn" and "new eruptivity" (at the time, "eruptivity" meant "intrusivity") to explain what he saw. From these terms it is evident that in 1907 he thought that partial melting was the principal process involved in the formation migmatite. In the same paper Sederholm (1907) introduced the term **anatexis** to describe the general case (*i.e.*, without restriction as to the degree of melting) of partial melting in the crust. In his later works, however, Sederholm (1923, 1926) placed more emphasis on the role of fluids and of assimilation in the formation of migmatites. Holmquist (1916), on the other hand, had worked in a regional metamorphic terrain, and he noticed that the metamorphic rocks in the very highest grade parts had developed leucocratic patches and veinlets; he called these rocks **venites**. In Holmquist's view, venites were formed by partial melting and the subsequent separation of the melt from the solid, in a process that he called metamorphic differentiation (today, the term metamorphic differentiation is used for subsolidus processes). Moreover, Holmquist (1916) believed that partial melting required conditions that were more extreme than those responsible for the regional metamorphism in the rest of the area, but that the same heat source had caused both. Thus, Holmquist (1916) introduced the term **ultrametamorphism** to emphasize the continuity between conditions of regional metamorphism and those for partial melting.

Further development of the terminology for migmatites was severely affected by the dispute over the origin of granites. Bowen (1915, 1928) fueled the controversy when he showed that granite magma was produced by the extreme fractional crystallization of basaltic magma, and that granite was not, therefore, a "primary" magma. Field geologists soon pointed out that the volume of granite in the continental crust was far too large to be accounted for by this mechanism. At the same time whole rock analyses appeared to indicate a progressive change in the composition of typical crustal rocks towards a granitic one with depth. The paradigm that granite was not a primary magma, coupled with the over-abundance of granite and the perceived tendency towards a more granitic composition with depth in the crust, lead to the concept of "granitization". The protagonists in the controversy over granitization soon split into "wet" and "dry" sects. The polarization of opinion on the origin of granitic rocks was so strong that, under the prevailing atmosphere a non-genetic, descriptive terminology had to be developed for migmatites and granites; the acme of this was the scheme used by Mehnert (1968) in his influential book.

The development of X-ray fluorescence analysis in the 1950s and early 1960s made high quality whole rock geochemical analyses widely available and enabled more systematic studies of the composition of metamorphic rocks to be made. Shaw (1954, 1956) compared the composition of low-grade and high-grade pelitic schist from the

Mineralogical Association of Canada Short Course 38, Quebec City, Quebec, p. 1–28

Littleton Formation, and showed that, apart from devolatization, prograde metamorphism was essentially isochemical, at least on the sample scale and, hence, that metasomatism was not a significant process in regional metamorphism of the continental crust. Studies of migmatites since then have found that partial melting is the principal process by which they formed; other processes such as metasomatism may occur, but they are of very minor importance and are, in any case, subsidiary to partial melting. Thus, the modern view is that migmatites are formed by partial melting, and this corresponds closely to the view of Holmquist, and to the early opinion of Sederholm formed by his observations at Hango. Consequently, there seems little point in maintaining a non-genetic description of rocks for which all the modern evidence indicates one causal process, partial melting. This contribution outlines a genetically based terminology for the parts of a migmatite.

Migmatites are high grade metamorphic rocks that have undergone partial melting; but unfortunately that is not very useful as a definition. Consider what happens during anatexis. If temperature becomes sufficiently high during prograde metamorphism, the rocks will begin to partially melt. Rocks of suitable composition could start to partially melt at around 650°C depending upon pressure, and will start to melt before others of less suitable composition, *i.e.*, the more fertile rocks melt first. Thus, in a typically heterogeneous portion of the crust, partial melting will have advanced more in some layers compared to others; some may not have melted at all. As rocks partially melt they switch from a single phase (solid) system to a two phase one (melt + solid) in which one phase is considerably less viscous and dense than the other; thus, under a suitable driving force the melt fraction tends to separate from the solid. Consequently, partially melted crust can become even more heterogeneous. In simple terms, four basic parts can be identified in a migmatite:

1) a part that did not melt and remained 100% solid,
2) a part that partially melted and retained its melt,
3) a part that partially melted and lost some, or virtually all, of its melt and,
4) a part that gained melt and could, therefore, potentially be derived from as much as 100% melt.

Thus, the definition of migmatite in terms of these idealized parts is:

Migmatite: a rock found in medium- and high-grade metamorphic areas that can be heterogeneous at the microscopic to macroscopic scale, and that consists of two, or more, petrographically different parts. One of these parts (see **neosome** below) must have formed by partial melting and contain rocks that are petrogenetically related to each other and to their protolith through partial melting or segregation of the melt from the solid fraction. The partially melted part typically contains pale-colored rocks that are quartzofeldspathic, or feldspathic, in composition, and dark-colored rocks that are enriched in ferromagnesian minerals. However, the partially melted part may simply have changed mineralogy, microstructure and grain size without developing (*i.e.*, without segregating into) separate light or dark parts.

Note that the proportions of each part in the migmatite are not specified. This is because their relative proportions are dependent on factors such as the temperature of metamorphism and how fertile, or infertile, the rocks were and may, therefore, vary greatly within and between migmatites. In addition, which parts are actually present in the outcrop of migmatite, and in what proportion is to a some degree dependent on how representative an outcrop is of the entire migmatite, *i.e.*, the size of the sample, or scale at which the observation is made. However, the underlying petrogenetic relationship between the key parts is partial melting. The parts of a migmatite are defined next.

THE PRINCIPAL PARTS OF A MIGMATITE

Figure 1-1 shows area of rock before (Fig. 1-1a) and after (Fig. 1-1b & c) partial melting has occurred. The rocks that have suitable bulk compositions (*i.e.*, the fertile rocks) have experienced partial melting, whereas the remainder have not. All those parts of the outcrop that have been modified by partial melting are called neosome meaning “new rock”. The modifications brought about by partial melting typically include an increase in the grain size and the progressive destruction of structures, such as foliation and small folds, that existed before the partial melting. Neosome generally contains only syn- and post-anatectic structures; older ones have been destroyed. However, structures that existed before partial melting are preserved in some neosomes, such as melt-depleted granulite (*e.g.*, Waters 1988, Guernina & Sawyer 2003). The term neosome is defined as follows.

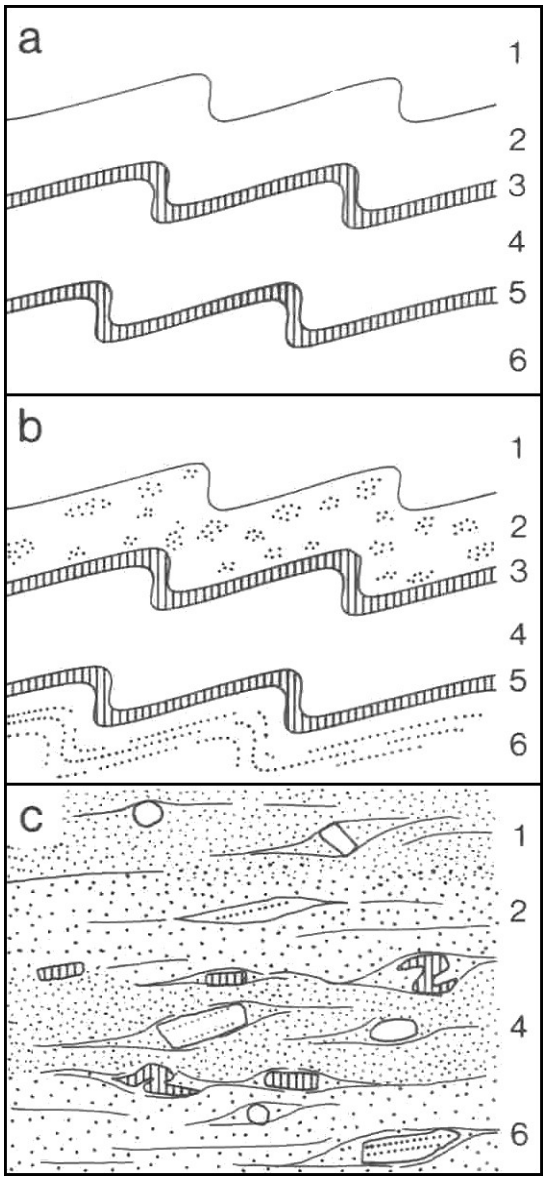

FIG. 1-1. Sketches of an outcrop before and after partial melting to illustrate protolith, neosome and paleosome parts in a migmatite, and the difference between a metatexite migmatite and a diatexite migmatite.
a) A hypothetical sequence of folded rocks before partial melting. The six mapped units are; 1 and 4 psammite, 2 and 6 pelite, whereas 3 and 5 are calc-silicate rocks.
b) The same sequence just after the start of partial melting. Neosome (dotted pattern) has formed in layers 2 and 6. Consequently, the pelite layers (2 and 6 in a) are the protolith; layers 1, 3, 4 and 5 did not partially melt (they are infertile), and so are the paleosome in this migmatite. Specifically, partial melting has resulted in the formation of patches of neosome in layer 2 and stromatic neosome in layer 6. Since the structure present in the pre-partial melting state (a) is still preserved, the migmatite in b is a metatexite migmatite.
c) The outcrop at a more advanced stage of partial melting. The psammite layers have now undergone extensive partial melting, thus layers 1 and 4 in (a) and (b) have become part of the protolith at this stage of development in the migmatite. The calc-silicate rocks still have not partially melted and remain paleosome (or resister) lithologies in this migmatite. However the resister layers have been disrupted as a result of dextral shearing during partial melting. The psammite layers and both pelite layers are now almost entirely neosome (dotted pattern), and contain schollen derived from the less fertile psammite and pelite layers (some of which contain stromatic neosome) and schollen derived from the calc-silicate paleosome. The structures that existed before the partial melting have been destroyed in this migmatite (compare a and c), and are replaced by structures that formed during anatexis, such as the flow structures outlined by the schlieren (black lines) and the asymmetry of the schollen; thus this is a diatexite migmatite. Although the meso- and microstructure in the former pelitic and psammitic layers are likely to be similar, they may still be distinguished and mapped as separate units on the basis of the different mineral assemblages in each.

Neosome: the parts of a migmatite newly formed by, or reconstituted by, partial melting. The neosome may, or may not, have undergone segregation, in which the melt and solid fractions are separated.

Comparing the before and after partial melting states in Figure 1-1, all the fertile rocks in the pre-partial melting state that became neosome after partial melting, are the protolith, or parent rock, of the neosome. Thus, protolith (or parent rock) is defined as follows.

Protolith, or parent rock: rocks present in the lower-grade parts (*i.e.*, below the "melt in" isograd) of a metamorphic area that are equivalent to those from which the neosome formed.

No migmatite that we see, therefore, contains protolith, because all rocks of suitable bulk composition will have partially melted and, therefore, been converted to neosome. Some rocks present in the pre-partial melting state (Fig. 1-1a) appear to have survived virtually unchanged into the post-partial melting state because they did not undergo partial melting (Fig. 1-1b). These rocks therefore, retain their structures that existed before the partial melting; these rocks are called paleosome meaning "old rock". The term paleosome is defined as follows.

Paleosome: the non-neosome part of a migmatite that was not affected by partial melting, and in which structures (such as foliations, folds, layering)

older than the partial melting are preserved. The microstructure (size, form and orientation of grains) is either unchanged, or only slightly coarsened by grain growth in the subsolidus state, compared to that in similar rocks just outside the region affected by anatexis.

A paleosome exists because it did not partially melt and become neosome (Olsen 1985), owing to its refractory bulk composition. Read (1957) referred to the prominent paleosome layers as **resisters**. Layers of calc-silicate, quartzite and metamafic rocks are common resister, or refractory, lithologies in migmatite terrains.

Terms specific to the neosome

Neosome is formed as a result of partial melting and, therefore, contains a fraction that was derived from the crystallization of the melt (or in rare circumstances the quenching of the melt to glass), another fraction that consists of the minerals that were in excess to the reaction that produced the melt and, the minerals that are the solid products of incongruent melting. If these parts have not separated in a migmatite (see example in Fig. 1-2a), but remain intimately mixed, the term neosome suffices as there are no other parts requiring specific terms. However, in the majority of migmatites, and especially those formed in regional metamorphic terrains, the melt and solid fractions become separated (see Fig. 1-2b) and, in that case, there is a need for terms to describe rocks that have formed from the two separated fractions. The solid fraction has both a higher density and viscosity than the melt fraction, and consequently, it tends to remain *in situ*; that one will be considered first. The part of the migmatite from which some, or all, of the melt fraction has been removed is called the residuum (the so-called restite) and is it defined as follows.

Residuum: the part of the neosome that is predominantly the solid fraction left after partial melting and the extraction of some, or all, of the melt fraction. Microstructures indicating partial melting may be present.

Residuum is a general term; there is no reference to rock color, or to a particular mineral assemblage, or to a group of minerals, attached to it. This is because the color and mineral assemblage in the residuum depends greatly on what rock type the protolith was. For bulk compositions that contain a very large proportion of light-colored minerals, such as feldspar or quartz, that are present in excess with respect to the reaction that produced the melt in the rock, the residuum that forms is also light-colored because it is dominated by quartz and feldspar. Examples of light-colored residua, are those generated from quartzite and leucogranite. In contrast, partial melting of many of the common rock types (*e.g.*, pelite, psammite and mafic rocks) in the Earth's crust typically generate residua in which ferromagnesian minerals are prominent constituents. Consequently, the residua generated from these rock types are generally melanocratic (Figs. 1-2b & c), and are given the special name melanosome.

Melanosome: the darker-colored part of the neosome in a migmatite that is rich in dark minerals such as biotite, garnet, cordierite, orthopyroxene, hornblende or clinopyroxene. The melanosome is the solid, residual fraction (*i.e.*, **residuum**) left after some, or all, of the melt fraction has been extracted. Microstructures indicating the former presence of melt may be present.

The complement to the residuum in a migmatite is the part that was derived from the anatectic melt, and this is called the **leucosome** because it is generally the light-colored part of a neosome. The anatectic melt generated at temperatures below 925°C is felsic, but at higher temperatures the bulk composition of the melt approaches the composition of the protolith, which is reached at *ca.* 1200°C (Vielzeuf & Holloway 1988), thus the part derived from the melt may no longer be leucocratic in migmatites formed at ultrahigh temperatures. Leucosome is defined as follows.

Leucosome: the lighter-colored part of the neosome in a migmatite, consisting dominantly of feldspar and quartz. The leucosome is that part of the migmatite derived from segregated partial melt; it may contain microstructures that indicate crystallization from a melt, or a magma. Leucosome may not necessarily have the composition of an anatectic melt; fractional crystallization and separation of the fractionated melt may have occurred.

There is much diversity within migmatites, therefore, the size, physical form, orientation and grain size are not factors in determining what is leucosome, residuum or melanosome. However, these parameters could be of significance in determining exactly how each rock in a migmatite formed, and so should all be recorded.

Although the residuum can be regarded as the *in situ* part of the neosome in most migmatites, that is not the case for the melt fraction; it is potentially mobile. Therefore, further terms that

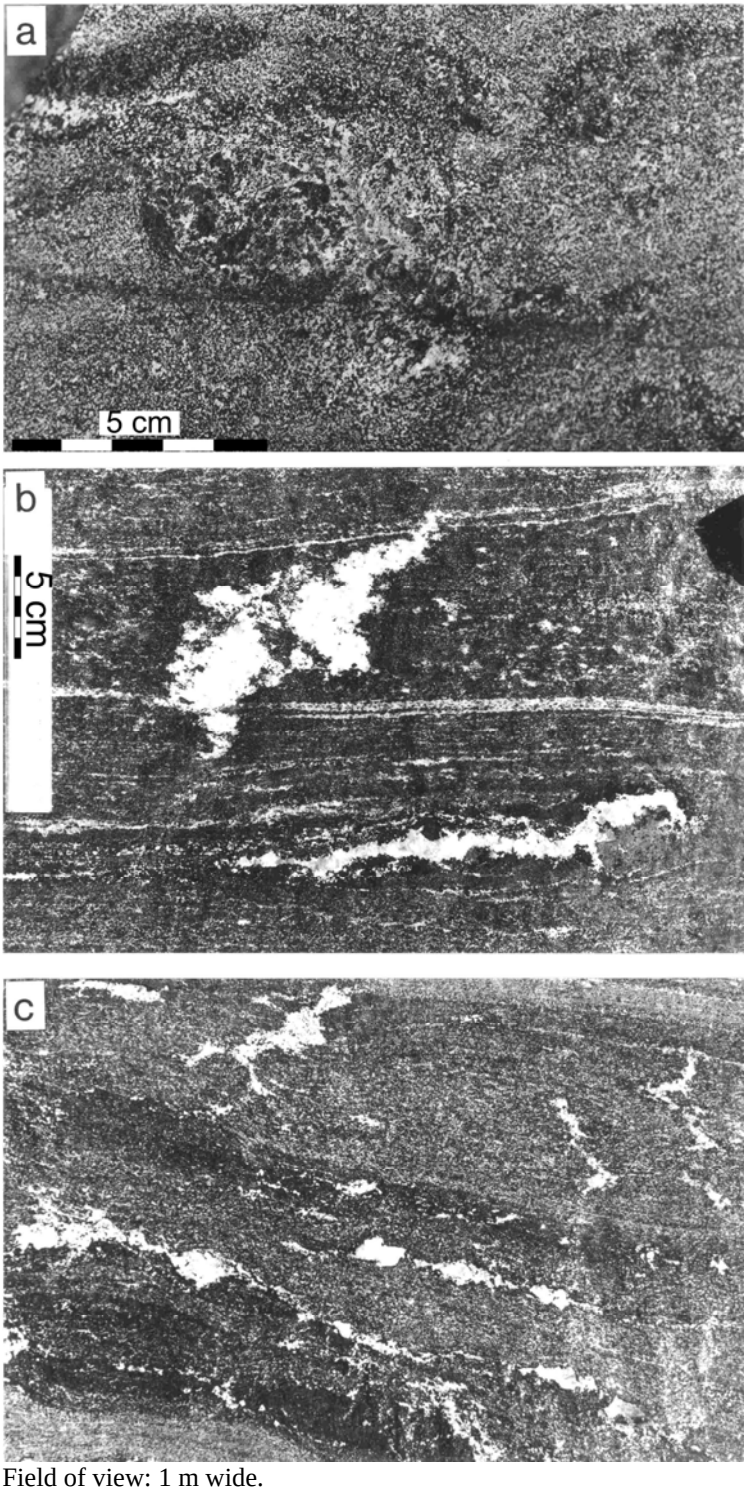

Field of view: 1 m wide.

FIG. 1-2. Neosome and paleosome. **a)** Migmatite formed from a very small degree of partial melting close to the onset of partial melting. A small patch of plagioclase + clinopyroxene + hornblende + garnet + quartz neosome has developed in an upper amphibolite-facies plagioclase + hornblende metamafic rock. The melt fraction and the residuum fractions did not separate into leucosome and melanosome, therefore, the neosome is unsegregated. The margins of this *in situ* neosome are diffuse, hence, it could also be termed nebulitic. The dark line crossing the photograph just below the centre is a post-anatectic fracture that contains a lower amphibolite-facies mineral assemblage.

b) Two patches of segregated neosome in a strongly layered (the layering predates most of the anatexis), upper amphibolite-facies hornblende + plagioclase metamafic schist. The neosome consists of a plagioclase + quartz leucosome surrounded by a melanosome that has a prominent inner part consisting of hornblende, and a less prominent outer part that contains hornblende + plagioclase. The modal fraction of plagioclase in the outer part increases outwards to merge with the mesocratic paleosome (*e.g.*, at the scale).

c) This migmatite developed from an upper amphibolite-facies migmatite mafic protolith and shows neosome in various stages of development. Dark layers of neosome are hornblende-rich and are interpreted to be residual (*i.e.*, melanosome), whereas the light colored plagioclase + quartz parts of the neosome are interpreted to be leucosome that crystallized from a tonalite melt that segregated from the melanosome. The migmatite also contains several meosocratic layers. The widest mesocratic layer in the upper half of the photograph contains leucosomes in asymmetric boudinage structures, and these have somewhat melanocratic rims. This mesocratic layer is, therefore, interpreted to record a less advanced stage of partial melting than the most melanocratic of the layers. Segregation of melt in the mesocratic layer occurred as it was being extended.

convey how far the melt fraction in a migmatite has moved from where it formed, to where it crystallized, may be useful for a more complete description of the leucosomes in a migmatite. This in turn may aid in the subsequent interpretation of the petrogenetic relationship between the parts derived from melt and the rocks around them. Three subdivisions of leucosome, shown schematically in Figure 1-3, may be useful.

***In situ* leucosome:** the product of crystallization of an anatectic melt, or part of an anatectic melt, that has segregated from its residuum, but has remained at the site where the melt formed.

In-source leucosome: the product of crystallization of an anatectic melt, or part of an anatectic melt, that has migrated away from the place where it formed, but is still within the confines of its source layer.

Leucocratic vein (sill or dyke): the product of crystallization of an anatectic melt, or part of an anatectic melt, that has migrated out of its source layer and has been intruded into another part of the migmatite which maybe nearby, or farther away.

Other parts of a migmatite

Migmatites commonly contain parts that are neither leucocratic nor melanocratic; these parts can be described as mesocratic (Fig. 1-4a, but see also Fig. 1-2c). In morphologically complex migmatites there may be many mesocratic domains each with a different color that results from subtle, and not so subtle, variations in mineral assemblage or grain size. The unfortunate term "mesosome" has been applied to these mesocratic domains. Mesosome is a contentious term because mesocratic rocks can occur in either the neosome or the paleosome parts of a migmatite. Whereas the petrogenetic significance of leucosome and melanosome are absolutely clear, they are by definition parts of the neosome, the petrogenetic significance of mesosome is compromised from the very outset by the fact that it could occur in both the neosome (rocks formed by partial melting) and paleosome (rocks that did not partially melt) in the very same migmatite. This ambiguity is also evident from past use; Henkes & Johannes (1981) used mesosome as a synonym for protolith, whereas Ashworth (1985) equate it with

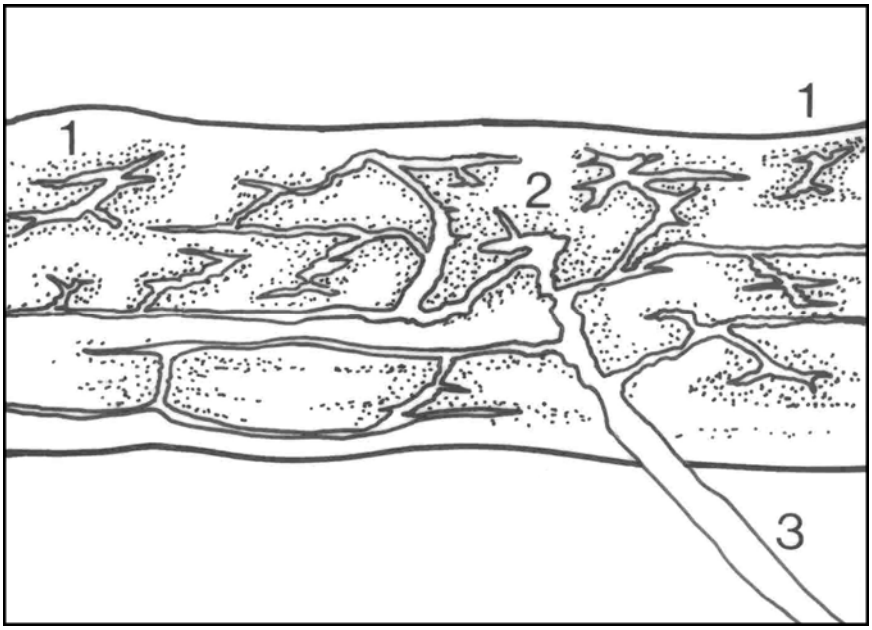

FIG. 1-3. Sketch to show the difference between *in situ* leucosome, in-source leucosome and leucocratic veins. The *in situ* leucosomes (1) in this migmatite occur at dilatant structures and are surrounded by melanosome (stippled pattern). Some *in situ* leucosomes have become linked together into a network of leucosomes that constitutes the channel system through which anatectic melt flowed as it left its source layer. The melt that has moved from where it formed, but has frozen within its source layer, constitutes the in-source leucosome (2); some parts of the in-source leucosome may have melanosome, but other parts do not. Where the in-source leucosome leaves its source layer altogether and enters a different layer in the migmatite, it becomes a leucocratic vein in that layer (3), and has no melanosome around it. That layer may, of course, contain its own *in situ* and in source leucosomes. This sketch is based on a migmatite from the Limpopo Mobile Belt, in which the *in situ* and in-source leucosomes formed in a mafic layer.

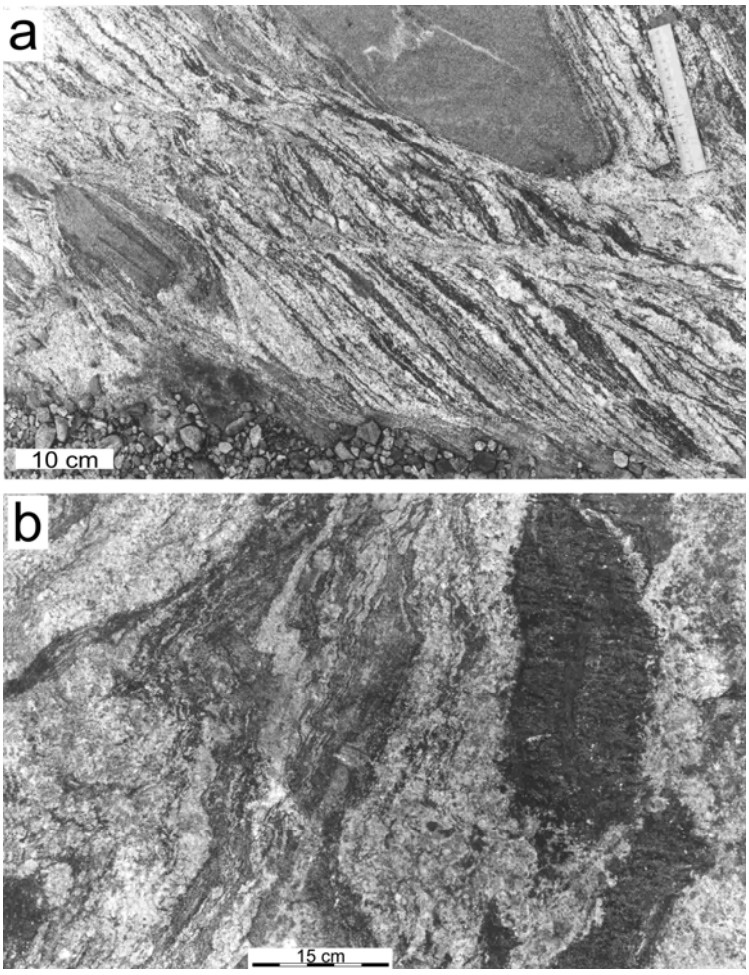

FIG. 1-4. Mesocratic paleosome and mesocratic neosome. **a)** The neosome part of this diatexite migmatite was derived from metapelitic rocks and consists of a cm-scale alternation of granitic leucosome (mineral assemblage plagioclase + quartz + K-feldspar) and melanosome which has the mineral assemblage plagioclase + cordierite + biotite + quartz + K-feldspar (sillimanite occurs as inclusions in cordierite). The paleosome occurs as two rafts of mesocratic, fine-grained plagioclase + quartz + biotite metapsammitic rocks. Some melt in the neosome part of this migmatite has segregated into three shear zones each with a top-to-the-left shear sense within the neosome part of this migmatite, therefore, these are in-source leucosomes. **b)** This granulite-facies migmatite consists entirely of neosome, and is located in the hinge of a fold. The leucocratic part is granitic in composition, and some of it may have been melt derived from the fold limbs and which moved along the pelitic layer and into the hinge during folding. The melanocratic rocks (upper right) contain the mineral assemblage garnet + orthopyroxene + biotite and, because they have virtually no feldspar or quartz left, are interpreted to be residuum (*i.e.*, melanosome). The mesocratic rocks (above the scale) contain the mineral assemblage biotite + cordierite + plagioclase + K-feldspar + quartz and are also interpreted to be residual and, therefore, part of the neosome also, but they are far less melt-depleted that the melanocratic portions. The folds outlined by the mesocratic layers formed during partial melting.

paleosome. This inconsistency continues in more recent literature, where some authors have used mesosome to describe intermediate-colored paleosome and then equated this with protolith, in clear contradiction to the definitions of both protolith and paleosome. For these reasons the term mesosome should be abandoned as it has no unique genetic significance. The rocks of intermediate color in a migmatite should simply be described as mesocratic. Moreover, because mesocratic rocks can occur in the neosome or paleosome (or both) of a migmatite, it is necessary when describing a particular mesocratic rock to state explicitly where that rock is located in the migmatite, *e.g.*, the paleosome as in Fig. 1-4a, or the neosome as in Fig. 1-4b.

Rarely, some adjacent parts in a migmatite are separated from each other by a narrow (< 2 cm) rim, or zone, that has a different composition, mineral assemblage or microstructure. The composition of these rims indicates that they are not the residuum left after extraction of anatectic melt and, therefore, the term **selvedge** is used to describe these.

Selvedge: a rim of rock of different color, composition, mineral assemblage or microstructure that may separate two different parts of a migmatite. Selvedges are not residuum material, and may be leucocratic, mesocratic or melanocratic.

Selvedges tend to have developed between a melt-rich part and melt-poor part of the neosome, or between a melt-rich part of the neosome and paleosome. Field observations from migmatites indicate that selvedges are most commonly developed around leucocratic veins (*e.g.*, Fig. 1-5); thus, the injected melt may not have been in

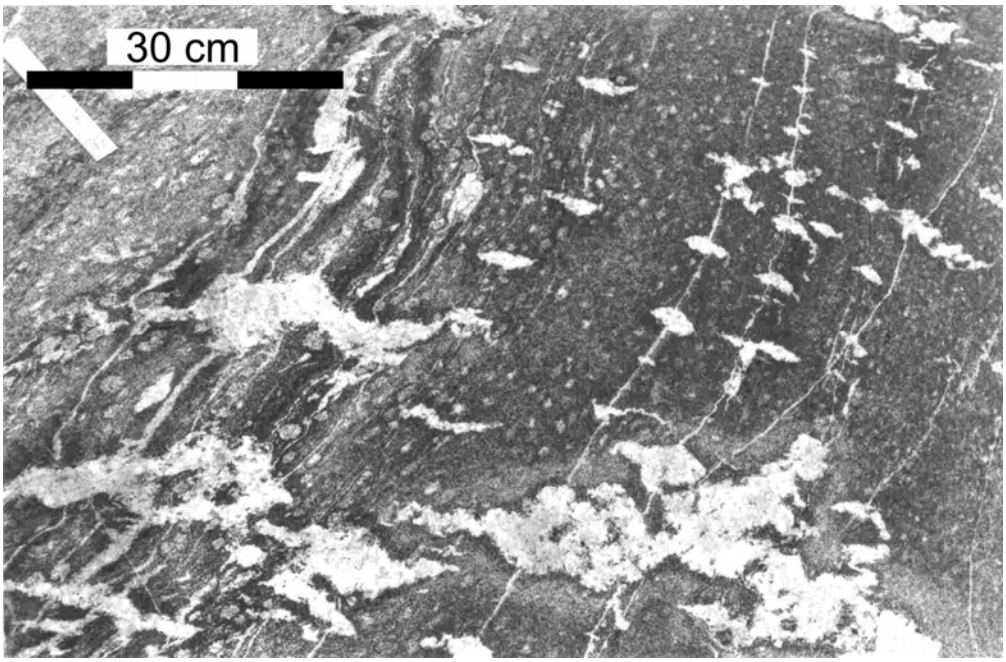

FIG. 1-5. The mafic rocks in this migmatite were folded during partial melting, and felsic melt intruded parallel to the axial planes of the folds, hence these are leucocratic veins, not leucosomes. A narrow mafic selvedge consisting of hornblende and biotite developed next to each felsic intrusion (*e.g.*, in the bottom left) and outside that a wider, light-colored selvedge developed in the plagioclase + hornblende + diopside + garnet metamafite by alteration of plagioclase (possibly to scapolite). Both selvedges are interpreted to have been formed by the interaction of the host rock with fluids that were released as the felsic melt crystallized.

chemical equilibrium with its host (either another part of the neosome or paleosome). Two main mechanisms can be envisaged for the formation of selvedges; 1) reaction between the host rock and an aqueous fluid that was exsolved as the melt that produced the leucosome or leucocratic vein crystallized and, 2) diffusional exchange of components between the injected anatectic melt (or the crystallized leucosome or leucocratic vein) and its adjacent host in response to gradients in activity.

The most common type of selvedge consists of a thin (mm-wide), biotite-rich (or in metamafic rocks a hornblende-rich) melanocratic rim around leucocratic veins, and some in-source leucosomes. Consequently, this type of selvedge is called a **mafic selvedge**. Mafic selvedges are also common at the margins of granitic dykes and sills intruded into low-grade country rocks; thus, mafic selvedges are not found only in migmatites.

Virtually all migmatite terrains contain felsic dykes that were intruded before, or after, the partial melting event. These are not leucosome (*i.e.*, *in situ* leucosome, in source leucosome or leucocratic veins), and should be called granite dykes (or granodiorite, tonalite, *etc*., dykes or sills as appropriate for their orientation) as they are no different from, and have the same origin as, felsic dykes or sills commonly found in lower-grade metamorphic terrains, or in non-metamorphosed rocks.

IDENTIFYING THE PARTS OF A MIGMATITE IN THE FIELD

Neosome

Neosome displays a wide range of morphology. It can occur as small scattered patches (*e.g.*, Fig. 1-2a) in a migmatite, or it can comprise the whole migmatite (*e.g.*, Fig. 1-4b). Irrespective of the scale or extent of the neosome, its identification hinges on recognizing the results of partial melting. This can be done by recognizing the microstructural and mineralogical changes that were brought about by partial melting. Neosome has a larger grain size than either the protolith or the adjacent paleosome; the presence of melt in the neosome may have facilitated the grain growth. Most neosome contains a mineral assemblage that is different from that of the protolith, typically one that is the product of an incongruent melting reaction. Neosomes, generally, do not preserve the

structures that existed in the protolith before partial melting. The structure (*e.g.*, foliation, folds, layering) and microstructure (shape, size and orientation of grains) that existed prior to partial melting are both degraded as the degree, and extent, of partial melting increases. The original structures and microstructure are replaced by new ones that develop during the neosome-forming processes, *e.g.*, partial melting and flow of the melt-rich part. These constitute the principal criteria available to identify the mesocratic, unsegregated neosomes that are formed in migmatites in which there was no segregation of the melt fraction from the solid fraction. However, in most migmatites, the melt fraction did separate from the residual fraction to a greater or lesser degree and, consequently, the presence of leucosome and residuum (*e.g.*, melanosome) are additional criteria by which segregated neosomes are identified (*e.g.*, Figs. 1-2b, 1-2c and 1-4a).

The recognition of neosome, whether it has segregated or not, is generally a simple matter in migmatites developed from mesocratic or melanocratic protoliths (*e.g.*, metagreywacke, metapelite, metadiorite and metamafic rocks). However, it is much more difficult if the protolith was leucocratic (*e.g.*, some granite, tonalite, trondhjemite and metapsammitic rocks) because of the lack of a contrast in color between the paleosome and neosome parts and within the neosome itself. The dilution of the mafic minerals by large amounts of feldspar and quartz in these rock types means that the subsequent changes in modal proportions brought about by partial melting produce only subtle changes in color, and these may be very difficult to detect in the field. Distinguishing the neosome from the paleosome in migmatites that developed from leucocratic protoliths may best be accomplished in the field by identifying changes in the microstructure (see Fig. 1-6), such as fabric or grain size, rather than relying on changes in mineral modes or color.

Residuum

Rocks derived from the residual material left after partial melting and extraction of the melt fraction are the major component of some granulite-facies migmatite terrains (Fig. 1-7a). This is because some of the melt generated (the degree of partial melting is rarely above 50%) has commonly escaped to form dykes and plutons of granite at higher levels in the crust. Many of the residual

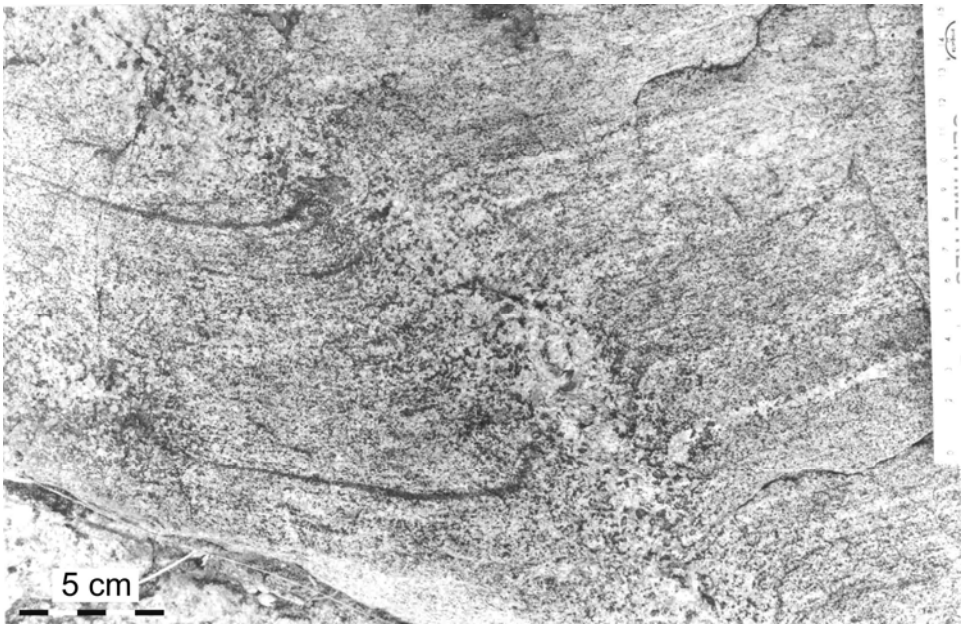

FIG. 1-6. The neosome in this migmatite formed in a small reverse shear in a leucocratic plagioclase + quartz + biotite psammite. The neosome contains the assemblage plagioclase + quartz + K-feldspar + orthopyroxene and is essentially the same color as the rocks around it. The neosome does not have conspicuous melanosome or leucosome parts to it, however it is easily recognized by its coarser grain size, and because it does not contain the prominent layering visible in the rocks (which could be considered as the protolith) on either side of it. Overall this could be called a patch-structured metatexite migmatite.

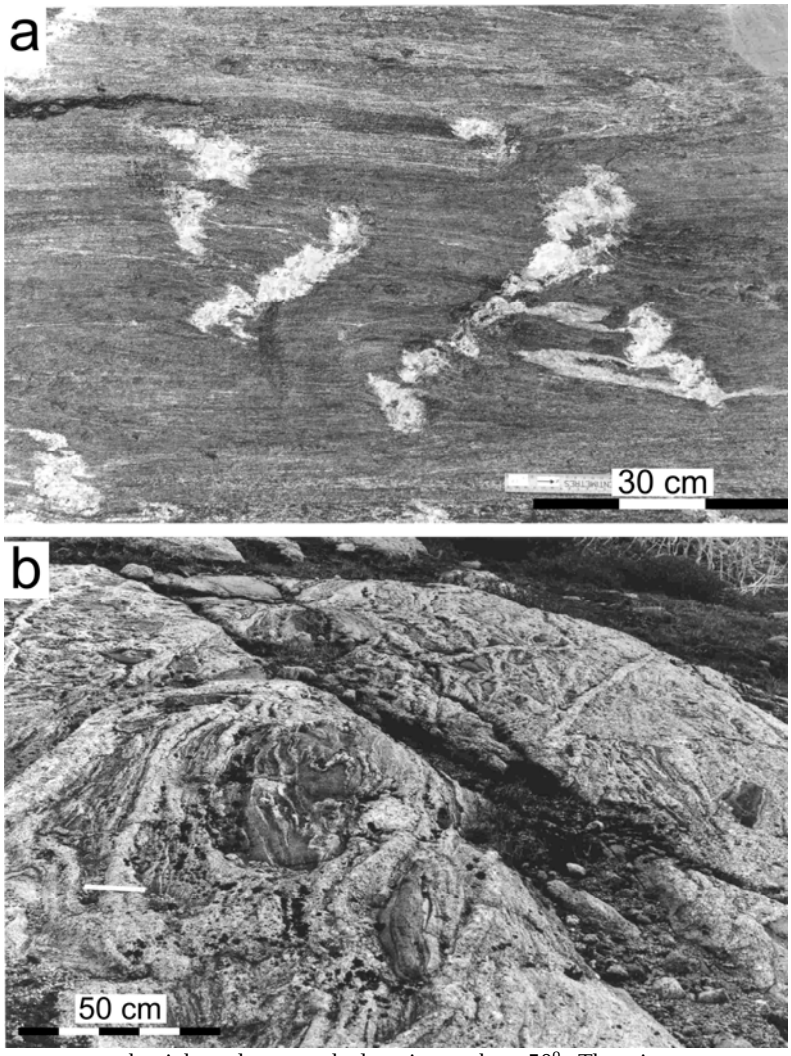

FIG. 1-7. Leucosomes and leucocratic veins. **a)** The dark rocks in this migmatite contain the mineral assemblage clinopyroxene + garnet + hornblende + plagioclase, and from their bulk chemical composition are interpreted to be the melt-depleted residuum from about 36% partial melting of metamafic rocks. The melting occurred during intense non-coaxial shearing that produced a strong foliation in the residual rocks, and folded some earlier tonalitic dikes. Differences in strain rate across foliation planes during the final stages of deformation resulted in the creation of abundant dilatant structures in the residual rocks. Anatectic melt migrated into these structures and, subsequently, crystallized to form the coarse-grained *in situ*, or in-source leucosomes that are evident in the centre of this photograph. Overall this could be called a dilation-structured metatexite migmatite.
b) This migmatite is crossed by several leucocratic veins that are typically about 10 cm wide. The ruler rests on a portion of one such leucocratic vein that is oriented parallel to the layering in the metatexite migmatite, however, farther on the vein curves to the right and crosses the layering at about 50°. The microstructure and modal composition of the leucocratic veins are the same as the stromatic leucosomes in the migmatite, and this suggests that the melt that formed the veins was also locally derived. Overall, this could be called a vein-structured metatexite migmatite, although it could also be considered vein-structured transitional migmatite between a metatexite and a diatexite morphology.

rocks in migmatites are overlooked. Perhaps the most familiar, and the easiest residual rocks to recognize in a migmatite, are those that occur as melanosome around the margin of an *in situ* leucosome (*e.g.*, Fig. 1-2b). However, melanocratic residual rocks in migmatites occur more commonly as diffuse patches, continuous layers (Fig. 1-2c) and, in some cases, irregularly shaped bodies (*e.g.*, Kenah & Hollister 1983, Sawyer 2001, White *et al*. 2004) in the neosome. Residual rocks that are not melanocratic can be particularly difficult to recognize in the field. For example, residual rocks are very widespread in some melt-depleted granulite terrains (*e.g.*, the Ashuanipi Subprovince), but they are the same (mesocratic) color as their psammitic protolith, and they still preserve cross bedding in places. Consequently, they have to be identified by their residual (plagioclase + orthopyroxene + quartz + biotite) mineral assemblage and whole rock composition (*e.g.*, Guernina & Sawyer 2003). Plagioclase-rich residual rocks derived from the partial melting of leucotonalite protolith in the Opatica Subprovince are also leucocratic, and they are identified principally by their microstructure, from which the loss of melt is inferred, and their whole rock compositions (Sawyer 1998).

Leucosome

The three divisions of leucosome can be recognized by a combination of their characteristics in the field (Fig. 1-3), and by the petrogenetic relationship between leucosome and its immediate host. However, if it is not possible to assign the leucosomes in a migmatite to one of these three categories, then the default term leucosome suffices.

In situ leucosome is, by definition in contact with its own residuum; in most cases as a melanosome around it. Contacts between the leucosome and residuum are generally diffuse on a millimetre- to centimetre-scale. The composition of *in situ* leucosome corresponds to an initial anatectic liquid or, if some melt was lost after crystallization had started, to a cumulate composition derived from an initial melt. The petrogenetic relationship between the leucosome and its host is specific; the leucosome was derived from the anatectic melt and came from where the adjacent residuum is located. However, if some loss of melt has occurred, there is an excess of residuum relative to leucosome.

An in-source leucosome is derived from melt that has moved from where it formed and, therefore, may be discordant and have sharp borders with its host rock (*e.g.*, Figs. 1-3 & 1-4b). Many in-source leucosomes, however, are oriented parallel to the compositional layering inherited from the protolith (*e.g.*, bedding) and have some diffuse and some sharp contacts. In-source leucosomes may have a composition corresponding to an initial anatectic melt, a cumulate or a fractionated anatectic melt. Because they are derived from a melt that has moved, in-source leucosomes are detached from their own specific residuum, but as they remain in their source layer, they are hosted by another, similar residuum (perhaps melanosome) that formed from the same protolith. Thus, there is a petrogenetic connection between the leucosome and its host, but they are not exact complements. For example, the host residuum may have formed from a slightly lower, or higher, degree of partial melting, or may have lost a higher, or lower, fraction of melt.

Leucocratic veins (or dykes if sufficiently large) are formed from anatectic melt that has moved away from its residuum (Fig. 1-3) and crystallized elsewhere in the migmatite (see Fig. 1-7b). Thus, it could be in a paleosome or a resister layer, or in another domain of neosome; for example, melt derived from a pelitic layer intruded into a neosome formed from a psammitic, or a mafic, protolith. Typically contacts between leucocratic veins and their host rocks are sharp; a selvedge may have developed at its edges. There is no direct petrogenetic relationship between the leucocratic vein and its immediate host rock; the age of crystallization in the former should be consistent with the metamorphic age in the latter. Leucocratic veins generally have compositions that indicate derivation from a fractionated anatectic melt, but some have compositions of an initial melt, and others compositions of cumulates.

Well-defined leucosomes are common in migmatites, but leucosomes that are poorly defined and form somewhat nebulous patches also occur. Many outcrops of migmatite contain several different forms and orientations of leucosome (*e.g.*, Oliver & Barr 1997). Some migmatites show petrological continuity (no cross-cutting contacts between leucosomes and a continuity of grain size and microstructure) from *in situ* leucosome that connect to in-source leucosome which, in turn, connect to leucocratic veins, hence all the portions of leucosome are inferred to have contained melt at the same time (Fig. 1-3); these arrays of linked leucosome are interpreted to mark the network of channels through which melt drained out of migmatites (Sawyer 2001, Guernina & Sawyer 2003, Marchildon & Brown 2003).

Many migmatites also contain felsic dykes that were not formed by the anatectic event which formed the neosome; most commonly the dykes are younger. Granite dykes typically have sharp contacts with their host and, because they were injected into cool hosts, may have fine-grained border zones (chilled margins). These felsic dykes are not leucosome and it is important to differentiate them (by their composition or age) from leucosomes, thus they are called granite (or granodiorite, tonalite, *etc.*) dykes.

THE FIRST ORDER MORPHOLOGY OF MIGMATITES

The terms that were given in the previous section describe the parts of a migmatite that develop as a consequence of partial melting; neosome with its melt-derived and residuum-derived parts, and the paleosome. These terms do not describe how the constituent parts of a migmatite are spatially arranged, or the overall morphology of a migmatite. Thus, another set of terms are required to describe the appearance of a migmatite. In most migmatites the arrangement of the parts results in a very complex morphology which can vary considerably from place to place. Consequently, it is most important to consider

whether or not the migmatite available for study in an outcrop is representative of the whole. The morphology of each migmatite is more than just the result of the processes associated with partial melting (*e.g.*, segregation of the melt). There are also a number of key factors, rather than processes, that contribute to the final appearance of a migmatite, and these need to be identified before the terms that describe the morphology of migmatites can be introduced. Four factors are immediately evident:

1) the nature of the rocks just before partial melting,
2) the extent of partial melting,
3) the rate of cooling, and
4) whether or not the rocks were deformed when they contained melt.

The first can be viewed as an internal factor, and the other three as external ones imposed on the rocks by the heat source, by the far-field stresses or by the local stresses.

First, consider the nature of the rocks prior to melting. When the metamorphic temperature becomes sufficiently high (> *ca.* 650°C) some of the rocks may begin to partially melt. The rocks that have bulk compositions that enable them to begin to partially melt are called "fertile", in contrast, the rocks that have bulk compositions that do not begin to partially melt at the metamorphic conditions attained in the migmatite are called "infertile". Of course, there are degrees of fertility; at the same temperature some rocks will produce more melt than others. Thus, we can envisage that the migmatite developed from a sequence of rocks dominated by infertile lithologies (*e.g.*, quartzite), but which contains a few thin layers of fertile rock (*e.g.*, pelite), will have a different appearance to one produced from a sequence consisting of few thin, infertile layers of quartzite within a thick pelitic sequence. Similarly, a sequence of thinly bedded siliciclastic metasedimentary rocks in which there is a wide range in rock fertility, will produce a migmatite that is morphologically different from one generated from a fertile, homogeneous protolith, such as a metagranite. The distribution of the fertile and infertile layers is clearly a factor in determining the morphological complexity of the final migmatite.

Second, the peak temperature reached during partial melting has a substantial effect. Returning to the example of a sequence of thinly bedded siliciclastic metasedimentary rocks, at the onset of partial melting (*ca.* 650°C) only the layer(s) with the most fertile composition will have started to produce melt and, at least in the initial stages, the partial melting will produce a few small, scattered patches of neosome. None of the other layers will have begun to partially melt and they are, therefore, paleosome in that migmatite. As the metamorphic temperature increases, progressively more and more of the layers will begin to melt. At the peak metamorphic temperature, of for example 900°C, a large proportion of the layers may have partially melted, and those with the most fertile compositions will have become neosome with a higher proportion of melt (high ratio of melt to residuum) than the neosome generated from the less fertile layers (lower ratio of melt to residuum). Should any infertile layers remain at that temperature, they will be the paleosome, although they will be coarser grained than they were at 650°C. Similarly, the migmatite generated from a homogeneous fertile protolith at 650°C may contain just a few scattered patches of neosome in a host that has not yet melted (*i.e.*, paleosome), whereas at 900°C partial melting in the same rock may be so pervasive that all of it has become neosome. These simple examples, illustrate that there will be significant differences in appearance due to the extent of partial melting between migmatites generated from identical protoliths, but at different metamorphic temperatures.

The third factor, duration of partial melting and particularly how rapidly cooling takes place affects the morphology of migmatites at the micro- and the meso-scales. In the most rapidly cooled rocks the partial melt is quenched to glass (see Holness 2008 and Cesare 2008 in this volume) and the minerals in the residuum have a small grain size. In migmatites that cooled a little more slowly the melt typically crystallizes to granophyre, and the minerals in the residuum are a little larger. In the slowest cooled terrains the melt fully crystallizes and the grain size is largest. Time also determines how far the melt fraction can have moved away from the residuum before it crystallizes. Thus, in addition to their smaller grain size, the leucosomes in migmatites from contact aureoles tend to be individually of smaller volume and more closely spaced than those from regional migmatite terrains.

The fourth factor, deformation, has two important effects; it produces differential stress that can drive the movement of melt, and it can result in a change in geometry, *e.g.*, by folding or by transposition, that can affect the final morphology of a migmatite. Differential stresses can be

produced on the grain scale (*e.g.*, Robin 1978, Wheeler 1987), and in heterogeneous rocks at a macroscopic scale between layers of different bulk viscosity (competence). Incompatibilities in the strain rate between layers that have different competencies result in the formation of dilatant structures, such as the inter-partitions between boudins. The combined effect of the gradients in differential stress and the local development of dilatancy is to provide both the driving force to move the melt fraction out of the matrix where it formed and the nearby dilatant sites where it collects (Sawyer 1994), and upon crystallization forms a leucosome. Deformation that drives the segregation of melt in a migmatite has the effect of enhancing its anisotropy by concentrating the melt into specific domains which become weaker. In contrast other parts of the neosome are made stronger during deformation because the proportion of melt there is greatly reduced, and the proportion of residual minerals, some of which are particularly strong (*e.g.*, garnet and pyroxene), increased. The segregation of melt has a marked feed-back effect in that further deformation is partitioned into the parts of a migmatite where the melt is concentrated because that is where it is weakest. This can result in folding or the transposition of the migmatite and produce morphologies that are strongly layered or attenuated. Thus, the morphology of migmatites that were deformed when they contained melt (*e.g.*, most regional metamorphic terrains) are very different from migmatites in which deformation did not occur, or was minor (*e.g.*, many contact aureoles and a few regional migmatite terrains).

Which of these four factors influences the overall morphology of migmatites the most can be gauged by comparing the changes in the appearance of migmatites across a large number of migmatite terrains. Such a comparison reveals that there are two basic morphologies of migmatite, whether they are from contact aureoles (Ballachulish Igneous Complex, Duluth Igneous Complex, Cooma) or from regional metamorphic terrains (Quetico, Ashuanipi and Opatica subprovinces, the St. Malo migmatite terrain, France, and the Broken Hill area, Australia).

In one morphology the structures (*e.g.*, bedding, foliation and micro- to meso-scale folds) that existed before partial melting began are preserved in a coherent manner so that their orientation and distribution can be mapped in the same way as in lower grade rocks that did not undergo anatexis. For this to have happened the proportion of the rock that was converted to neosome must have been sufficiently small that enough of the old structures are preserved such that a coherent picture of the old structure remains. In the other morphology, the structures that pre-date partial melting are no longer preserved in a coherent, mappable way. Typically they remain only in variously oriented fragments of paleosome, or in some cases residuum, that are scattered in neosome (compare Figs. 1-1a & c). The principal structures in these migmatites are those that formed during partial melting and before solidification, typically a magmatic or submagmatic foliation, compositional layering or flow banding and various small relics of paleosome or residuum-rich neosome, commonly oriented in an imbricate fashion and enveloped in a flow banding.

These two morphologies of migmatite are called metatexite and diatexite respectively, and they represent the first order descriptive terms for the morphology of migmatites; they are defined as follows.

Metatexite: a migmatite that is heterogeneous at the outcrop scale, and in which coherent pre-partial-melting structures are widely preserved in the paleosome (where the microstructure appears unchanged) and, possibly in the melanosome (residuum) part of the neosome where the fraction of melt was low. The neosome part is generally segregated into leucosome and melanosome, but neosome in which melt and residuum did not segregate may also occur.

Diatexite: a migmatite in which neosome is dominant and melt was pervasively distributed throughout. Pre-partial-melting structures are absent from the neosome, and are commonly replaced by syn-anatectic flow structures (*e.g.*, magmatic or submagmatic foliations, schlieren), or by isotropic neosome. Neosomes are diverse, reflecting a large range in the fraction of melt, and they can range from predominantly leucocratic to predominantly mesocratic (*e.g.*, unsegregated melt and residuum) to predominantly melanocratic. Paleosome occurs as rafts and schollen, but may be absent.

The distribution of metatextite and diatexite migmatites follows a similar pattern in all migmatite terrains where both occur; some migmatite terrains contain only migmatites with the metatexite morphology. The metatexite migmatites typically occur in the lower temperature parts of migmatite terrains and diatexite migmatites occur in the higher-temperature part and could, therefore, be interpreted as the consequence of an increase in the

fraction of melt (M_f) present. In some migmatite terrains the passage from metatexite to diatexite migmatites is gradational; typically continuous layers of paleosome and residuum in metatexite progressively become disrupted and enclosed in unsegregated neosome or leucosome, then the fragments tend to become rotated and finally they become small and rounded relics in diatexite. However, the change from metatexite migmatite to diatexite migmatite is abrupt in some migmatite terrains. For example, White *et al*. (2005) argued that ingress of aqueous fluid at the peak metamorphic temperature lowered the local solidus temperature to below the ambient metamorphic temperature which caused a sudden increase in the fraction of melt and that this was responsible for the abrupt appearance of diatexite migmatites at Round Hill in Australia. On the other hand, Solar & Brown (2001) correlated the abrupt change from metatexite to diatexite migmatite in Maine to a sharp change in the regional strain. It could be interpreted that the switch in the morphology from metatextite to diatexite in migmatites is a direct consequence of the increase in the degree of partial melting and, therefore, that the presence of diatexite migmatites reflects a higher peak metamorphic temperature (or a_{H2O} in the case of H_2O-fluxed melting). In a closed system where melt was neither lost nor gained this would be correct. However, this is an over simplistic view of natural migmatites because migmatites are commonly not closed systems. Guernina & Sawyer (2003) have shown that metatexite migmatites formed in depleted granulite terrains where the metamorphic temperatures was about 900°C, because the melt was continually removed from the rocks, and hence the system was open. Sawyer (1998) and Sawyer *et al*. (1999) showed that the melt generated in one part of a migmatite can be moved and accumulated in another where the structures that pre-date partial melting are eventually erased creating a diatexite migmatite. Thus, the transition from metatexite to diatexite is primarily due to an increase in the fraction of melt (M_f) in the migmatite. In a closed system the fraction of melt is equal to the degree of partial melting (F), but in an open system it is not. Diatexite migmatites formed in a closed system where M_f corresponds to F could be called **primary diatexite migmatites**, and those formed in open systems where M_f does not correspond to F could be called **secondary diatexite migmatites**.

The first-order morphological division of migmatites into metatexite and diatextite is represented on Figure 1-8 as a function of the fraction of melt. The fraction of melt at which the transition from metatexite to diatexite morphology occurs is conjectural; three possibilities are shown on Fig 1-8. In the simplest model (Fig. 1-8a) the matrix framework loses cohesion when the fraction of melt reaches about 0.26 and the contacts between the crystals, treated as uniformly packed, rigid spheres, are lost. However, most rocks consist of a

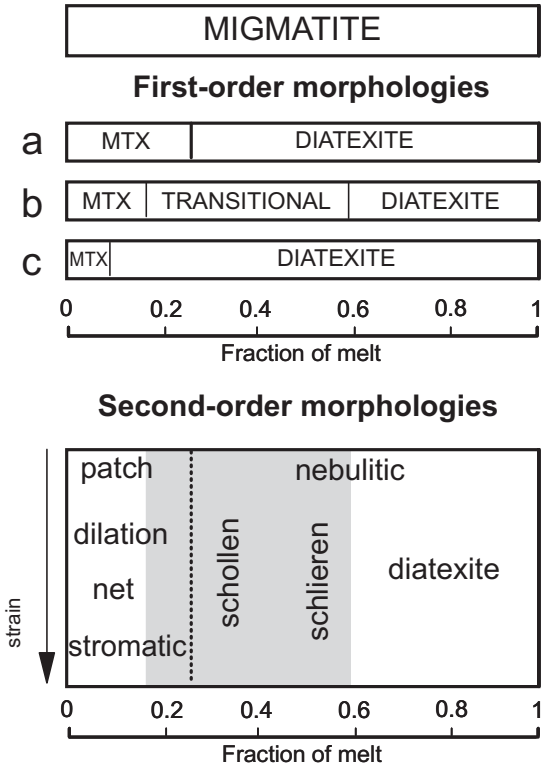

FIG. 1-8. The first- and second-order divisions for migmatites. Three positions for the transition from metatexite (MTX) to diatexite morphology are shown. Two (a & b) are for partially molten rocks that are suspensions of crystals in a melt, and one (c) is for a partially molten rock in which anatectic melt occurs as a film on most of the grain boundaries. For a rock consisting of uniform rigid spheres (a), the transition occurs at a fraction of melt of about 0.26, for rock containing a range of particle shapes and sizes (b) it lies between 0.16 and 0.6, but if movement between the grains occurs by processes such as grain boundary sliding or solution-precipitation, it could lie at fractions of melt as low as 0.08 (c). The second order morphologies for metatexite and diatexite migmatites are shown with reference to the fraction of melt (increasing from left to right) with the transition defined by model (a) shown as a dashed line, and the transitional domain from model (b) shown as a grey field.

range of particle sizes and shapes, and the onset of magma flow when a suspension of crystals in melt forms could occur (Fig. 1-8b) with a fraction of melt as low as 0.16 or as high as 0.6 (Lejeune & Richet 1995, Renner *et al.* 2000). If the deformation mechanism was not a melt dominated one, but involved processes such as grain boundary sliding and the dissolution, diffusion and precipitation of minerals through a thin intergranular film of melt, then the disruption of pre-anatectic structures, and the transition from metatexite to diatexite morphology could, potentially, occur at far lower fractions of melt, perhaps as little as 0.07 (Fig. 1-8c) corresponding to the "melt connectivity transition" of Rosenberg & Handy (2005). Presently, estimates of the fraction of melt present at the transition from metatexite to diatexite migmatite come from geochemical methods and suggest that it occurs at M_f *ca.* 0.2, which corresponds approximately to the rheological threshold where a suspension of crystals in melt forms; this threshold has been variously called the "rheologically critical melt percentage" (Arzi 1978), the "melt extraction threshold" (Vigneresse *et al.* 1996), and the "solid-to-liquid transition" (Rosenberg & Handy 2005). However, studies aimed at elucidating the deformation mechanisms that occurred in migmatites are needed to understand better how the transition from metatexite to diatexite is accomplished.

The first-order division of migmatites into metatexite and diatexite is based on the fraction of melt present in the migmatite. Other factors such as, the original distribution of lithologies in the protolith, whether or not deformation occurred when the rocks contained partial melt, and how the partially melted rocks responded to deformation, all contribute to the final morphology of a migmatite. However, the effects of these contributing factors are superimposed on a basic metatexite (Figs. 1-9 & 1-10) or diatexite (Figs. 1-11 & 1-12) pattern. Therefore, these factors can be viewed as having a second-order effect on the final morphology that a migmatite develops, these second order effects will be considered next.

THE SECOND ORDER MORPHOLOGIES OF MIGMATITES

Terms appropriate to metatexite migmatites

Structure at the very onset of partial melting. At the onset of partial melting the fraction of melt in a migmatite is, of course, very small and this precludes the development of an eye-catching morphology. Nevertheless, it is very important to identify these migmatites because their appearance defines the lower-grade limit to migmatite terrains. Partial melting in a rock typically starts at a few dispersed sites (see Fig. 1-2a) where the conditions are optimal for the melt-producing reaction to proceed. However, in some cases melting may begin at many locations that are dispersed throughout the rock, *i.e.*, melting is pervasive throughout the volume of rock. The first macroscopic evidence that partial melting has occurred in a rock is the development of thin, fine-grained quartzofeldspathic films along the grain boundaries between the reactant minerals, which may have become rounded and have developed a sugar-like, macroscopic appearance. The thin leucocratic films are crystallized melt (*e.g.*, Holness & Clemens 1999, Sawyer 1999, Holness & Watt 2002). The term **nebulitic** may be an appropriate descriptive term for some examples of this incipient stage of neosome formation. If there are no sharp boundaries or no clearly defined shape to the neosome the migmatite is then described as a nebulitic metatexite migmatite.

Patch structure As the fraction of melt generated by partial melting increases the neosome part becomes more conspicuous and easier to recognize in the field. If partial melting occurred at discrete sites and the neosome has grown into scattered small, macroscopically visible domains, the term **patch migmatite** is applicable. Patch-shaped neosome was one of the first to be recognized in migmatites; Sederholm (1907) called them "blind ending" and regarded them as characteristic of the incipient stages of partial melting (see also Weber & Barbey 1986, McLellan 1988, Grant & Frost 1990, Hobson *et al*. 1998, Sawyer 1991, Timmermann *et al*. 2002, Slagstad *et al*. 2005). However, Sederholm's comment refers to incipient melting in the layer containing the patch neosome. For example, although partial melting may have just begun and produced small patches of neosome in a metapsammite layer (Fig. 1-9a), it may have started much earlier in an adjacent metapelitic layer and already have produced a great deal of melt there before the psammite began to partially melt. As partial melting continues, the patches of neosome grow and complex lobate shapes may form as neighboring patches of neosome coalesce.

The melt and solid fractions with a neosome patch may or may not have separated. Neosome that has not undergone segregation is mesocratic, and it is recognized by its coarser grain size and its

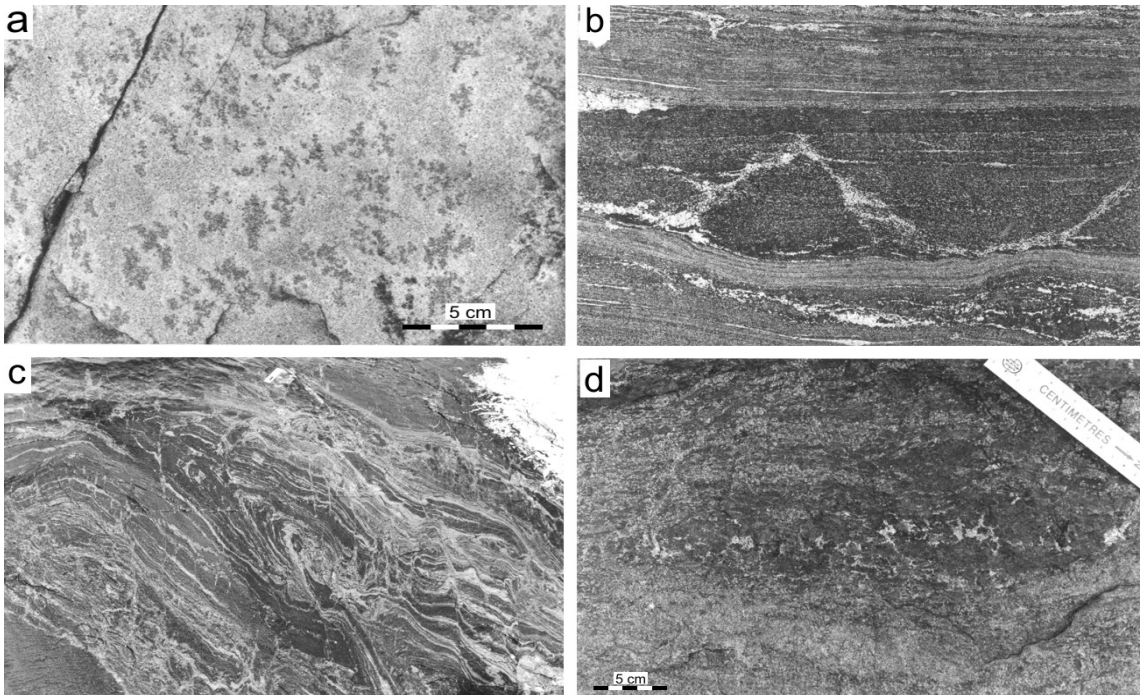

FIG. 1-9. Examples of patch-structured and dilation-structured metatexite migmatites. **a)** Patch-structured neosome developed in a granulite-facies plagioclase + quartz + biotite metapsammite. The metapsammite that remains between the patches of neosome is the paleosome in this metatexite migmatite; it is mesocratic and fine-grained. Patches of neosome are up to 2 cm across and have aggregates of dark colored crystals of orthopyroxene in their centres; that forms the melanosome in the migmatite. The outer portion of the patches of neosome contains the paragenesis plagioclase + quartz + K-feldspar and these are the leucosome part of the migmatite. **b)** Dilation-structured metatexite migmatite. Leucosome in the coarse-grained plagioclase + hornblende metamafic layer in the centre of the photograph are located in dilatant structures that formed as a result of shear failure during layer-parallel extension. **c)** Numerous dilatant sites were created in the thin, competent layers during folding of this plagioclase + clinopyroxene + orthopyroxene + quartz mafic granulite. Melt migrated into these sites and resulted and formed the complex array of leucosomes in this migmatite. Some leucosomes are located between the layers (hence these could be said to be stromatic), and become noticeably thicker in the fold hinges. Other leucosomes occupy many small normal-sense shears that are oriented at about 45° to the axial trace of the fold. **d)** Leucosomes in this migmatite are located in small dilatant sites that have formed in a melanocratic patch of garnet + orthopyroxene + biotite residuum in a sequence of granulite-facies metapelitic rocks. The competent melanosome developed short extension fractures due to extension parallel to the layering. Nearby anatectic melt then migrated into the fractures.

isotropic microstructure (Fig. 1-2a) that results from the elimination by partial melting of the pre-anatectic structures, still present in the surrounding paleosome. Large patches of unsegregated neosome can, if they have diffuse borders, be called nebulitic patch migmatites. In segregated patches of neosome the residuum may occur as an outer rim to the neosome patch. Alternatively, the solid, residual phase(s) may occur at the core of the neosome and be surrounded by an annulus or "moat" of leucosome (*e.g.*, Fig. 1-9a), some of which may be derived from anatectic melt and some of which (*e.g.*, K-feldspar) may be the solid products of the melting reaction (Waters & Whales 1988, Stüwe & Powell 1989, Powell & Downes 1990, Waters 2001, White *et al*. 2004). Many neosomes in patch metatexite migmatites have bulk chemical compositions that are similar to that of their host rocks (or protolith) and thus can be interpreted to have formed *in situ* in a closed system. However, some patches of segregated neosome have bulk compositions that are enriched in residual material; these are *in situ* neosomes that formed in an open system and have lost some of their melt fraction. Typically the melt fraction moved just a short distance and collected to form in-source leucosomes nearby and which are distinguished by the paucity of associated residual material (*e.g.*, Sawyer *et al.* 1999).

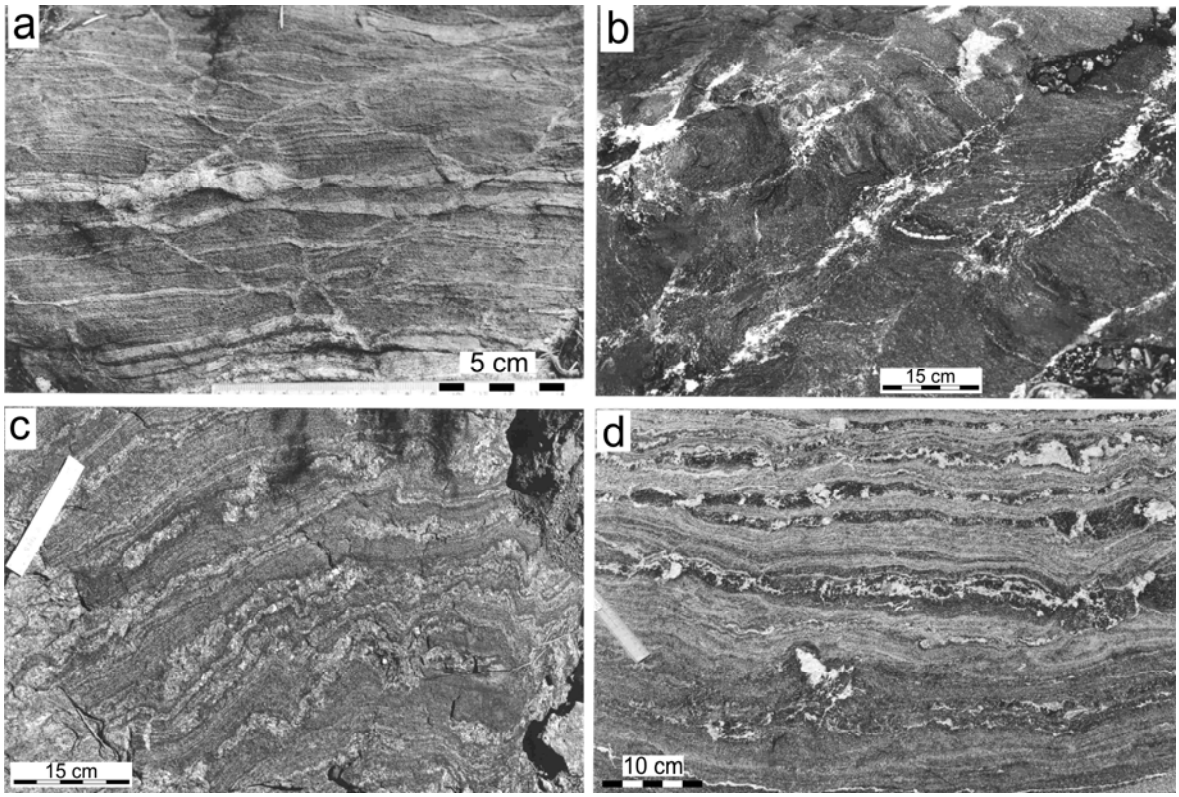

FIG. 1-10. Examples of net-structured and stromatic metatexite migmatites. **a)** Incipient net-structured metatexite migmatite in the contact aureole of the Duluth Igneous Complex. The net-like pattern results from one set of leucosomes oriented parallel to the bedding (*i.e.*, stromatic leucosomes) and two sets of leucosomes that occupy extensional shears oriented at about 45° to the bedding, that together enclose polygonal-shaped blocks of semipelitic paleosome. **b)** Incipient net-structured metatexite migmatite from a regional metamorphic terrain. The net-like pattern arises from a set of thin leucosomes parallel to the foliation in the metamafic paleosome, and a second, much more prominent set, that occur along small shear planes oriented at approximately 70° to the foliation. Coarse-grained clinopyroxene + hornblende + garnet melanosome is associated with the second set of leucosomes, hence, they are interpreted to be *in situ* or in-source leucosomes. **c)** The stromatic morphology in this migmatite is created by multiple injections of melt subparallel to the foliation and the transposed bedding in granulite-facies semipelitic rocks. The stromata generally do not have mafic selvedges, thus the injected melt may have been in equilibrium with its host. Thus, the melt from which the stromatic leucosomes crystallized may have been generated from similar rocks nearby, and the stromata may be viewed as in-source leucosome, or as leucocratic veins. **d)** The stromatic morphology of this migmatite was inherited from its protolith which acquired a strong banding as a result of non-coaxial strain. However, this tectonic layering has been considerably enhanced by later partial melting. The fertile layers produced, and lost, up to 36% melt and this resulted in the formation of prominent layers of competent, hornblende-rich melanosome that underwent boudinage and thus attracted some melt back to them. The less fertile, and the infertile layers in the migmatite are mesocratic; they are neosome and paleosome respectively.

Patch migmatites are generally preserved in the parts of migmatites where the strain was low, such as in competent lithologies, or in large-scale pressure shadows. Transposition of migmatites when they contained melt attenuates the patches of neosome (*e.g.*, Timmermann *et al*. 2002) into much higher aspect ratio shapes, and is one of the ways in which stromatic metatexite migmatites are formed (see below).

Dilation structure. When the melt fraction in a migmatite becomes mobile, typically as a result of deformation, it moves away from where it was formed and collects in the nearest stable, low-pressure sites (Sawyer 1994, Sawyer *et al*. 1999). The leucosomes mark the places where some, or all, of the melt crystallized in a migmatite. These places are either where the melt formed, the channels along which it moved through the migmatite, or the

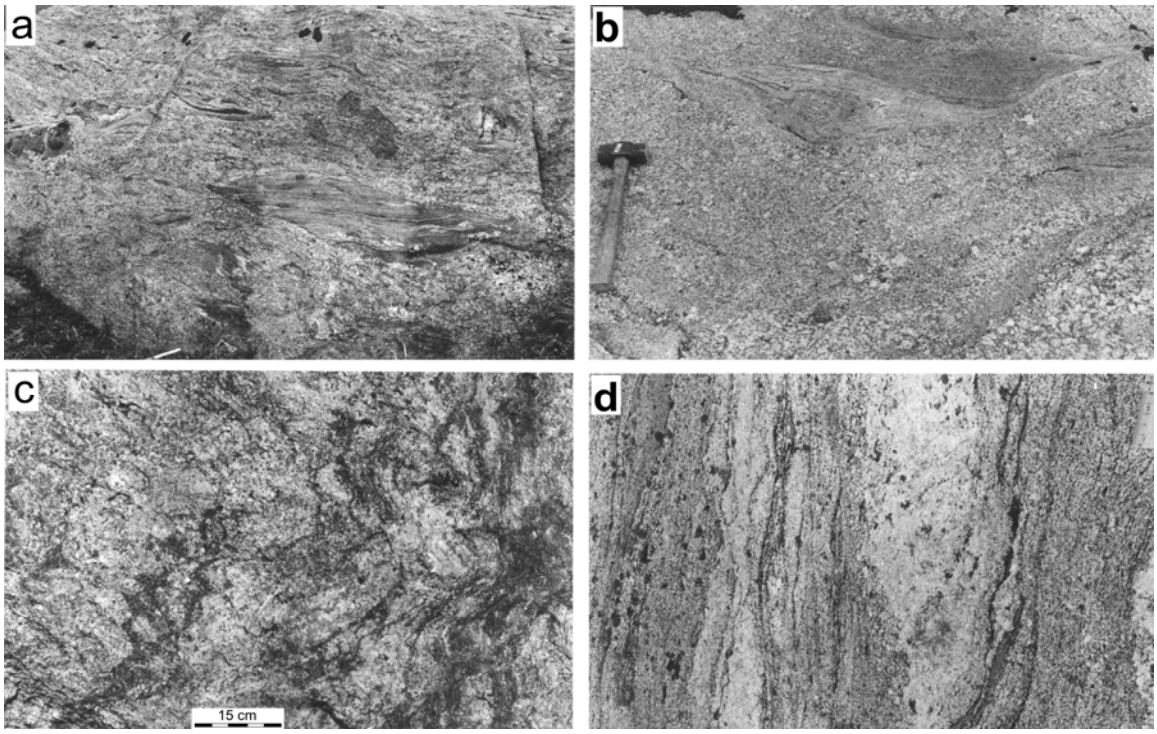

FIG. 1-11. The morphological varieties of diatexite migmatite. **a)** Schollen-structured diatexite migmatite from a psammitic and pelitic protolith. The coarse-grained, mesocratic neosome (plagioclase + quartz + K-feldspar + biotite + orthopyroxene) contains many oriented schollen. Most are of melt-depleted plagioclase + quartz + biotite + orthopyroxene psammite (*i.e.,* neosome), but a few are of vein quartz and, hence, are paleosome. Compositional banding attributed to flow in the mesocratic neosome can be seen in the upper part of the photograph. Photograph is 3.2 m wide. **b)** The protolith for this schollen-structured diatexite migmatite was leucotonalite. The schollen are rich in plagioclase, and were either derived from infertile rocks (paleosome), or the residuum (neosome) left after melting. The neosome enclosing the schollen displays some variation in microstructure and its bulk composition indicates that it was derived largely from anatectic melt that was redistributed within the migmatite, rather than introduced from an external source. **c)** This schlieren-structured diatexite migmatite had a pelitic protolith; the schlieren appear to be the melt-depleted remains of pelitic layers. The bulk composition indicates that a substantial amount of granitic melt has been introduced; therefore this is a secondary diatexite. Biotite in the schlieren may be the result of reaction between the introduced melt and residual cordierite or orthopyroxene in the relics of pelite. **d)** The individual schlieren in this schlieren-structured diatexite migmatite are thin, and are mostly composed of imbricate flakes of biotite. Thus, the schlieren may have formed by the impingement and aggregation of biotite crystals rotating in diatexite magma. The bulk composition of this diatexite migmatite (excluding the leucocratic vein) is very similar to its pelitic protolith, hence this migmatite formed in a closed system and is a primary diatexite. Photograph is 60 cm across.

places where the melt was able to collect (Sawyer 2001). Therefore, the distribution of leucosomes in a migmatite is, to a considerable extent, controlled by the distribution of the competent lithologies, because these determine where the incompatibilities of strain rate, that ultimately lead to dilatancy, will be in the rock. The term **dilation-structured** metatexite migmatite (*cf.* surreitic structure of Mehnert 1968) is used to describe a metatexite migmatite in which the distribution and geometry of the leucosomes is controlled principally by the dilatant structures that were present, such as the inter-boudin partitions, loci of shear failure (Fig. 1-9b), pressure shadows, dilated bedding planes in fold hinges (Fig. 1-9c), and extension fractures (Fig. 1-9d) or tension gashes.

Consider a sequence of metasedimentary rocks consisting mostly of fertile pelite but which contains a few layers of competent, infertile lithologies, such as quartzite or calc-silicate rocks. If boudinage begins in the sequence during partial melting, the melt generated in the pelite layers will migrate and collect in the inter-partition spaces as they grow in the competent layers, because these are the sites of low pressure in the migmatite. Thus, the distribution of the leucosome, and hence the

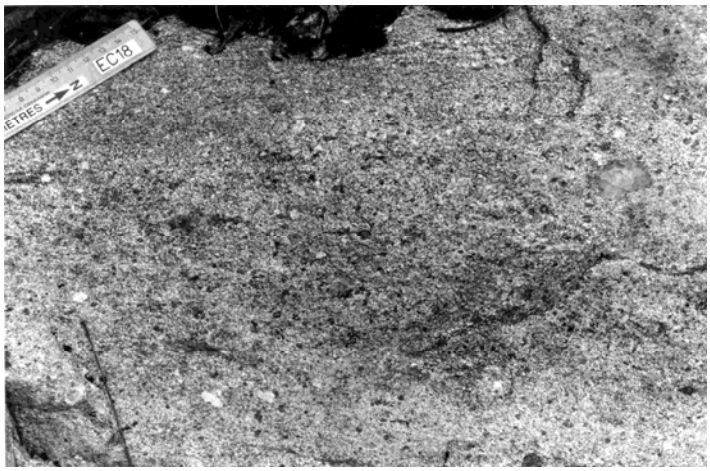

FIG. 1-12. Diatexite migmatites with a simple morphology are characteristic of the highest grade parts of many migmatite terrains where the proportion of neosome is very high. There are no prominent schlieren, schollen or compositional banding. Thus, no qualifying descriptive term needs be added to "diatexite". However, this diatexite migmatite has a strong magmatic foliation that is defined by the preferred orientation of tabular, and prismatic, crystals of cordierite, plagioclase, K-feldspar, biotite and, in places, sillimanite. The bulk composition of this migmatite is very similar to its pelitic protolith, hence, this is a primary diatexite.

morphology of the migmatite, depends on the competent layers. In addition to the distribution of the competent layers there are two other critical factors, the thickness of the competent layers and the total strain. At the start of boudinage, the boudins will not have separated far and consequently the leucosomes are thin and elongated at a high angle to the layering. The angle will depend on whether tensile failure or shear failure occurred in the layer. Generally, leucosomes that are hosted by the thin competent layers will be closer together than those in thicker layers. As strain accumulates the boudins move apart, the leucosome in the inter-partition space becomes progressively wider and eventually its long axis will be oriented parallel to the layering; this is more likely for the thinnest of the competent layers. Thus, both the original distribution of rocks and the subsequent deformation influence the morphology that the migmatite develops. If the fertile layers have an intrinsic anisotropy, such as a strong foliation, they may undergo an internal asymmetric boudinage induced by the incompatibility of strain rates across either the foliation planes, or other internal compositional boundaries. Melt in these layers will migrate into these dilatant asymmetrical structures. The leucosomes that form when the melt crystallizes may be regularly spaced, but they are typically oriented at a much shallower angle to the layering than the leucosomes in the nearby competent layers.

Layers may become progressively stronger as a migmatite forms if the melt fraction migrates from them, and results in an increase in the modal proportion of strong minerals such as garnet and pyroxene. Such residual layers may eventually become sufficiently strong that they fail and develop extensional fractures (see Fig. 1-9d), which then suck melt back into the residuum from adjacent rocks, or else provide a refuge for some of the last increments of melt produced by the residual layer itself.

The leucosome in dilational-structured metatexite migmatites may not be *in situ* because the melt it formed from has migrated into the site. Therefore, most are either in-source leucosomes, or else leucocratic veins.

Net structure. A net structure is developed where leucosomes (or neosome) occur in two, or more, systematically oriented sets that together create a net-like pattern which outline lozenge- or polygonal-shaped domains of darker rock that is either of paleosome, neosome that has melted less, or residuum. Net-structure (*cf.* diktyonitic structure of Mehnert 1968) is one of the most common morphological varieties displayed by metatexite migmatite. Sederholm (1907) considered their appearance to be another (with patch-structured neosome) indicator of partial melting in the foliated older granite at Hango. Net-structured metatexite migmatites (Fig. 1-10a) are the first macroscopic evidence that partial melting has occurred in the pelitic and semipelitic rocks of the contact aureole to the Duluth Igneous Complex (*e.g.*, the Linwood Lake area). Patches of neosome are developed in the slightly lower grade rocks farther from the contact, but the patches are so small (<2 mm across in rocks with a grain size of 0.1 mm) that they can only be reliably identified in thin section.

Typically, the net-like pattern is the result of the intersection of one set of leucosomes that is parallel to the compositional layering (*e.g.*, bedding) and a second set located in small shears or

shear band structures that formed during layer-parallel extension. In some cases the leucosomes are bordered by melanosome *(e.g.*, Fig. 1-10b), thus melt migrated by porous flow a short distance from where it formed to where it collected to make the leucosome (*e.g.*, McLellan 1988, Sawyer 1991, Brown 1994, Oliver *et al.* 1999). This scenario has been confirmed by the experiments on analog materials of Rosenberg & Handy (2000). They showed that the onset of partial melting causes deformation to be concentrated into narrow shear bands, and that further increments of melt move into these shear bands. Melt may migrate into, or out of, shear bands depending on whether they are lengthening or shortening (Mancktelow 2002), or if there is a change in the relative orientation of the principal stress direction and the shear band (Simakin & Talbot 2001a & b). Leucosomes in the highest grade net-structured metatexite migmatites are wider and they may be without borders of residual material (*e.g.*, Oliver & Barr 1997), suggesting that the structures received melt from much farther away.

Stromatic structure Metatexite migmatites that are characterized by numerous, thin parallel and laterally persistent neosome are said to have a stromatic, or layered, structure. In most cases the layered structure is due to stroma (the individual layers) of leucosome (Fig. 1-10c), but they could equally be layers of residual material or melanosome (see Fig. 1-10d), or unsegregated neosome. In most migmatites the stromata are sheet-like (longer than the outcrop), but in some migmatites they occur as high aspect ratio lenses that are tens of centimetres long. Stromatic-structured metatexite migmatites have been studied far more than the other types, principally because of the curious regularity of the spacing between the layers in some examples; four principal mechanisms have been proposed to account for this morphology.

1) Multiple injections of anatectic melt along adjacent, parallel planes of foliation, bedding (*lit-par-lit*) or any other weakness (*e.g.*, Fig. 1-10c). In this case the leucocratic layer cannot, of course, be *in situ* neosome or leucosome.
2) Short-range segregation of melt from its residuum. Thus, the resulting stromata consist of leucosome and its complementary residual material (Brown *et al.* 1995). The leucosomes in this scheme are either *in situ* or, perhaps, in-source.
3) Partial melting of the fertile layers in a sequence that consists of thin, alternating layers (beds) of different composition (*e.g.*, Johannes 1983, Gupta & Johannes 1986, Johannes *et al.* 1995). The neosome commonly segregates with the leucosome forming in the centre of the layer and biotite-rich melanosome at its margins. Because the neosome and its segregated parts are confined to a particular (fertile) layer or bed, they are *in situ*.
4) Park (1983) considered that the transposition of a migmatite while it contained melt could result in a strongly layered morphology. During deformation, neosomes (leucosome and residuum) that were initially equant in shape (*e.g.*, patch morphology) become attenuated into thin, high aspect ratio shapes and are simultaneously rotated into parallelism (*e.g.*, Timmermann *et al.* 2002). This type of transformation of the morphology of a migmatite is most commonly observed at the metre-scale in outcrops of metatexite migmatites that contain a mesoscopic ductile shear zone, however, much more extensive regions of stromatic migmatites occur in crustal-scale shear zones (Brown & Solar 1998a, 1998b, Solar & Brown 2001, Marchildon & Brown 2003).

It seems evident that a number of different mechanisms can produce a stromatic morphology in a metatexite migmatite. Some stromatic-structured migmatites form because their protolith was strongly layered. Others formed by the repeated injection of melt along parallel planes of weakness during anatexis, and still others are the result of a drastic modification of precursor morphology by intense deformation.

Terms appropriate to diatexite migmatites

As the fraction of melt increases in a metatexite migmatite the pre-anatectic structures in the migmatite are progressively destroyed as more neosome is created. However, new micro- and macrostructures are produced during anatexis and they become evident in the neosome. The precise morphology that is developed depends on whether or not deformation occurred and on the original distribution of the fertile rock types.

Nebulitic structure If there was essentially no deformation during partial melting, and consequently the melt fraction and residuum did not separate, the resulting migmatite consists of scattered ghost-like remnants of paleosome within a coarser-grained, diffuse mesocratic neosome; such a

morphology is called a nebulitic diatexite migmatite (or nebulite). Nebulitic diatexite migmatites occur in contact aureoles, but in regional migmatite terrains they tend to be restricted to areas of low syn-anatectic strain. Because these migmatites contain a fraction of melt well above the "melt connectivity threshold" defined by Rosenberg & Handy (2005), they are mechanically very weak. Consequently, they would readily undergo bulk flow if there was penetrative deformation and then the neosome would develop a foliation and a compositional banding.

Schollen structure The transition from a metatexite migmatite to a diatexite migmatite in the field is commonly characterized by an increase in the proportion of neosome and the progressive disruption of the more competent layers (typically paleosome and residuum) into tabular fragments called "schollen" (singular scholle) or "rafts" that become rotated into different orientations. Thus, deformation during partial melting is a significant factor in destroying the coherence of the old structures. Moreover, shear stresses drive the movement of the neosome and results in the formation of a magmatic (or sub-magmatic) foliation and compositional banding in the diatexite magma as it flows. In many migmatite terrains the first diatexite migmatites are characterized by the presence of many tabular pieces of paleosome and residuum-rich neosome that have moderate to high aspect ratios; migmatites with such a morphology are called **schollen-structured** (or raft-structured) diatexite migmatites (see Fig. 1-11a). Schollen become progressively fewer and smaller away from the transition from metatexite migmatites (*i.e.*, to higher grade in the migmatite terrain). Schollen of less competent lithologies are commonly attenuated into elongate, lenticular shapes as can be seen in Figure 1-11b. The last-remaining schollen generally consist of the most competent of the local resister lithologies, *e.g.*, calc-silicate rocks and pieces of quartz vein that, commonly, have highly rounded shapes, an effect attributed to erosion of the scholle in the moving diatexite magma.

Schlieren structure A compositional banding commonly develops in diatexite migmatites concomitant with the reduction in the number and size of schollen. Typically the compositional banding, which contains imbricated tabular crystals, is deflected around schollen and may be perturbed into tight asymmetric flow folds. These features all suggest that the banding was attenuated and deformed with the diatexite magma as it flowed. Felsic bands in the neosome are typically a few centimetres wide and each has a slightly different modal composition or microstructure. Thin bands rich in mafic minerals are also common, and the term "schliere" (plural schlieren) is given to a particular type which consists of thin (generally <10 cm) layers composed of oriented, platy or elongate minerals, most commonly biotite, but examples with plagioclase, sillimanite, orthopyroxene or amphibole are also known. The microstructure of a schliere commonly shows a marked imbricate arrangement of the tabular crystals, and this has been interpreted to indicate that the schliere formed by the impingement and aggregation of platy minerals that were freely rotating in a flowing magma (Milord & Sawyer 2003). However, in other migmatites the schlieren have microstructures that have been interpreted as evidence that they are the highly residual remains of fertile layers after the extraction of a very large fraction of melt (see Fig. 1-11c). Schlieren in general appear to contain a high concentration of accessory minerals, such as apatite and zircon, in addition to biotite, and consequently schlieren tend to have bulk compositions that resemble residual rocks in many aspects. However, the source of the minerals and how they were assembled to make schlieren remains in need of further, in-depth study. Diatexite migmatites in which schlieren are a significant component are called **schlieren-structured** (or schlieric) diatexite migmatites (*e.g.*, Fig. 1-11d).

The quintessential diatexite structure The proportion of schlieren and schollen decreases away from the transition from metatexite migmatites, and the result of this is to create diatexite migmatites that have a somewhat simpler appearance because they are essentially all neosome (see Fig. 1-12). These diatexite migmatites contain structures that formed during partial melting; typically a foliation defined by the orientation of tabular or platy minerals, most commonly plagioclase and biotite that was acquired during flow in a magmatic, or a submagmatic, state. Compositional banding may also be evident as variations in the microstructure or the modal proportions of the minerals but, generally, such variations in microstructure and rock type from place to place are subtle. The rather bland appearance of the diatexite migmatites in the highest grade parts of migmatite terrains led Mehnert (1968) and Solar & Brown (2001) to refer

to these as homogeneous diatexites. Although the variations in appearance may be subtle, particularly at the scale of an individual outcrop (say 100 m^2), there are, nevertheless, variations in bulk composition and microstructure that are of major petrological significance to the interpretation of the processes that occurred during the formation of these migmatites. For example, Sawyer (1998) was able to recognize melt-rich (up to nearly 100% melt) and residuum-rich parts within seemingly uniform diatexite migmatites in the Opatica Subprovince, and concluded that there was considerable movement of the melt fraction from place to place within the diatexite migmatites. Milord *et al*. (2001) were able to divide the uniform-looking diatexite migmatites in the St. Malo terrain into leucocratic, mesocratic and melanocratic diatexite, which they showed corresponded to melt-rich, unsegregated and residuum-rich rocks respectively. Mäkitie (2001) distinguished between different diatexite migmatites on the basis of a characteristic ferromagnesian mineral, biotite in one case and orthopyroxene in the other. As there is no distinctive morphology to these diatexite migmatites, there is no qualifying descriptive term, they can be considered as *the* quintessential **diatexite migmatites**. In some migmatite terrains these are the dominant form of diatexite migmatite.

Effect of deformation on the morphology of diatexite migmatites

High shear strains have been shown to generate a stronger preferred alignment of minerals in magmas (Ildefonse *et al*. 1992, 1997, Arbaret *et al*. 1996, 1997). Thus, the effect of higher shear strains on a diatexite magma is to produce a stronger magmatic foliation, a better alignment of schollen and better parallelism of flow banding, all of which results in a more strongly foliated or layered appearance to the schollen- and schlieren-structured diatexite migmatites, but it does not create a distinctive new morphology. The effect of high shear strains on the diatexite magmas that contain few schollen or schlieren is not very conspicuous, simply because they lack suitable macroscopic markers to record it.

Diatexite migmatites can contain a significant fraction of melt (generally >30%), and as they cool the melt fraction begins to crystallize. The first to crystallize is plagioclase (generally), then quartz and K-feldspar and lesser amounts of ferromagnesian minerals. The minerals that crystallize first are generally large, and subhedral to euhedral in form. After about 55% crystallization, there are sufficient crystals to create a loose-packed framework of crystals that touch at their corners; this framework can sustain weak stresses. Once the melt fraction is reduced to about 25% there are sufficient crystals that the framework is locked, it becomes rigid, and can support substantial stresses. If deformation occurs during crystallization of the diatexite, the loose packed structure of the framework is rearranged (*e.g.*, Vigneresse *et al*. 1996) to a more densely packed and stronger configuration in which many crystals touch along their faces and the volume of interstitial pore space is locally reduced. In effect deformation compacts the framework structure and this makes it stronger and, eventually, creates dilatancy in it. The excess melt, that is expelled as the pore space is reduced, migrates away to fill dilatant structures, most commonly fractures, that form in the rigid framework of early-formed crystals as it becomes more densely packed. Hence many diatexite migmatites contain arrays of felsic patches, veins and dykes that post-date the magmatic foliation and compositional flow banding; some of these have sharp contacts, but many have somewhat diffuse margins and this is evidence that the host had not yet solidified. The felsic patches, veins and dykes in diatexite migmatites are generally very leucocratic (K-feldspar + quartz + plagioclase) and have evolved bulk compositions that are consistent with derivation from the expelled interstitial melt.

Exactly the same process occurs in the parts of granite plutons that undergo deformation as they crystallize; the movement of fractionated melt from the interstitial pore space into fractures that form in the framework of crystals results in the formation of late-stage veins (*e.g.*, Cuney *et al*. 1990, Pons *et al*. 1995, John & Stunitz 1997, Sawyer 2000). Overall, therefore, the movement of melt into the low-pressure, dilatant sites that develop when a diatexite migmatite is deformed as it crystallizes is analogous to movement of melt from the pores to the space between the boudins in a dilation-structured metatexite migmatite. However, in the first the dilatancy becomes possible as the rigid framework grows by crystallization, and in the second it is possible because of the prior existence of strong (paleosome) lithologies.

OTHER MORPHOLOGIES OF MIGMATITE

Vein-structured and fold-structured migmatites are two morphologies that fall outside of the

first and second order divisions for descriptive terms used for migmatites. This is because both vein- and fold-structured morphologies can develop in either metatexite or diatexite migmatites.

Vein structure

Vein-structured migmatites contain one or more sets of leucocratic veins that are superimposed on a migmatite that has any one of the morphologies appropriate for metatexite or diatexite migmatites (*e.g.*, Fig. 1-7b). It could even be superimposed on a fold-structured migmatite. The veins are typically emplaced after the peak of anatexis, but before the migmatite had solidified. In diatexite migmatites for example, the emplacement of leucocratic veins commonly post-dates the formation of flow-related structures, such as foliation, schlieren and compositional banding and, hence, it is interpreted to have occurred during the late stages of crystallization when the framework of crystals had become sufficiently strong that it could fracture. The composition of the leucocratic veins in some vein-structured migmatites indicates that they crystallized from a fractionated anatectic melt derived from rocks similar in composition to their hosts, but that had formed at a slightly greater depth (Sawyer 1987, Sawyer & Barnes 1988). If the veins belong to a younger anatectic event, and were emplaced well after the migmatite had crystallized, then the term veined migmatite applies.

Fold structure

The term **fold-structured** migmatite applies if the folding occurred when the migmatite, either a metatexite or a diatexite migmatite, contained melt. The folds that develop in migmatites display a wide range of geometries that are determined by the relative competencies and thicknesses of the layers during folding and the mechanism (*i.e.*, passive folding, buckling or bending) by which the folds formed.

In metatexite migmatites that contain many competent layers, folds commonly develop by buckling and the strong layers tend to have parallel, or concentric, fold profiles. However, folds with similar profiles tend to develop when all the layers have approximately the same, low competence. Many studies from metatexite migmatite terrains have noted that there is generally far more leucosome present in the core regions of folds, especially the antiformal cores, than on the flanks (Allibone & Norris 1992, Collins & Sawyer 1996). These observations suggest that melt migrates from the fold limbs and collects in the cores as the folds grow and progressively tighten, an interpretation that has been confirmed by analog models (*e.g.*, Barraud *et al*. 2004). The melt that moves from the limbs and into the core region fills the various dilatant sites that develop there (see Fig. 1-9c) as the fold tightened. Thus the leucosomes in folds are commonly located:

1) between, and parallel to, bedding planes that have dilated in the fold hinges,
2) in arrays of planar structures that are oriented parallel to the axial surface of the fold,
3) in arrays of radially oriented tensile fractures formed in the most competent of the folded layers (generally a resister lithology) and,
4) in variously oriented shears within the fold that are commonly related to shortening of strong layers in the hinge region, and where the layers were extended on the fold limbs.

Why melt should collect in planes that are oriented parallel to the axial surface of a fold has long interested structural geologists, and Brown & Rushmer (1997) and Vernon & Paterson (2001) have discussed this problem.

The folds in diatexite migmatites commonly develop as a result of flow instabilities, *i.e.*, they are passive flow folds, and may be quite different in appearance to those that form in metatexite migmatites. Disharmonic or convoluted styles with many discontinuities (ductile shears) parallel to the compositional layering are common. Although the local geometry of the folds is commonly non-planar and non-cylindrical, the orientation of structures generally remains consistent.

If folding occurred after the migmatite had already fully crystallized, then the term folded migmatite applies.

THE IMPORTANCE OF A CONSISTENT SCALE FOR OBSERVATION

The term **layer-confined** migmatite describes a migmatite in which partial melting has occurred only in certain layers or beds, *i.e.*, the fertile ones; the term is developed from "bedded migmatite" introduced by Greenfield *et al.* (1996) to describe migmatites in which partial melting has affected the pelitic layers, but not the adjacent psammitic ones. This concept is not new, and the migmatites described by Gupta & Johannes (1982, 1986) and Johannes (1983) are equivalent. The published accounts of layer-confined migmatites describe a wide range of morphologies in the layers (or beds) that have partially melted. Neosome types range in

morphology from patch, dilation-structured, net-structured to stromatic-structured. Some of the fertile layers have been converted entirely to neosome so that all traces of pre-anatectic structure in the layer have been lost, and thus could be said to have diatexite morphology. However, this is not the best way to consider these migmatites. Scale was mentioned earlier in this chapter as a critical factor in the study of migmatites. Because migmatites are complex and heterogeneous rocks they must be viewed at a sufficiently large scale to be representative of the whole migmatite. Moreover, to use a nomenclature or classification scheme consistently, all the migmatites must treated in the same way; in this case that means viewed at the same length scale. Since the overall orientation and geometry of the pre-anatectic bedding and other structures can be traced out very well by using the intervening infertile paleosome layers, layer-confined migmatites are, in fact, just a small sample of a much larger migmatite that is clearly a metatexite migmatite. Viewed in this context the descriptive terms "layer-confined" or "bedded migmatite" arise simply because the emphasis has been placed on too-small-a scale (*i.e.*, the bed scale). In other words, the term "layer-confined" or "bedded migmatite" refers to a scale of observation that is inconsistent (too small) with that implicit in application of the first- and second-order morphological terms outlined above. This is why I have excluded layer-confined (and "bedded migmatite") from the terms used to describe the first order and second order morphology of migmatites.

CONCLUSION

Migmatites are found in metamorphic terrains where partial melting has occurred. Thus, the deciding factor in whether, or not, a rock is a migmatite, is evidence that some part of it must have partially melted. Not all the parts of a migmatite contain evidence for partial melting. Some parts (the paleosome) may not have melted at all, and other parts (the leucosome) may have crystallized from the melt fraction that has segregated.

The constituent parts of a migmatite, *i.e.*, the paleosome and neosome (which is further divided into residuum and leucosome) are arranged in an often-bewildering array of configurations, that gives migmatites their typically complex appearance. The factors which contribute to this complexity include the type, range and disposition of lithologies in the protolith of the migmatite, the temperature at which partial melting occurred, how fast the migmatites cooled, and whether or not deformation occurred during partial melting. Despite this, there are just two first-order morphological types of migmatite; metatexite migmatites, in which structures that existed before partial melting remain coherent and mappable, and diatexite migmatites in which the structures that existed before partial melting have been destroyed and replaced by new ones that formed during partial melting and as the migmatite crystallized. This first-order division reflects how pervasive the anatectic melt was in the migmatite, metatexite migmatites contained a lower fraction of melt than diatexite migmatites. However, how the melt was segregated also influences the morphology, and this is generally determined by the differential stresses that existed in the migmatite.

A second-order of morphological terms applies to both metatexite and diatexite migmatites. The terms applicable to metatexite migmatites are based principally on how the neosome is distributed, and so reflect the nature of the protolith, and how the migmatite responded to deformation. Diatexite migmatites also show considerable variation in their morphology, but the second-order terms that describe these, are based on the remnants of the paleosome and residuum left in the neosome.

The heterogeneous nature of virtually all migmatites means that the scale at which observations are made is an important consideration when describing migmatites. Rarely are small outcrops representative of a migmatite as a whole, and this is particularly the case for metatexite migmatites.

ACKNOWLEDGEMENTS

Over the past several years my thoughts on the nomenclature and mapping of migmatites have benefited greatly from discussions with many people, and in particular I would like to thank Mike Brown, Richard White, Pierre Barbey, Bernard Bonin, Robert Martin and Isabelle Milord. I also thank Richard Cox for his comments on the present version.

REFERENCES

ALLIBONE, A.H. & NORRIS, R.J. (1992): Segregation of leucogranite microplutons during synanatectic deformation: an example from the Taylor Valley, Antarctica. *J. Metamorphic Geol.* **10**, 589-600.

ARBARET, L., DIOT, H. & BOUCHEZ, J.-L. (1996): Shape fabrics of particles in low concentration suspensions: 2D analog experiments and application to tiling in magma. *J. Struct. Geol.* **18**, 941-950.

ARBARET, L., DIOT, H., BOUCHEZ, J.-L., LESPINASSE, P. & de SAINT-BLANQUAT, M. (1997): Analogue 3D simple shear experiments of magmatic biotite subfabrics. In *Granite: From Segregation of Melt to Emplacement Fabric*, Bouchez, J.-L., Hutton, D. H. W. & Stephens, W. E. (editors), pp. 129-143. Kluwer Academic Publisher, Dordrecht.

ARZI, A.A. (1978): Critical phenomena in the rheology of partially melted rocks. *Tectonophysics* **44** 173-184.

ASHWORTH, J.R. (1985): Introduction. In *Migmatites*, Ashworth, J.R. (editor), pp 1-35. Blackie, Glasgow.

BARRAUD, J., GARDIEN, V., ALLEMAND, P. & GRANDJEAN, P. (2004): Analogue models of melt-flow networks in folding migmatites. *J. Struct. Geol.* **26**, 307-324.

BOWEN, N.L. (1915): Crystallization-differentiation in silicate liquids. *Am. J. Sci.* **39,** 175-191.

BOWEN, N.L. (1928): *The Evolution of the Igneous Rocks*. Princeton University Press, New Jersey, 334 pp.

BROWN, M. (1994): The generation, segregation, ascent and emplacement of granitic magma: the migmatite-to-crustally-derived granite connection in thickened orogens. *Earth Sci. Rev.* **36**, 83-130.

BROWN, M. & RUSHMER, T. (1997): The role of deformation in the movement of granitic melt; views from the laboratory and the field. In *Deformation-enhanced Fluid Transport in the Earth's Crust and Mantle*. Holness, M.B. (editor), pp. 111-144. The Mineralogical Society Series **8**, Chapman and Hall, London.

BROWN, M. & SOLAR, G.S. (1998a): Shear-zone systems and melts: feedback relations and self-organisation in orogenic belts. *J. Struct. Geol.* **20**, 211-227.

BROWN, M. & SOLAR, G.S. (1998b): Granite ascent and emplacement during contractional deformation in convergent orogens. *J. Struct. Geol.* **20**, 1365-1393.

BROWN, M., AVERKIN, Y.A., MCLELLAN, E.L. & SAWYER, E.W. (1995): Melt segregation in migmatites. *J. Geophys. Res.* **100**, 15, 655-679.

CESARE, B. (2008): Crustal melting: Working with enclaves. *In* Working with Migmatites (E.W. Sawyer & M. Brown, eds.). *Mineral. Assoc. Canada, Short Course* **38**, x-x.

COLLINS, W.J. & SAWYER, E.W. (1996): Pervasive granitoid magma transfer through the lower-middle crust during non-coaxial compressional deformation. *J. Metamorphic Geol.* **14**, 565-579.

CUNEY, M., FRIEDRICH, M., BLUMENFELD, P., BOURGUIGNON, A., BOIRON, M.C., VIGNERESSE, J.-L., & POTY, B. (1990): Metallogenesis in the French part of the Variscan orogen. Part 1: U preconcentrations in the pre-Variscan and Variscan formations – a comparison with Sn, W and Au. *Tectonophysics* **177**, 39-57.

GRANT, J.A. & FROST, B.R. (1990); Contact metamorphism and partial melting of pelitic rocks in the aureole of the Laramie Anorthositic Complex, Morton Pass, Wyoming. *Am. J. Sci.* **290,** 425-472.

GREENFIELD, J.E., CLARKE, G.L., BLAND, M. & CLARKE, D.L. (1996): *In situ* migmatite and hybrid diatexite at Mt. Stafford, central Australia. *J. Metamorphic Geol.* **14**, 413-426.

GUERNINA, S. & SAWYER, E.W. (2003): Large-scale melt-depletion in granulite terranes: an example from the Archaean Ashuanipi subprovince of Quebec, *J. Metamorphic Geol.* **21**, 181-201.

GUPTA, L.N. & JOHANNES, W. (1982): Petrogenesis of a stromatic migmatite (Neulag, southern Norway). *Journal of Petrology* **23**, 548-567.

GUPTA, L.N. & JOHANNES, W. (1986): Genetic model for the stromatic migmatites of the Rantasalmi-Sulkava area, Finland. *J. Petrol.* **27**, 521-539.

HENKES, L. & JOHANNES, W. (1981): The petrology of a migmatite (Arvika, Värmland, western Sweden). *Neues Jahrb. Mineral. Abhand.* **141**, 113-133.

HOBSON, A., BUSSY, F. & HERNANDEZ, J. (1998): Shallow-level migmatization of gabbros in a metamorphic contact aureole, Fuerteventura Basal Complex, Canary Islands, *J. Petrol.* **39**, 1025-1037.

HOLMQUIST, P.J. (1916): Swedish Archaean structures and their meaning. *Bull. Geol. Inst. Uppsala* **15,** 125-148.

HOLNESS, M. (2008): Decoding migmatite microstructures. *In* Working with Migmatites

(E.W. Sawyer & M. Brown, eds.). *Mineral. Assoc. Canada, Short Course* **38**, 57-76.

HOLNESS, M. & CLEMENS, J.D. (1999): Partial melting of the Appin quartzite driven by fracture-controlled H_2O infiltration in the aureole of the Ballachulish Igneous Complex, Scottish Highlands. *Contrib. Mineral. Petrol.* **136**, 154-168.

HOLNESS, M.B. & WATT, G.R. (2002): The aureole of the Traigh Bhàn na Sgùrra sill, Isle of Mull: reaction driven microcracking during pyrometamorphism. *J. Petrol.* **43**, 511-534.

ILDEFONSE, B., LAUNEAU, P., BOUCHEZ, J.L. & FERNANDEZ, A. (1992): Effect of mechanical interactions on the development of shape preferred orientations: A two dimensional experimental approach. *J. Struct. Geol.* **14**, 73-83.

ILDEFONSE, B., ARBARET, L., & DIOT, H. (1997): Rigid particles in simple shear flow: is their preferred orientation periodic or steady state? In *Granite: from segregation of melt to emplacement fabrics*, Bouchez, J.-L., Hutton, D. H. W. & Stephens, W. E. (editors), pp. 177-185. Klüwer Dordrecht.

JOHANNES, W. (1983): On the origin of layered migmatites. In *Migmatites, Melting and Metamorphism*, Atherton, M.P. & Gribble, C.D. (editors), pp 234-248. Shiva, Nantwich.

JOHANNES, W., HOLTZ, F. & MÖLLER, P. (1995): REE distribution in some layered migmatites: constraints on their petrogenesis. *Lithos* **35**, 139-152.

JOHN, B.E. & STUNITZ, H. (1997): Magmatic fracturing and small-scale melt segregation during pluton emplacement: evidence from the Adamello Massif (Italy). In *Granite: From Segregation of Melt to Emplacement Fabrics*, Bouchez, J.-L., Hutton, D. H. W. & Stephens, W. E. (editors), pp. 55-74. Klüwer, Dordrecht.

KENAH, C. & HOLLISTER, L.S. (1983); Anatexis in the Central Gneiss Complex, British Columbia. In *Migmatites, Melting and Metamorphism*, Atherton, M.P. & Gribble, C.D. (editors), pp 142-162. Shiva, Nantwich.

LEJEUNE, A.-M. & RICHET, P. (1995): Rheology of crystal-bearing silicate melts: an experimental study at high viscosities. *J. Geophys. Res.* **100**, 4215-4229.

MÄKITIE, H. (2001): Eastern margin of the Vaasa Migmatite Complex, Kauhava, western Finland: preliminary petrography and geochemistry of the diatexites. *Bull. Geol. Soc. Finland* **73**, 35-46.

MANCKTELOW, N.S. (2002): Finite-element modelling of shear zone development in viscoelastic materials and its implication for the localisation of partial melting. *J. Struct. Geol.* **24**, 1045-1053.

MARCHILDON, N. & BROWN, M. (2003): Spatial distribution of melt-bearing structures in anatectic rocks from southern Brittany, France: implications for melt transfer at grain- to orogen-scale. *Tectonophysics* **364**, 215-235.

MCLELLAN, E.L. (1988): Migmatite structures in the Central Gneiss Complex, Boca De Quadra, Alaska. *J. Metamorphic Geol.* **6**, 517-542.

MEHNERT, K.R. (1968): *Migmatites and the origin of granitic rocks. Developments in Petrology* **1.** Elsevier, Amsterdam. 393 pp.

MILORD, I., & SAWYER, E.W. (2003): Schlieren formation in diatexite migmatite: examples from the St. Malo migmatite terrane, France. *J. Metamorphic Geol.* **21**, 341-362.

MILORD, I., SAWYER, E.W. & BROWN, M. (2001): Formation of diatexite migmatite and granite magma during anatexis of semi-pelitic metasedimentary rocks: an example from St. Malo, France. *J. Petrol.* **42**, 487-505.

OLIVER, N.H.S. & BARR, T.D. (1997): The geometry and evolution of magma pathways through migmatites of the Halls Creek Orogen, Western Australia. *Mineral. Mag.* **61,** 3-14.

OLIVER, N.H.S., BODORKOS, S, NEMCHIN, A.A., KINNY, P.D. & WATT, G.R. (1999): Relationships between zircon U-Pb SHRIMP ages and leucosome type in migmatites of the Halls Creek Orogen, Western Australia. *J. Petrol.* **40**. 1553-1575.

OLSEN, S.N. (1985): Mass balance in migmatites. In *Migmatites*, Ashworth, J.R. (editor), pp 145-179. Blackie, Glasgow.

PARK, A.K. (1983): Lit-par-lit migmatite fabrics in a metagabbro-anorthosite complex, Sygnefjell, Jotunheim, south Norway. In *Migmatites, Melting and Metamorphism*, Atherton, M.P. & Gribble, C.D. (editors), p 296. Shiva, Nantwich.

PONS, J., BARBEY, P., DUPUIS, D. & LEGER, J.M. (1995): Mechanisms of pluton emplacement and structural evolution of 2.1 Ga juvenile continental crust: the Birimian of southwestern Niger. *Precamb. Res.* **70**, 281-301.

POWELL, R. & DOWNES, J. (1990): Garnet porphyroblast-bearing leucosomes in metapelites: mechanisms, phase diagrams and an example from Broken Hill, Australia. In *High Temperature Metamorphism and Crustal Anatexis*, Ashworth, J.R & Brown, M. (editors) pp.105-123. Mineralogical Society Series **2**, Unwin Hyman, London.

READ, H. H. (1957): *The Granite Controversy*. London, Thomas Murby & Co. 430 pp.

RENNER, J., EVANS, B. & HIRTH, G. (2000): On the rheologically critical melt fraction. *Earth Planet. Sci. Lett.* **181**, 585-594.

ROBIN, P-Y.F. (1978): Pressure solution at grain-to-grain contacts. *Geochim. Cosmochim. Acta* **42**, 1383-1389.

ROSENBERG, C.L. & HANDY, M.R. (2000): Syntectonic melt pathways during simple shearing of a partially molten rock analogue (norcamphor-benzamide). *J. Geophys. Res.* **105**, 3135-3149.

ROSENBERG, C.L. & HANDY, M.R. (2005): Experimental deformation of partially melted granite revisited: implications for the continental crust. *J. Metamorphic Geol.* **23**, 19-28.

SAWYER, E.W. (1987): The role of partial melting and fractional crystallization in determining discordant migmatite leucosome compositions. *J. Petrol.* **28**, 445-73.

SAWYER, E.W. (1991): Disequilibrium melting and the rate of melt-residuum separation during migmatization of mafic rocks from the Grenville Front. *J. Petrol.* **32**, 701-738.

SAWYER, E.W. (1994): Melt segregation in the continental crust. *Geology* **22**, 1019-1022.

SAWYER, E.W. (1998): Formation and evolution of granite magmas during crustal reworking: the significance of diatexites. *J. Petrol.* **39**, 1147-1167.

SAWYER, E.W. (1999): Criteria for the recognition of partial melting. *Phys. Chem. Earth (A)* **24**, 269-279.

SAWYER, E.W. (2000): Grain-scale and outcrop-scale distribution and movement of melt in a crystallizing granite. *Trans. R. Soc. Edinburgh: Earth Sci.* **91**, 73-85.

SAWYER, E.W. (2001): Melt segregation in the continental crust: distribution and movement of melt in anatectic rocks. *J. Metamorphic Geol.* **19**, 291-309.

SAWYER, E.W. & BARNES, S.-J. (1988): Temporal and compositional differences between solidus and anatectic migmatite leucosomes from the Quetico metasedimentary belt Canada. *J. Metamorphic Geol.* **6**, 437-450.

SAWYER, E.W., DOMBROWSKI, C. & COLLINS, W.J. (1999): Movement of melt during synchronous regional deformation and granulite-facies anatexis, an example from the Wuluma Hills, central Australia. In *Understanding Granites; integrating New and Classical Techniques*, Castro, A., Fernández, C. & Vigneresse, J.-L. (editors), pp. 221-237. *Geological Society of London Special Publication*, **158**, London.

SEDERHOLM, J.J. (1907): Om granit och gneis, deras uppkomst, uppträdande och utbredning inom urberget i Fennoskandia. *Bull. Commission géologique de Finlande* **23**, 110pp.

SEDERHOLM, J.J. (1923): On migmatites and associated Precambrian rocks of southwestern Finland I: The Pellinge region. *Bull. Commission géologique de Finlande* **58**, 158 pp.

SEDERHOLM, J.J. (1926): On migmatites and associated Precambrian rocks of southwestern Finland II: The region around the Barösundsfjärd west of Helsingfors and neighbouring areas. *Bull. Commission géologique de Finlande* **77**, 143 pp.

SHAW, D.M. (1954): Trace elements in pelitic rocks. *Geol. Soc. Am., Bull.* **65**, 1151-1182.

SHAW, D.M. (1956): Geochemistry of pelitic rocks Part III: major elements and general geochemistry. *Geol. Soc. Am., Bull.* **67**, 919-934.

SIMAKIN, A. & TALBOT, C. (2001a): Tectonic pumping of pervasive granitic melts. *Tectonophysics* **332**, 387-402.

SIMAKIN, A. & TALBOT, C. (2001b): Transfer of melt between microscopic pores and macroscopic veins in migmatites. *Phys. Chem. Earth* **26**, 363-367.

SLAGSTAD, T., JAMIESON, R.A. & CULSHAW, N.G. (2005): Formation, crystallization and migration of melt in the mid-orogenic crust: Muskoka domain migmatites, Grenville Province, Ontario. *J. Petrol.* **46**, 893-919.

SOLAR, G.S. & BROWN, M. (2001): Petrogenesis of migmatites in Maine, USA: possible source of peraluminous leucogranite in plutons? *J. Petrol.* **42**, 789-823.

STÜWE, K. & POWELL, R. (1989): Metamorphic segregations associated with garnet and

orthopyroxene porphyroblast growth: two examples from the Larsemann Hills, East Antartica. *Contrib. Mineral. Petrol.* **103**, 523-530.

TIMMERMANN, H., JAMIESON, R.A., PARRISH, R.R. & CULSHAW, N.G. (2002): Coeval migmatites and granulites, Muskoka domain, southwestern Grenville Province, Ontario. *Can. J. Earth Sci.* **39**, 239-258.

VERNON, R.H. & PATERSON, S.R. (2001): Axial-surface leucosomes in anatectic migmatites. *Tectonophysics* **335**, 183-192.

VIELZEUF, D. & HOLLOWAY, J.R. (1988): Experimental determination of the fluid-absent melting relations in the pelitic system: Consequences for crustal differentiation. *Contrib. Mineral. Petrol.* **98**, 257-276.

VIGNERESSE, J.-L., BARBEY, P. & CUNEY, M. (1996): Rheological transitions during partial melting and crystallization with application to felsic magma segregation and transfer. *J. Petrol.* **37**, 1579-1600.

WATERS, D.J. (1988): Partial melting and the formation of granulite facies assemblages in Namaqualand, South Africa. *J. Metamorphic Geol.* **6**, 387-404.

WATERS, D.J. (2001): The significance of prograde and retrograde quartz-bearing intergrowth microstructures in partially melted granulite-facies rocks. *Lithos* **56**, 97-110.

WATERS, D.J. & WHALES, C.J. (1984): Dehydration melting and the granulite transition in metapelites from southern Namaqualand, S. Africa. *Contrib. Mineral. Petrol.* **88**, 269-275.

WEBER, C. & BARBEY, P. (1986): The role of water, mixing processes and metamorphic fabric in the genesis of the Baume migmatites (Ardèche, France), *Contrib. Mineral. Petrol.* **92**, 481-491.

WHEELER, J. (1987): The significance of grain-scale stresses in the kinetics of metamorphism. *Contrib. Mineral. Petrol.* **97**, 397-404.

WHITE, R.W., POWELL, R. & HALPIN, J.A. (2004): Spatially-focussed melt formation in aluminous metapelites from Broken Hill, Australia. *J. Metamorphic Geol.* **22**, 825-845.

WHITE, R.W., POMEROY, N.E. & POWELL, R. (2005): An *in situ* metatexite-diatexite transition in upper amphibolite facies rocks from Broken Hill, Australia. *J. Metamorphic Geol.* **23**, 579-602.

CHAPTER 2: IDENTIFYING THE PARTS OF MIGMATITES IN THE FIELD

E.W. Sawyer
Department of Applied Science,
Université du Québec à Chicoutimi,
Chicoutimi, Quebec, G7H 2B1, Canada
ewsawyer@uqac.ca

INTRODUCTION

For some geologists migmatites are, for one reason or another, the specific interest of their research, but for most migmatites are just one of several rock types that happen to occur in the area they work in. Both groups need, nevertheless, to find a way to represent the migmatites on a map in such a way that accurately portrays what is in the outcrop and conveys the information necessary for interpreting the geological history of the map area, and perhaps beyond. This chapter addresses some of the problems related to identifying the constituent parts of partially melted rocks in the field, whether in a regional (upper amphibolite and granulite facies) or in a contact metamorphic setting. The connection between tectonics, or structure, and the appearance of migmatites in the field are discussed by Solar (2008: Chapter 7).

Much of the work that has been done on migmatites in the past has been petrological. Common themes have been the conditions at which migmatites form, the composition of the minerals and anatectic melt(s) in migmatites, determining how much partial melting has occurred and by which mechanism, and the identification of the numerous processes (*e.g.*, segregation, crystallization, magma flow, *etc.*) that may occur during anatexis. The wider petrological problem of how migmatites are connected to the formation of granite is also a perennial theme (Brown 1994, Brown & Rushmer 1997, Sawyer 1998, Solar & Brown 2001), and is one that goes beyond just migmatites, since it is also at the core of the major petrological problem of how the continental crust came to be differentiated. Studies that encompass both structural (used here in the tectonic, as opposed to morphological, sense) and petrological aspects in migmatites have largely been concerned with segregation of the melt fraction (Oliver & Barr 1997, Sawyer 2001, Marchildon & Brown 2003), or the connection between major shear zones and the movement of granitic magmas through the crust (Brown & Solar 1998, Solar & Brown 2001, Brown 2008).

A new perspective on the significance of migmatites has emerged following theoretical studies on the effect that weak layers in the crust have in controlling the development of orogens and plateaus (*e.g.*, Block & Royden 1990, Royden 1996, Clark & Royden 2000, McQuarrie & Chase 2000). The presence of even a small amount of melt (fraction of melt M_f <0.07) in rocks has been shown to reduce their strength greatly (Rosenberg & Handy 2005), thus migmatites are viewed as the most likely candidates for weak layers, or zones, in the middle and deep levels of active orogens. Thermal-mechanical models of orogens (*e.g.*, Beaumont *et al.* 2004) produce regions in the middle and lower crust in which the flow of material carries the isotherms in the direction of both the pro- and retro-wedges. Erosion of the surface of the orogen focuses and facilitates a more rapid movement of the material through the orogen. After a certain period of contraction the temperature in the orogen surpasses that of the solidus, and partial melting occurs. During subsequent contraction the development of the orogen is very strongly controlled by the outward flow of hot, weak, partially melted rocks in the middle and lower crust in what are called "channel flows". Consequently, interest in the role that migmatites may have in geodynamics is growing rapidly. New research into the geometry, kinematics and timing of channel flows in deeply eroded ancient orogens adds tectonics, structure (*e.g.*, Vanderhaeghe *et al*. 1999, Vanderhaeghe & Teyssier 2001, Williams & Jiang 2005, Brown & Gibson 2006), deformation processes, rheology (Závada *et al*. 2007) and geochronology (Hinchey *et al*. 2006) to the more traditional subjects of research in migmatites. This widening range of interests in migmatites means that mapping of them should cover features of use to both the petrologists and geodynamicists (see Solar 2008).

Mineralogical Association of Canada Short Course 38, Quebec City, Quebec, p. 29–36

THE BASIC UNITS

Field work is principally the examination of the centimetre- to metre-scale details in rocks, even if the final objective is to produce an orogen-scale map. The small scale reveals the details in petrography, petrology, structure, morphology and the temporal relationships between the constituent parts of a migmatite, or between a migmatite and its adjacent rocks, that provide the information necessary to understand the larger scale. Maps at the outcrop-, or smaller scales, are made to illustrate specific spatial relationships among the various parts of a migmatite, such as leucosome and residuum (Sawyer 2001), or between a specific part and some other feature, such as the structural sites in which the leucosome are located (Oliver & Barr 1997). Therefore, the most common map units at this scale are simply the parts of a migmatite; neosome, leucosome, residuum (or melanosome) and paleosome. The reader is referred to chapter 1 of this volume for full definitions of these terms, and others used in this chapter.

The main parts

Neosome is that part of a migmatite that has partially melted. The melt fraction and the solid fraction may not have separated, and such a neosome is termed unsegregated. Unsegregated neosome, such as at Mount Stafford in central Australia, indicates that partial melting occurred in the absence of deviatoric stresses (*i.e.*, in so-called static melting). Some diatexite migmatites (*e.g.*, in the Quetico Subprovince) also are examples of unsegregated neosome, but the flow structures they contain indicate the existence of shear stresses. In general, partial melting is accompanied by deviatoric stresses (*i.e.*, so-called dynamic melting) and these drive the separation of melt from its residual solids, thus in most migmatites the neosome has segregated into melt-rich and melt-poor parts. The part that was derived from the anatectic melt is called the leucosome, whereas the part derived from material from which some, or virtually all, of the melt fraction has been removed is called the residuum. Leucosome can be subdivided into *in-situ* leucosome, in-source leucosome and leucocratic veins depending upon how far the melt they have crystallized from moved. Melanosome is a particular kind of residuum; one that has a high proportion of dark coloured minerals and is, therefore, melanocratic. Paleosome is the part of a migmatite which did not partially melt because it had an inappropriate bulk composition. Not all the parts of a migmatite may be present in a small area or outcrop. Moreover, there may be more than one type of each in an outcrop. The degree of partial melting and the extent to which the melt and solid fractions separated is rarely the same from place to place in a migmatite; hence neosome typically displays a range of colours, mineral proportions and morphological complexity.

The correct identification of the parts of a migmatite is, of course, a prerequisite to any sampling or taking of measurements in a migmatite, whether for petrological, geochemical, structural or even dating purposes, because each part has formed in a different manner and thus records different information. Paleosome lithologies are generally competent and strain is, therefore, partitioned into the surrounding neosome. Consequently, paleosome preserves the oldest (*i.e.*, pre-anatectic) structures and microstructures in a migmatite because they have not been modified, or eradicated, by the combined effects of partial melting and high strain. Paleosome does not contain syn-anatectic structures or microstructures indicative of partial melting.

The parts derived from the anatectic melt, or from regions that contained a moderate fraction of melt (M_f greater than about 0.07) were the weakest parts of a migmatite and, therefore, experienced the highest syn-anatectic strain, because the strain was partitioned into them. Thus, they contain structures and microstructures (*e.g.*, magmatic foliation) that formed during flow of the melt, or magma, and its subsequent crystallization. Deformation of these parts of a migmatite after they have partially crystallized leads to the development of a framework of touching crystals and results in the separation of the remaining, fractionated melt into fractures that develop in the framework, or to other low pressure structures. Thus, the composition of leucosomes may not necessarily represent an anatectic melt; the majority of leucosomes in migmatites have, in fact, plagioclase-rich compositions and can be modeled as accumulates (Sawyer 1987, 2008) of early formed crystals.

The residuum parts of migmatites have some of the characteristics of both the paleosome and the leucosome. Residua formed by the episodic loss of melt, such that they never at any stage contained more than a few percent of melt (they were in effect drained systems), may still preserve pre-anatectic structures such as foliations and folds, and even delicate sedimentary structures (Waters & Whales 1984, Guernina & Sawyer 2003). Microstructures

that formed during partial melting or subsequent crystallization (Sawyer 2001, Holness 2008) are commonly preserved in the residual parts of migmatites. Many of the residual parts of migmatites contained a sufficiently large fraction of anatectic melt during some part of their history that they became weak, and underwent ductile deformation and subsequent recrystallization facilitated by the presence of the melt; these residual rocks may have partially or wholly lost their pre-anatectic structures and microstructures.

Analysis of the whole rock compositions in order to understand the processes that occurred in migmatites generally begins from a "starting point" composition and, ideally, includes examples of the end products of the processes considered. In the case of partial melting these are the initial composition of the rock, the melt and the residuum respectively. Thus, sampling for petrological or geochemical purposes also requires that the specific parts of a migmatite are correctly identified in the field. Residual rocks contain the solid products of incongruent melting reactions, plus the phases that were in excess to the melting reaction; thus they also are ideal samples for petrological studies of the melting reactions. Minerals that crystallized from the melt are a minor constituent of residual rocks, and may even be absent. The melt-rich parts of migmatites (leucosome and many diatexite migmatites) are, of course, dominated by the products of crystallization of the anatectic melt and may or may not contain residual or refractory material. However, a leucosome or diatexite need not record the composition of the initial anatectic melt; fractional crystallization can result in the accumulation of the early formed crystals and, hence, the development of a melt with an evolved composition. The only component of petrological or geochemical significance that generally is not readily retrievable from most migmatites is the protolith; this is unfortunate because knowledge of the initial composition of rocks is virtually essential. The protolith has to be found in the lower grade rocks that are the non-melted equivalents to the neosome in the migmatite (see Sawyer 2008: chapter 1, Figure 1-1), which is why it is important to map both sides of the "melt-in" isograd (see below). Unsegregated neosome contains both residual and melt components and could, if it formed in a closed system (*i.e.*, no melt has leaked from, or been added, to it), be the equivalent to protolith in terms of bulk composition.

Relative chronology in migmatites

Most mapping invariably involves the construction of a relative chronology in the rocks that are studied. In crystalline rocks this chronology is generally provided by intrusive relationships and the successive overprinting of older structural features, such as foliation planes and folds, by newer ones. Consequently, in many migmatite terrains a relative chronology is provided by the sequence of fold and foliation structures they contain, and the familiar D_1, D_2... notation of structural geologists is commonly applied; this approach works well in metatexite migmatites because markers that existed before anatexis (*i.e.*, bedding) still remain. For most practical purposes the paleosome and residuum parts of migmatites can be considered to be immobile and to have remained essentially *in situ*, and they generally form the layers that are used to define the folds or contain the structures from which a structural chronology can be established. The melt fraction in migmatites, however, is mobile because of its lower viscosity and density, thus it can move into the dilatant sites along bedding and foliation planes, in the axial surfaces of folds, in shear bands, between boudins and at the hinges of folds (*e.g.*, Collins & Sawyer 1996, Barraud *et al*. 2004), created by the successive episodes of deformation that produce the structures used to establish the relative chronology. Thus, the parts of a migmatite derived from the anatectic melt (*in situ* leucosomes, in-source leucosomes, leucocratic veins, diatexite migmatites and unsegregated neosomes) are commonly tied to the structural chronology by their position in the migmatite. This has led to the idea of "generations" of leucosome in migmatites. A common observation is that the earliest "generations" of leucosome have undergone boudinage whereas the later "generations" have not. Thus, the earliest "generation" of leucosome are interpreted to have been more competent and, therefore, to have been solid prior to the formation of the later "generations" of parallel-sided leucosome. Consequently, it has been proposed that in some terrains each successive "generation" of leucosome represents a separate anatectic event, M_1, M_2...*etc*. separated by periods of time when the temperature declined to below the solidus. This interpretation assumes that the only way a leucosome can become competent is if it is solid, *i.e.*, fully crystallized. This may not always be the case.

An interpretation for "generations" of leucosome

Numerical modeling of collision zones (*e.g.*, Beaumont *et al*. 2004) show that once suprasolidus temperatures have been reached, they are maintained for long periods of time in the middle and lower crust of orogens. This appears to be supported by dating from regional migmatite terrains which shows that metamorphic temperatures remained above the solidus for periods of time as long as 40 m.y. (*e.g.*, Zaleski *et al*. 1999, Rubatto *et al.* 2001). Furthermore, detailed petrographic studies of the contacts between the successive "generations" of leucosomes in some regional migmatites have failed to demonstrate cross-cutting relationships and truncations. The contacts are, in these cases, gradational, without abrupt changes in the mineral assemblage, proportions of minerals or grain size; there is, in fact, petrological continuity (*e.g.*, Marchildon & Brown 2003) between the successive leucosomes in the various structural sites. Consequently, it can be concluded that the leucosomes in the various structural sites all contained melt at the same time, and were in fact all part of a linked array. Lastly, the migmatites developed in short-lived (thousands of years) contact aureoles where anatexis was clearly related to a single anatectic event, also show successive "generations" of leucosome located in progressively younger structural sites as determined by the successive development and overprinting of structures. Thus, it appears unreasonable in some cases to equate each "generation" of leucosomes to a separate melting event with the temperature cycling back and forth across the solidus.

Partial melting in migmatites occurs as the temperature rises, *i.e.*, in the prograde part of the *P–T* history. If the local pressure gradients provide a sufficient driving force during the prograde stage, the anatectic melt in the migmatite moves first by porous flow from the grain boundaries where it formed and then by channel flow to nearby low-pressure dilatant sites where it collects. The segregation of melt at this stage involves the separation of melt from its solid residuum. The network of melt-filled channels remains filled with melt provided that no new dilatancy forms. However, if new pressure gradients and dilatant sites were to develop because of, for example, a change in the orientation and magnitude of the stresses (perhaps due to a new episode of folding), then the melt in the migmatite moves from the old sites to the newer, more stable ones. If the old sites are optimally oriented the melt in them could be completely removed, and the only evidence for their former existence would be the residuum left behind (Sawyer 2001).

Once the temperature starts to decline, anatectic melt is no longer generated and the melt in the migmatite begins to crystallize. Thus, if at some time after crystallization has begun there is a reorientation of the stresses (*i.e.*, a new deformation, the D_2 folding event, for example), new pressure gradients and dilatant sites are created. The fraction of melt in the migmatite responds and migrates toward to the new dilatant sites and collects there. However, the minerals that have already crystallized from the anatectic melt do not move, they remain in the previous network of channels and dilatant sinks and become the first "generation" of leucosome. The segregation of melt at this stage has created: 1) a low viscosity, crystal-free melt that has an evolved bulk composition that is located in the new channels and dilatant sites and, 2) a high-viscosity leucosome which consists of the early crystallization products (mostly plagioclase) and some trapped melt that is located in the old channels and dilatant sites. If, later, another change in the stresses (D_3) perturbs the pressure gradients and again creates new dilatant sites, then the cycle is repeated. The melt, now more evolved, moves to the new dilatant sites but leaves behind the minerals that crystallized from it to form the second "generation" of leucosomes in the migmatite. The crystal-rich material left in the earlier "generation" of dilatant structures will be deformed by the later deformation; it could become boudinaged or folded depending upon its orientation, and undergo a reduction in grain size.

The segregation process separates anatectic melt from the residuum when metamorphic temperatures are rising, but when temperature declines the cessation of melting and the onset of crystallization changes what is produced by the segregation process; it now separates the remaining anatectic melt from its crystallization products. The successive creation of new dilational sites and pressure gradients attracts the diminishing volume of melt that remains in the migmatite and creates the next "generation" of leucosome. The old "generation" of leucosomes is much more competent than the new because it is the aggregate of the early crystallization products that contained some trapped melt, whereas the new one is essentially all melt. Moreover, the old "generations" of leucosome become progressively more competent as the fraction of melt in them declines,

either by migrating away or by crystallization. Hence leucosomes formed in a single anatectic event can display a wide range of competencies and diverse locations in a migmatite. This mechanism also explains the common observation that the oldest "generations" of leucosomes are commonly rich in plagioclase (the mineral that crystallizes first) and that successive "generations" have progressively more evolved compositions that are rich in K-feldspar. Except at the onset of partial melting, the majority of leucosomes in a migmatite are not *in situ*; the leucosomes mark either the channels through which the melt migrated or the dilatant sites where it collected. Hence, in-source leucosomes and leucocratic veins predominate in most migmatites, and the residuum, which marks the place where the melt formed, is not directly attached to leucosome.

Although most leucosomes and arrays of leucosome in migmatites are better explained by the migration of melt driven by deformation as the melt crystallized, there are examples where some of the felsic melt produced in the early stages of an anatectic event was solid before the later leucosomes were formed. The St.-Malo migmatite terrain in Brittany locally contains fine-grained, layer-parallel felsic dykes that have been interpreted to be derived from anatectic melt that formed by water-present melting at the start of anatexis. This anatectic melt intruded into cool rocks outside the "melt-in" isograd, however, their host rocks later underwent partial melting as the isotherms advanced higher in the crust and passed the fine-grained and now competent dykes.

TERRAIN-SCALE MAPS

Terrain-scale maps would be expected to reveal the distribution of partially melted rocks and make some distinction that differentiates higher grade migmatites from lower grade ones, and show the differences in the structural style and geometry between migmatites and the lower grade rocks and between higher grade and lower grade migmatites.

The units used in mapping in high grade metamorphic terrains are commonly based on lithological or petrological characteristics. For migmatites these could be the first order division of migmatites (anatexites) into metatexite and diatexite. The lower temperature boundary of migmatites in the field is defined by the start of partial melting (the "melt-in" isograd). Since metatexite migmatites preserve the coherent layering and structures that existed prior to anatexis, the same units, formations or groups that were identified in the non-melted rocks should be traceable into the metatexite migmatites, at least close to the "melt-in" isograd. This is extremely important because it enables the neosome in the migmatite to be correlated with their equivalent rocks on the low temperature side of the "melt-in" isograd, and thus lead to the identification of protolith. Similarly, paleosome or resister lithologies should also be identified in the migmatite and correlated with the same rocks at lower grades. If paleosome layers remain coherent they provide a means of tracing the change in the geometry of structures across the "melt-in" isograd, through the metatexite migmatites and potentially into diatexite migmatites. Whether isograds are parallel or oblique to lithological contacts, or whether isograds cross or not, has long been of fundamental interest to metamorphic petrologists. The configuration of the "melt-in" and other isograds in migmatites should be shown on maps wherever possible, as they can provide information on the source of heat, the mechanism of heat transfer and whether or not an influx of aqueous fluid induced partial melting.

The change from metatexite to diatexite migmatite is easily recognized in the field. The change corresponds to the point where the fraction of melt in the migmatite has increased above a certain threshold value so that pre-anatectic structures are eliminated due to:

1) bulk flow, in which a thin film of melt develops on virtually all the grain boundaries (M_f >0.07) and the grains roll or slide past each other,
2) magma flow, in which the melt fraction increases such that that the contacts between solid grains retreat and the grains are able to rotate in the melt, or
3) in the absence of deformation that the fraction of melt becomes so high that the contacts between grains have retreated so far apart that old structures appear to have faded away (*i.e.*, a nebulitic diatexite).

In the majority of cases the transition from metatexite to diatexite is a function of temperature. However, in one case it has been shown (White *et al*. 2005) to correspond to an increase in the degree of partial melting caused by an influx of H_2O, and in another to an influx of felsic magma (Greenfield *et al*. 1996).

The coherence of the pre-anatectic structures that characterize metatexite migmatites is lost in diatexite migmatite. Therefore, the lithological units

that have been traced from non-melted rocks and into the metatexite migmatites are no longer traced in the diatexite migmatites. Although diatexite migmatites are easy to identify in the field, they are difficult to subdivide on a lithological basis. Some workers (*e.g.*, Mäkitie 2001) have distinguished between biotite diatexite and orthopyroxene diatexite. The systematic identification of the mineral paragenesis in diatexite migmatites should lead to a lithological subdivision into, for example, pelitic diatexite (*e.g.*, cordierite + garnet + sillimanite + K-feldspar assemblage) or psammitic diatexite (orthopyroxene) that reflects the composition of the protolith. Other workers have used subdivisions that reflect variation in the fraction of melt within the diatexite migmatite, *e.g.*, the residual diatexite and melt-rich diatexite divisions of Sawyer (1998) and the leucocratic, mesocratic and melanocratic diatexite migmatites of Milord *et al.* (2001). These divisions reflect the migration of melt within diatexite migmatites, and may be useful for showing the petrological variation within diatexite migmatites from zones of channel flow.

The proportion of felsic intrusive bodies in many migmatite terrains increases with metamorphic grade. The contacts between metatexite migmatites and bodies of granite intruded into them are, generally, sharp and readily apparent. Unfortunately, many of the contacts between diatexite migmatites and granites can be difficult to locate precisely as they are petrologically indistinct.

INTERMEDIATE SCALE MAPS

There is a need for information at a scale between the individual parts of a migmatite and that of the terrain. Medium scale maps that typically cover from a square kilometre to several hundred km^2 can be used to reveal how the distribution of anatectic melt in a migmatite is related to the large structures in a region. Brown & Solar (1998) and Solar & Brown (2001) mapped at this scale to show a strong correlation between strain and the morphology of migmatites across major, crustal scale shear zones. This scale can also be used to illustrate the distribution of melt-rich and melt-depleted rocks around large fold structures in migmatites, such as the dome structures that are associated with zones of channel flow.

Anatectic melt is the mobile phase in migmatites and, therefore, it moves and collects in the low pressure sites, and because of its lower density tends move upward in the crust and collect in suitable traps or at various barriers. A map that shows the distribution of regions where residual rocks predominate (*i.e.*, regions that have experienced a net loss of melt) and the regions that have an increased abundance of leucocratic dykes (vein-structured migmatites), or thicker leucosomes (commonly fold hinges) or contain leucocratic diatexite migmatites, (*i.e.*, regions that have experienced a net addition of melt) reveal the large scale pattern of mass (anatectic melt) transfer in the continental crust. Such regions can also be revealed by changes in the morphology of the migmatites (see Solar 2008). The second level division of morphology in migmatites, patch, dilational, net and stromatic divisions for metatexite migmatites, and the nebulitic, schollen, schlieren subdivisions of diatexite, plus vein- and fold-structured migmatites, could serve as map units to accomplish this. These morphologies reflect differences in

1) the fraction of melt present in a migmatite,
2) the form of the protolith (a thinly bedded protolith results in a migmatite that has a different morphology from one developed from a massive protolith) and,
3) deformation, both how much strain affected the rocks and how the individual domains of neosome, residuum or paleosome responded to deformation (*e.g.*, ductile or brittle response, or whether boudinage rather than folding occurred).

Strain gradients in migmatites affect the morphology of migmatites in various ways; for example a change in the morphology from patch to stromatic metatexite migmatite, by a progressive change to higher aspect ratio shapes for the lozenge-shaped blocks between leucosomes in net-structured metatexite migmatites, or by the progressive development of a more pronounced compositional banding in diatexite migmatites owing to more intense flow as syn-anatectic strain increases.

CONCLUSION

Migmatites can be complex looking rocks and mapping them can be a daunting task. However, it is encouraging that there are just four basic parts, although these may occur in a bewildering number of different geometrical relationships. The identification of the parts is essential for the mapping and sampling of migmatites and is easier if the processes that have contributed to their formation are considered. Once the basic parts are identified the next task to the determine how they came to be assembled the way they are; and is this

principally due to metamorphic grade, to the nature of the protolith, to the effects of deformation, the migration of anatectic melt, or to the length of time the migmatite contained partial melt?

ACKNOWLEDGEMENTS

I would like to thank Mike Brown, Richard White, Pierre Barbey, Bernard Bonin, Robert Martin and Isabelle Milord for numerous discussions on migmatite. Over the past years I have been fortunate enough to be been shown many migmatites in the field, I am particularly grateful to Claude Hérbert, Fernado Bea, Olivier Vanderhaeghe, Gary Solar, Steven Hauck and Mark Seversen.

REFERENCES

BARRAUD, J., GARDIEN, V., ALLEMAND, P. & GRANDJEAN, P. (2004): Analogue models of melt-flow networks in folding migmatites. *J. Struct. Geol.* **26**, 307-324.

BEAUMONT, C., JAMIESON, R.A., NGUYEN, M.H. & MEDVEDEV, S. (2004): Crustal channel flows: 1 Numerical models with applications to the tectonics of the Himalayan-Tibetan orogen. *J. Geophys. Res.* **109**, B06406, 29 p.

BLOCK, L. & ROYDEN, L.H. (1990): Core complex geometries and regional-scale flow in the lower crust. *Tectonics* **9**, 557-567.

BROWN, M. (1994): The generation, segregation, ascent and emplacement of granitic magma: the migmatite-to-crustally-derived granite connection in thickened orogens. *Earth Sci. Rev.* **36**, 83-130.

BROWN, M. (2008): Granites, migmatites and residual granulites: relationships and processes. *In* Working with Migmatites (E.W. Sawyer & M. Brown, eds.). *Mineral. Assoc. Can., Short Course* **38**, 97-144.

BROWN, M. & RUSHMER, T. (1997): The role of deformation in the movement of granitic melt; views from the laboratory and the field. In: HOLNESS, M.B. (editor) *Deformation-enhanced Fluid Transport in the Earth's Crust and Mantle*, pp. 111-144. The Mineralogical Society Series **8**, Chapman and Hall, London.

BROWN, M. & SOLAR, G.S. (1998): Shear-zone systems and melts: feedback relations and self-organisation in orogenic belts. *J. Struct. Geol.* **20**, 211-227.

BROWN, R.L. & GIBSON, H.D. (2006): An argument for channel flow in the southern Canadian Cordillera and comparison with Himalayan tectonics. In: Law, R. D., Searle, M. P. & Godin, L. (eds.) *Channel Flow, Ductile Extrusion and Exhumation in Continental Collision Zones.* Geol. Soc., London, Spec. Pub. **268**, 543-559.

CLARK, M.K. & ROYDEN, L.H. (2000): Topographic ooze: building the eastern margin of Tibet by lower crustal flow. *Geology* **28**, 703-706.

COLLINS, W.J. & SAWYER, E.W. (1996): Pervasive granitoid magma transfer through the lower-middle crust during non-coaxial compressional deformation. *J. Metamorphic Geol.* **14**, 565-579.

GREENFIELD, J.E., CLARKE, G.L., BLAND, M. & CLARKE, D.L. (1996): *In situ* migmatite and hybrid diatexite at Mt. Stafford, central Australia. *J. Metamorphic Geol.* **14**, 413-426.

GUERNINA, S. & SAWYER, E.W. (2003): Large-scale melt-depletion in granulite terranes: an example from the Archaean Ashuanipi subprovince of Quebec, *J. Metamorphic Geol.* **21**, 181-201.

HINCHEY, A.M. CARR, S.D., MCNEILL, P.D. & RAYNER, N. (2006): Paleocene-Eocene high-grade metamorphism, anatexis and deformation in the Thor-Odin dome, Monashee complex, southeastern British Columbia. *Can. J. Earth Sci.* **43**, 1341-1365.

HOLNESS, M. (2008): Decoding migmatite microstructures. *In* Working with Migmatites (E.W. Sawyer & M. Brown, eds.). *Mineral. Assoc. Canada, Short Course* **38**, 57-76.

MÄKITIE, H. (2001): Eastern margin of the Vaasa Migmatite Complex, Kauhava, western Finland: preliminary petrography and geochemistry of the diatexites. *Bull. Geol. Soc. Finland* **73**, 35-46.

MARCHILDON, N. & BROWN, M. (2003): Spatial distribution of melt-bearing structures in anatectic rocks from southern Brittany, France: implications for melt transfer at grain- to orogen-scale. *Tectonophys.* **364**, 215-235.

MCQUARRIE, N. & CHASE, C.G. (2000): Raising the Colorado Plateau. *Geology* **28**, 91-94.

MILORD, I., SAWYER, E.W. & BROWN, M. (2001): Formation of diatexite migmatite and granite magma during anatexis of semi-pelitic metasedimentary rocks: an example from St. Malo, France. *J. Petrol.* **42**, 487-505.

OLIVER, N.H.S. & BARR, T.D. (1997): The geometry and evolution of magma pathways

through migmatites of the Halls Creek Orogen, Western Australia. *Mineral. Mag.* **61,** 3-14.

ROSENBERG, C.L. & HANDY, M.R. (2005): Experimental deformation of partially melted granite revisited: implications for the continental crust. *J. Metamorphic Geol.* **23**, 19-28.

ROYDEN, L. H. (1996): Coupling and decoupling of the crust and mantle in convergent orogens: Implications for strain partitioning in the crust. *J. Geophys. Res.* **101**, 17679-17705.

RUBATTO, D., WILLIAMS, I. S. & BUICK, I. S. (2001): Zircon and monazite response to prograde metamorphism in the Reynolds Range, Central Australia. *Contrib. Mineral. Petrol.*, **140**, 458-468.

SAWYER, E.W. (1987): The role of partial melting and fractional crystallization in determining discordant migmatite leucosome compositions. *J. Petrol.* **28**, 445-73.

SAWYER, E.W. (1998): Formation and evolution of granite magmas during crustal reworking: the significance of diatexites. *J. Petrol.* **39**, 1147-1167.

SAWYER, E.W. (2001): Melt segregation in the continental crust: distribution and movement of melt in anatectic rocks. *J. Metamorphic Geol.* **19**, 291-309.

SAWYER, E.W. (2008): *Atlas of Migmatites*. The Canadian Mineralogist, Special Publication 9. NRC Research Press, Ottawa, Ontario. 371p.

SOLAR, G.S. (2008): The interplay between tectonics/structure and migmatite morphology in the field. *In* Working with Migmatites (E.W. Sawyer & M. Brown, eds.). *Mineral. Assoc. Can., Short Course* **38**, 145-157.

SOLAR, G.S. & BROWN, M. (2001): Petrogenesis of migmatites in Maine, USA: possible source of peraluminous leucogranite in plutons? *J. Petrol.* **42**, 789-823.

VANDERHAEGHE, O. & TEYSSIER, C. (2001): Partial melting and flow in orogens. *Tectonophys.* **342**, 451-472.

VANDERHAEGHE, O., TEYSSIER, C., & WYSOCZANSKI, R. (1999): Structural and geochronological constraints on the role of partial melting during the formation of the Shuswap metamorphic core complex at the latitude of the Thor-Odin dome, British Columbia. *Can. J. Earth Sci.* **36**, 917-943.

WATERS, D.J. & WHALES, C.J. (1984): Dehydration melting and the granulite transition in metapelites from southern Namaqualand, S. Africa. *Contrib. Mineral. Petrol.* **88**, 269-275.

WHITE, R.W., POMEROY, N.E. & POWELL, R. (2005): An *in situ* metatexite-diatexite transition in upper amphibolite facies rocks from Broken Hill, Australia. *J. Metamorphic Geol.* **23**, 579-602.

WILLIAMS, P.F. & JIANG, D. (2005): An investigation of lower crustal deformation: evidence for channel flow and its implications for tectonics and structural studies. *J. Struct. Geol.* **27**, 1486-1505.

ZALESKI, E., VAN BREEMEN, O. & PETERSON, V. L. (1999): Geological evolution of the Manitouwadge greenstone belt and Wawa-Quetico subprovince boundary, Superior Province, Ontario, constrained by U-Pb zircon dates of supracrustal and plutonic rocks. *Can. J. Earth Sci.* **36**, 945-966

ZAVÁDA, P., SCHULMANN, K., KONOPÁSEK J., ULRICH, S. & LEXA, O. (2007): Extreme ductility of feldspar aggregates – melt-enhanced grain boundary sliding and creep failure: rheological implications for felsic lower crust. *J. Geophys. Res.* **112**, B10210. DOI 10.1029/2006JB004730.

CHAPTER 3: CRUSTAL MELTING: WORKING WITH ENCLAVES

Bernardo Cesare
Dipartimento di Geoscienze, Università di Padova
and C.N.R., Istituto di Geoscienze e Georisorse
Corso Garibaldi, 37, I-35137 Padova,
Italy
E-mail: bernardo.cesare@unipd.it

INTRODUCTION

In another chapter in this volume (Holness 2008), emphasis has been placed on the problems related to the recognition of microstructures indicating the presence of melt in migmatites, and on how these problems may be in part circumvented, for example by studying pyrometamorphosed rocks.

More generally, despite being by far the most important and voluminous witness of how the partially melted, deep levels of the crust should look like (review in Brown 2007), migmatites suffer from one major problem: their slow cooling. Grant (1985) nicely outlined that "*Although we have been discussing partial melting of pelitic rocks, more of what we now see in a pelitic migmatite is probably attributable to re-crystallisation*". In other words, migmatitic complexes mostly represent an anatectic product which has been affected by further modifications of microstructure (summary in Holness 2008), phase assemblage (*e.g.*, Kriegsman and Hensen 1998), phase composition (*e.g.*, Cesare *et al.* 2008) and physical properties (*e.g.*, Ferri *et al.* 2007).

Experimental studies (reviewed by Clemens 2006) provide considerable, essential information for the interpretation of migmatites, by reproducing the *P–T–X* conditions relevant for the partial melting of the mid to deep crust, and by defining, as a result, the main melting reactions, the chemistry of phases, the compositions of melts and the fertility of different parent rocks. However, owing to their small size, rapid run times and in some cases simplified chemical systems, experimental simulations cannot fully represent the behavior of natural anatectic environments, so that a significant gap in the knowledge of how partial melting actually takes place in nature remains.

In this chapter I will describe how metasedimentary enclaves in volcanic rocks (very rare although probably overlooked) may help fill the gap mentioned above. Brought to the surface from depths of *ca*. 20 km by volcanic eruptions, the rock fragments enclosed in the volcanic rocks of the Neogene Volcanic Province (NVP) of SE Spain can be considered as "natural experimental charges" (*e.g.*, Downes *et al.* 2004), because their rapid cooling has allowed the preservation of the anatectic melt as glass. Unlike the pyrometamorphic rocks referred to by Holness (2008) the enclaves described here have a much deeper origin, and an inferred genetic relation to the lavas in which they are hosted.

The enclaves in the volcanic rocks of the NVP have been extensively studied in the last decade (Cesare *et al.* 1997, 2002, 2003a, 2003b, 2003c, 2005, 2007, Cesare & Maineri 1999, Cesare 2000, Álvarez-Valero *et al.* 2005, 2007, Acosta-Vigil *et al.* 2007, Álvarez-Valero & Kriegsman 2007, Ferri *et al.* 2007) and the reader may refer to these papers for the details of their geology, petrology, mineralogy, geochronology and rock physics. Here I will review some of their main bearings for the petrogenesis of anatectic metapelite, focusing, unless specified, on the enclaves from the localities of El Hoyazo. Here one can observe two main types of enclaves: the Bt–Grt–Sil (Fig. 3-1a) and the Spl–Crd types (Fig. 3-1b). The former, more abundant in the field and most studied, is represented by well foliated, Qtz-free rocks consisting of Grt–Pl–Bt–Sil–Gph–glass±Ilm±Crd±Kfs±Spl (mineral abbreviations after Kretz 1983). The bulk composition of the enclaves is highly residual (*ca*. 44 wt.% SiO_2, 31% Al_2O_3, 10% FeO_{tot}), and their thermobarometric study indicates equilibration temperature of 850±50°C and pressure of 5–7 kbar. According to Cesare *et al.* (1997), these rocks represent the residue (restite) after anatexis of graphitic metapelite and extraction of 40–60 wt.% granitic melt, contaminated by mafic magmas (Benito *et al.* 1999) and now represented by the host dacite.

Mineralogical Association of Canada Short Course 38, Quebec City, Quebec, p. 37-55

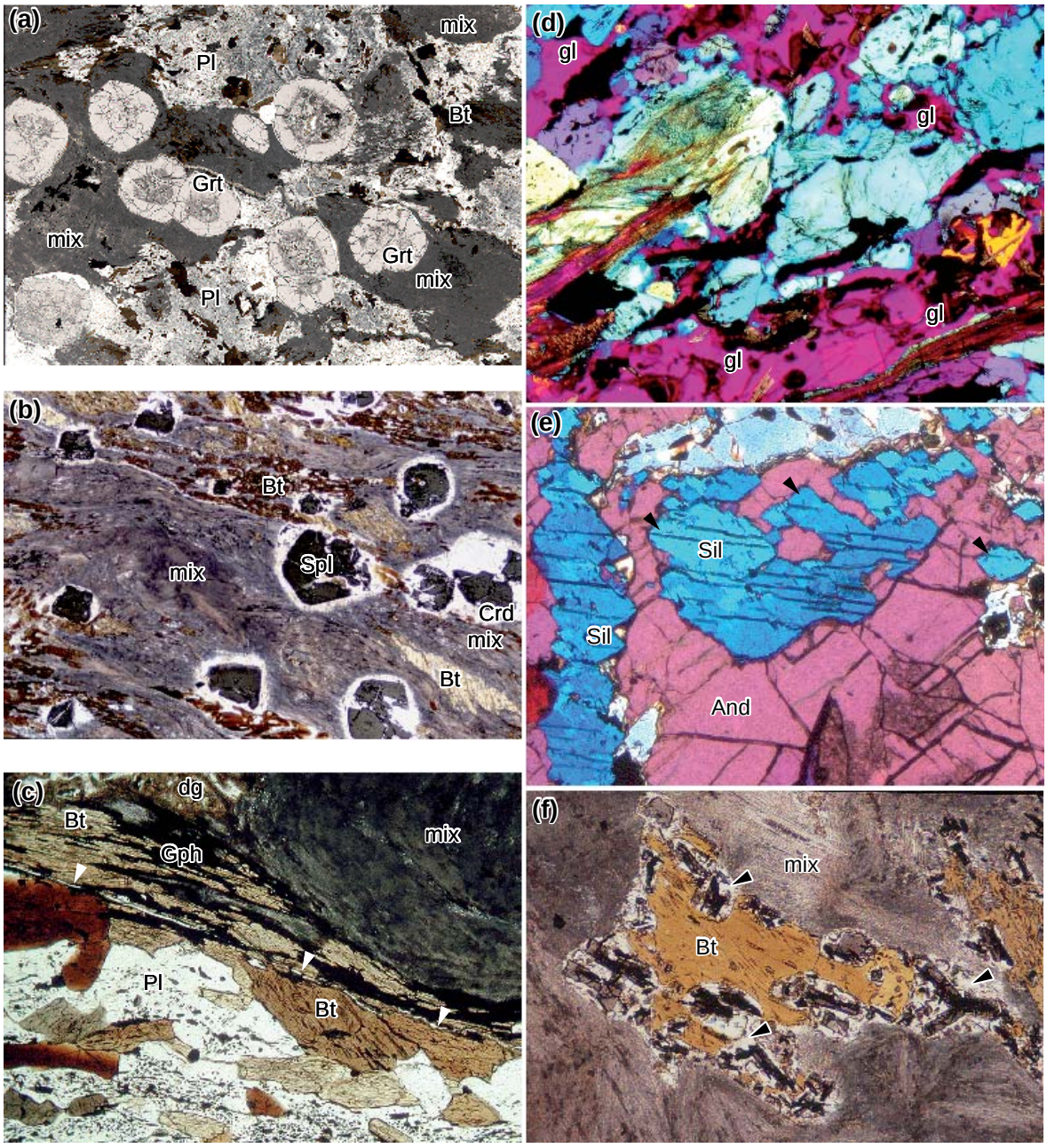

Fig. 3-1. a) Typical Bt-Grt-Sil enclave from El Hoyazo. Note the abundant aggregates of "mix", commonly in contact with euhedral porphyroblasts of garnet. The darker cores of garnet contain abundant inclusions of melt. Plane-polarized light; width of field 30 mm. **b)** Typical Spl-Crd enclave from El Hoyazo. The matrix around spinel is mainly composed of "mix" and biotite, whereas coronae around spinel consist of cordierite or K-feldspar. Plane-polarized light; width of field 5 mm. **c)** Thin film of glass (arrows) along the foliation marked by biotite, graphite and "mix". A patch of devitrified, weathered glass (dg) is visible at the strain shadow around the nodule of mix. Plane-polarized light; width of field 5 mm. **d)** A thick layer of glass (gl, red-violet) in the lower portion of the image is connected to an intergranular network of thinner glass films in the upper portion. In the network, melt coats rounded crystals. Crossed polars with 530 nm accessory plate; width of field 4.2 mm. **e)** Prismatic sillimanite (blue, arrows) topotactically replacing andalusite (pink). Crossed polars with 530 nm accessory plate; width of field 0.8 mm. **f)** Microstructure of biotite melting in the Qtz-free Bt-Grt-Sil enclaves of El Hoyazo. Products of melting include glass (arrows), spinel and ilmenite. Plane-polarized light; width of field 0.7 mm.

WHY ENCLAVES?

Extending to volcanic settings the terminology discussed and defined by Didier & Barbarin (1991) and Didier & Maury (1991), I will distinguish *xenoliths* – extraneous pieces of rocks in magmas (no genetic relations) – from (*cognate*) *enclaves* – fragments showing genetic links to their host rocks. The added value of enclaves, discussed in detail below, is that they bear regional-scale information on the source region of magmas: in the case of metapelitic protoliths, the residual enclaves can be compared with the melanosomes of migmatites and regarded as equivalents.

The uniqueness of enclaves in volcanic rocks for the understanding of crustal melting and the behavior of migmatites can be understood by considering a schematic *T*–*t* diagram such as in Figure 3-2, which shows the different trajectories that rocks undergoing partial melting (either regionally or by contact with magmas) may exhibit. After the peak of metamorphism and anatexis, the cooling of regionally metamorphosed migmatite and granulite terrains (field 1) may take 10^6–10^7 years, and that of enclaves in plutonic rocks (field 2) 10^5–10^6 years. Conversely, that of enclaves in volcanic rocks (path 3) may take 10^{-5}–10^{-1} years (minutes to months): this is the only geological process by which the evidence of melting can be preserved. Figure 3-2 also shows the difference between enclaves and pyrometamorphic xenoliths (path 4). The latter did not share the slow prograde path of the other rocks, and were suddenly heated during entrainment in the host lava (discussion in Holness 2008). It follows that the importance of enclaves in volcanic rocks is given by the combination of extremely rapid cooling and deep crustal provenance. In this perspective, the definition of "*erupted migmatites*" attributed by Zeck (1970) to the enclaves of El Hoyazo in the NVP is most appropriate.

While enclaves (and xenoliths as well) are widespread in mafic volcanic rocks and therefore have become the main subject of study in mantle petrology and geochemistry (*e.g.,* Nixon 1987), the same cannot be said for crustal enclaves in felsic volcanic rocks, especially those that contain partial melts, which are rare and more subject to dissolution during transport (Tsuchiyama 1986). In addition to being rare, crustal enclaves and xenoliths also have other drawbacks, intrinsic to their nature, when compared to migmatites. These are the small size, the lack of outcrop continuity and the lack of precise information on their source, that make it difficult to extrapolate from them on to a regional scale.

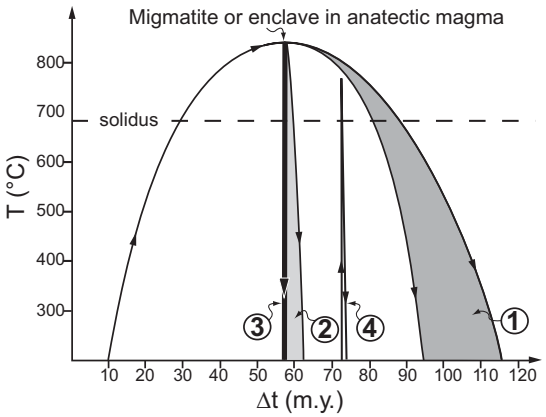

FIG. 3-2. Schematic temperature (*T*) – time elapsed (Δ*t*) diagram with model trajectories of migmatite and granulite (field 1), of enclaves and xenoliths in intrusive rocks (field 2), of enclaves in volcanic rocks (path 3) and of pyrometamorphosed xenoliths (path 4). See text for discussion.

The genetic relationship of rock fragments to host magma is a very important issue, especially in connection with the possibility of retrieving information about the source regions of granite. It is obvious that if the enclaves we observe are the residues of melting (restite) that are genetically linked to a specific magmatic rock, then we can learn a lot more about the regional process of anatexis.

Vernon (2007) has discussed in detail the problem of identifying restite in S–type magmas, concluding that microstructural and isotopic evidence is either against restite or is ambiguous. Among the case studies in support of Vernon's analysis are the enclaves of El Hoyazo that are the subject of this chapter, for which we propose a residual (restite) origin (Cesare *et al.* 1997, Cesare *et al.* 2003a, Perini *et al.*, in press).

I believe that *demonstrating* the residual (restitic) nature of enclaves in volcanic rocks is probably an impossible goal, since we are distant in time and space from the locus where the melting occurred. Therefore, data can only *support* a restite origin that should be generally evaluated and discussed in terms of likelihood and consistency, rather than proof. Except for the origin of melt inclusions in garnet (discussed below), I am not going into the details of the restite problem applied to the enclaves of El Hoyazo, because it is beyond the scope of this chapter. I would only reaffirm that when currently available data from these rocks are considered, they are consistent with restite.

MELT (AT LAST!)

As outlined above, the uniqueness of enclaves (and xenoliths) in volcanic rocks is the preservation of melt, quenched by rapid cooling, in the form of glass. This is the only situation where one can actually talk about "melt", whereas in most other occurrences the term melt is used for its crystallization products or for single mineral phases pseudomorphing the microstructural sites of former melt (*e.g.*, Holness 2008). In the NVP lavas, fresh, undevitrified glass occurs throughout the enclaves in various microstructural domains.

Intergranular films

Glass is commonly present in films and layers of variable thickness, orientation and aspect ratio depending on the mineralogy of, and the degree of melt extraction from, the rock. In strongly foliated, residual (feldspar-poor) samples, glass films are some tens of micrometres thick (Fig. 3-3) and often oriented parallel to the foliation defined by the preferred orientation of biotite, sillimanite and graphite (Fig. 3-1c). Films of glass may also coat the porphyroblasts of garnet (Fig. 3-4), and in all cases there is no mineralogical control on the location of glass films, *i.e.,* glass is not located between reactant minerals. Although some glass fills thin veinlets at a high angle to the foliation (Fig. 3-5), the preferential location of glass films parallel to the layering supports the observations of Guernina & Sawyer (2003) and suggests a control by externally imposed stresses.

In less foliated, more feldspathic enclaves, glass films are thicker (>100 μm) and may form an interconnected network around rounded crystals (Fig. 3-1d).

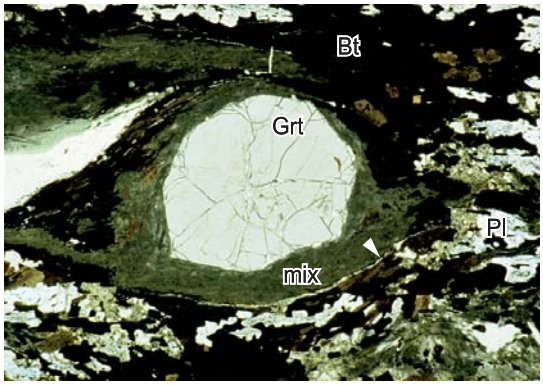

FIG. 3-3. Thin film of glass (arrows) parallel to the foliation that is deflected around a porphyroblast of garnet. Garnet shows euhedral crystal faces toward "mix". Plane-polarized light; width of field 12 mm.

A less common occurrence of glass films is at boundaries between reacting phases, in particular biotite and sillimanite (Cesare 2000, Ferri *et al.* 2007). These microstructures, described in detail below, develop in a static regime, and the glass film (>50 μm) also contains the other products of a melting reaction (*e.g.*, spinel, ilmenite, orthopyroxene).

Glass pockets

Locally, glass is present in large (>500 μm across) pockets located at strain shadows around

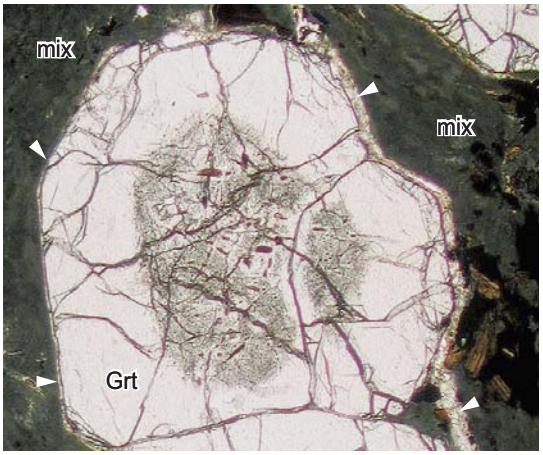

FIG. 3-4. Garnet porphyroblast, with core containing many inclusions of melt and biotite, coated by a thin film of glass (arrows). Garnet shows euhedral crystal faces toward "mix". Plane-polarized light; width of field 5 mm.

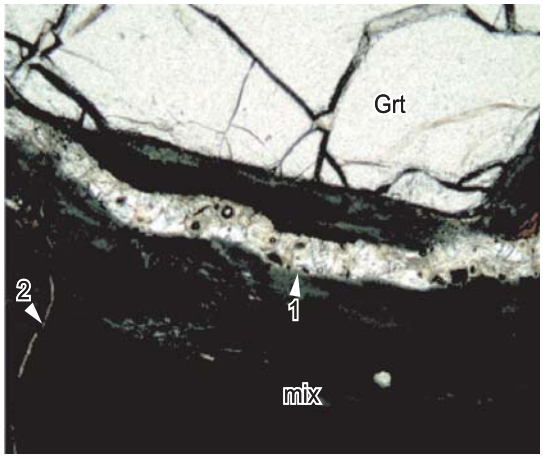

FIG. 3-5. Close-up of a Grt-"mix" boundary from the same sample as in previous figure, showing a thick (*ca*. 100 μm), foliation-parallel layer of partly devitrified glass (1) and a much thinner (<10 μm) glass veinlet quasi-orthogonal to the foliation (2). Plane-polarized light; width of field 1.5 mm.

garnet (Fig. 3-6). This microstructure is mostly observed in the intensely foliated Bt–Grt–Sil enclaves that contain garnet porphyroblasts up to 1 cm in diameter. Other pockets are observed in statically melted, glass-rich graphitic enclaves, and contain an intergrowth of glass and graphite (Fig. 3-7) indicating C–O–H fluid–melt–rock interactions (*e.g.*, Cesare & Maineri 1999).

"Mix"

The last mode of occurrence of interstitial glass is a peculiar intergrowth with acicular sillimanite (fibrolite according to the definition of Pattison 1992), defined as "mix" by Cesare (2000). The "mix" forms layers elongate parallel to the foliation (see Fig. 3-1b) but also nodular aggregates, up to 1 cm across, with size and spatial distribution similar to that of garnet. In the same thin section, "mix" is observed both at the contact with euhedral garnet porphyroblasts, suggesting textural equilibrium, and as faceted knots that partially or totally pseudomorph the garnet (Fig. 3-8, see also Cesare 2000, Fig. 1). This controversial behavior can be interpreted either as the result of replacement (by "mix") of a chemically unstable garnet in favor of a stable one, or as the result of a kinetically controlled behavior of garnet, with growth or dissolution in the different compositional domains of the rock as modeled by Foster (1986). Backscattered SEM imaging (Fig. 3-9) and chemical analyses (Cesare 2000) provide details of the "mix": it consists of a two-phase combination of sillimanite and a rhyolitic melt in proportions that vary from *ca*. 25 wt.% to *ca*. 40 wt.% melt.

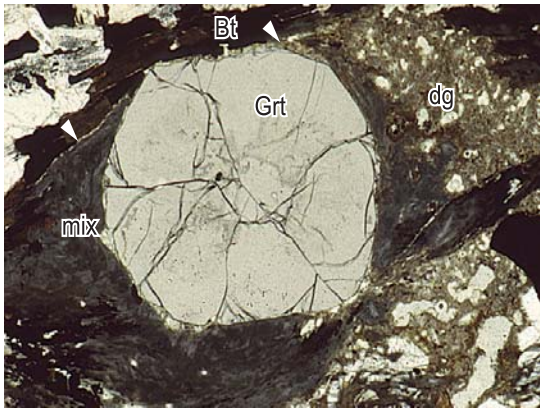

FIG. 3-6. Large pocket of devitrified glass (dg) in the strain shadow of a porphyroblast of garnet. Thin foliation-parallel films of glass are also visible (arrows). Plane-polarized light; width of field 10 mm.

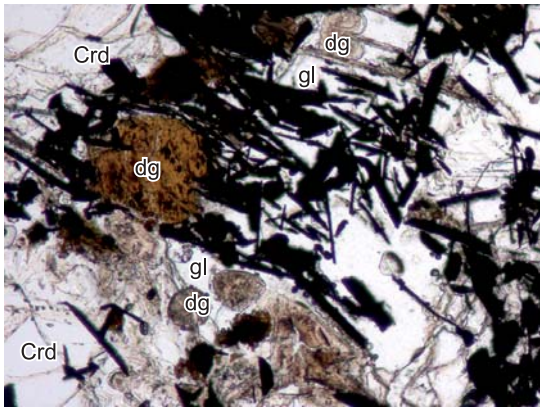

FIG. 3-7. Intergrowth of graphite lamellae (black) and fresh (gl, colorless) or devitrified (dg, brown) glass in a pocket located among cordierite crystals. Plane-polarized light; width of field 2 mm.

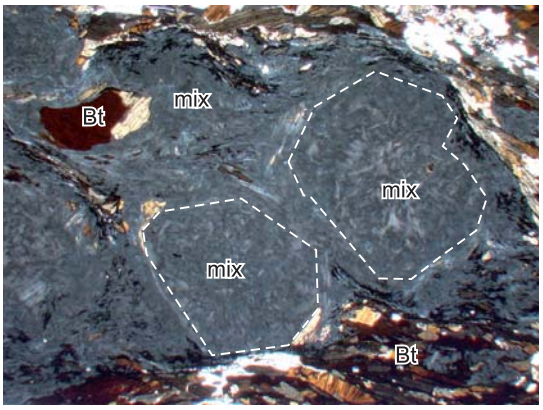

FIG. 3-8. Faceted knots of "mix" which have size and shape compatible with pseudomorphs after garnet, in a Bt-Grt-Sil enclave from El Hoyazo. Plane-polarized light; width of field 8.5 mm.

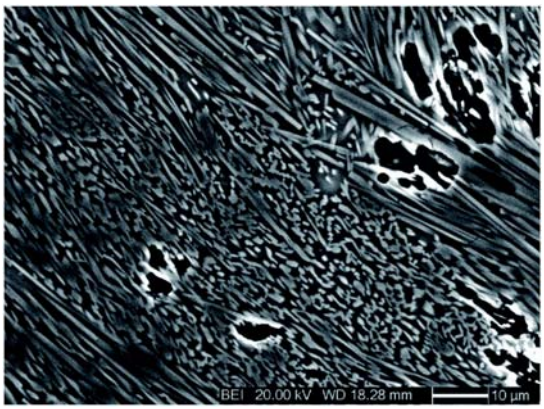

FIG. 3-9. Backscattered SEM image of the "mix" aggregate, consisting of acicular sillimanite (lighter gray) and interstitial glass (darker gray).

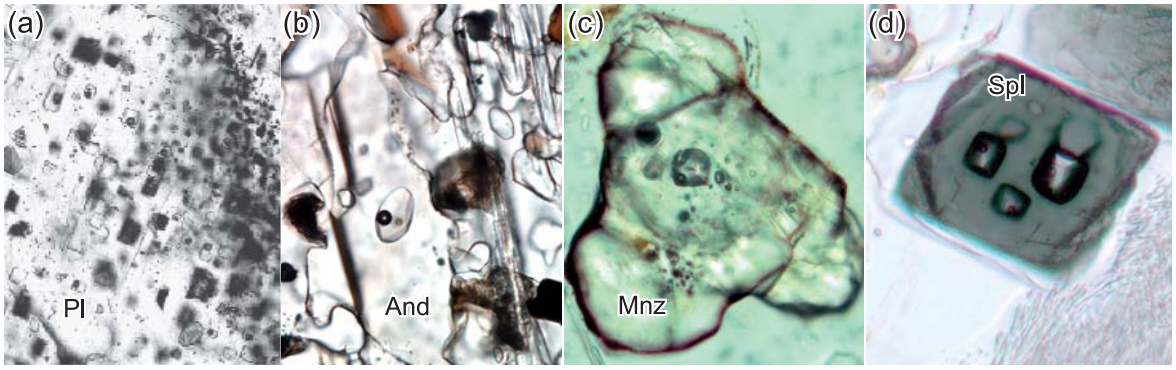

FIG. 3-10. Examples of melt inclusions in various hosts from the enclaves of the NVP. **a)** regular, negative crystal, melt inclusions in plagioclase. Plane-polarized light; width of field 0.5 mm. **b)** isolated melt inclusion in andalusite from Mazarrón. Plane-polarized light; width of field 0.3 mm. **c)** one large and many small melt inclusions in monazite. Plane-polarized light; width of field 200 μm. **d)** negative crystal melt inclusions in spinel. Plane-polarized light; width of field 200 μm.

Dealing with rock fragments that underwent rapid decompression, one question to be asked is if the interstitial glass forming the films, pockets and "mix" described above could result from the impregnation of microfractures by melt from the host lava, rather than being the anatectic melt in equilibrium with the solid assemblage at depth? Although infiltration in a fracture network formed during decompression is commonly observed in mantle xenoliths (*e.g.*, Faure *et al.* 2001), this phenomenon can be ruled out in the enclaves from El Hoyazo, since the composition of the intergranular glass in the enclaves is markedly different to that of the host dacite (Cesare *et al.* 1997).

Melt inclusions

Even if they actually contain glass (quenched melt), the term "melt inclusion" is generally preferred and used (*e.g.*, Webster 2006), and I will adopt it here. Probably the most relevant feature of the enclaves of the NVP is that melt inclusions are present and abundant in all the types of enclave, and in virtually all the minerals, including plagioclase, garnet, cordierite, biotite, spinel, ilmenite, andalusite, corundum, quartz, apatite, zircon and monazite (Fig. 3-10, see also Cesare *et al.* 1997, 2003b, 2003c, 2007, Cesare & Maineri 1999, Álvarez-Valero *et al.* 2005, 2007, Acosta-Vigil *et al.* 2007). For some mineral hosts (*e.g.*, andalusite, cordierite, zircon) this is the first ever occurrence of melt inclusions to be reported (source: Fluid Inclusion Research, volumes 1–31). In general melt inclusions have a maximum size that rarely exceeds 50 μm (up to 100 μm in plagioclase or cordierite) and contain clear, undevitrified glass, commonly with one or more shrinkage bubbles (Fig. 3-11). This has allowed the chemical composition of glasses in inclusions to be analyzed by *in situ* techniques such as EMP and LA–ICP–MS (*e.g.*, Cesare *et al.* 2003a). The shape of the inclusions ranges from spherical to irregular to a faceted negative crystal, and is a function of the type of host mineral and of the time that the enclaves resided at high temperature. In places, as described in detail by Acosta-Vigil *et al.* (2007) the presence of daughter crystals of the host (*e.g.*, ilmenite, plagioclase) or of other phases (*e.g.*, alkali feldspar in plagioclase) indicates post-entrapment crystallization of the melt or interaction between the melt and its host. The zonal arrangement (Sobolev & Kostyuk 1975, Bodnar & Student 2006) of melt inclusions within their hosts is particularly evident in garnet (Fig. 3-12), where inclusions are typically concentrated at the core of crystals. This is consistent with a primary origin (Roedder 1984), *i.e.*, with entrapment of glass droplets by the host mineral during its growth.

A primary origin for the melt inclusions is crucial in determining the petrogenetic significance of enclaves: in fact, it in turn implies that the host mineral has grown in the presence of melt and therefore attests to a partial melting event of peritectic nature (*i.e.*, an incongruent melting reaction). Since this interpretation has recently been challenged by Vernon (2007), I will discuss this issue in detail below.

ORIGIN AND SIGNIFICANCE OF GLASS INCLUSIONS IN CRUSTAL ENCLAVES

The process proposed by Vernon (2007) for the origin of melt inclusions in garnet crystals from

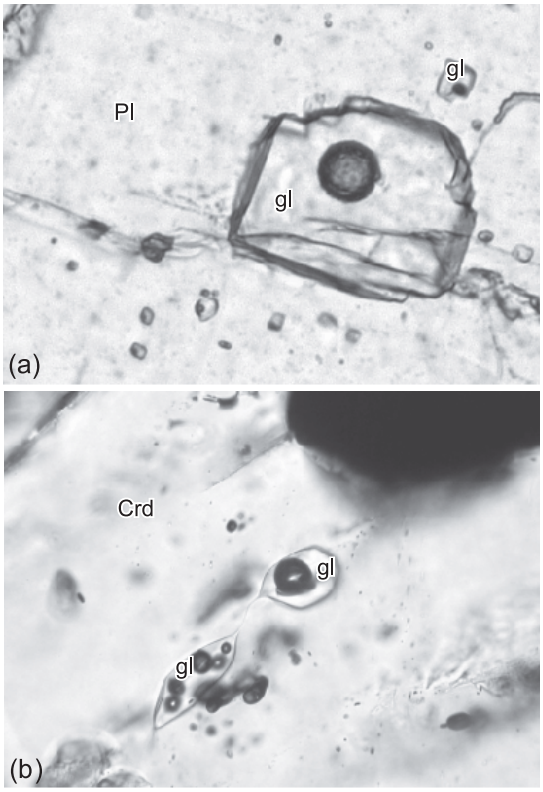

FIG. 3-11. Examples of melt inclusions containing clear and undevitrified glass (gl). **a)** negative crystal-shaped melt inclusions in plagioclase. Plane-polarized light; width of field 180 μm. **b)** irregular inclusion in cordierite, showing many shrinkage bubbles and "necking down" (Roedder, 1984). Plane-polarized light; width of field 120 μm.

the enclaves of El Hoyazo is "melting in response to loss of stability of a mineral assemblage" that "may conceivably produce melt droplets dispersed all through the grains of the unstable mineral if inclusions were originally present, which is a common situation in metamorphic assemblages". Continuing that "instability of inclusion-rich cores during the melting, rather than incorporation of melt droplets during growth" is suggested, he concluded that "glass inclusions must have formed later" than garnet. In essence the mechanism proposed (hereafter termed "*inclusion melting*") is the melting of mineral inclusions contained within an already present garnet. This model, while not unfeasible, is subject to severe constraints, keeping in mind that (for further details see Acosta-Vigil *et al.* 2007): i) melt inclusions in garnet from El Hoyazo are composed of undevitrified glass (see Fig. 3-12b), an empty shrinkage bubble and, in a few cases, include graphite or heavy element(s)-bearing minerals as

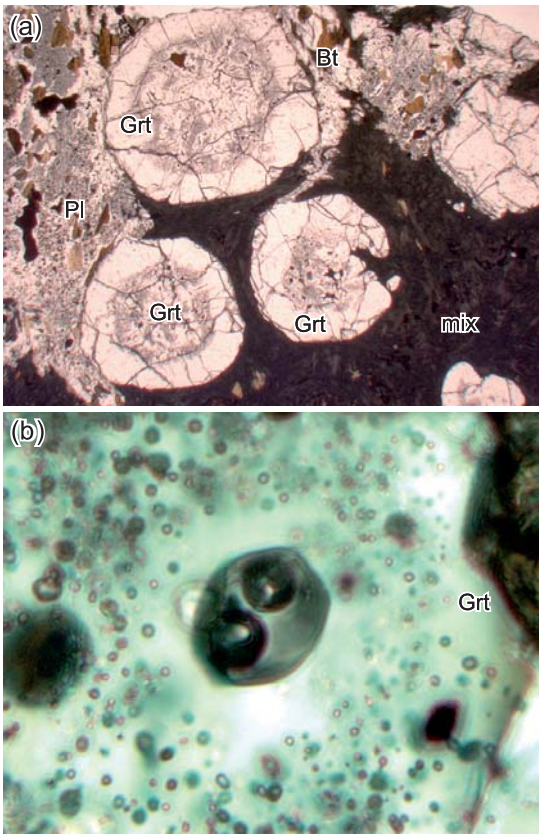

FIG. 3-12. Representative features of melt inclusions in garnet from Bt-Grt-Sil enclaves from El Hoyazo. **a)** zonal arrangement of inclusions at the core of garnet porphyroblasts. Plane-polarized light; width of field 8.5 mm. **b)** enlargement of inclusion-rich zone in garnet, showing that inclusions are composed of clear glass and shrinkage bubble(s), and are optically free of solid phases. Plane-polarized light; width of field 80 μm.

the only other mineral phases over hundreds of inclusions observed; ii) inclusions are composed of a leucogranitic peraluminous glass containing significant amounts of Na, K, Ca, Ti, P; and iii) other mineral inclusions in garnet, separate from melt inclusions, are rare and consist of graphite, ilmenite, biotite and sillimanite.

Considering the mass-balance and microstructural constraints on the theoretical behavior of a mineral inclusion (I) in a mineral host (H, in our case garnet), and its melting to produce a melt (M) and possible peritectic phases (P), the possibilities are: eutectic melting (I + H = M) and peritectic (incongruent) melting (I + H = M + P). Eutectic melting produces a M that, compositionally, must lie between I and H. There are no known minerals that may form a eutectic granitic

composition, such as the suite of inclusions observed in garnet, in combination with garnet. Therefore this possibility can be ruled out. Peritectic (incongruent) melting would produce, along with M, significant and detectable amounts of solids within the inclusion. Depending on the nature of I, these P phases could include spinel, ilmenite, sillimanite, corundum and orthopyroxene. Again, this possibility seems inapplicable to those melt inclusions in the garnet crystals from El Hoyazo because, when examined optically, or on backscattered electron images, they do not contain any solid minerals that could be the peritectic phases.

In addition to the mass-balance and microstructural constraints, further constraints are imposed by thermodynamics. The I + H system is chemically pretty simple, but it is rather unusual. Possible inclusions of I phases in the garnet from metapelitic rocks might be biotite, muscovite, quartz, plagioclase and sillimanite. Apart from the unavoidable constraint of there being necessary peritectic products, most of these binaries would have extremely high melting temperatures, or would not melt at all. For example, muscovite inclusions in garnet would not melt at P <10 kbar, T <850°C (Holland & Powell 2001).

Based on the above observations, the *only* way by which "inclusion melting" could take place is that H, rather than a single mineral, includes an *aggregate* of reactant I phases that always happen to occur in exactly the right modal proportions to enable the reaction to be complete congruent melting. Examples would be aggregates of Kfs + Sil + Qtz or Qtz + Pl + Kfs: if in the right modal proportions, these could melt without leaving peritectic (P) phases in the residue (Johannes & Holtz 1996). Note, however that these assemblages are very rare (they are restricted to subsets of the CKNASH system) and also require the presence of an aqueous fluid phase (H_2O) in order to melt at a geologically reasonable temperature (<1000°C, Johannes & Holtz 1996). Theoretically, melting could even occur at low, "minimum melt" temperatures if the inclusion contained the six phases Ms–Ab–Bt–Kfs–Qtz–H_2O (Thompson 1982) in the correct proportions.

At El Hoyazo, where thousands of fresh, P-free melt inclusions are observed within each garnet (and Pl, Hc, Ilm, Crd, *etc.*, as well), where preserved I are single crystals of either Bt, Sil, Ilm, Gph, Zrn, Ap or Mnz, and where glass compositions have a very narrow compositional range (Acosta-Vigil *et al.* 2007), "inclusion melting" would work only if for *each* melt inclusion there was originally an aggregate of solids and H_2O, *each* with exactly the *same* proportions of reactant phases.

Based on the above considerations, I conclude that although Vernon's (2007) model cannot be ruled out, the requirements for it to have operated are so geologically unreasonable, that it is extremely unlikely to be the correct explanation. Furthermore, I believe that this conclusion can be generalized beyond the El Hoyazo example to include all melt inclusions in crustal rocks. Further details on how melt inclusions are trapped during the growth of garnet and plagioclase hosts are provided by Acosta-Vigil *et al.* (2007).

PRESERVATION OF HIGH TEMPERATURE ASSEMBLAGES

In keeping with the products of experimental quenching, enclaves have the great advantage of not being affected by late stage retrogression and re-equilibration upon cooling. This implies that the phase assemblages and the phase compositions are the same as, or the closest possible to, those that existed at the time of anatexis. Since the dimensions of the crystals and the glass inclusions are big enough to enable several analytical techniques to be used, all the phases in the enclaves have been subjected to an extensive chemical characterization, and this has allowed a better understanding of the mineralogy of high temperature (HT) metapelitic systems.

Chemistry and crystallography of minerals

Table 3-1 reports the representative composition of minerals and of the bulk rock in a typical Bt–Grt–Sil enclave from El Hoyazo and can be considered representative of this enclave type (see also Cesare *et al.* 1997, 2003a, 2005).

Biotite has provided important information that is commonly erased by retrograde processes in migmatites and granulites (*e.g.*, Cesare *et al.* 2008) on the relationships between H and Ti contents in high temperature metapelitic rocks. By integrating EMP data with the direct measurement of H by SIMS and Fe^{3+} by Mossbauer spectrometry, Cesare *et al.* (2003b) have demonstrated the importance of dehydroxylation and Ti-oxy exchange [$(Fe, Mg)^{2+}$ + 2(OH) = Ti + 2O]. Along with its implications on the thermodynamic model of biotite (recently updated by White *et al.* 2007) the Ti-oxy exchange

TABLE 3-1. Representative composition of mineral phases and bulk rock in a typical Bt-Grt-Sil enclave (Ssmple HO50) from El Hoyazo.

Phase	Bt	Grt	Crd	Pl	Kfs	Sil	Ilm	melt	bulk rock
SiO_2	34.43	36.97	48.19	61.19	64.93	36.52	0.04	72.68	47.71
TiO_2	4.86	0.01	0.00	0.02	0.01	0.00	53.34	0.09	1.37
Al_2O_3	18.84	20.55	32.29	24.38	18.79	61.83	0.18	13.16	26.84
Cr_2O_3	0.06	0.02	0.02	0.01	0.00	0.01	0.03	0.02	n.a.
FeO	23.44	37.00	11.74	0.01	0.06	0.20	45.56	0.74	9.83
MnO	0.04	1.28	0.10	0.00	0.02	0.00	0.29	0.01	0.12
MgO	6.35	3.46	6.64	0.00	0.00	0.05	0.89	0.11	2.16
CaO	0.01	1.03	0.01	6.01	0.17	0.06	0.02	0.30	2.58
Na_2O	0.41	0.00	0.11	7.35	2.32	0.01	n.a.	1.72	2.91
K_2O	8.55	0.01	0.10	0.82	12.03	0.04	n.a.	5.58	2.97
L.O.I.	--	--	--	--	--	--	--	--	2.67
Total	96.99	100.34	99.20	99.80	98.32	98.72	100.34	94.40	99.14

has important consequences on high temperature petrogenesis, the most important being a major decrease (30–40%) in the availability of H_2O to the system, which in turn affects the estimates of melt productivity and the mass balance calculations of all Bt-bearing reactions during crustal melting (discussion in Cesare *et al.* 2003a).

Plagioclase in the Bt–Grt–Sil enclaves is homogeneous, with a relatively sodic ($An_{27–33}$) composition, which might seem incompatible with the high inferred equilibration temperatures (850 ±50°C). Note, however, that similar compositions are reported in experimental studies of partial melting of metagreywacke and semipelitic bulk compositions in the range 800–900°C (*e.g.*, Montel & Vielzeuf 1997, Nair & Chacko 2002), and that also in regional migmatites a sodic composition of plagioclase turns out to be present both in the melt-derived fraction and in the residuum (*e.g.*, Gupta & Johannes 1982, Kenah & Hollister 1983).

Graphite is extremely abundant in the enclaves, which may contain up to 1.2 wt.% carbon (Ferri *et al.* 2007). The degree of ordering (crystallinity) of the different textural generations of graphite has been determined by Raman spectroscopy (Cesare & Maineri 1999), who found that the highest state of ordering was in the fine-grained crystals associated with the melt inclusions in plagioclase (Fig. 3-13) and the lowest was in the coarse lamellae and aggregates in the rock matrix. These variations have been interpreted to be related to the progressive graphitization of the sedimentary carbonaceous matter (French 1964, Beyssac *et al.* 2002), and as the evidence for the syn-anatectic precipitation of highly crystalline graphite during fluid-present melting (Cesare & Maineri 1999).

Other minerals, not occurring in the Bt–Grt–Sil enclaves, are worthy of mention.

Spinel is hercynite-rich (X_{Mg} = 0.13–0.22) and Zn-poor, and very common in the Spl–Crd enclaves of El Hoyazo and also at the Mazarrón and Mar Menor localities. It commonly forms euhedral mm-sized crystals, and it is these that have had their intracrystalline cation ordering studied by single crystal X-ray diffraction. Interestingly, these Mg-hercynite crystals display the largest disordering observed in natural spinel, with cation ordering

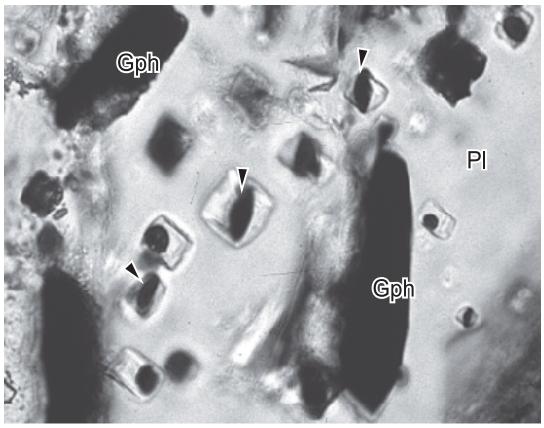

FIG. 3-13. Graphite (black) and melt inclusions in plagioclase. Tiny graphite crystals occur sparsely within some melt inclusions (arrows). These graphite lamellae represent solid inclusions and not daughter crystals and exhibit the highest crystalline ordering. Plane-polarized light; width of field 130 μm.

closure temperatures in the range 700–900°C (Lavina, pers. comm., 2008). These data indicate that in rapidly cooled rocks, intracrystalline cation ordering in spinel may provide additional constraints to thermometry.

Al_2SiO_5 polymorphs are also common in the enclaves: fibrolite dominates, whereas prismatic sillimanite is much rarer. Andalusite is common at Mazarrón and Mar Menor, and in the former locality it is commonly pseudomorphed by prismatic sillimanite (Fig. 3-1e). The direct topotactic (crystallographically controlled) transformation of andalusite to sillimanite was characterized by TEM in samples from Mazarrón (Cesare *et al.* 2002), where it was observed that the two lattices are rotated by ~2.5° around a_{And} (= b_{Sil}) with respect to the topotactic relationship previously proposed in the literature ($c_{And} \parallel c_{Sil}$, $a_{And} \parallel b_{Sil}$, $b_{And} \parallel a_{Sil}$, Vernon 1987). In addition, the finding of microscopic lamellae of sillimanite within seemingly homogeneous andalusite has important implications for the interpretation of phase equilibria in aluminous metapelite, as it suggests that many "andalusite-grade" rocks might in fact contain optically undetectable sillimanite, and that a correct assessment of the And–Sil transition should be rigorously performed by TEM investigation.

Chemistry of melts

As outlined before, the enclaves of the NVP offer the unique possibility of determining the composition of natural anatectic melts, both those occurring as intergranular films and, especially, those trapped as melt inclusions in the various mineral hosts. After some preliminary characterization (Cesare *et al.* 1997, 2003c, 2005, Cesare 2000, Cesare & Gómez-Pugnaire 2001), the systematic study of the composition of glasses in the Bt–Grt–Sil enclaves of El Hoyazo has been undertaken by Acosta-Vigil *et al.* (2007), who obtained the first dataset of anatectic melts from natural pelitic rocks. Unlike the case of rapidly melted xenoliths in lavas (*e.g.*, Braun & Kriegsman 2001, Salvioli Mariani *et al.* 2005), where glasses exhibit very large compositional ranges, the melts in the enclaves we studied are remarkably homogeneous in composition. They are granitic, peraluminous and felsic (leucogranite), with a moderate Aluminum Saturation Index (Table 3-2). Interestingly, there are systematic differences in the glass compositions from different textural settings in the enclaves, but all glasses from a specific textural location (i.e., within a specific host mineral) all have comparable compositions. These relationships are maintained between different enclaves in an outcrop, and have been interpreted as recording the evolution of the composition of the melt during prograde anatexis of the quartz-poor metapelite. Because H_2O concentrations are below the saturation levels for granitic melts at the inferred pressures of melting (*e.g.*, Holtz *et al.* 1995), Acosta-Vigil *et al.* (2007) concluded that crustal anatexis occurred under H_2O-undersaturated

TABLE 3-2: Representative compositions of glasses in the enclaves of the NVP.

Host	Plagioclase	Garnet	Cordierite	Ilmenite	Andalusite	Interstitial
Source	1	1	1	1	2	3
SiO_2	73.28	71.26	73.42	70.68	71.21	70.47
TiO_2	0.08	0.10	0.07	0.31	0.09	0.21
Al_2O_3	12.64	14.44	14.01	15.69	13.87	15.10
FeO_{tot}	1.15	1.72	1.31	2.58	1.46	1.13
MnO	0.02	0.08	0.04	0.07	0.15	0.03
MgO	0.15	0.05	0.04	0.13	0.12	0.13
CaO	0.24	0.60	0.93	0.96	0.61	1.03
Na_2O	2.85	3.61	3.41	3.55	2.72	3.57
K_2O	5.00	4.97	4.92	4.92	5.74	5.76
P_2O_5	0.21	0.37	0.20	0.31	n.a.	n.a.
F	0.06	0.08	0.05	0.07	n.a.	n.a.
Cl	0.04	0.01	0.45	0.01	0.27	n.a.
Total	95.72	97.29	98.85	99.28	96.15	97.43

All data refer to melt inclusions (hosted by mineral listed in first row) except for the rightmost column of interstitial glass rimming biotite melting to hercynite. Sources of data: 1) Acosta-Vigil *et al*. (2007); 2) Cesare et al. (2003c); 3) Cesare (2000).

conditions. In fact, the compositions of the melt in the inclusions compare closely to those of glasses produced by experimental, fluid-absent partial melting of metapelitic rocks (*e.g.*, Le Breton and Thompson 1988, Vielzeuf and Holloway 1988, Patiño Douce & Johnston 1991).

The composition of the glass within the melt inclusions has also been a key to constraining the much-debated location of the Al_2SiO_5 triple point in *P–T* space. Andalusite in the *xenoliths* from Mazarrón (here the genetic link to the host lava is less straightforward) shows the systematic occurrence of large and primary primary melt inclusions (see Fig. 3-10b), and these were analyzed by EMP and LA–ICP–MS (Cesare *et al.* 2003c). Based on the content of the volatile elements, B, Cl and F, and on the occurrence of graphite in these rocks, the displacement of the wet granite solidus in P–T space was calculated, and compared to the location of the And–Sil equilibria from Holdaway (1971) and Pattison (1992). Because an And + melt stability field, as observed in the enclaves, was generated using the And–Sil equilibrium of Pattison (1992), but not with that of Holdaway (1971), the former is preferred and should be used.

While there is little doubt that the composition of glass in the inclusions from the enclaves is that of a partial melt produced by anatexis, the connection with migmatites is less straightforward. In general, leucosome in migmatites is not considered to be primary anatectic melt because of the possible presence of restitic phases and/or cumulus phenomena (*e.g.*, Sawyer 1987, Solar & Brown 2001). Alternative methods should be sought: on the basis of the example of enclaves from the NVP, one might look for former melt inclusions also in migmatites and granulites. Target host minerals should be the peritectic phases (*i.e.*, garnet, orthopyroxene and spinel) that grow during the melting reaction and, therefore, have more potential to trap droplets of melt. In slowly cooled regional anatectic rocks the melt inclusion will have crystallized to an aggregate of different minerals (quartz, feldspars and micas), and this is what should be expected. One example of former melt inclusions in granulite can be observed in Fig. 3-14 (Ferrero, pers. com.). These microcrystalline aggregates within garnet from the "khondalite" of the Kerala Khondalite Belt of SE India are mainly composed of quartz, feldspars and biotite, have been experimentally melted at *ca*. 950 °C, and the homogenized composition can then be analyzed by EMP.

MELTING REACTIONS

In the enclaves, melting reactions are outlined by microstructures that involve intergranular films of glass which are commonly well preserved and can be analyzed, allowing a better chemical characterization of the melt-producing reaction. In many cases the most straightforward microstructures indicate a static event that overprints and postdates the main anatectic assemblage (*e.g.*, Bt–Grt–Sil).

The melting of biotite in the Qtz-free, Bt–Grt–Sil enclaves has been modeled by Cesare (2000) through the study of peculiar reaction rims that are composed of glass, spinel and ilmenite, and which occur at the contact between biotite and "mix" (Fig. 3-1f). After detailed microstructural and microchemical characterization (glass composition reported in Table 3-2), algebraic analysis (Fisher 1989, Cesare 1999) was performed in the nine-component (Al–Ca–Fe–K–Mg–Mn–Na–Si–Ti), nine-phase (Bt_1–Bt_2–Grt–Spl–Ilm–melt–mix–Pl_1–Pl_2) system, and provided the balance:

$$0.78\ Bt_1 + 1.95\ Pl_1 + 2.82\ mix + 0.32\ Grt = 0.25\ Ilm + 5.00\ melt + 0.30\ Bt_2 + 2.53\ Spl + 1.03\ Pl_2 \quad (1)$$

This relationship is in agreement with the observed textures and can, therefore, be considered a good model for the incongruent melting of biotite in the Qtz-free enclaves (Cesare 2000). As this reaction requires garnet and plagioclase as reactants, the reaction volume must be larger than the site at which the melt is produced, where these two phases are not present. Ferri *et al.* (2007) have reproduced the same reaction experimentally in cores of Bt–Grt–Sil enclaves melted at 950°C and 5 kbar.

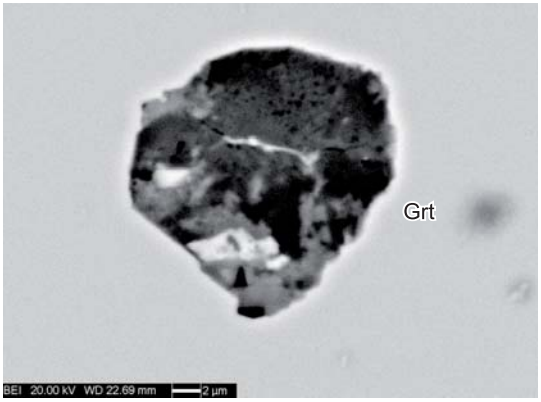

FIG. 3-14. Backscattered SEM image of a polycrystalline inclusion in garnet from a metapelitic granulite ("khondalite") of the Kerala Khondalite Belt, probably representing a former melt inclusion, crystallized during slow cooling (courtesy S. Ferrero).

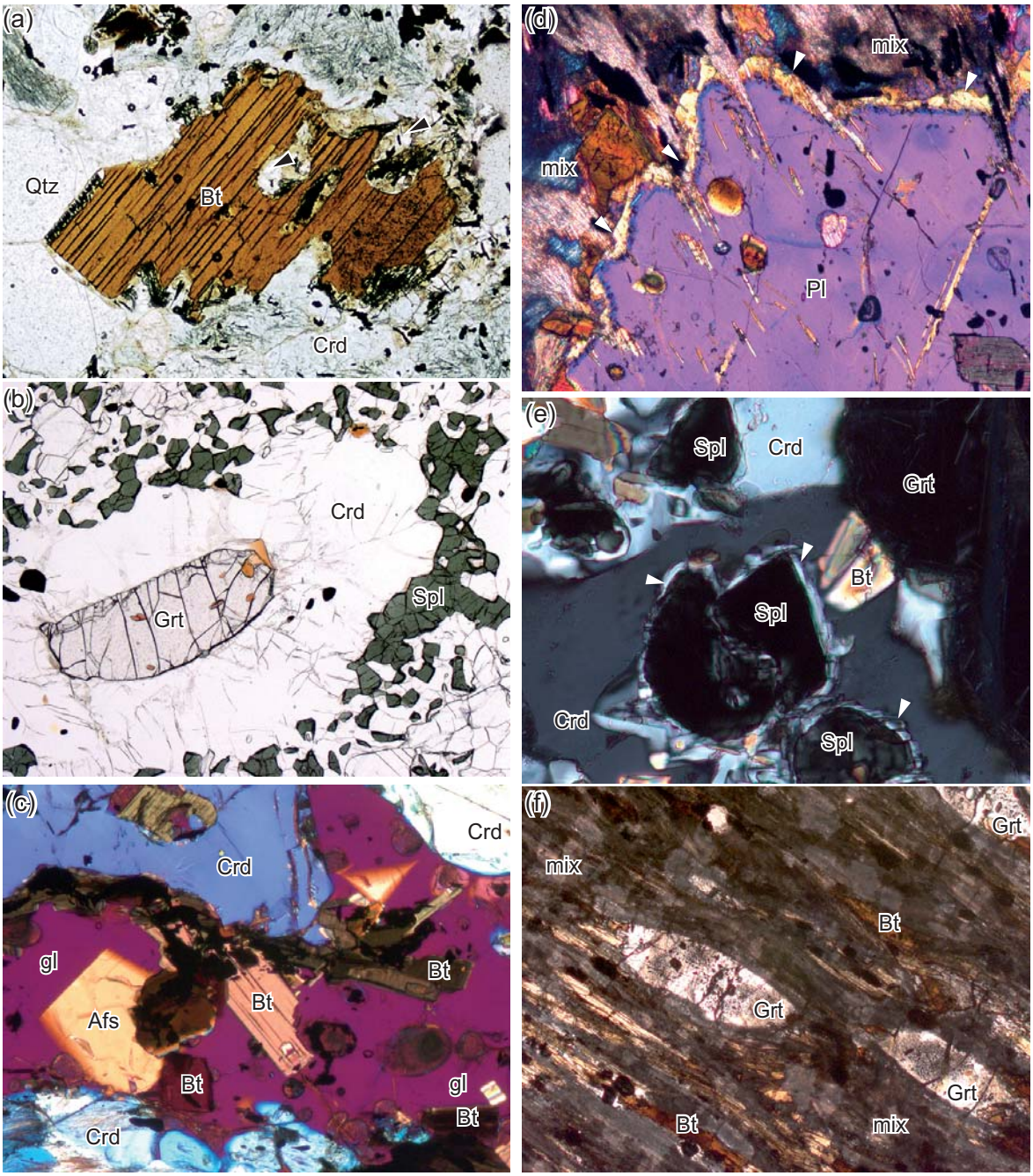

FIG. 3-15. **a)** Microstructure of biotite melting in the Qtz-Crd rocks of El Hoyazo. Products of melting include glass (arrows), orthopyroxene and ilmenite. Note uneven distribution of the reaction rim. Plane-polarized light; width of field 0.6 mm. **b)** Reaction corona of cordierite and spinel in a khondalite from the Kerala Khondalite Belt. Plane-polarized light; width of field 8 mm. **c)** Euhedral crystallites of alkali feldspar (Afs) and biotite in a thick glass layer bounded by embayed cordierite (right). Crossed polars with 530 nm accessory plate; width of field 0.4 mm. **d)** Sodic rim (yellow, arrows) overgrowing a crystal of more calcic plagioclase (purple) at the contact with a "mix". Crossed polars with 530 nm accessory plate; width of field 0.85 mm. **e)** Thin rim of plagioclase (arrows) around spinel in the Crd-bearing coronae around garnet. Crossed polars; width of field 0.3 mm. **f)** "Elliptical garnets" from a highly deformed enclave of El Hoyazo. Plane-polarized light; width of field 3 mm.

A similar reaction microstructure is observed in Qtz-bearing enclaves, namely in the Qtz–Crd rocks (as in the definition of Zeck 1970) of El Hoyazo. Here, biotite shows evidence of instability and decomposition (Fig. 3-15a), and a reaction rim up to 100 μm in thickness and consisting of glass, orthopyroxene and ilmenite (Fig. 3-16) has developed. The reaction proceeds only at the Qtz–Bt grain boundaries, whereas adjacent Bt–Crd interfaces remained stable.

In this example, mass balance calculations in the simplified KFMASH–Ti system indicate that the reaction inferred from textural analysis:

$$\text{Bt} + \text{Qtz} = \text{melt} + \text{Opx} + \text{Ilm} \qquad (2)$$

similar to those produced experimentally, for example in the H_2O-saturated melting of Ms + Qtz (Rubie & Brearley 1990).

A third example of microstructures formed by a melting reaction is observed both at El Hoyazo and Mazarrón, and consists of spinel + cordierite + K-feldspar + plagioclase + glass coronae around garnet (Fig. 3-17). These microstructures indicate the breakdown of garnet during decompression and slight heating, and have been characterized by Álvarez-Valero *et al.* (2007). Also in this case the reaction corona developed statically and glass is present between the product phases. However, unlike in the previous examples, the glass occurs mostly as melt inclusions in spinel and cordierite, and only rarely forms an intergranular film. Once again, the full microchemical characterization of phases (including the glass) in the rock has enabled an algebraic analysis of the development of the corona. Although the microstructures are suggestive of a model reaction such as

$$\text{Grt} + \text{Sil}\ (+\text{Pl}) = \text{Spl} + \text{Crd} + \text{Kfs} + \text{melt}, \qquad (3)$$

matrix analysis in the NCKFMASH system indicates the (unbalanced) reaction

$$\text{Grt} + \text{Sil} + \text{Bt} + \text{Pl}_1 = \text{Spl} + \text{Crd} + \text{Pl}_2 + \text{Kfs} + \text{melt} \qquad (4)$$

as the preferred model for the melting reaction (Álvarez-Valero *et al.* 2007).

Although this approach does not always lead to unequivocal results and interpretations, the modeling of melting reactions in enclaves and xenoliths represents a significant improvement, because analyzed, rather than assumed, melt compositions can be considered. Therefore, it has important implications for the petrogenesis of migmatites and granulites, where similar microstructures occur commonly (*e.g.,* Fig. 3-15b).

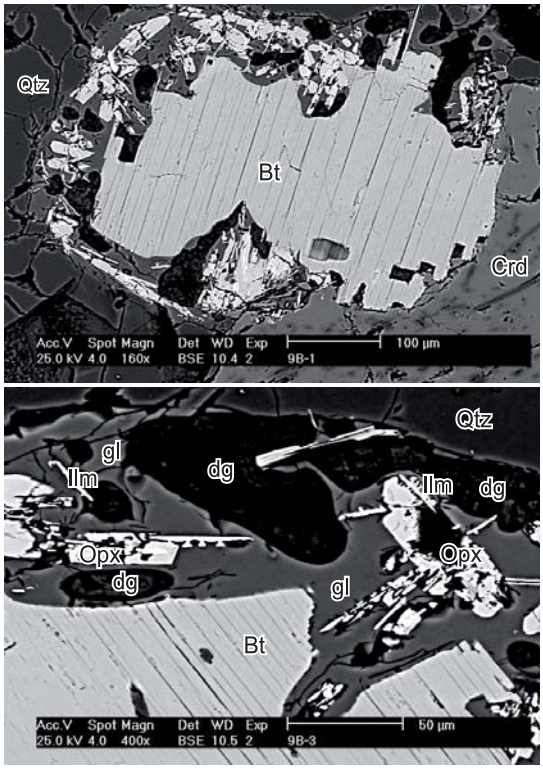

FIG. 3-16. **a)** Backscattered SEM image of a microstructure such as in Fig 3-15a. Note the kinetic control on reaction progress, with extensive reaction at the boundaries with quartz, and little or no reaction at the boundaries with cordierite. **b)** Close-up of a reaction rim around biotite, displaying fresh (gl) and weathered (dg) glass, elongate orthopyroxene and acicular to dendritic ilmenite.

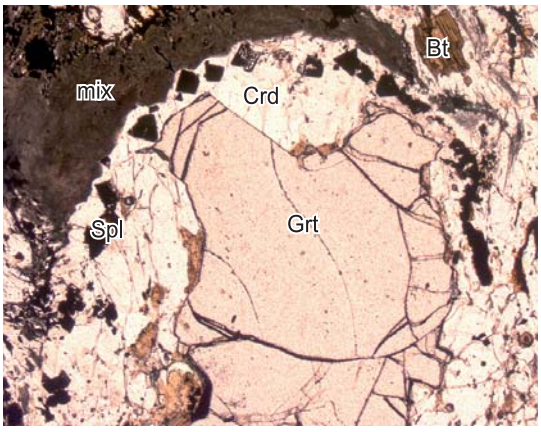

FIG. 3-17. Reaction corona of spinel, cordierite and K-feldspar replacing garnet in an enclave from El Hoyazo. Crossed polars; width of field 8.5 mm.

MELT-CONSUMING (CRYSTALLIZATION) FEATURES

Along with providing insights on the prograde, melt-producing history of high-grade metapelite, the enclaves of the NVP also display local evidence of melt-consuming features, and these can be compared with the microstructures formed during crystallization that are observed in migmatites.

A first example is represented by the small (a few tens of μm) euhedral crystallites of alkali feldspars and biotite that can be observed at the boundaries or within the thickest films of glass in melt-rich enclaves (Fig. 3-15c). These microstructures are comparable to the euhedral crystals rimmed by pseudomorphic quartz and K-feldspar after melt films (*e.g.*, Vernon 2004, Holness 2008– this volume, Figure 4-10), of which they represent the very initial stage of development. Depending on which minerals occur at the boundary with the glass film, the crystallization product may form overgrowths rather than single crystallites, highlighting a kinetic control on nucleation. This is observed when plagioclase is involved: in this case an overgrowth of different composition (alkali feldspar or more albitic plagioclase) projects topotactically towards the "mix" or glass layer (Fig. 3-15d).

Another melt-consuming feature is represented by symplectic intergrowths of biotite–plagioclase or biotite–K-feldspar. The former type is observed as partial pseudomorphs after garnet (Fig. 3-18, see also Figure 2f in Álvarez-Valero *et al.* 2007) and has been interpreted as evidence of a slight cooling event, with partial crystallization, before the eruption of the lavas that host the enclaves.

A similar genetic interpretation has been proposed for the thin rims of plagioclase around spinel (Fig. 3-15e) in the coronae after garnet from the same rocks (Álvarez-Valero *et al.* 2007). These rims represent partial to total "pseudomorphs" after melt, and they are very similar to the microstructures observed in migmatites and granulite discussed by Holness (2008).

INFORMATION ON DYNAMICS

One of the most important features of the enclaves of the NVP is that they show evidence of having been deformed during melting. The syn-anatectic origin of the foliation and other deformation features in the enclaves has been questioned by Vernon (2007) on the basis of his interpretation of melt inclusions in garnet. Since, as outlined above, the "inclusion melting" process proposed by Vernon (2007) is untenable, we can confidently conclude that garnet has indeed grown during melting, and reaffirm the microstructural evidence of syntectonic melting described by Cesare *et al.* (1997), Cesare and Gómez-Pugnaire (2001) and Álvarez-Valero *et al.* (2005).

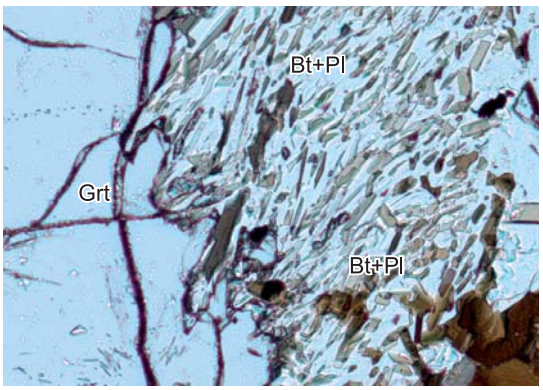

FIG. 3-18. Fine-grained aggregate of biotite and plagioclase partially replacing garnet. Plane-polarized light; width of field 1.5 mm.

A first evidence of the syn-anatectic origin of the main foliation of most enclaves is that it anastomoses around porphyroblasts that contain primary melt inclusions. This is observed both around porphyroblasts of garnet at El Hoyazo and around porphyroblasts of plagioclase at Mazarrón (Cesare & Gómez-Pugnaire 2001). A spectacular example comes from the Bt–Grt–Sil enclaves from El Hoyazo, where the foliation that anastomoses around garnet is marked by the helicitic arrangement of melt inclusions in plagioclase (Fig. 3-19), rather than biotite–sillimanite–glass folia as is generally observed. This microstructure implies the growth of garnet in the presence of melt, and the subsequent deflection of the foliation around it. Growth of plagioclase seems to postdate development of the foliation, but might also be coeval with it. Regardless of the actual timing of the growth of plagioclase, the helicitic foliation included in it and outlined by melt inclusions, attests to a prolonged history of crystallization and deformation in the presence of a melt phase, *i.e.*, during anatexis.

In some cases, melting was accompanied by intense deformation and pressure-solution phenomena. One example is provided by the elliptical garnets (Fig. 3-15f) studied by Álvarez-Valero *et al.* (2005), which show evidence of truncation of the internal pattern of melt inclusions at high strain

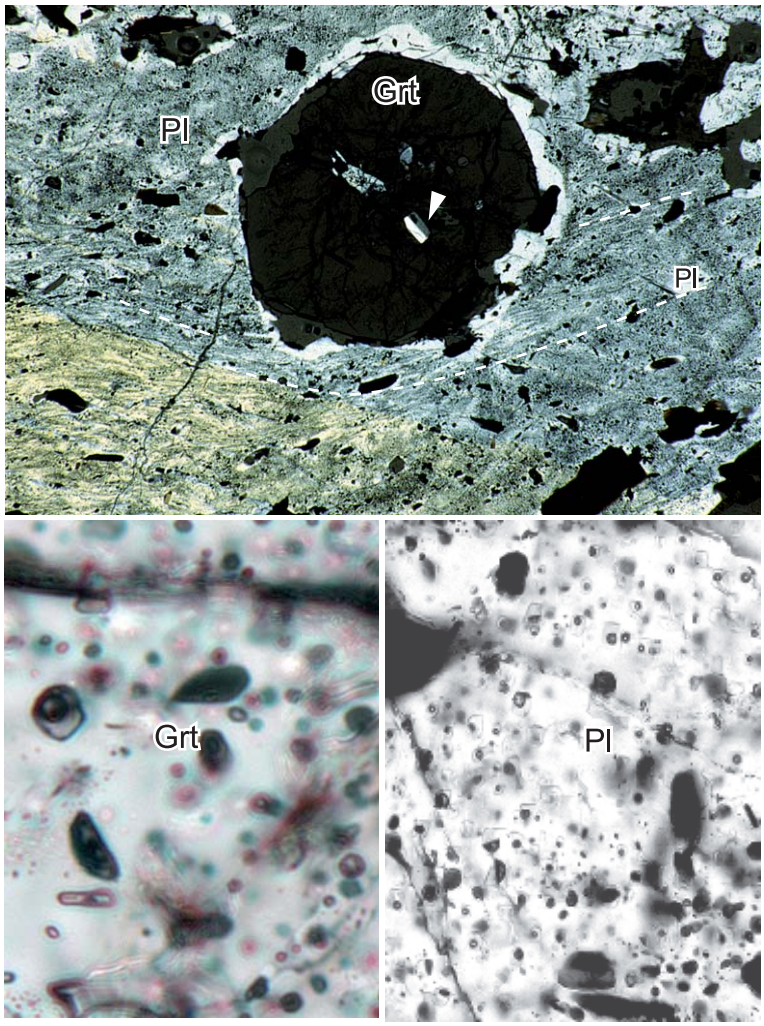

FIG. 3-19. **a)** Porphyroblast of garnet with melt inclusions (enlarged in **b)**) surrounded and enclosed by plagioclase. The garnet includes a Carlsbad-twinned plagioclase (arrow). The plagioclase contains an internal foliation deflecting around garnet, outlined by graphite and melt inclusions (enlarged in **c)**). Crossed polars; width of field 20 mm.
b) close-up of garnet core containing many melt inclusions. Plane-polarized light; width of field 80 μm.
c) close-up of plagioclase containing many melt inclusions and graphite (black). Plane-polarized light; width of field 0.2 mm.

zones, and the redeposition of new garnet and biotite at the strain shadows. Dissolution was probably promoted by the movement of melt away from high-strain zones in the direction along the foliation planes which anastomose around the crystals of garnet. A similar example is observed in quartzofeldspathic enclaves from El Hoyazo, where intensely foliated domains consisting mainly of fibrolitic sillimanite and melt, alternate with layers that have a more granoblastic microstructure (Fig. 3-20a). Also the origin of highly oriented sillimanite folia in these rocks is syn-anatectic, as indicated by the presence of melt inclusions in the lenticular crystals of quartz that are elongate parallel to the foliation (Fig. 3-20b). All the above microstructures demonstrate that the enclaves were not involved in a "static" or contact-melting type of environment, but that melting occurred when the crust was deforming as a coherent body, in a regional-scale process.

The identification of a syn-anatectic deformation in the enclaves demonstrates that the enclaves can provide unique pieces of information about the actual state and dynamic behavior of the partially melted crust. In connection with defining the pathways that the melt followed as it escaped from its residuum, it has been observed that in the most residual, feldspar-poor samples, the intergranular melt is preferentially located on thin, layer-parallel folia, whereas glass-filled fractures oriented at a high angle to the foliation are less common (Figs. 3-1c, 3-5). This supports the conclusion of Cesare *et al.* (1997) that, on a length-scale of up to tens of centimetres, deformation-assisted escape of melt occurred by flow parallel to lithological anisotropies.

It should be noted that the proposition that the deformation recorded by the microstructures in the enclaves occurred before their fragmentation

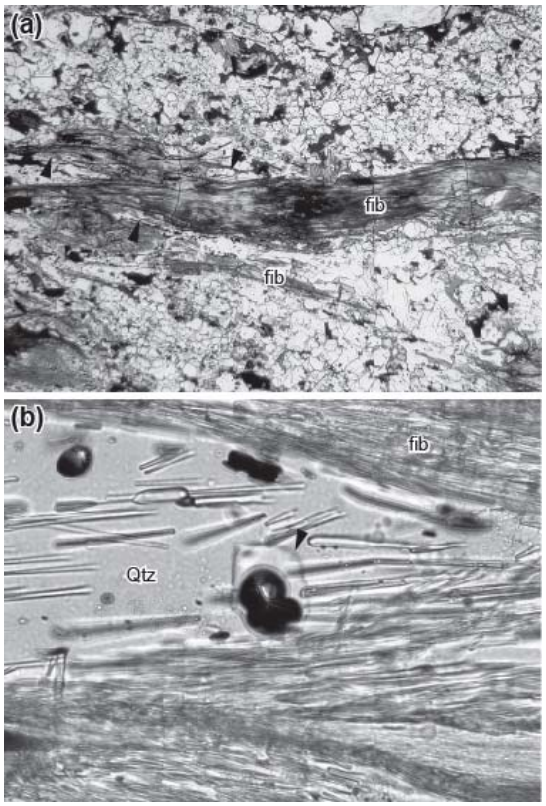

FIG. 3-20. **a)** Quartzofeldspathic enclave with a fibrolite-rich, intensely oriented layer in the central part of the image. Thinner fibrolite folia anastomose in the left-hand side (arrows). Plane-polarized light; width of field 3 mm. **b)** Enlargement of a lenticular quartz crystal wrapped by sillimanite folia. The quartz contains a melt inclusion (arrow). Plane-polarized light; width of field 80 μm.

and inclusion in the lava is not contradicted by the presence of the static microstructures that are present in some of the enclaves that were studied and which have been described above (*e.g.*, biotite-melting reactions and cordierite–spinel coronae after garnet). In fact, the latter microstructures are late with respect to the foliation, and are interpreted as having formed after fragmentation of the metapelite and its entrainment in the lava as enclaves, and during the time which the enclaves were resident in the magma chamber prior to eruption (Álvarez-Valero *et al.* 2007).

CONCLUSIONS

Unfortunately, rocks such as those described in this chapter seem to be very rare in nature, but a careful and focused reinvestigation of outcrops of S-type felsic volcanic rocks is likely to reveal (many) further occurrences. For example, crustal enclaves, xenoliths and xenocrysts with many similarities to those of the NVP occur at Lipari (Eolian islands, Italy; Barker 1989), where garnet and andalusite contain primary melt inclusions (Clarke *et al.* 2005).

Along with the drawback of being rare, enclaves and xenoliths also suffer from the major uncertainty on the location and nature of their source, and from their small size, that may prevent extrapolation of the results obtained from them to regional scale; this may lead one to question their relevance for the overall understanding of anatexis.

Despite these problems intrinsically related to being fragments of rock in "foreign" magmas, the case studies summarized above should suffice to indicate that information from enclaves represents an important complement to field-based studies of migmatite complexes and experimental simulation of crustal melting.

ACKNOWLEDGEMENTS

I wish to thank A. Acosta-Vigil, F. Ferri, and L. Tajcmanova for critically reading this paper, and E. Sawyer for review and for inviting me to take part in this workshop on migmatites. Financial support from Italian MIUR (PRIN 2005-047810) and C.N.R. (Euromargins ESF Eurocore)

REFERENCES

ACOSTA-VIGIL, A., CESARE, B., LONDON, D. & MORGAN, G.B.VI (2007): Microstructures and composition of melt inclusions in a crustal anatectic environment: the metapelitic enclaves within El Hoyazo dacites, SE Spain. *Chem. Geol.* **237**, 450-465.

ÁLVAREZ-VALERO, A.M. & KRIEGSMAN, L.M. (2007): Crustal thinning and mafic underplating beneath the Neogene Volcanic Province (Betic Cordillera, SE Spain): evidence from crustal xenoliths. *Terra Nova* **19**, 266-271.

ÁLVAREZ-VALERO, A.M., CESARE, B. & KRIEGSMAN, L.M. (2005): P-T paths in crustal enclaves: Examples from the Neogene Volcanic Province, Spain. *Geochim. Cosmochim. Acta* **68**, A665-A665 Suppl. S.

ÁLVAREZ-VALERO, A.M., CESARE, B. & KRIEGSMAN, L.M. (2007): Formation of spinel-cordierite-feldspar-glass coronas after garnet in metapelitic xenoliths: Reaction modelling and geodynamic implications. *J. Metamorph. Geol.* **25**, 305-320.

BARKER, D. S. (1987). Rhyolites contaminated with metapelite and gabbro, Lipari, Aeolian Islands, Italy: products of lower crustal fusion or of assimilation plus fractional crystallization? *Contrib. Mineral. Petrol.,* **97**, 460–472.

BODNAR, R.J. & STUDENT, J.J. (2006): Melt inclusions in plutonic rocks: petrography and microthermometry. *In:* Melt Inclusions in Plutonic Rocks (J.D. Webster, *ed.*) Min. Assoc. Can. Short Course **36**, 1-25.

BRAUN, I. & KRIEGSMAN, L.M. (2001): Partial melting in crustal xenoliths and anatectic migmatites: a comparison. *Phys. Chem. Earth, A* **26**, 261-266.

BROWN, M. (2007): Crustal melting and melt extraction, ascent and emplacement in orogens: mechanisms and consequences. *J. Geol. Soc. London* **164**, 709-730.

CESARE, B. (1999) Multi-Stage pseudomorphic replacement of garnet during polymetamorphism: 2. Algebraic analysis of mineral assemblages. *J. Metamorphic Geol*. **17**, 735-746.

CESARE, B. (2000): Incongruent melting of biotite to spinel in a quartz-free restite at El Joyazo (SE Spain): Textures and reaction characterization. *Contrib. Mineral. Petrol.* **139**, 273-284.

CESARE, B. & GÓMEZ-PUGNAIRE, M.T. (2001): Crustal melting in the Alborán domain: constraints from the xenoliths of the Neogene Volcanic Province. *Phys. Chem. Earth, A* **26**, 255-260.

CESARE, B. & MAINERI, C. (1999): Fluid-present anatexis of metapelites at El Joyazo (SE Spain): constraints from raman spectroscopy of graphite. *Contrib. Mineral. Petrol.* **135**, 41-52.

CESARE, B., SALVIOLI MARIANI, E. & VENTURELLI, G. (1997): Crustal anatexis and melt extraction in the restitic xenoliths at El Hoyazo (SE Spain). *Mineral. Mag.* **61**, 15-27.

CESARE, B., GÓMEZ-PUGNAIRE, M.T., SANCHEZ-NAVAS, A. & GROBETY, B. (2002): Andalusite - sillimanite replacement (Mazarrón - SE Spain): microstructural and TEM study. *Am. Mineral.* **87**, 433-444.

CESARE, B., CRUCIANI, G. & RUSSO, U. (2003a): Hydrogen deficiency in Ti-rich biotite from anatectic metapelites (El Joyazo - SE Spain): crystal-chemical aspects and implications for high-temperature petrogenesis. *Am. Mineral.* **88**, 583-595.

CESARE, B., GÓMEZ-PUGNAIRE, M.T. & RUBATTO, D. (2003b): Residence time of S-type anatectic magmas beneath the Neogene Volcanic Province of SE Spain: a zircon and monazite SHRIMP study. *Contrib. Mineral. Petrol.* **146**, 28–43.

CESARE, B., MARCHESI, C., HERMANN, J. & GÓMEZ-PUGNAIRE, M.T. (2003c): Primary melt inclusions in andalusite from anatectic graphitic metapelites: Implications for the position of the Al_2SiO_5 triple point. *Geology* **31**, 573-576.

CESARE, B., MELI, S., NODARI, L. & RUSSO, U. (2005): Fe^{3+} reduction during biotite melting in graphitic metapelites: another origin of CO_2 in granulites. *Contrib. Mineral. Petrol.* **149**, 129-140.

CESARE, B., MAINERI, C., BARON TOALDO, A., PEDRON, D. & ACOSTA-VIGIL, A. (2007): Immiscibility between carbonic fluids and granitic melts during crustal anatexis: a fluid and melt inclusion study in the enclaves of the Neogene Volcanic Province of SE Spain. *Chem. Geol.* **237**, 433-449.

CESARE, B., SATISH-KUMAR, M., CRUCIANI, G., POCKER, S. & NODARI, L. (2008): Formation of glass-bearing spinel-cordierite-feldspars coronas after garnet in metapelitic xenoliths. Reaction modelling and geodynamic implications. *Am. Mineral.* **93**, 327-338.

CLARKE, D.B., DORAIS, M., BARBARIN, B., BARKER, D., CESARE, B., CLARKE, G.L., BAGHDADI, S.E., FÖRSTER, H-J., GAETA, M., GOTTESMAN, B., JAMIESON, R.A., KONTAK, D.J., KOLLER, F., GOMES, C.L., LONDON, D., MORGAN, G.B., NEVES, L., PATTISON, D.R.M., PEREIRA, J., PICHAVANT, M., RAPELA, C.W., RENNO, A.D., RICHARDS, S., ROBERTS, M., ROTTURA, A., SAAVEDRA, J., SIAL, A.N., TOSSELI, A.J., UGIDOS, J.M., UHER, P., VILLASECA, C., VISONA, D., WHITNEY, D.L., WILLIAMSON, B. & WOODWARD, H.H., (2005). Occurrence and origin of andalusite in peraluminous felsic igneous rocks. *J. Petrol.* **46**, 441-472.

CLEMENS, J. D. (2006): Melting of the continental crust: fluid regimes, melting reactions and source-rock fertility. *In*: Evolution and Differentiation of the Continental Crust (M. Brown and T. Rushmer, *eds*.) Cambridge University Press, 297-331.

DIDIER, J. AND BARBARIN B. (1991): The different type of enclaves in granites: Nomenclature. *In*: Enclaves and Granite Petrology (J. Didier & B.

Barbarin, *eds.*), Developments in Petrology **13**, 19-23.

DIDIER, J. & MAURY, R.C. (1991): The outstanding contribution of Alfred Lacroix to the study of enclaves in magmatic rocks. *In*: Enclaves and Granite Petrology (J. Didier & B. Barbarin, *eds.*), Developments in Petrology **13**, 25-32.

DOWNES, H., BEARD, A. & HINTON, R. (2004): Natural experimental charges; an ion-microprobe study of trace element distribution coefficients in glass-rich hornblendite and clinopyroxenite xenoliths. *In*: Trace Element Fingerprinting: Laboratory Studies and Petrogenetic Processes (S.Y. O'Reilly & R. Vannucci, *eds.*) Lithos **75**, 1-17.

FAURE, F., TROILLIARD, G., MONTEL, J.M. & NICOLLET, C. (2001): Nano-petrographic investigation of a mafic xenolith (Maar de Beaunit, Massif Central, France). *Eur. J. Mineral.* **13**, 27-40.

FERRI, F., BURLINI, L., CESARE, B. & SASSI, R. (2007): Seismic properties of lower crustal xenoliths from El Hoyazo (SE Spain): Experimental evidence up to partial melting. *Earth Planet. Sci. Lett.* **253**, 239-253.

FISHER, G.W. (1989): Matrix analysis of metamorphic mineral assemblages and reactions. *Contrib. Mineral. Petrol.* **102**, 69-77.

FOSTER, C.T. (1986) Thermodynamic models of reactions involving garnet in a sillimanite/ staurolite schist. *Mineral. Mag.*, **50**, 427-439.

FRENCH, B.M. (1964): Graphitization of organic material in a progressively metamorphosed Precambrian iron formation. *Science* **146**, 917-918.

GRANT, J.A. (1985): Phase equilibria in partial melting of pelitic rocks. *In:* High Temperature Metamorphism and Crustal Anatexis (J.R. Ashworth and M. Brown, *eds.*) Unwin Hyman, London, 105-144.

GUERNINA, S. & SAWYER, E.W. (2003): Large-scale melt-depletion in granulite terranes; an example from the Archean Ashuanipi Subprovince of Quebec. *J. Metamorphic Geol.* **21**, 181-201.

GUPTA, L.N. & JOHANNES, W. (1982): Genetic model for the stromatic migmatites of the Rantasalmi-Sulkava area, Finland. *J. Petrol*, **27**, 521-539

HOLDAWAY, M.J. (1971): Stability of andalusite and the aluminosilicate phase diagram. *Am. J. Science* **271**, 97-131.

HOLLAND, T. & POWELL, R. (2001): Calculation of phase relations involving haplogranitic melts using an internally consistent thermodynamic dataset. *J. Petrol.* **42**, 673-683.

HOLNESS, M.B. (2008): Decoding migmatite microstructures. *In* Working with Migmatites (E.W. Sawyer & M. Brown, eds.). *Mineral. Assoc. Canada, Short Course* **38**, x-x+22.

HOLTZ, F., BEHRENS, H., DINGWELL, D.B. & JOHANNES, W. (1995): Water solubility in haplogranitic melts. Compositional, pressure and temperature dependence. *Am. Mineral.* **80**, 94-108.

JOHANNES, W. & HOLTZ, F. (1996): Petrogenesis and experimental petrology of granitic rocks. (W. Johannes & F. Holtz, *eds.*) Minerals and Rocks Series Vol. 22. XIII, Berlin: Springer-Verlag, 335 p.

KENAH, C. & HOLLISTER, L.S. (1983) Anatexis in the Central Gneiss Complex, British Columbia. In: Migmatites, Melting and Metamorphism (Atherton and Gribble, *eds.*), Proceedings of the Geochemical Group of the Mineralogical Society, Shiva Geology Series, 142-162.

KRETZ, R., 1983, Symbols for rock-forming minerals: *Am. Mineral*. **68**, 277-279.

KRIEGSMAN, L.M. & HENSEN, B.J. (1998): Back reaction between restite and melt: Implications for geothermobarometry and pressure-temperature paths. *Geology* **26**, 1111-1114.

LE BRETON, N. & THOMPSON, A.B. (1988): Fluid-absent (dehydration) melting of biotite in metapelites in the early stages of crustal anatexis. *Contrib. Mineral. Petrol.* **99**, 226-237.

MONTEL, J.M. & VIELZEUF, D. (1994): Partial melting of metagreywackes. Part 2. Compositions of minerals and melts. *Contrib. Mineral. Petrol.* **128**, 176-196.

NAIR, R. & CHACKO, T. (2002): Fluid-absent melting of high-grade semi-pelites; P-T constraints on orthopyroxene formation and implications for granulite genesis. *J. Petrol.* **43**, 2121-2142.

NIXON, P.H. (1987): Mantle Xenoliths. (P.H. Nixon, *ed.*), New York: John Wiley, 844p.

PATIÑO-DOUCE, A.E. & JOHNSTON, A.D. (1991): Phase equilibria and melt productivity in the pelitic system; implications for the origin of peraluminous granitoids and aluminous granulites. *Contrib. Mineral. Petrol.* **107**, 202-218.

PATTISON, D.R.M. (1992): Stability of andalusite and sillimanite and the Al_2SiO_5 triple point; constraints from the Ballachulish aureole, Scotland. *J. Geology* **100**, 423-446.

PERINI G., CESARE B., GÓMEZ-PUGNAIRE M.T., GHEZZI, S., TOMMASINI S. Armouring effect in decoupling Sr-Nd isotopes during disequilibrium crustal melting: the case study of frozen migmatites from El Hoyazo and Mazarrón, SE Spain. *Eur. J. Mineral*., in press.

ROEDDER, E. (1984): Fluid inclusions (P.H. Ribbe, *ed.*) Rev. Mineral. **12**, 646 p.

RUBIE, D.C. AND BREARLEY, A.J. (1990) A model for rates of disequilibrium melting during metamorphism. In: High Temperature Metamorphism and Anatexis (Ashworth and Brown, *eds*.), Unwin-Hyman Ltd, 57–86.

SALVIOLI MARIANI, E., RENZULLI, A., SERRI, G., HOLM, P.M. & TOSCANI, L. (2005): Glass-bearing crustal xenoliths (buchites) erupted during the Recent activity of Stromboli (Aeolian Islands). *Lithos* **81**, 255-277.

SAWYER, E.W. (1987): The role of partial melting and fractional crystallization determining discordant migmatite leucosome compositions. *J. Petrol.* **28**, 445-473.

SOBOLEV, V.S. & KOSTYUK, V.P. (1975): Magmatic crystallization based on a study of melt inclusions. *Fluid Incl. Res.* **9**, 182-253 (translated from original publication in Russian).

SOLAR, G.S. & BROWN, M. (2001): Petrogenesis of migmatites in Maine, USA; possible source of peraluminous leucogranite in plutons? *J. Petrol.* **42**, 789-823.

TSUCHIYAMA, A. (1986): Melting and dissolution kinetics: application to partial melting and dissolution of xenoliths. *J. Geophys. Res.* **91**, 9395-9406.

VERNON, R.H. (1987) Oriented growth of sillimanite in andalusite, Placitas-Juan Tabo area, New Mexico, U.S.A. *Can. J. Earth Sci.* **24**, 580–590.

VERNON, R.H. (2004): A practical guide to rock microstructure. Cambridge, Cambridge University Press, 594 p.

VERNON, R.H. (2007): Problems in identifying restite in S-type granites of southeastern Australia, with speculations on sources of magma and enclaves. *Can. Mineral.* **45**, 147-178.

VIELZEUF, D. & HOLLOWAY, J.R. (1988): Experimental determination of the fluid-absent melting relations in the pelitic system. *Contrib. Mineral. Petrol.* **98**, 257-276.

WEBSTER, J.D. (2006): Melt inclusions in Plutonic Rocks (J.D. Webster *ed.*) Min. Assoc. Canada, Short Course **36**.

WHITE, R. W., POWELL, R., AND HOLLAND, T. J. B. (2007) Progress relating to calculation of partial melting equilibria for metapelites. *J. Metamorphic Geol*. **25**, 511–527

ZECK, H.P. (1970): An erupted migmatite from Cerro de Hoyazo, SE Spain. *Contrib. Mineral. Petrol.* **26**, 225-246.

CHAPTER 4: DECODING MIGMATITE MICROSTRUCTURES

Marian B. Holness
Department of Earth Sciences, University of Cambridge,
Downing Street, Cambridge, CB2 3EQ
United Kingdom
E-mail: marian@esc.cam.ac.uk

INTRODUCTION

While centimetre-scale pockets and layers of solidified melt (*leucosomes*) are clearly visible in migmatites in the field, if most of the melt were drained from the rock, or if anatexis only produced small amounts of melt, information about the previous distribution of partial melt would be essentially confined to the grain scale. This contribution is concerned with these grain-scale records of partial melting.

Following Brodie *et al.* (2002) the term *microstructure* will be used to describe the spatial arrangement, relative size and internal features of grains, instead of the sometimes ambiguous *texture* which is commonly also used for preferred orientation (and is therefore synonymous with *microfabric*). However, in keeping with the extensive literature on the equilibrium geometry of melt-bearing and solid crystalline aggregates, the terms *textural equilibrium* and *textural maturation* respectively will be used to describe the lowest energy microstructure and the processes by which this microstructure is attained.

Quite apart from a central role in developing our understanding of the actual process of crustal melting (Brown 2007), the distribution of partial melts at the grain scale has been the subject of much recent attention due to its profound effect on rock rheology (Arzi 1978, van der Molen & Paterson 1979, Dell'Angelo & Tullis 1988, Davidson *et al.* 1994, Rutter & Neumann 1995, Rosenberg & Riller 2000) and importance to melt segregation (Brown 1994, Sawyer 2001, Marchildon & Brown 2002). Criteria for establishing the presence and distribution of former melt are based on evidence for the progress of known melt-producing reactions such as a consideration of the *P–T* conditions of metamorphism (were they sufficient to result in melting?). Microstructural evidence for particular melt-producing reactions, such as the presence of phases formed during incongruent melting, may also be used. Mineral grains formed during melting often grow with well-defined crystal faces (Figs. 4-1a, 4-2a; Kenah & Hollister 1983, Vernon & Collins 1988, Grant & Frost 1990, Brown 2001, Sawyer 2001, Marchildon & Brown 2003, White *et al.* 2004, Vernon 2004)). Planar growth faces are also a characteristic of grains crystallizing early from the liquid during solidification (Fig. 4-1c). Other microstructural evidence includes an assessment of the distribution of residual rocks left by almost complete extraction of melt (Kenah & Hollister 1983, Sawyer 1994), and symplectic replacement textures indicative of melting reactions operating in reverse during solidification (Fig. 4-1b; Ashworth & McLellan 1985, Nyman *et al.* 1995, Brown & Raith 1996, Hartel & Pattison 1996, Sawyer 1999, 2001, Kriegsman 2001, Waters 2001, Guernina & Sawyer 2003). Extensive back-reaction during cooling may, in some cases, result in the complete obliteration of evidence for grain-scale melt distribution (Sawyer 2001).

Other criteria are based on more general microstructural features in which no particular melting reaction is implicated. These include grain size (Ashworth & McLellan 1985), consideration of the proportion of inter-phase grain boundaries compared to those between grains of the same phase (Ashworth 1976, Dougan 1983), the presence of idiomorphic grains, which may be chemically zoned (Mehnert 1968, Dougan 1979, Platten 1982, Pattison & Harte 1988), granophyric intergrowths of quartz and feldspar (Fig. 4-1d; *e.g.,* Grant & Frost 1990, Harte *et al.* 1991, Holness & Watt 2002), and evidence for low viscosity flow (Sawyer 2001, Vernon 2000).

Further criteria for the former presence of melt are based on the similarity of some migmatite microstructures to experimentally produced, melt-bearing, texturally equilibrated microstructures (*e.g.,* Jurewicz & Watson 1985). Harte *et al.* (1991) suggested that highly cuspate single grains with low

Mineralogical Association of Canada Short Course 38, Quebec City, Quebec, p. 57-76

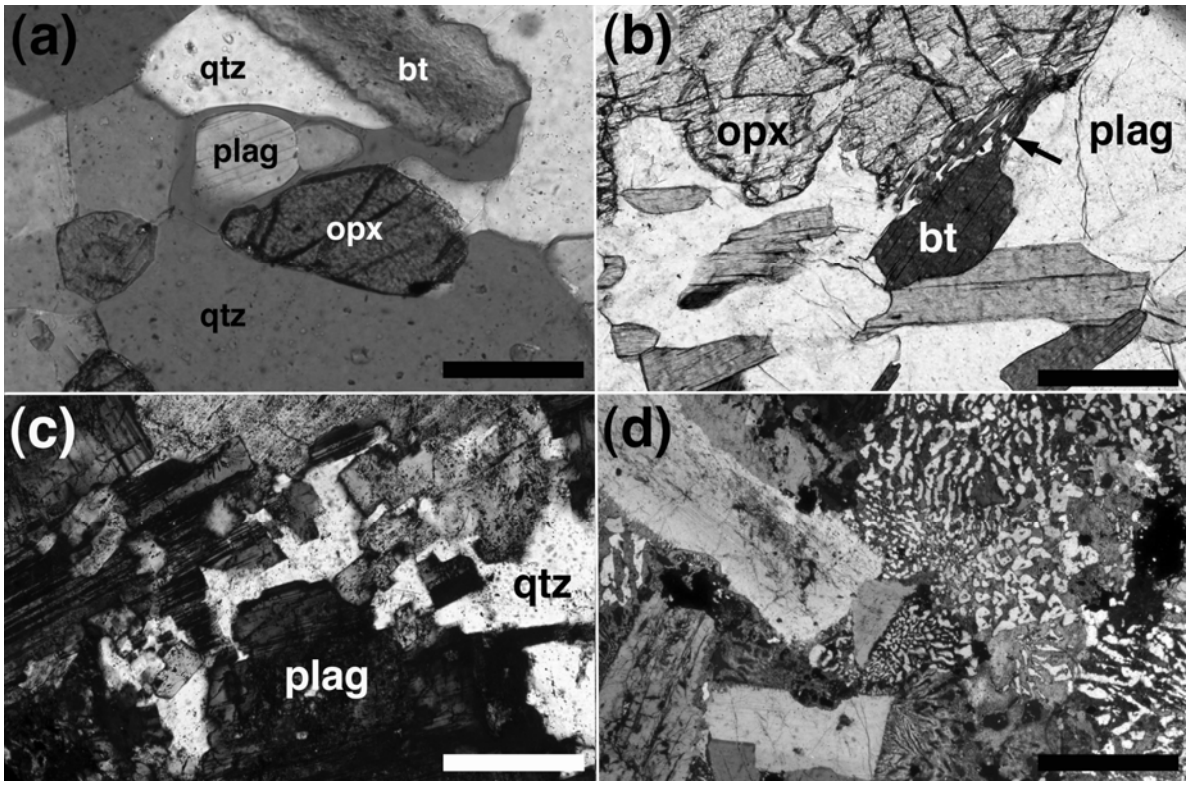

FIG. 4-1. **a)** Regionally metamorphosed granulite facies migmatite from the Ashuanipi Subprovince, Quebec, in which melt formed by biotite breakdown has been replaced by K-feldspar. Note the rounded shape of the peritectic orthopyroxene at the base of the grain in this image, while the upper surface, in contact with former melt, is faceted. Scale bar is 200 μm long. **b)** Biotite-quartz intergrowths (arrowed) formed at the margins of a peritectic orthopyroxene grain in a regionally metamorphosed metapelitic granulite, Ashuanipi Subprovince, Quebec. Scale bar is 200 μm long. **c)** Melt pool defined by oikocrystic quartz enclosing euhedral plagioclase crystals which grew directly from the liquid. Contact metamorphosed Lewisian Gneiss, Isle of Rum, Scotland. Scale bar is 200 μm long. (d) Granophyric intergrowths of quartz and feldspar, nucleating on euhedral crystals of plagioclase. Contact metamorphosed Lewisian Gneiss, Isle of Rum, Scotland. Scale bar is 1 mm long.

dihedral angles in pelitic migmatites grew within, and mimicked the shape of, texturally equilibrated melt-filled pores. This interpretation was foreshadowed by Platten (1982, 1983), who ascribed similar textures to the former presence of melt without making the connection with textural equilibrium, and has been embraced by all succeeding studies of grain-scale melt distributions in all but the shallowest crustal environments (*e.g.,* Holness & Clemens 1999, Rosenberg & Riller 2000, Sawyer 1999, 2001, Marchildon & Brown 2002). These features have been termed *interserts* (Rosenberg & Riller 2000), *pseudomorphs after melt* (Marchildon & Brown 2002) or *melt pseudomorphs* (*e.g.,* Harte *et al*. 1993, Clemens & Holness 2000, Brown 2001, Walte *et al*. 2005). Although the term *pseudomorph* is usually used to describe a grain of one mineral assuming the shape of another (literally having a "*false form*"), using it to describe a mineral grain assuming the shape of a liquid-filled pore is probably valid because the key indicator of the grain's origin is its shape.

THE IMPORTANCE OF TIMESCALE

Much has already been said in the excellent recent reviews of melt-related microstructures in migmatitic rocks (*e.g.,* Sawyer 1999, 2001, Marchildon & Brown 2002), although few (*e.g.,* Sawyer 2001) have emphasized the importance of the timescale of the anatectic event. Migmatites in regional terranes commonly form over millions of years with a polybaric temperature–time path. Conversely, the thermal history in contact aureoles is controlled by depth of emplacement and by the dimensions and temperature of the intrusion, resulting in typical anatectic timescales of years to hundreds of thousands of years. Since the final microstructures in solidified migmatites result from

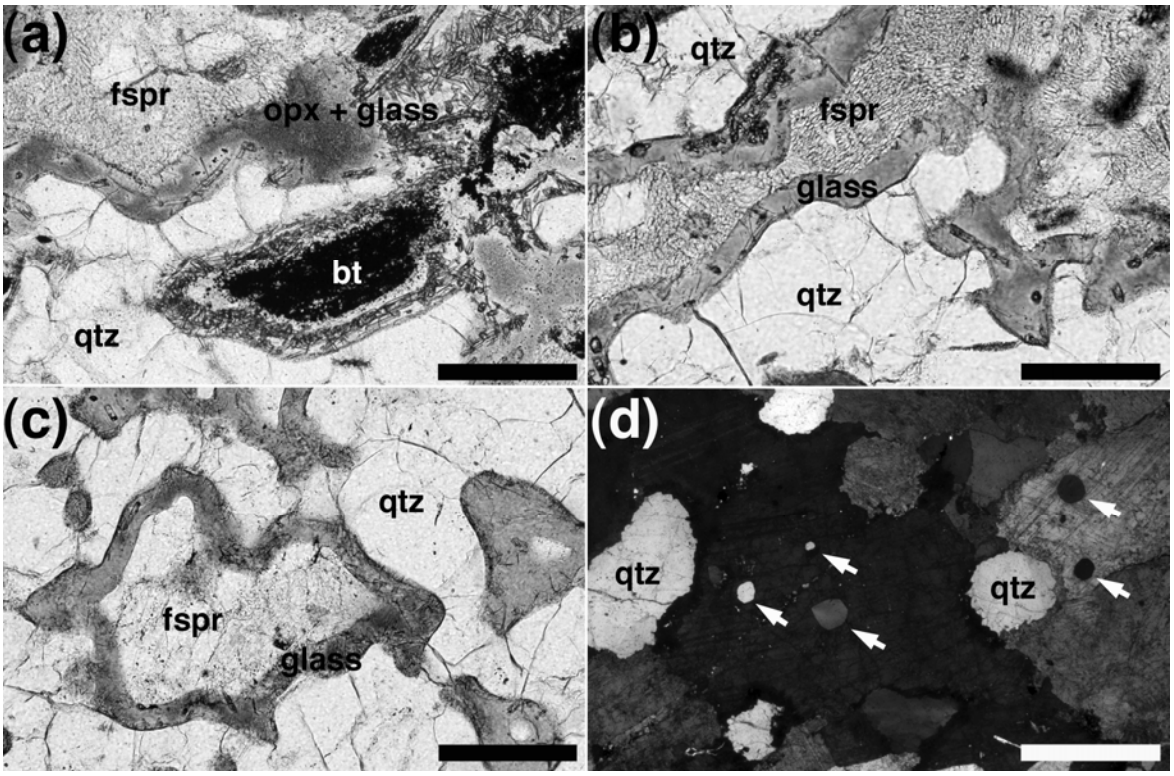

FIG. 4-2. **a)**, **b)** and **c)** Glassy melt rims in partially melted psammitic rocks from the pyrometamorphic aureole of the Glenmore Gabbro plug, Ardnamurchan, Scotland. Scale bars are 200 μm long. Note the acicular orthopyroxene grains which grew consequent to the breakdown of the biotite (**a** and **b**), and the parallelism of the grain boundary melt films, indicating no relative movement of liquid and residuum. **d)** Contact metamorphosed quartzofeldspathic Lewisian Gneiss, Isle of Rum, Scotland. Grain boundaries separating quartz and feldspar are undulose and lobate, due to solidification of melt rims. In contrast, isolated inclusions of quartz within individual feldspar grains have smooth outlines (arrows). Scale bar is 1 mm long.

the interplay between melting, melt-present textural equilibration, nucleation and growth during solidification, and the extent to which microstructures continue to evolve in the sub-solidus, the range of possible metamorphic timescales results in a wide range of microstructures.

Understanding microstructural evolution is complicated by the fact that most migmatites are fully crystalline. However, both the microstructures due to solidification, and the extent of sub-solidus microstructural modification, are a consequence of the timescale of the metamorphic event and, by understanding how microstructural development throughout the heating/cooling cycle can be affected by the rate at which it occurs, the petrographer should be able to read back from a thin section to obtain a picture of the anatectic event itself.

WHAT DOES MELTING LOOK LIKE?

Due to the long timescales involved it is almost impossible to find an anatectic rock preserving unmodified microstructures dating from the early stages of melting during regional metamorphism. Such primary textures are invariably overprinted. Access to the earliest stages of reaction, during which the melt distribution and geometry are totally controlled by the kinetics of reaction, is only possible via laboratory experiments and by examination of natural examples in which the timescales of the metamorphic event were short. Such natural examples are confined to the aureoles around small shallow magmatic conduits, and to crustal xenoliths and enclaves in volcanic rocks (see Cesare 2008).

The earliest signs of incipient melting are only preserved in very extreme environments or in experimental simulations. Brearley (1987a, 1987b) demonstrated that biotite breakdown during pyrometamorphism of a pelitic xenolith entrained in a dolerite dyke involved *in situ* melt generation. Over a matter of hours the temperature of biotite breakdown was overstepped by as much as 250˚C,

resulting in the development of a fine-grained mixture of melt, oxides, new biotite and spinel.

Once melting is well underway, progressively thicker melt films form, separating reactant grains (Figs. 4-2a, b, c; Butler 1961, Mehnert *et al.* 1973, Büsch *et al.* 1974, Paquet & François 1980, Platten 1982, 1983, Cesare 2000, Holness 1999, Braun & Kriegsman 2001, Holness & Watt 2002, Holness *et al.* 2005a, Acosta-Vigil *et al.* 2006). The distribution of these melt films can be used as an indicator for closed or open-system behavior. For example, if water were required for melting to occur (*e.g.,* for the reaction quartz + feldspar + H_2O = melt), melt film distribution would be controlled by the distribution of H_2O. Inclusions of feldspar within single quartz grains, that are isolated from the grain boundary network and thus can be kept dry, would only begin to melt once the temperatures had attained that of the H_2O-absent quartz + feldspar = melt reaction (Fig. 4-2d; Holness & Watt 2002, Holness *et al.* 2005a). The initial rate of growth of melt films may be rapid, followed by a much slower growth rate (Holness *et al.* 2005a). This slowing of the progress of melting may be a consequence of the consumption of the H_2O originally present on the grain boundaries, followed by slower H_2O-absent melting.

An important consequence of the volume increase associated with fluid-absent melting reactions, such as muscovite breakdown, is the development of overpressure which can result in hydrofracturing (Clemens & Mawer 1992). This is very clearly seen in experimental charges (Connolly *et al.* 1997, Rushmer 2001) and in some pyrometamorphic aureoles (Fig. 4-3; Holness & Watt 2002, Holness *et al.* 2005a).

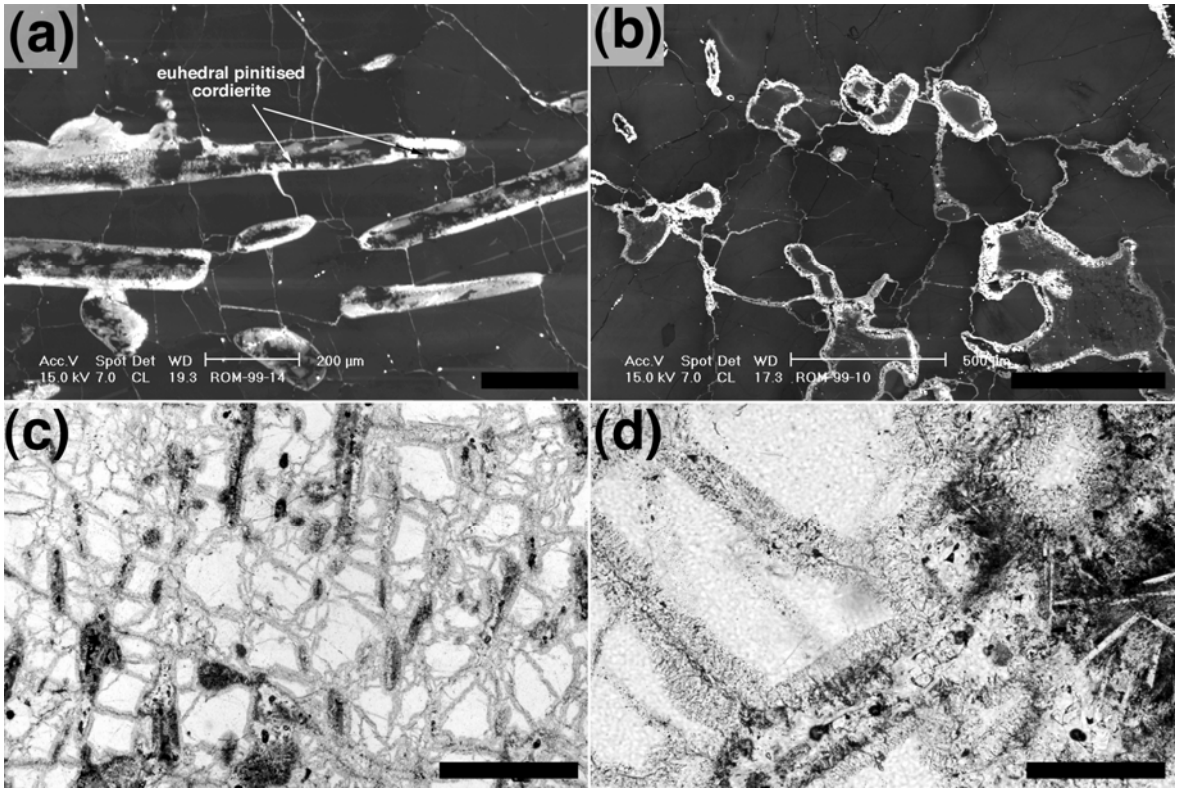

FIG. 4-3. **a)** Muscovite-bearing quartzite from the aureole of the Traigh Bhan na Sgurra sill, Mull, Scotland, imaged using cathodoluminescence. The elongate muscovite has been replaced by a fine-grained aggregate of cordierite, mullite and K-feldspar. Note the brightly luminescing cracks radiating from the reacted muscovite. Scale bar is 200 µm long. From Holness & Watt (2002). **b)** Feldspathic quartzite from the aureole of the Traigh Bhan na Sgurra sill, Mull, Scotland, imaged using cathodoluminescence. Brightly luminescing fine-grained granophyric intergrowths form on all quartz–feldspar grain boundaries, with radiating granophyre-filled cracks emanating from the melt rims. Scale bar is 500 µm long. From Holness & Watt (2002). **c)** Muscovite-bearing quartzite from the aureole of the Traigh Bhan na Sgurra sill, Mull, Scotland, plane-polarized light. Note the intense fracturing associated with partial melting. Scale bar is 1 mm long. **d)** Close-up of melt-filled cracks shown in (c). Note the quartz overgrowths on the crack walls. Scale bar is 200 µm long.

In aureoles around magmatic conduits, deviatoric stresses are small or absent and the melt remains *in situ*. Relative movement of solid and melt occurred once the melt fraction reached 40 vol.% in a pyrometamorphic aureole at Glenmore, but this may have been triggered by the onset of overpressure associated with fluid-absent melting (Holness *et al.* 2005a). However, around a longer-lived basaltic conduit on the Isle of Rum, quartzo-feldspathic rocks in which the melt fraction reached 95 vol.% still contain planar arrays of refractory accessory grains, preserving bedding and demonstrating the complete absence of melt movement (Holness 1999).

How relevant are these observations to deeper environments?

The unusual nature of shallow pyrometamorphic environments means we can see what melting looked like at the onset of reaction, but the trade-off is that we cannot confidently extrapolate to deeper and more long-lived systems in which timescales may be sufficient to permit other processes such as melting with small temperature oversteps, melt segregation/extraction and textural maturation. Thus, in regional metamorphic environments, microstructures that preserve information about the presence of melt occur principally in residual rocks. A further complication is that the microstructures preserved in these longer-lived systems reflect a much later stage when melting and melt segregation were in decline or finished (Sawyer 2001).

Although internally generated hydrofracturing during melting is commonly observed in pyrometamorphic aureoles (Fig. 4-3; Holness & Watt 2002, Holness *et al.* 2005a), there is little preserved microstructural evidence for hydrofracturing in the deep crust (Sawyer 1999). Watt *et al.* (2000) interpreted brightly luminescing planar features, forming a complex intra-grain network of fractures in quartz from granulite-facies migmatites, as healed melt-bearing fractures. If this interpretation is correct, the apparent absence of any major element signature in the fractures means that the melt was expelled completely from the fracture network. Given the complexity of the network and the absence of any preferred fracture orientation, complete expulsion of melt by compaction or shearing seems unlikely. It is possible the fractures contained only C–O–H fluids.

Holyoke & Rushmer (2002) demonstrated experimentally that the physical behavior of a melting rock depends also on the nature of the reaction. Melting associated with muscovite breakdown involves a burst of melt production over a short temperature interval, leading to fracturing. Conversely, biotite breakdown involves steadier melt production associated with a continually changing biotite composition. Melt has time to move along grain boundaries and there is a lower build-up of fluid overpressure. Microstructural and compositional evidence that slowly produced melt, such as that formed during regional granulite-facies metamorphism, has time to be drained continually from its source was provided by Sawyer (2001) and Guernina & Sawyer (2003).

If the melt-production rate is sufficiently low, the melt distribution can be controlled by the minimization of interfacial energies during textural maturation. Since textural maturation is a diffusive process it requires reaction and deformation rates to be commensurate with grain-boundary mass transport.

Texturally equilibrated melt geometries

Melt distribution in texturally equilibrated systems is controlled by the minimization of internal energies. The melt geometry and its interconnectivity are functions of melt fraction (*i.e.*, porosity, ϕ), the melt–solid dihedral angle (Θ), and the extent of anisotropy of interfacial energies. The population of dihedral angles is controlled by the balancing of the two interfacial energies involved: the grain boundary energy between the two grains of the same phase, γ_b, and the energy of the interface between the two different phases, γ_i (Fig. 4-4a). For isotropic materials Θ satisfies the relation:

$$\gamma_b = 2\gamma_i \cos\left(\frac{\Theta}{2}\right) \qquad (1)$$

(Smith 1948), but since most materials of interest to geologists have significant anisotropy of interfacial energy (*e.g.*, Kretz 1966, Vernon 1968, Laporte *et al.* 1997), the equation above is modified to incorporate torque forces which act to rotate interfaces to lower energy orientations (Herring 1951, Hoffman & Cahn 1972, Cahn & Hoffman 1974). This stabilizes planar interfaces at pore corners (*e.g.*, Kretz 1966, Vernon 1968, Laporte & Watson 1995, Cmíral *et al.* 1997, Lupulescu & Watson 1999, Laporte & Provost 2000), partial or complete faceting of pore walls (Wolf & Wyllie 1991, Laporte 1994, Laporte & Watson 1995,

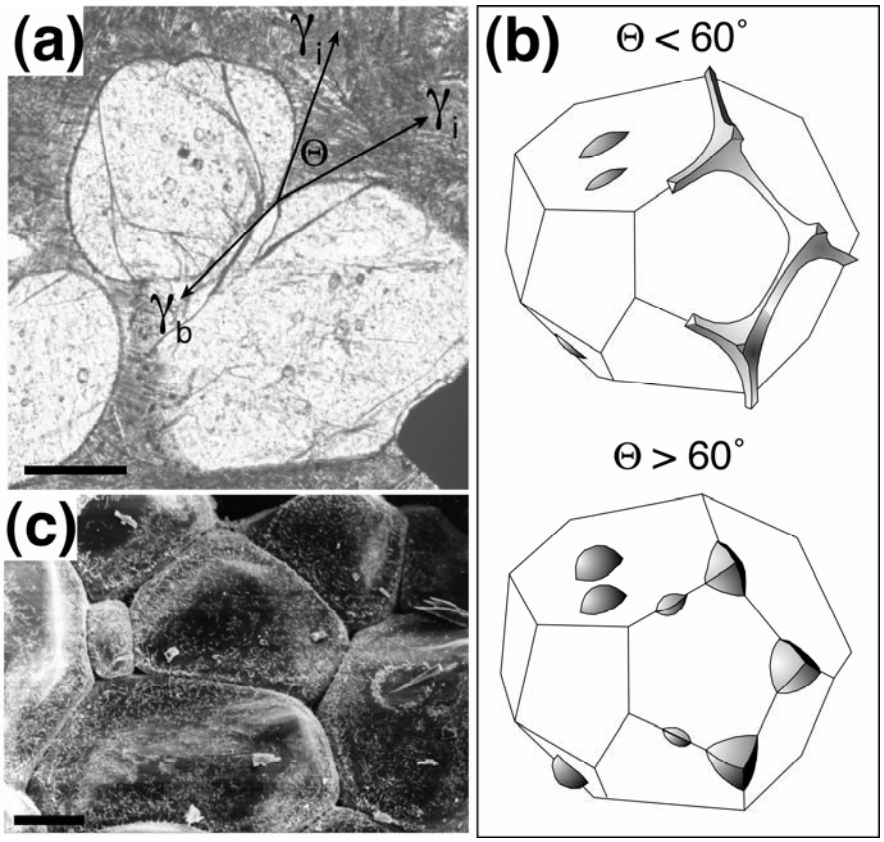

FIG. 4-4. **a)** Clumps of rounded pigeonite phenocrysts in textural equilibrium with the andesitic fine-grained matrix, Isle of Mull, Scotland (from Holness 2006). The direction of the force exerted by the energy of the grain boundary is labeled γ_b, while that of the interface between melt and solid is shown as γ_i. The dihedral angle, Θ, is a function of the balance between these two energies. Scale bar is 500 μm long. **b)** Cartoon showing the difference in equilibrium melt topology for dihedral angles above and below the critical value of 60˚ for melt interconnectivity. After Watson & Brenan (1987). **c)** Experimental charge in which quartz was equilibrated with brine at 9.4 kbar and 800˚C: the dihedral angle under these conditions is less than 60˚ (Holness 1992). Note the channels on all three-grain junctions. The small acicular crystals scattered on the quartz surface formed during the quench. Scale bar is 20 μm long.

Lupulescu & Watson 1999), and results in a range of possible equilibrium dihedral angles, depending on the relative orientation of the solid grains (Herring 1951, Laporte & Provost 2000).

For geologically relevant systems the melt–solid dihedral angle is less than 60˚ [see Holness (2006) for a recent review] with a standard deviation of ~15˚ (Laporte & Provost 2000, Holness 2006) so the equilibrium distribution is one of interconnected channels along three-grain junctions (Figs. 4-4b, c; Smith 1964, Beeré 1975, von Bargen & Waff 1986). For isotropic materials these channels remain open and interconnected even for vanishingly low porosities but, since all minerals are anisotropic to some extent, there is a threshold level for interconnectivity of $\phi <$ few vol.% (Wark & Watson 1998, Maumus *et al.* 2004, Price *et al.* 2006, Yoshino *et al.* 2006).

In a system in which liquid can move freely, complete textural equilibrium will entail melt flow until it reaches the minimum energy porosity. This ranges from 0 vol.% (at Θ > 60˚) to ~23 vol.%, or the porosity required for complete disaggregation, for Θ = 0˚ (Park & Yoon 1985, Cheadle 1989). For the likely range of melt–solid dihedral angles in geological systems (20–40˚, Holness 2006), the minimum energy porosity is 10–18 vol. % (Cheadle 1989).

Are crustal melt geometries controlled by textural equilibrium?

Much of our understanding of the process of textural maturation has been obtained from studies of fully solidified plutonic igneous rocks (Hunter 1987, Holness *et al.* 2005b, Higgins 2006). These show that textural maturation towards equilibrium

takes place in a series of stages, the earliest of which is the rotation of grain boundaries in the vicinity of three-grain junctions to achieve the equilibrium dihedral angle (Holness *et al.* 2005b, Higgins 2006). The melt geometry resulting from reaction will result only coincidentally in a melt–solid–solid junction with the equilibrium angle (20–40˚). For instance, melt films on inter-phase boundaries (Fig. 4-5a) will result in an initial angle at melt–solid–solid junctions of ~ 180˚, which is far from equilibrium. The greatest driving force for microstructural change is therefore likely to be present at these junctions, and will result in the rotation of large areas of grain boundary, in the manner of an opening or closing book, as the angle approaches the equilibrium value (Fig. 4-5b, Holness *et al.* 2005b).

As a consequence of the angle change, the grain boundaries in the vicinity of the pore corner develop a step-change in curvature. Since changes in mean curvature increase the energy of the interface, the pore wall must move in order to attain constant mean curvature, at least in isotropic systems (*e.g.*, Holness & Siklos 2000). There is thus a complex interplay between the gradually changing angle at the melt–solid–solid junction and the propagation of a change in grain boundary orientation and curvature further from the junction.

Since continuous films of liquid on grain boundaries are only stable for melt–solid dihedral angles of 0˚ (Smith 1964), thin films of melt will neck down to form strings of melt-filled lenses of a shape controlled by the dihedral angle (which is always > 0˚ for systems of geological interest). Melt-filled, intra-grain cracks formed by hydro-fracture will heal, leading to arrays of melt-filled inclusions with a shape controlled by the interfacial energies of the host crystal (Vernon 1968).

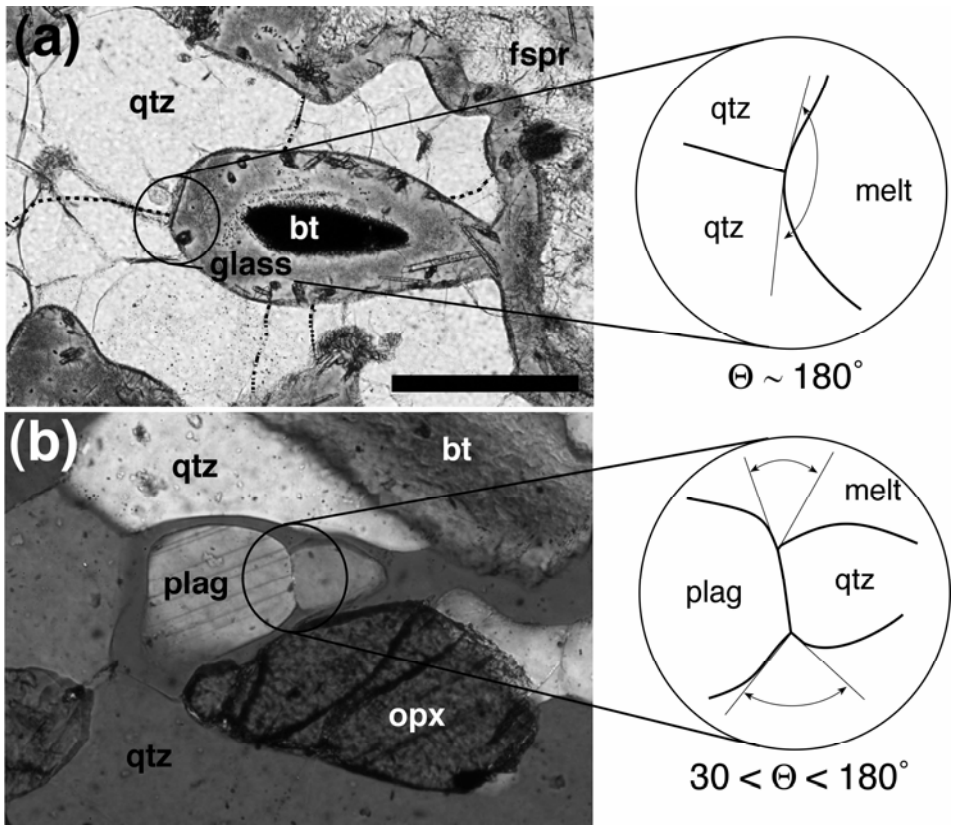

FIG. 4-5. **a)** Glassy, partially melted metasedimentary rock from the pyrometamorphic aureole of the Glenmore plug, Ardnamurchan. The scale bar is 200 μm long. The dihedral angle formed at grain boundaries (drawn as dotted lines in the quartz) truncated by melt films on intra-phase grain boundaries is of the order of 180˚. This is far from equilibrium and for lower rates of melting these angles decrease by the rotation of large areas of grain boundary. **b)** Textures formed during lower rates of melting are exemplified by the regionally metamorphosed metasedimentary granulite of the Ashuanipi sub-province, Quebec, in which melt films are pseudomorphed by K-feldspar. However, even at these low rates, the angle may not attain the equilibrium values (20–40˚). The angle highlighted here is of the order of 100˚. Scale bar is 200 μm long.

Considerations of the reduction in free energy tell us that textural equilibrium in a melt-present system in which the liquid is free to move will cause the infiltration of melt along previously dry three-grain junctions (Watson 1982). The rates of this process have been measured experimentally (Daines & Kohlstedt 1993, Hammouda & Laporte 2000), but we have no direct observations of the process on the grain-scale.

The extent to which the melt distribution will attain the minimum energy configuration partly depends on the balance of reaction rate and textural adjustment. A further important control on the extent of textural equilibrium is the rate and mechanism of deformation during anatexis. Although diffusion creep does not result in a melt distribution different from the static case, melt distribution during dislocation creep is markedly different. During dynamic recrystallization of experimental charges, actively migrating grain boundaries at all possible orientations contain transient films of melt which break up into isolated droplets once deformation ceases (Urai 1983, Jin *et al.* 1994). At higher differential stresses (≥ 100MPa for grain sizes 10–25 μm for olivine basalt aggregates), melt becomes concentrated in elongate pockets aligned subparallel to the maximum compressive stress (Ave'Lallemant & Carter 1970, Hirth & Kohlstedt 1995, Kohlstedt & Zimmerman 1996, Daines & Kohlstedt 1997).

Observation of microstructures in crustal rocks demonstrates that the balance between textural maturation, reaction and deformation is only very rarely in favor of textural equilibrium. Low dihedral angles at the corners of cuspate grains inferred to have pseudomorphed melt-filled pores (Holness & Clemens 1999, Rosenberg & Riller 2000 Clemens & Holness 2000, Marchildon & Brown 2002) only rarely form populations consistent with melt–solid textural equilibrium (Rosenberg & Riller 2000), and most commonly have angles intermediate between melt–solid and solid–solid equilibrium (Fig. 4-5b).

The low angles expected for equilibrated silicic melts (Holness 2006) should lead to most of the melt residing in tubular channels on three-grain junctions in a rock containing less than the disaggregation melt fraction of 23 vol.% (Smith 1964, Beeré 1975, Cheadle 1989). A cut through a texturally equilibrated rock with no preferred crystallographic orientation will result in these tubular channels being sectioned predominantly at high angles to their length, so the tubular melt pockets would generally appear as cuspate pockets at three-grain junctions. The dominance of elongate pockets on two-grain junctions, observed in regionally metamorphosed migmatites containing as little as 5 vol.% melt (Figs. 4-6a, b; Sawyer 1999, 2001) cannot be accounted for by random cross-sectioning (*cf.* Wark *et al.* 2003) but must reflect a dominance of grain-boundary melt films. Such melt films are commonly present on grain boundaries between reactant phases (Figs. 4-6a, b; Sawyer 2001) demonstrating an absence of textural equilibrium on the grain-scale in these rocks.

Examples in which melt does not reside predominantly on reactant grain boundaries are rarely described. Rosenberg & Riller (2000) described microstructures very similar to texturally equilibrated experimental charges in partially melted, non-deformed, granitic rocks from the aureole of the Sudbury Igneous Complex, and a similar example from the aureole of the Duluth Igneous Complex is shown in Fig. 4-6.

Rosenberg & Riller (2000), Sawyer (2000) and Marchildon & Brown (2003) describe an inferred grain-scale melt distribution in rocks undergoing shearing during anatexis which is dominated by melt-filled pockets aligned perpendicular to the elongation direction defined by mineral lineation fabrics. However, Sawyer (2001) and Guernina & Sawyer (2003) show that melt in more slowly deformed rocks tends to occupy pockets elongate parallel to rock foliation, consistent with the rock fabric being the first-order control on the grain-scale melt distribution in regional metamorphic rocks in which mica is both the source of the melt and also the fabric-defining mineral (Fig. 4-6b). Melt distribution thus appears to be controlled predominantly by reaction kinetics and externally imposed stresses, with texturally equilibrated distributions occurring only rarely.

What about rocks from which melt was extracted?

Melt distributions preserved in shallow, short-lived, pyrometamorphic aureoles are unlikely to be representative of those developed during regional metamorphism. Not only do longer timescales permit an approach to melt–solid textural equilibrium, but they also result in lower melting rates and melt migration. Given sufficient time, melt can be almost completely extracted to form a metatexite with a markedly different bulk composition to that of the protolith (Sawyer 2001).

Sawyer (2001) showed that relatively rapidly

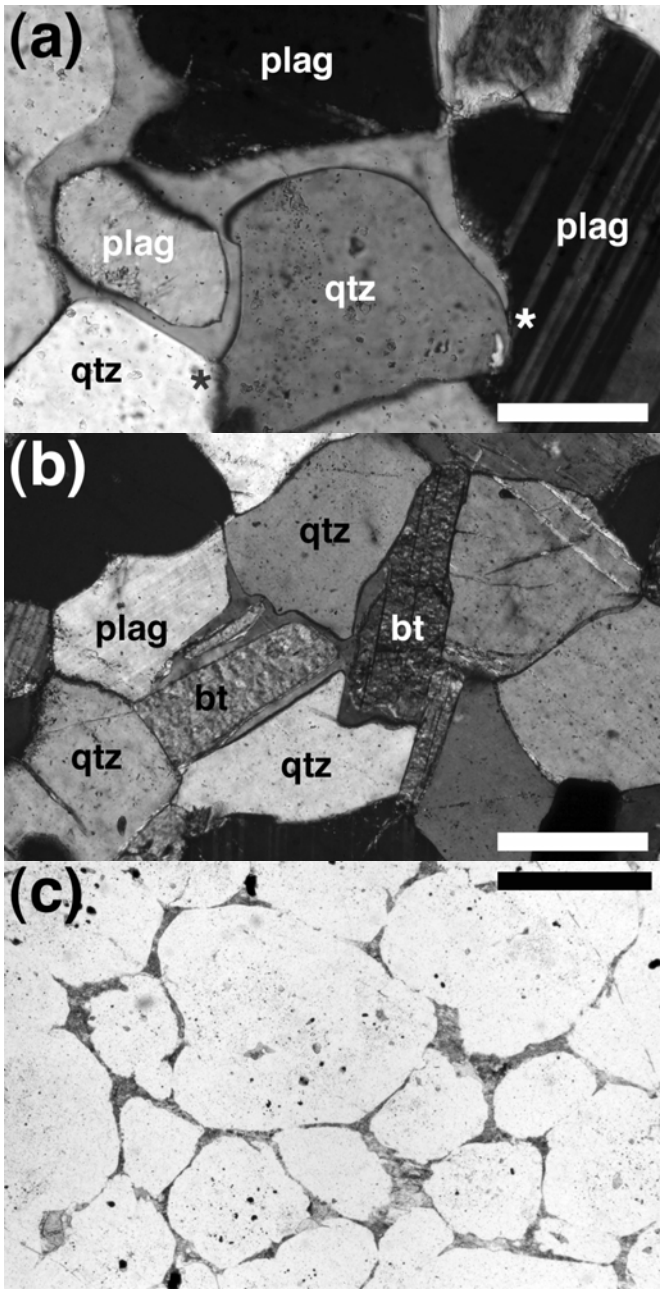

FIG. 4-6. **a)** and **b)** Photomicrographs of meta-sedimentary rocks from the regionally metamorphosed, granulite-facies, Ashuanipi Subprovince, Quebec, in which melting resulted from the reaction biotite + quartz + plagioclase = orthopyroxene + melt. The last vestiges of melt are now replaced by thin grain-boundary films of K-feldspar. Note how the films of former melt occur on grain boundaries between reactant phases.

a) The two melt–solid–solid junctions marked by asterisks are far from either melt–solid or solid–solid equilibrium. That marked with a black asterisk is ~100˚, while that marked by a white asterisk is ~30˚. Scale bar is 200 μm long.

b) Note how the melt is concentrated in films surrounding the biotite grains: if the biotite grains are aligned, defining a foliation, the melt films will be aligned too. Scale bar is 200 μm long.

c) Migmatite from the aureole of the Duluth Igneous Complex, Minnesota. The area shown comprises rounded quartz grains (white) separated by elongate and cuspate grains of plagioclase (grey). Each plagioclase grain is approximately one quartz grain diameter in length. Scale bar is 1 mm long.

cooled rocks (such as those in the aureole of the 2 kbar Duluth Igneous Complex) retain much of their partial melt, preserving an interconnected melt network in at least some parts of the rock volume (on a thin-section scale) and enabling identification of melt sources and sinks. In contrast, the residual melt left in melt-depleted regional granulite-facies rocks is much less than the total inferred to have been produced during the entire melting event: the remaining melt volume may even be less than that required for interconnectivity, demonstrating that slowly heated rocks with a low melt production rate can be almost completely drained. In the deep crust, such continual draining of melt during anatexis means that the melt fraction is never allowed to attain values at which the rock starts to deform easily, and this can result in the preservation of fine-scale sedimentary structures in rocks from which up to 40 vol.% melt has been extracted (Guernina & Sawyer 2003).

SOLIDIFICATION

The preceding discussion of the grain-scale distribution of melt during and after the melting process itself, especially that in deeper crustal environments, is entirely dependent on reading back through solidification, *i.e.,* on being able to infer the former presence of melt from the microstructure. This, in essence, is what migmatite petrography is about, as the rocks are always solid by the time we get to look at them. In this section I will show how the wide range of observed microstructures formed during solidification is a result of the interplay between nucleation and growth of solid phases, with the two dominant controls being the timescale of cooling and the size of the melt pockets.

Rapidly cooled rocks

If the cooling rate is sufficiently rapid, melt is quenched to glass, regardless of the size of the melt pocket – in such cases we can be confident of having an exact snapshot of the melt distribution. This is the case for some pyrometamorphic aureoles (Fig. 4-2; Butler 1961, Holness *et al.* 2005) and for crustal enclaves and xenoliths in volcanic rocks (Cesare 2008). As the cooling rate decreases, *i.e.,* as the depth of the melting event, or the diameter of the pluton (for contact metamorphism) increases, the extent to which the melt is undercooled before nucleation and growth of the solid phases is reduced. This results in a progression from supercooled melt (glass) through finely crystallized melt to an increasingly coarse polycrystalline aggregate. This can be illustrated by a consideration of quartzofeldspathic rocks from a series of contact aureoles.

Pyrometamorphism at 120 bar around the 50 m diameter gabbro plug at Glenmore, Ardnamurchan, resulted in glassy melt rims separating quartz and feldspar (Fig. 4-2; Butler 1961, Holness *et al*. 2005a). Solidification of melt rims in the arkose from the 150 bar aureole of the gabbro plug in Kinloch, Isle of Rum, and in pelite from the 600 bar aureole of the Traigh Bhan na Sgurra sill (Holness & Watt 2002) resulted in a fine granophyric intergrowth (Figs. 4-3, 4-7a). Solidification of melt rims in amphibolitic gneiss during heating by the Rum Igneous Complex at 100–200 bar formed a much coarser granophyric intergrowth, in which quartz paramorphs after tridymite are visible (Figs. 4-7b, c; Holness & Isherwood 2003).

If melt films on quartz–feldspar grain boundaries are cooled more slowly than those of the very shallow pyrometamorphic aureoles the granophyric intergrowths become much coarser-grained. If the grain size becomes commensurate with that of the melt film thickness the result is an aggregate of equigranular, equant grains of feldspar and quartz which has been termed a *string of beads texture* (Fig. 4-7d, Holness & Isherwood 2003) with randomly oriented individual grains. For lower nucleation rates, melt solidification may result in highly irregular quartz–feldspar grain boundaries, with each grain having highly cuspate and spiky extensions (Figs. 4-7e, f). This microstructure forms when both components of the melt film nucleated entirely on the side-walls, growing into the melt to form an intergrowth.

As the cooling rate decreases further, for larger or deeper contact aureoles, the extended timescale permits the onset of melt migration, resulting in the grain-scale draining of melt from its localized source and segregation into large pockets. The range of pore sizes now forms a further variable which controls solidification microstructures.

In the deeper parts of the contact aureole associated with the Rum Layered Suite (Holness & Isherwood 2003) and in that associated with the 3 kbar, 10 km diameter, Ballachulish Igneous Complex (Pattison & Harte 1988) solidification microstructures vary with the size of the melt-filled pockets. The largest pockets may be filled with granophyre (Fig. 4-1d), or by oikocrysts with abundant inclusions (Fig. 4-1c; Grant & Frost 1990, Harte *et al.* 1991, Pattison & Harte 1988). Thick films of melt are preserved as polycrystalline aggregates, while the smallest pores (the thinnest melt films and pockets bounded by three grains) are generally pseudomorphed by single crystals of the volumetrically minor phase (Fig. 4-6). These grains have lower dihedral angles against their walls than expected for solid-state textural equilibrium (*e.g.,* Harte *et al.* 1991, Holness & Clemens 1999, Rosenberg & Riller 2000, Marchildon & Brown 2002), and their neighbors have a rounded shape (Fig. 4-6c).

The mineral forming the pseudomorph is commonly different to that of the pore walls. For example, for quartz-dominated volumes it is feldspar which forms the pseudomorphs, while in feldspar-dominated volumes it is quartz (*e.g.,* Harte *et al.* 1991, Rosenberg & Riller 2000). Examples of quartz, alkali and plagioclase feldspar pseudomorphs are most common although other minerals (such as cordierite and biotite) may also form pseudomorphs. The pseudomorph may be

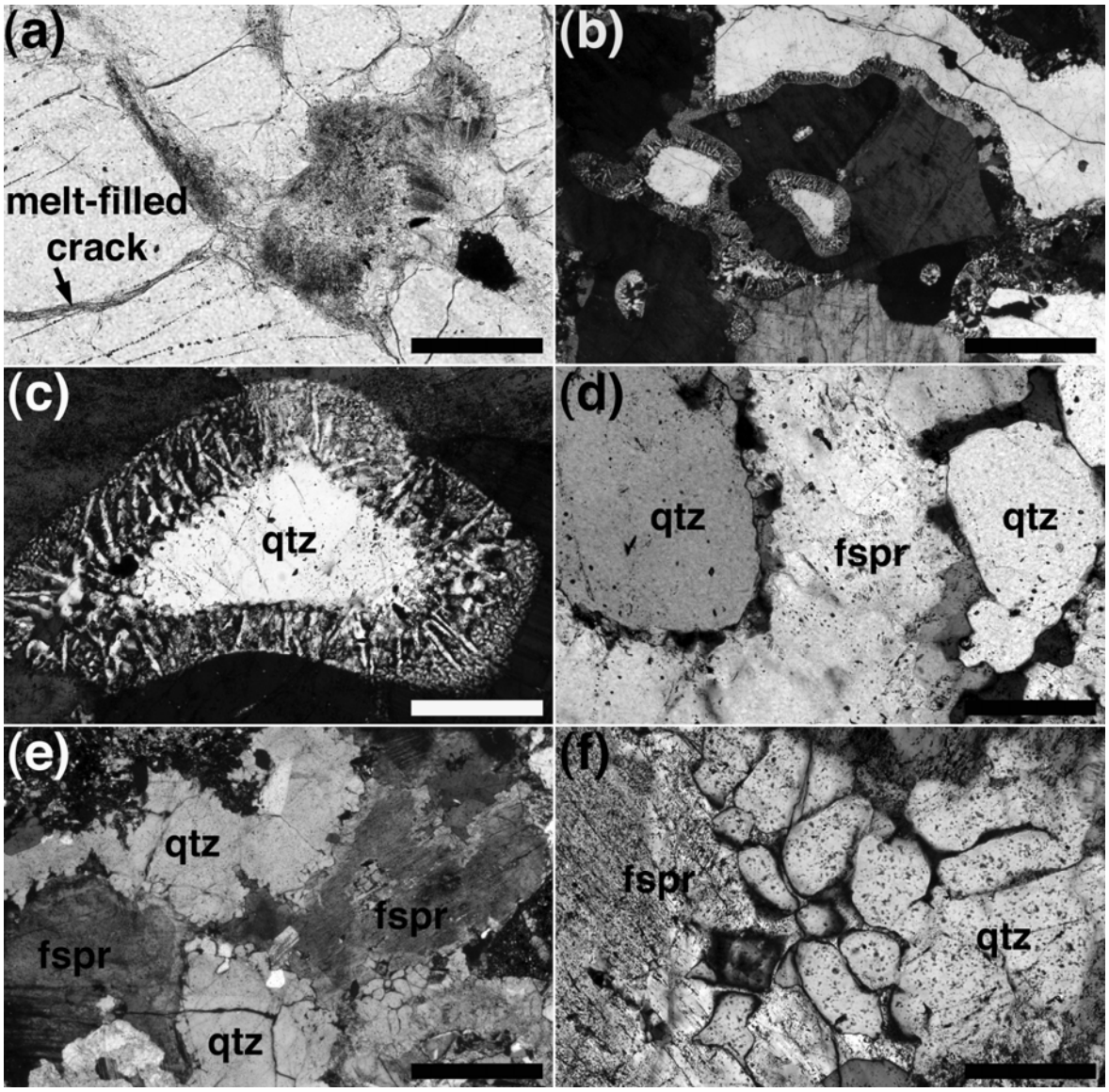

FIG. 4-7. A progression of solidification microstructures developed in grain boundary melt films in quartzofeldspathic rocks as the cooling rate decreases. **a)** Fine-grained granophyre replacing a melt pool in the 600 bar aureole of the Traigh Bhan na Sgurra sill, Isle of Mull, Scotland. Scale bar is 200 μm long. **b)** Continuous and parallel-sided granophyric rims separating quartz and feldspar in gneiss from the 100–200 bar aureole of the Rum Igneous Complex, Scotland. Scale bar is 1 mm long. **c)** Close-up view of the granophyric rim from b), showing the elongate quartz paramorphs after tridymite. Scale bar is 200 μm long. **d)** The string-of-beads texture developed in more slowly cooled, deeper parts of the Rum aureole. Quartz paramorphs after tridymite are absent. Scale bar is 200 μm long. **e)** Highly cuspate quartz-feldspar grain boundaries are the manifestation of coarse-grained intergrowths of quartz and feldspar, in which the two phases nucleate and overgrow the walls of the melt rim. Gneiss from the deeper parts of the Rum aureole. Scale bar is 1 mm long. **f)** Close-up of e) showing the highly cuspate grain boundaries. Scale bar is 200 μm long.

formed of the same mineral as the walls, albeit of a different composition (*e.g.,* plagioclase, Sawyer 2001).

The difference in solidification textures between larger pores, which crystallize to poly-minerallic aggregates, and small pores, in which single grains crystallize (Fig. 4-8), is observed within a single rock at a constant cooling rate: it probably reflects an increasing barrier to nucleation as the pore size becomes smaller (*e.g.,* Melia & Moffitt 1964, Cahn 1980, Scherer 1999, Putnis & Mauthe 2001).

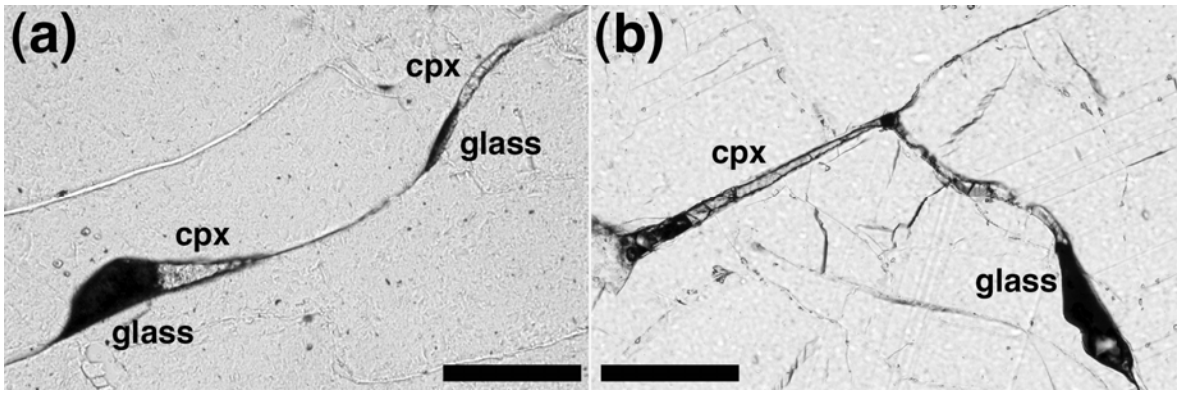

FIG. 4-8 – Gabbroic nodules entrained in a basaltic lava cone in Iceland, in which glass-filled pores between plagioclase grains are partially filled by clinopyroxene. Note how there is no overgrowth of the pore walls by plagioclase and that the clinopyroxene perfectly inherits the pore shape. Scale bar in both images is 200 μm long.

Very slowly cooled migmatites

As the depth of anatexis increases, granophyric intergrowths are confined to larger and larger melt pools. They are not found in deep crustal migmatites and appear to be essentially a shallow to mid-crustal phenomenon. Although their composition approximates that of the ternary minimum in the system Or–Ab–Qtz, the intergrowths are probably controlled more by kinetic factors such as the rates of growth and diffusion in the adjacent melt, together with a low nucleation rate for both minerals (see Vernon (2004) for a review of the literature).

For migmatites in the mid- to deep-crust, the texture is again controlled by the size of melt domains. Large melt pockets crystallize to poly-minerallic aggregates containing either the solid products of melting reactions (*e.g.,* White *et al*. 2004) or idiomorphic grains formed during cooling (Grant & Frost 1990, Sawyer 2001, Marchildon & Brown 2002), enclosed by single crystals of another phase. In contrast, small melt pockets (typically those bounded by fewer than 4 grains) may be partially or wholly filled by a single grain. Interstitial grains may form perfect pseudomorphs of a melt-filled pore (clinopyroxene in the gabbroic example shown in Figs. 4-8a, b), with no overgrowth of the pore walls even for a multiply-saturated liquid. Other examples show well-developed overgrowth of the pore walls, followed by growth of a single phase which infills the remaining porosity (the lower part of Fig. 4-9).

The composition of individual pseudo-morphs is unlikely to represent the composition of the last liquid in that particular pore: even if other components of the liquid solidified on the walls of the pore itself, some of the liquid must have solidified elsewhere, forming pseudomorphs themselves, overgrowths on existing grains or idiomorphic grains (in larger pores). The formation of single-grain pseudomorphs therefore necessitates mass transport through the pore network on at least the grain scale.

If averaged over a centimetre length-scale, the composition of all pseudomorphs approximates the residual liquid. Table 4-1 gives four examples of melt compositions estimated from point-counting melt pseudomorphs within single thin-sections of

TABLE 4-1 – Composition of pseudomorphed melt pockets, determined by point counting 1000 points per section. From Holness & Sawyer (2008).

	Melt fraction %	Quartz %	Plagioclase %	K-feldspar %	
Duluth aureole pelite	6.4	39	35	26	Sawyer (2001)
B1-384-20	25.1	45	24	31	
Ashuanipi metagreywacke **BL86-091A**	5.4	37	22	41	
Ashuanipi metagreywacke **BL86-044A**	4.2	37	26	37	

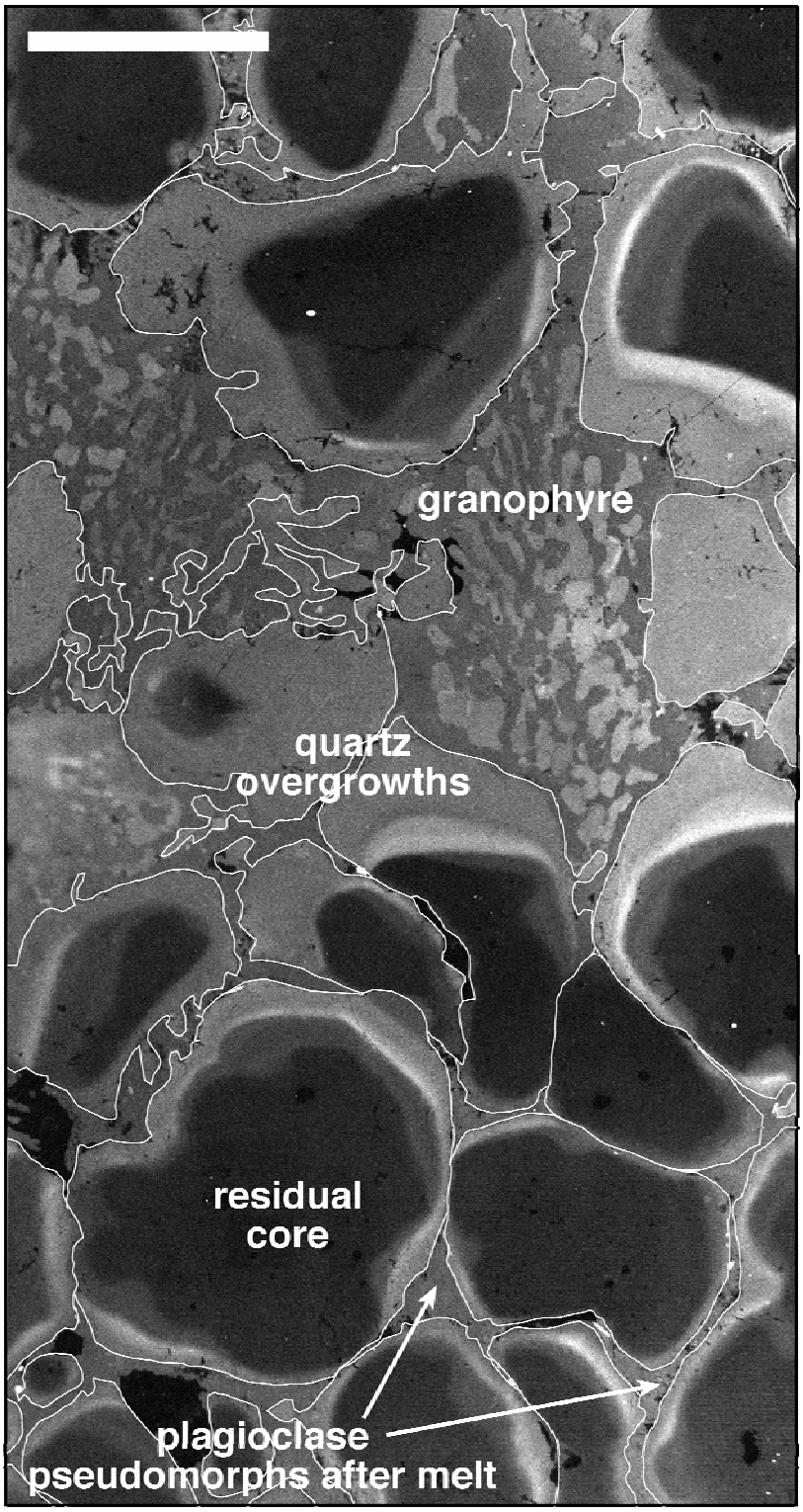

FIG. 4-9 – Partially melted quartz-rich layer of the Biwabik Iron Formation from the aureole of the Duluth Complex, Minnesota, imaged using cathodoluminescence, in which the dominant quartz grains are surrounded by elongate and cuspate plagioclase grains. The same rock is illustrated in Fig. 4-6c, under plane polarized light. The individual quartz grains are outlined in white and show four different growth zones. The dark interiors are residual material, while the three successive overgrowths record a period of increasing temperature (increasing CL brightness) with a final period during which the granophyric intergrowths grew in the large pore. The regions with a low melt fraction have a late-stage pore structure infilled by plagioclase. The scale bar is 1 mm long.

metasedimentary migmatites, and these are of broadly granitic composition. Overgrowth of residual grains depletes the bulk composition of the pseudomorphs in the phase which forms the dominant residual phase. The data from the two examples of granulite-facies metagreywacke from Ashuanipi in Table 4-1 show a low modal proportion of plagioclase, probably because plagioclase is the major residual phase in both these rocks: it is easy to underestimate the amount of overgrowth on residual plagioclase, especially if the overgrowths are thin or in optical continuity with their substrate.

A microstructural record charting progressive crystallization is rarely preserved in migmatites, but the partially melted Biwabik Iron Formation from the aureole of the Duluth Igneous Complex (Fig. 4-6c) displays a complex record of melting and solidification preserved in variations in cathodoluminescent intensity in quartz grains (Fig. 4-9). The sample comprises clinopyroxene and Fe-oxides (not shown in Figs. 4-6 or 4-9) together with rounded quartz grains separated by elongate and cuspate plagioclase. Brightness of quartz under cathodoluminescence approximately corresponds to temperature, as the main factor controlling the brightness is Ti content (Wark & Watson 2006, Wiebe *et al*. 2007, Holness & Sawyer 2008). The four generations of quartz shown in Fig. 4-9 record melting of the protolith (with the lobate margins of the dark cores reminiscent of partially resorbed reactant minerals in migmatites) with three subsequent overgrowths during solidification. The final stage of quartz growth is associated with the granophyre.

The quartz overgrowths on the residual grains bounding the largest pores show that at the metamorphic peak the melt was saturated only in quartz. This melt occupied ~20 vol.% of the quartz-rich regions (of which about half now comprises plagioclase) and formed much larger, scattered pockets (Fig. 4-9). During cooling, crystallization of kinetically favored overgrowths on the quartz residual grains proceeded until the liquid moved onto the quartz–feldspar cotectic. At this point feldspar nucleated, and quartz and feldspar grew simultaneously to form granophyric intergrowths in the largest pores. Cathodoluminescent images of the largest granophyre-filled pores demonstrate that undulose quartz–feldspar boundaries signify *simultaneous* crystallization of quartz and feldspar. In contrast, the smooth quartz–feldspar grain boundaries in the smaller pores denote *sequential* growth, with feldspar crystallizing alone following quartz overgrowth on the pore walls. The critical pore width at which this change occurs is ~250 μm (Fig. 4-9). In some pores quartz continued crystallizing until the pore was completely filled.

There is no kinetic barrier to overgrowth of pore walls. However, crystallization of the phases not forming the pore walls requires homogeneous nucleation. While this becomes easier as overgrowth on the walls proceeds (which increases the concentration of the other phases in the remaining liquid) the smaller the pore, the greater the supersaturation required for nucleation (Scherer 1999). Nucleation of the minor phase therefore cannot occur until the temperature has decreased to create sufficient undercooling to overcome the barrier to nucleation. Once nucleation does occur, the remaining melt in the small pores is replaced by plagioclase. In the case of the Biwabik migmatite, this plagioclase growth must have been accompanied by quartz overgrowth elsewhere, as the rejected quartz component migrated through the remaining porosity away from the growing plagioclase.

In the Biwabik rock, nucleation delay appears to have promoted melt–solid textural equilibration, and it is these equilibrium angles which are inherited by the plagioclase pore-filling. But in other migmatites, such as those shown in Figs. 4-6a and b, dihedral angles recorded by the pseudomorphs are far from melt–solid equilibrium (*e.g.*, Marchildon & Brown 2002). For these rocks this implies both that any nucleation delay was insufficient to promote melt–solid textural equilibration before the melt was replaced by the pseudomorph, and also that overgrowth on the walls of melt-filled pores in the vicinity of the pore corners was minimal.

WHAT HAPPENS IN THE SUB-SOLIDUS?

Although there has been little or no modification of peak microstructures in rocks metamorphosed at very shallow levels in the crust, the long timescales required for cooling and eventual exposure of rocks metamorphosed and melted at deeper levels in the crust inevitably result in significant post-peak modification of rocks from the mid to lower crust. The peak mineral assemblage may be (partially) replaced by one stable at lower temperatures and pressures. Another important effect is that of deformation: many microstructural records of partial melting, such as fine granophyric intergrowths and elongate

pseudomorphs of grain-boundary melt pockets, are highly susceptible to recrystallization during ductile deformation. Originally monocrystalline pseudomorphs of thin melt films become polygonized, and a clear record of melt distribution will only be preserved in rocks which have not undergone post-peak deformation. A less obvious, but no less important, change is that of solid-state textural maturation during which microstructures inherited from the melt-present stage evolve toward lower energy configurations. A common manifestation of this is grain-size coarsening during static annealing.

Textural maturation in the sub-solidus differs from the melt-present case in that mass transfer is dominated by grain boundary diffusion, which is significantly slower than transport through a liquid. Furthermore, while sub-solidus textural maturation of microstructures in monominerallic domains is rapid as it only necessitates mass movement *across* grain boundaries (Hunter 1987), equilibration in

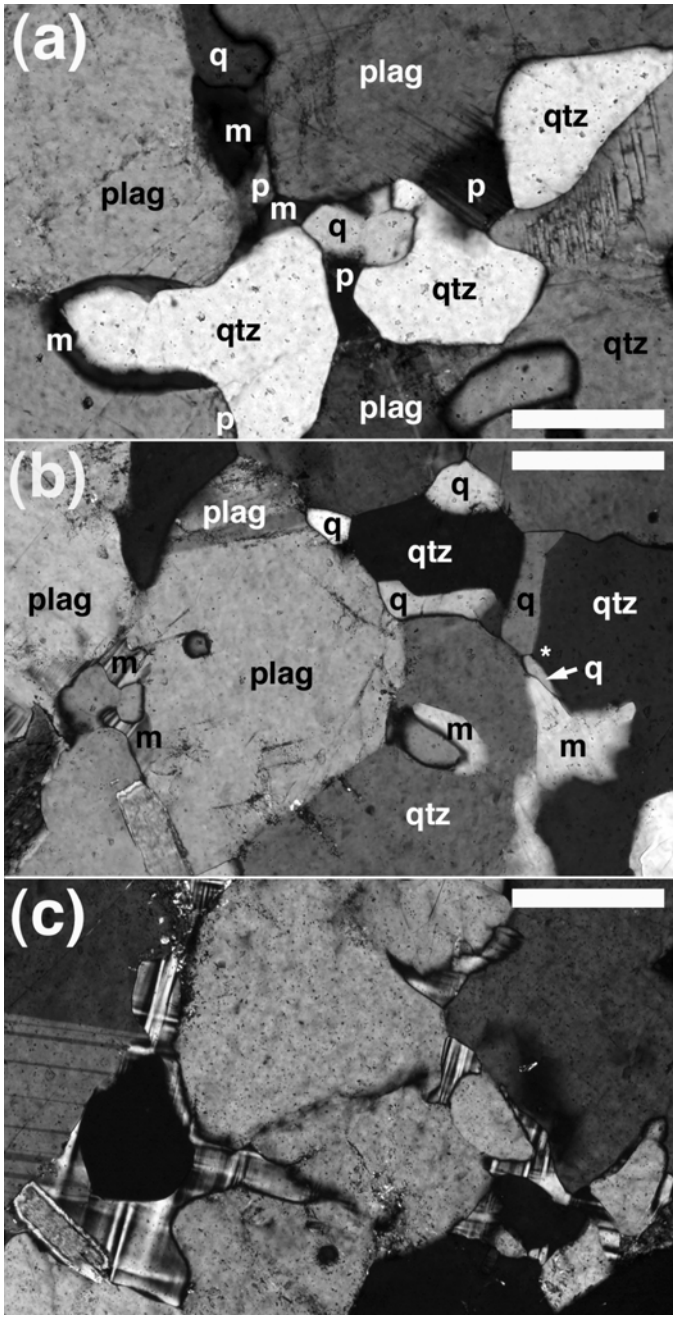

FIG. 4-10. Photomicrographs of an upper amphibolite-facies migmatite from the Opatica Subprovince, Quebec. **a)** An annealed and recrystallized string-of-beads texture developed between reacting grains of plagioclase and quartz. The larger grains are interpreted as residuum and are marked qtz and plag, while the crystals solidified from thick grain boundary melt films are marked m (microcline), q (quartz) and p (plagioclase). Note how the microcline within the thinner melt film (bottom left corner of image) is elongate and cuspate, in contrast to the quartz and plagioclase grains within the thicker melt film. The plagioclase residual grain at the top centre of the image has an extension with a slightly different extinction position separating the two white quartz residual grains. This extension nucleated on the plagioclase residual grain during solidification of the thick melt film. Scale bar is 200 μm long. **b)** String of quartz grains forming a polycrystalline pseudomorph of a grain boundary melt film. The asterisk marks the spot where four quartz grains meet, two of which are formed from solidified melt. The two three-grain junctions have 120˚ angles, demonstrating an approach to sub-solidus textural equilibrium. Note again that the microcline shapes are cuspate. Scale bar is 200 μm long. **c)** Microcline pseudomorphs after melt films. Note the cuspate shape denoting only a limited approach to sub-solidus textural equilibrium, although the dihedral angles at the corners have increased somewhat in the sub-solidus. Scale bar is 200 μm long.

polymineralic domains requires mass transport *along* grain boundaries and is therefore sluggish. It is rare to find completely equilibrated solid-state microstructures in polymineralic rocks.

Similarities in both the structure and composition of silicate phases lead to similar interfacial energies, and hence dihedral angles of ~120˚. Typical median angles fall in the range 100–140˚ (*e.g.,* Kretz 1966, Vernon 1968, 1970), with standard deviations of 10–20˚ (Vernon 1968, 1970). For the particular case of the grains that pseudomorph porosity there is potentially a large difference between the angle inherited by the pseudomorph (20–40˚ for melt–solid equilibrium) and that of solid-state equilibrium. Studies of gabbroic intrusions demonstrate that the closure temperature for the earliest (and thus most strongly driven) stage of textural maturation is of the order of 1000˚C for ~10 km diameter intrusions in the shallow (<2 kbar) crust (Holness *et al.* 2005, 2007). This demonstrates that *sub-solidus* textural maturation of anatectic rocks is not possible for shallow, short-lived events and is most likely to be important only for regional scale medium- to high-pressure migmatites.

Although published studies of dihedral angles at the corners of pseudomorphed pores in migmatites suggest that sub-solidus textural equilibrium is not generally achieved (Holness & Clemens 1999, Rosenberg & Riller 2000, Marchildon & Brown 2002), this conclusion is biased by the dominance of samples containing cuspate grains. A full assessment of the extent of sub-solidus textural equilibration of solidified melt-bearing rocks must include rocks in which melt-bearing microstructures are not as well preserved. Polycrystalline solidified melt films would be polygonized, perhaps having undergone some grain growth, and idiomorphic grains and cuspate interstitial grains would become rounded. Such structures are visible in the upper amphibolite-facies migmatites from the Opatica Subprovince in Quebec, thought to be the exhumed roots of an Archean mountain belt (Sawyer & Benn 1993). In the example shown in Fig. 4-10, recrystallised string-of-beads melt films display 120˚ junctions at intra-phase boundaries, and microcline pseudomorphs are rounded with high dihedral angles (Fig. 4-10). While this demonstrates that an approach to sub-solidus textural equilibrium can occur in slowly cooled migmatitic terranes, it is questionable whether melt-related microstructures could be recognizable with a closer approach to equilibrium than that shown by this sample. Recognition of the former presence of melt in more strongly equilibrated migmatites would be dependent on the presence of peritectic phases, a depleted bulk composition, and hand specimen or outcrop-scale features.

ACKNOWLEDGEMENTS

I am grateful to Ed Sawyer for inviting me to participate in the *Working With Migmatites* Short Course, and to his support and collaboration while researching for this project. Helpful reviews by Michael Higgins and Bernardo Cesare significantly improved an earlier version of this contribution.

REFERENCES

ACOSTA-VIGIL, A., LONDON, D. & MORGAN, G.B., VI (2006): Experiments on the kinetics of partial melting of a leucogranite at 200 MPa H_2O and 690–800˚C: compositional variability of melts during the onset of H_2O-saturated crustal anatexis. *Contrib. Min. Pet.* **151**, 539-557.

ARZI, A.A. (1978): Critical phenomena in the rheology of partially-molten rocks. *Tectonophysics* **44**, 174-184.

ASHWORTH, J.R. (1976): Petrogenesis of migmatites in the Huntly–Portsoy area, north-east Scotland. *Min. Mag*. **40**, 661-682.

ASHWORTH, J.R. & MCLELLAN, E.L. (1985): Textures. In *Migmatites* (Ashworth, J.R. ed.), Blackie, Glasgow. pp 180-203.

AVE'LALLEMANT, H.G. & CARTER, N.L. (1970): Syntectonic recrystallization of olivine and modes of flow in the upper mantle. *Geol. Soc. Amer. Bull*. **81**, 2203-2220.

BEERÉ, W. (1975): A unifying theory of the stability of penetrating liquid phases and sintering pores. *Acta Metall*. **23**, 131-138.

BRAUN I. & KRIEGSMAN, L.M. (2001): Partial melting in crustal xenoliths and anatectic migmatites: a comparison. *Phys. Chem. Earth*, **26A**, 261-266.

BREARLEY, A.J. (1987a): A natural example of the disequilibrium breakdown of biotite at high temperature: TEM observations and comparison with experimental kinetic data. *Min. Mag*. **51**, 93-106.

BREARLEY, A.J. (1987b): An experimental and kinetic study of the breakdown of aluminous biotite at 800˚C: reaction microstructures and mineral chemistry. *Bull. Minéral*. **110**, 513-532

BRODIE, K.H., FETTES, D., HARTE, B. & SCHMIDT, R. (2002): *Towards a unified nomenclature in metamorphic petrology. 3. Structural terms, including fault rocks.* A proposal on behalf of the IUGS Subcommision on the Systematics of Metamorphic Rocks. Recommendations. http://www.bgs.ac.uk/SCMR/docs/papers/paper_3.pdf

BROWN, M. (2001): Orogeny, migmatites and leucogranites: a review. *Proc. Indian Acad. Sci. (Earth Planet. Sci.)*, **110**, 313-336.

BROWN, M. (1994): The generation, segregation, ascent and emplacement of granite magma: the migmatite-to-crustally-derived granite connection in thickened orogens. *Earth Sci. Rev*. **36**, 83-130

BROWN, M. (2007) Crustal melting and melt extraction, ascent and emplacement in orogens: mechanisms and consequences. *J. Geol. Soc. Lond*. **164**, 709-730.

BROWN, M. & RAITH, M. (1996): First evidence of ultrahigh-temperature decompression from the granulite province of southern India. *J. Geol. Soc. Lond*. **153**, 819-822.

BÜSCH, W., SCHNEIDER, G. & MEHNERT, K.R. (1974): Initial melting at grain boundaries. Part II: melting in rocks of granodioritic, quartz dioritic and tonalitic composition. *Neues Jahrb. Mineral, Abhand.* **1974**, 345-370.

BUTLER, B.C.M. (1961): Metamorphism and metasomatism of rocks of the Moine Series by a dolerite plug in Glenmore, Ardnamurchan. *Min. Mag.* **32**, 866-897.

CAHN, J.W. (1980): Surface stress and the chemical equilibrium of small crystals: I. The case of the isotropic surface. *Acta Metall*. **28**, 1333-1338.

CAHN, J.W. & HOFFMAN, D.W. (1974): A vector thermodynamics for anisotropic surfaces, II. Application to curved surfaces. *Acta Metall.* **22**, 1205-1214.

CESARE, B. (2000): Incongruent melting of biotite to spinel in a quartz-free restite at El Joyazo (SE Spain): textures and reaction characterization. *Contrib. Min. Pet*. **139**, 273-284.

CESARE, B. (2008): Crustal melting: working with enclaves. *In* Working with Migmatites (E.W. Sawyer & M. Brown, eds.). *Mineral. Assoc. Canada, Short Course* **38**, 37-55.

CHEADLE, M.J. (1989): Properties of texturally equilibrated two-phase aggregates. *Unpublished PhD thesis, University of Cambridge*. pp. 166.

CLEMENS, J.D. & HOLNESS, M.B. (2000): Textural evolution and partial melting of arkose in a contact aureole: a case study and implications. *Electronic Geosci.* **5**, 4.

CLEMENS, J.D. & MAWER, C.K. (1992): Granitic magma transport by fracture propagation. *Tectonophysics* **204**, 339-360.

CMÍRAL, M., FITZ GERALD, J.D., FAUL, U.H. & GREEN, D.H. (1997): A close look at dihedral angles and melt geometry in olivine-basalt aggregates: a TEM study. *Contrib. Min. Pet.***130**, 336-345.

CONNOLLY, J., HOLNESS, M., RUBIE, D. & RUSHMER, T. (1997): Reaction-induced microcracking: an experimental investigation of a mechanism for enhancing anatectic melt extraction. *Geology* **25**, 591-594.

DAINES, M.J. & KOHLSTEDT, D.L. (1993): A laboratory study of melt migration. *Phil. Trans. Roy. Soc. London* **342A**, 43-52.

DAINES, M.J. & KOHLSTEDT, D.L. (1997): Influence of deformation on melt topology in peridotites. *J. Geophys. Res*. **102**, 10257-10272.

DAVIDSON, C., SCHMID, S.M. & HOLLISTER, L.S. (1994): Role of melt during deformation in the deep crust. *Terra Nova* **6**, 133-142.

DELL'ANGELO, L.N. & TULLIS, J. (1988): Experimental deformation of partially melted granitic aggregates. *J. Met. Geol*. **6**, 495-515.

DOUGAN, T.W. (1979): Compositional and modal relationships and melting reactions in some migmatitic metapelites from New Hampshire and Maine. *Am. J. Sci*. **279**, 897-935.

DOUGAN, T.W. (1983): Textural relations in melanosomes of selected specimens of migmatite pelitic schists: implications for leucosome-generating processes. *Contrib. Min. Pet*. **83**, 82-98.

GRANT, J.A. & FROST, B.R. (1990): Contact metamorphism and partial melting of pelitic rocks in the aureole of the Laramie anorthosite complex, Morton Pass, Wyoming. *Am. J. Sci*. **290**, 425-472.

GUERNINA, S. & SAWYER, E.W. (2003): Large-scale melt-depletion in granulite terranes: an example from the Archean Ashuanipi Subprovince of Quebec. *J. Met. Geol*. **21**, 181-201.

HAMMOUDA, T. & LAPORTE, D. (2000): Ultrafast mantle impregnation by carbonatite melts. *Geology* **28**, 283-285.

HARTE, B., PATTISON, D.R.M. & LINKLATER, C.M. (1991): Field relations and petrography of partially melted pelitic and semi-pelitic rocks. In *Equilibrium and kinetics in contact metamorphism: the Ballachulish Igneous Complex and its aureole*. (Voll, G., Töpel, J., Pattison, D.R.M., & Seifert, F., eds.). Springer-Verlag, Berlin. pp 181-210.

HARTE, B., HUNTER, R.H. & KINNY, P.D. (1993): Melt geometry, movement and crystallisation, in relation to mantle dykes, veins and metasomatism. *Phil. Trans. R. Soc. Lond*. **342A**, 1-21.

HARTEL, T.H.D. & PATTISON, D.R.M. (1996): Genesis of the Kapuskasing (Ontario) migmatitic mafic granulites by dehydration melting of amphibolite: the importance of quartz to reaction progress. *J. Met. Geol*. **14**, 591-611.

HERRING, C. (1951): Surface tension as a motivation for sintering. In *Physics of Powder Metallurgy* (KINGSTON, W.E., ed.), pp. 143-179. McGraw-Hill, New York.

HIGGINS, M.D. (2006): *Quantitative textural measurements in igneous and metamorphic petrology*, Cambridge University Press, UK, pp. 265.

HIRTH, J.G. & KOHLSTEDT, D.L. (1995): Experimental constraints on the dynamics of the partially molten upper mangle: deformation in the diffusion creep regime. *J. Geophys. Res*. **100**, 1981-2001.

HOFFMAN, D.W. & CAHN, J.W. (1972): A vector thermodynamics for anisotropic surfaces, I. Fundamentals and applications to plane surface junctions. *Surface Sci.* **31**, 368-388.

HOLNESS, M.B. (1992): Equilibrium dihedral angles in the system quartz–CO_2–H_2O–NaCl at 800˚C and 1–15 kbar: the effects of pressure and fluid composition on the permeability of quartzites. *Earth Planet. Sci. Lett.* **114**, 171-184.

HOLNESS, M.B. (1999): Contact metamorphism and anatexis of Torridonian arkose by minor intrusions of the Rum Igneous Complex, Inner Hebrides, Scotland. *Geol. Mag*. **136**, 527-542.

HOLNESS, M.B. (2006): Melt–solid dihedral angles of common minerals in natural rocks *J. Pet.* **47**, 791-800

HOLNESS, M.B. & CLEMENS, J.D. (1999): Partial melting of the Appin Quartzite driven by fracture-controlled H_2O infiltration in the aureole of the Ballachulish Igneous Complex, Scottish Highlands. *Contrib. Min. Pet*. **136**, 154-168.

HOLNESS, M.B. & ISHERWOOD, C. (2003): The aureole of the Rum Tertiary Igneous Complex, Inner Hebrides, Scotland. *J. Geol. Soc. London* **160**, 15-27.

HOLNESS, M.B. & SAWYER, E.W. (2008): On the pseudomorphing of melt in migmatites. Submitted to *Journal of Petrology*.

HOLNESS, M.B. & SIKLOS, S.T.C. (2000): Rates of textural equilibration in fluid-bearing systems: kinetic limitations to surface-energy controlled permeability. *Chem. Geol.* **162**, 137-153.

HOLNESS, M.B. & WATT, G.R. (2002): The aureole of the Traigh Bhan na Sgurra sill, Isle of Mull: reaction-driven micro-cracking during pyrometamorphism. *J. Pet.* **43**, 511-534.

HOLNESS, M.B., DANE, K., SIDES, R., RICHARDSON, C. & CADDICK, M. (2005a): Melting and melt segregation in the aureole of the Glenmore Plug, Ardnamurchan. *J. Met. Geol*. **23**, 29-43.

HOLNESS, M.B., CHEADLE, M.J. & MCKENZIE, D. (2005b): On the uses of changes in dihedral angle to decode late-stage textural evolution in cumulates. *J. Pet*. **46**, 1565-1583.

HOLNESS, M.B., TEGNER, C., NIELSEN, T.F.D. & STRIPP, G. (2007) A textural record of solidification and cooling in the Skaergaard Intrusion, East Greenland. *J. Pet*., in press.

HOLYOKE, C.W. III & RUSHMER, T. (2002): An experimental study of grain scale melt segregation mechanisms in two common crustal rock types. *J. Met. Geol*. **20**, 493-512.

HUNTER, R.H. (1987): Textural equilibrium in layered igneous rocks. In *Origins of Igneous Layering* (Parsons, I., ed.). Dordrecht: D. Reidel. pp. 473–503.

JIN, Z., GREEN, H.W. & ZHOU, Y. (1994): Melt topology in partially molten mantle peridotite during ductile deformation. *Nature* **372**, 164-167.

JUREWICZ, S.R. & WATSON, E.B. (1985): The distribution of partial melt in a granitic system: the application of liquid phase sintering theory. *Geochim. Cosmochim. Acta* **49**, 1109-1121.

KENAH, P. & HOLLISTER, L.S. (1983): Anatexis in the Central Gneiss complex, British Columbia. In *Migmatites, melting and metamorphism* (Atherton, M.P. & Gribble, C.D., eds.) Cheshire, England, Shiva, 142-162.

KOHLSTEDT, D.L. & ZIMMERMAN, M.E. (1996): Rheology of partially molten mantle rocks. *Ann. Rev. Earth Plan. Sci*. **24**, 41-62.

KRETZ, R. (1966): Interpretation of the shape of mineral grains in metamorphic rocks. *J. Pet.* **7**, 68-94.

KRIEGSMAN, L.M. (2001): Partial melting, partial melt extraction and partial back reaction in anatectic migmatites. *Lithos* **56**, 75-96.

LAPORTE, D. (1994): Wetting behavior of partial melts during crustal anatexis: the distribution of hydrous silicic melts in polycrystalline aggregates of quartz. *Contrib. Min. Pet.* **116**, 486-499.

LAPORTE D. & PROVOST, A. (2000): Equilibrium geometry of a fluid phase in a polycrystalline aggregate with anisotropic surface energies: Dry grain boundaries. *J. Geophys. Res.* **105**, 25937-25953.

LAPORTE, D. & WATSON, E.B. (1995): Experimental and theoretical constraints on melt distribution in crustal sources: the effect of crystalline anisotropy on melt interconnectivity. *Chem. Geol.* **124**, 161-184.

LAPORTE, D., RAPAILLE, C. & PROVOST, A. (1997): Wetting angles, equilibrium melt geometry, and the permeability threshold of partially molten crustal protoliths. In *Granite: From segregation of melt to emplacement fabrics*. (Bouchez, J.-L., Hutton, D.H. & Stephens, W.E., eds.) pp. 31-54. Kluwer Acad., Norwell, Mass.

LUPULESCU, A. & WATSON, E.B. (1999): Low melt fraction connectivity of granitic and tonalitic melts in a mafic crustal rock at 800˚C and 1 GPa. *Contrib. Min. Pet.* **134**, 202-216.

MARCHILDON, N. & BROWN, M. (2002): Grain-scale melt distribution in two contact aureole rocks: implications for controls on melt localization and deformation. *J. Met. Geol*, **20**, 381-396.

MARCHILDON, N. & BROWN, M. (2003): Spatial distribution of melt-bearing structures in anatectic rocks from Southern Brittany, France: implications for melt transfer at grain- to orogen-scale. *Tectonophysics* **364**, 215-235.

MAUMUS, J., LAPORTE, D. & SCHIANO, P. (2004): Dihedral angle measurements and infiltration property of SiO_2-rich melts in mantle peridotite assemblages. *Contrib. Min. Pet.* **148**, 1-12.

MEHNERT, K.R. (1968): *Migmatites and the Origin of Granitic Rocks*. Elsevier, Amsterdam.

MEHNERT, K.R., BÜSCH, W. & SCHNEIDER, G. (1973): Initial melting at grain boundaries of quartz and feldspar in gneisses and granulites. *Neues Jahrb. Mineral Monatsh.* **4**, 165-183.

MELIA, T.P. & MOFFITT, W.P. (1964): Crystallization from aqueous solution. *J. Colloid Sci*. **19**, 433-447.

NYMAN, M.W., PATTISON, D.R.M. & GHENT, E.D. (1995): Melt extraction during formation of K-feldspar + sillimanite migmatites, west of Revelstoke, British Columbia. *J. Pet*. **36**, 351-372.

PAQUET, J. & FRANÇOIS, P. (1980): Experimental deformation of partially melted granitic rocks at 600–900˚C and 250 MPa confining pressure. *Tectonophysics* **68**, 131-146.

PARK, H.H. & YOON, D.N. (1985): Effect of dihedral angle on the morphology of grains in a matrix phase. *Metall. Trans*. **16**, 923-928.

PATTISON, D.R.M. & HARTE, B. (1988): Evolution of structurally contrasting anatectic migmatites in the 3-kbar Ballachulish aureole, Scotland. *J. Met. Geol.* **6**, 475-494.

PLATTEN, I.M. (1982): Partial melting of feldspathic quartzite around late Caledonian minor intrusions in Appin, Scotland. *Geol. Mag*. **119**, 413-419.

PLATTEN, I.M. (1983): Partial melting of semi-pelite and the development of marginal breccias around late Caledonian minor intrusives in the Grampian Highlands of Scotland. *Geol. Mag*. **120**, 37-49.

PRICE, J.D., WARK, D.A., WATSON, E.B. & SMITH, A.M. (2006): Grain-scale permeabilities of faceted polycrystalline aggregates. *Geofluids* **6**, 302-318.

PUTNIS, A. & MAUTHE, G. (2001): The effect of pore size on cementation in porous rocks. *Geofluids* **1**, 37-41.

ROSENBERG, C.L. & RILLER, U. (2000): Partial melt topology in statically and dynamically recrystallized granite. *Geology* **28**, 7-10.

RUSHMER, T. (2001): Volume change during partial melting reactions: implications for melt extraction, melt geochemistry and crustal rheology. *Tectonophysics* **342**, 389-405.

RUTTER, E.H. & NEUMANN, D.H.K. (1995): Experimental deformation of partially molten Westerley Granite under fluid-absent conditions, with implications for the extraction of granitic magmas. *J. Geophys.Res*. **100**, 15697-15715.

SAWYER, E.W. (1994): Melt segregation in the continental crust. *Geology* **22**, 1019-1022.

SAWYER, E.W. (1999): Criteria for the recognition of partial melting. *Phys. Chem. Earth* **24**, 269-279.

SAWYER, E.W. (2000): Grain-scale and outcrop-scale distribution and movement of melt in a crystallising granite. *Trans. Roy. Soc. Ed.: Earth Sciences* **91**, 73-85.

SAWYER, E.W. (2001): Melt segregation in the continental crust: distribution and movement of melt in anatectic rocks. *J. Met. Geol*. **19**, 291-309.

SAWYER, E.W. & BENN, K. (1993): Structure of the high-grade Opatica Belt and adjacent low-grade Abitibi subprovince, Canada: an Archean mountain front. *J. Struct. Geol.* **15**, 1443-1458.

SCHERER, G.W. (1999): Crystallization in pores. *Cem. Concrete Res*. **29**, 1347-1358.

SMITH, C.S. (1948): Grains, phases and interfaces: an interpretation of microstructure. *Trans. Metall. Soc. AIME* **175**, 15-51.

SMITH, C.S. (1964): Some elementary principles of polycrystalline microstructure. *Metall. Rev*. **9**, 1-48.

URAI, J.L. (1983): Water-assisted dynamic recrystallization and weakening in polycrystalline bischoffite. *Tectonophysics* **96**, 125-157.

VAN DER MOLEN, I. & PATERSON, M.S. (1979): Experimental deformation of partially-melted granite. *Contrib. Min. Pet.* **70**, 299-318.

VERNON, R.H. (1968): Microstructures of high-grade metamorphic rocks at Broken Hill, Australia. *J. Pet*. **9**, 1-22.

VERNON, R.H. (1970): Comparative grain-boundary studies of some basic and ultrabasic granulites, nodules and cumulates. *Scot. J. Geol* **6**, 337-351.

VERNON, R.H. (2004): *A practical guide to rock microstructure*. Cambridge University Press, UK. 594 p.

VERNON, R.H. & COLLINS, W.J. (1988): Igneous microstructures in migmatites. *Geology* **16**, 1126-1129.

VON BARGEN, N. & WAFF, H.S. (1986): Permeability, interfacial areas and curvatures of partially molten systems: results of numerical computations of equilibrium microstructures. *J. Geophys. Res*. **91**, 9261-9276.

WALTE, N.P., BONS, P.D & PASSCHIER, C.W. (2005): Deformation of melt-bearing systems – insight from *in situ* grain-scale analogue experiments. *J. Struct. Geol*. **27**, 1666-1679.

WARK, D.A. & WATSON, E.B. (1998): Grain-scale permeabilities of texturally equilibrated, monomineralic rocks. *Earth Planet. Sci. Lett*. **164**, 591-605.

WARK, D.A. & WATSON, E.B. (2006): The TitaniQ: a titanium-in-quartz geothermometer. *Contrib. Min. Pet.* **152**, 743-754.

WARK, D.A., WILLIAMS, C.A., WATSON, E.B. & PRICE, J.D. (2003): Reassessment of pore shapes in microstructurally equilibrated rocks, with implications for permeability of the upper mantle. *J. Geophys. Res*. **108**, doi:10.1029/2001JB 001575.

WATERS, D.J. (2001): The significance of prograde and retrograde quartz-bearing intergrowth microstructures in partially melted granulite-facies rocks. *Lithos*, **56**, 97-110.

WATSON, E.B. (1982): Melt infiltration and magma evolution. *Geology* **10**, 236-240.

WATSON, E.B. & BRENAN, J.M. (1987): Fluids in the lithosphere, I: Experimentally determined wetting characteristics of CO_2–H_2O fluids and their implications for fluid transport, host rock physical properties, and fluid inclusion formation. *Earth Planet. Sci. Lett*. **85**, 497-515.

WATT, G.R., OLIVER, N.H.S. & GRIFFIN, B.J. (2000): Evidence for reaction-induced micro-fracturing in granulite facies migmatites. *Geology* **28**, 327-330.

WHITE, R.W., POWELL, R., & HALPIN, J.A. (2004): Spatially focussed melt formation in aluminous metapelites from Broken Hill, Australia. *J. Met. Geol*. **22**, 825-845.

WIEBE, R.A., WARK, D.A. & WATSON, E.B. (2007): Insights from quartz cathodoluminescence zoning into crystallization of the Vinalhaven granite, coastal Maine. *Contrib. Min. Pet.* in press.

WOLF, M.B. & WYLLIE, P.J. (1991): Dehydration-melting of solid amphibolite at 10 kbar – textural development, liquid interconnectivity and applications to the segregation of magmas. *Min. Pet.* **44**, 151-179.

YOSHINO, T., PRICE, J.D., WARK, D.A. & WATSON, E.B. (2006): Effect of faceting on pore geometry in texturally equilibrated rocks: implications for low permeability at low porosity. *Contrib. Min. Pet*. **152**, 169-186.

CHAPTER 5: INSIGHTS GAINED FROM THE PETROLOGICAL MODELING OF MIGMATITES: PARTICULAR REFERENCE TO MINERAL ASSEMBLAGES AND COMMON REPLACEMENT TEXTURES

Richard W. White
Institute of Geosciences, University of Mainz,
Mainz D55099,
Germany
E-mail: rwhite@uni-mainz.de

INTRODUCTION

The processes of high-grade metamorphism, partial melting and migmatite formation are intimately connected, with it being difficult to consider one in isolation of the others. Of particular importance is the relationship between the reactions that produce typical upper amphibolite and granulite-facies assemblages and the production of melt. Equally important, but less commonly considered, is the role of melt crystallization in the development of common retrograde assemblages and textures that are critical in the interpretation of *P–T* paths.

Silicate liquid or melt is an important constituent in most high-temperature reactions especially those involving a hydrous mineral (mica or amphibole) on the low-temperature side of the reaction. These reactions typically form both the high-grade anhydrous or near-anhydrous assemblages that typify granulite and are the main melt-producing reactions in crustal rocks.

Within this view there are some key points that can be made based on observation and the use of phase diagrams. These are:

1. As the melting reactions and those that produce high-temperature mineral assemblages are one and the same, the textural evolution of those assemblages will exert a first order control on the melting process and the spatial distribution of melt production.
2. The ability to model mineral assemblage evolution in high-grade metamorphic rocks provides key constraints on the production of melt as a function of pressure, temperature and, with adequate geochronology, time.
3. The presence of granulite facies assemblages in most rock compositions (particularly metasedimentary rocks) is consistent with the production and loss of melt regardless of whether evidence for the former presence of melt in these rocks (such as leucosomes) is preserved. That is, rocks that are not migmatites did not necessarily escape partial melting.
4. The crystallization of melt and the development of hydrous high-grade retrograde minerals and textures are intimately linked, with the cessation of high-*T* retrograde mineral growth commonly controlled by the final crystallization of melt.

With the advent of large internally consistent datasets (*e.g.,* Holland & Powell 1985, 1990, 1998, Berman 1988), sophisticated activity–composition methodologies (*e.g.,* Holland & Powell 1996a, 1996b; Powell & Holland 1993, 1999) and computer programs to utilize them (*e.g.,* THERMOCALC, Powell & Holland 1988, Perplex, Connolly 1990), quantitative mineral equilibria modeling of rocks has become relatively common. These methods allow us to build a theoretical mineral equilibria framework in which to investigate metamorphism including suprasolidus equilibria for migmatites.

In this chapter I outline the basic features of calculated phase diagrams for partially melted rocks and their use in the interpretation of migmatites. In addition, these diagrams are used to highlight the relationships between the evolution of the solid phases in terms of changing mineral assemblages and mineral proportions, and the formation and crystallization of melt. The common replacement and reaction textures seen in migmatites generally represent the only evidence of the changes that have occurred and provide vital constraints on migmatite evolution.

PHASE EQUILIBRIA MODELING OF MELTING AND MELT-BEARING ROCKS

The quantitative phase diagrams presented in this chapter were calculated using THERMOCALC version 3.26i and an updated internally consistent dataset (Holland & Powell 1998, ds55 created Nov.

Mineralogical Association of Canada Short Course 38, Quebec City, Quebec, p. 77-96

2003). The *a–x* relationships for each chemical system are those given in Table 1 of White *et al*. (2007) with the addition of gedrite from Diener *et al*. (2007). With the exception of Fig. 5-1, all diagrams were calculated in the NCKFMASHTO model system. The following mineral abbreviations are used: quartz, q; garnet, g; sillimanite, sill; cordierite, cd; orthopyroxene, opx; K-feldspar, ksp; plagioclase, pl; biotite, bi; muscovite, mu; gedrite, ged; ilmenite, ilm; magnetite, mt; silicate melt, liq.

Constraints from petrogenetic grids

P–T grids or *P–T* projections provide the basic "backbone" of invariant and univariant mineral equilibria that control the more complex higher variance relationships in rocks (*e.g.*, Hensen 1971, Powell & Holland 1990, White *et al*. 2007). Even though grids can generally only be constructed for relatively simple chemical systems, they do provide a clear and relatively simple overview of the stable reactions and hence mineral assemblages that may form during high-grade metamorphism.

The minimum chemical system in which to consider partial melting reactions in metapelitic rocks is the K_2O–FeO–MgO–Al_2O_3–SiO_2–H_2O (KFMASH) system. Simpler systems such as FMAS & FMASH, while commonly used for the interpretation of UHT granulites, give no information on the role of a melt phase or the micas in mineral assemblage evolution and are of little use

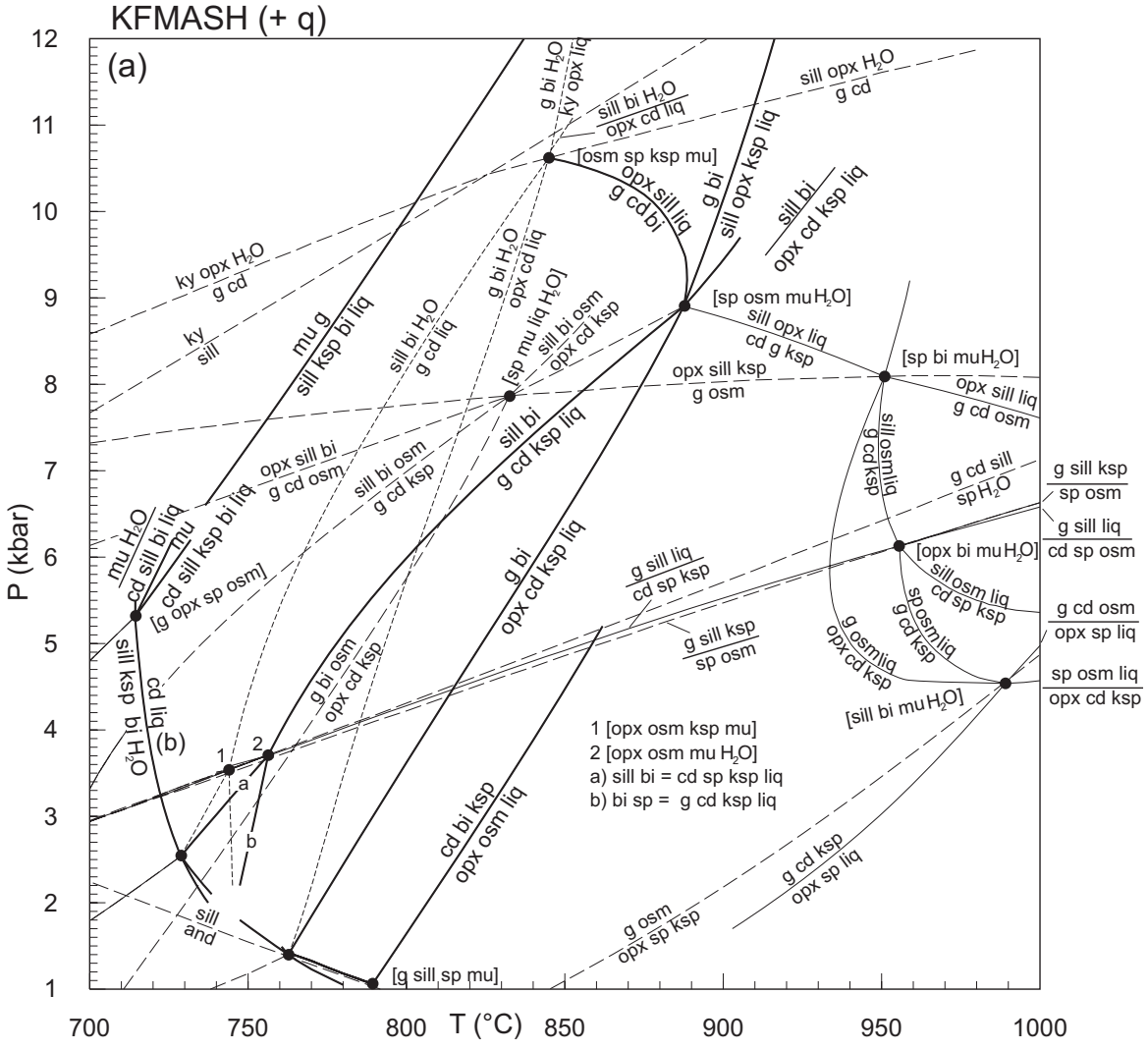

FIG. 5-1. Calculated petrogenetic grid in KFMASH modified from White *et al*. (2007). The main melt-producing reactions are shown in bold lines, other melt-producing reactions are shown as thin solid lines. Melt-absent equilibria are shown as long-dashed lines and reactions with coexisting melt and H_2O (other than the wet solidus) are shown as short-dashed lines.

in studying migmatites. The phase relations within the KFMASH system can be shown qualitatively in *P–T* grids and AFM compatibility triangles in much the same way as the lower temperature KFMASH relationships were illustrated by Thompson (1957). By projecting from quartz, K-feldspar and melt, the KFMASH system is reduced to the ternary AFM system allowing qualitative compatibility diagrams to be produced. With the addition of experimental results, quantitative *P–T–X* constraints can be placed on many of the reactions. Examples of qualitative and semiquantitative KFMASH (± TO) grids include Grant (1985), Clarke *et al*. (1989), Grant & Frost (1990), Dasgupta *et al*. (1995), and Carrington & Harley (1995).

The development of a thermodynamic model for haplogranitic melt (Holland & Powell 2001, White *et al*. 2001) allowed quantitative calculations of melt-bearing equilibria to be undertaken using an internally consistent thermodynamic dataset. The key univariant equilibria for metapelitic systems can be seen in a quantitative KFMASH grid (Fig. 5-1). These univariant equilibria define the basic mineral assemblage stability topology for high-*T* metapelite. Despite the large number of stable reactions present in Fig. 5-1, a number of them are melt-absent and/or H_2O-bearing above the wet solidus and are unlikely to be "seen" by common rock compositions during prograde metamorphism. Of the stable melt-bearing reactions, only a handful can produce a significant amount of melt. The main melting reactions are those with muscovite or biotite on the low-*T* side and melt on the high-*T* side and are shown as thicker lines in Fig. 5-1.

At low *P* (below ≈ 3.5 kbar), only biotite-breakdown melting reactions occur, as muscovite is typically consumed subsolidus. Here, the reaction between biotite and sillimanite produces cordierite and spinel (Fig. 5-1, reaction a). In less aluminous rocks, the reaction

$$\text{bi} + \text{g} + \text{q} = \text{opx} + \text{cd} + \text{ksp} + \text{liq} \qquad (1)$$

may be seen at higher *T*. Typically, these low-*T* reactions only affect Fe-rich rocks. At higher *P* (P ≈ 3.5–9 kbar), the reaction between biotite and sillimanite produces the common garnet + cordierite bearing assemblages,

$$\text{bi} + \text{sill} + \text{q} = \text{g} + \text{cd} + \text{ksp} + \text{liq} \qquad (2).$$

At higher *T*, reaction 1 may be seen by subaluminous (below the g–cd tie line in AFM) metapelite as well as metagreywacke. In addition, partial melting reactions consuming muscovite also occur at pressures above about 5 kbar. At pressures above approximately 9 kbar, the biotite-consuming melting reactions produce the UHT assemblage of coexisting sillimanite and orthopyroxene (Fig. 5-1).

Constraints from pseudosections

While the phase relationships in KFMASH are extremely useful for considering the main partial melting reactions in metapelitic rocks in a general sense, they are of limited use in considering partial melting in specific rock compositions, and for gaining a quantitative view of the *P–T* conditions at which the key reactions occur (*e.g.,* White *et al*. 2007). In addition, the use of petrogenetic grids to understand the melting process leads to an over-emphasis on univariant equilibria and an under-emphasis on the role of higher variance equilibria on the melting process. For specific rocks, phase diagrams drawn for a fixed composition or a compositional vector (pseudosections) are extremely useful, as such diagrams consider both low and high variance equilibria. *P–T* pseudo-sections, drawn for a fixed bulk rock composition, can effectively be viewed as multivariant mineral assemblage "maps" in *P–T* space. However, there are limitations to their use, especially regarding the choice of components in the system to be modeled (see White *et al*. 2007 for discussion). Quantitative phase equilibria modeling can be undertaken in compositionally large systems (*e.g.,* NCKFMASHTO, MnNCKFMASHTO) using sophisticated activity composition (*a–x*) models that represent a close, but not complete or perfect, representation of natural systems.

Figure 5-2 is a pseudosection calculated for a metapelite composition in the system NCKFMASHTO. In this larger chemical system equivalents to some of the KFMASH univariants occur as narrow multivariant fields. These include the key partial melting reactions involving the breakdown of coexisting mu–q, bi–sill and bi–g. Pseudosections can be contoured for mineral mole proportions and mineral composition variables, allowing a great deal of the information preserved in rocks to be integrated within a single thermo-dynamic framework. Melt mole percent contours are shown in Fig. 5-2 for a rock saturated in H_2O at the wet solidus. Due to the different amount of H_2O required to saturate the rock in a H_2O fluid at different pressures along the wet solidus, the amount of fluid present at the low-*P* part of the solidus (below about 4 kbar) is an over-estimation, and hence will overestimate the amount of melt

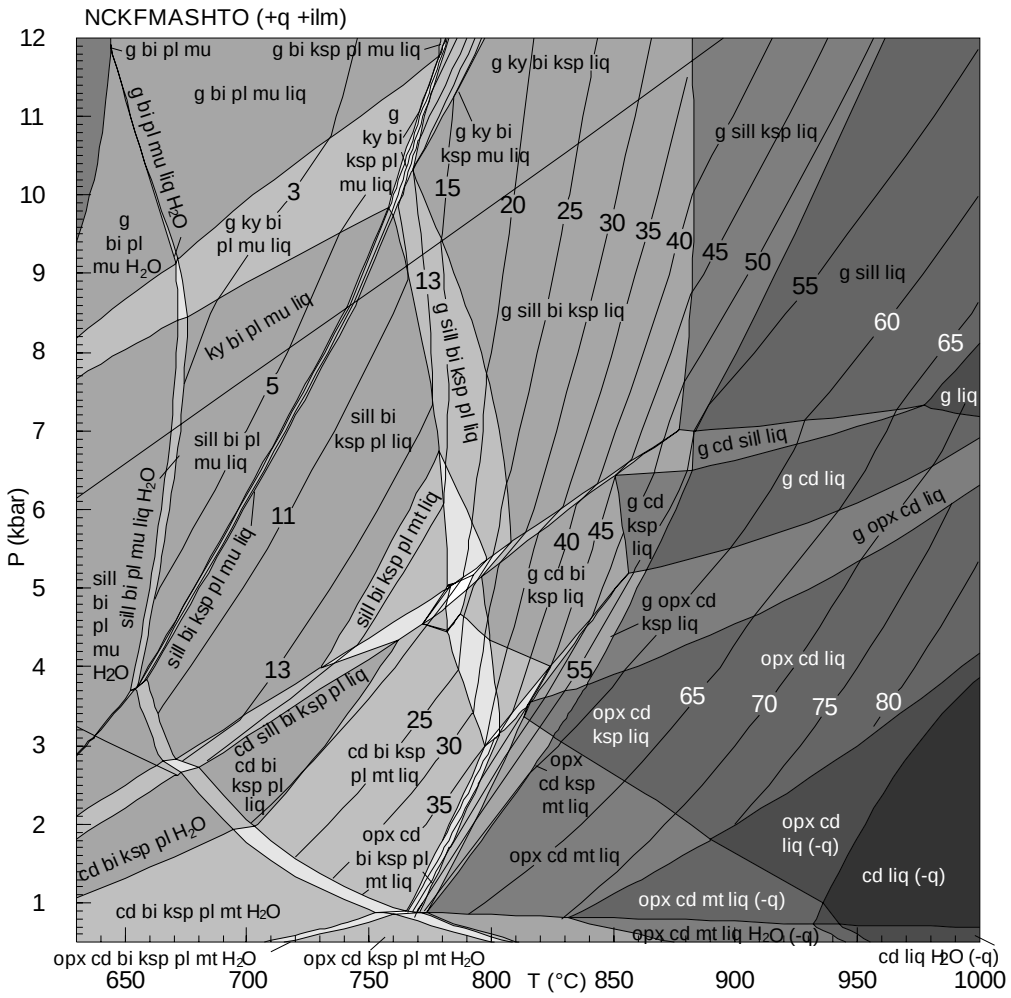

FIG. 5-2. Calculated pseudosection for a metapelite composition (modified from White *et al*. 2007). Contours shown are mole percent melt.

produced along an isobaric heating line at these low pressures. Furthermore, as the diagram is drawn for a fixed composition, processes such as melt loss are not considered. Thus the amount of melt at high-*T* can be very high (>40%). The effects of melt loss are discussed later. However, it is the general disposition of contours that is of most importance. Fields with closely spaced contours represent pulses in melt production, associated with the consumption of mica. At temperatures above the stability of mica the increase in the melt proportion is largely related to the consumption of quartz and feldspars as the melt becomes progressively drier with increasing *T*.

The relationships between the production of melt and changes in mineral assemblages and mineral proportions for some isobaric heating paths are shown in Fig. 5-3. These plots show the main changes in mineral mole proportions and the change in the proportion of melt for isobaric heating paths at 4, 5.5 and 8 kbar. In each of the plots the segments with steep increases in melt proportion represent the major lower variance partial melting reactions. These segments also coincide with temperature intervals in which the most profound changes in mineral proportions occur. It is typically these fields in which profound textural changes may also occur, giving clues to the prograde and or retrograde history.

A useful comparison with the partial melting equilibra in the metapelitic composition is provided by a pseudosection drawn for a metagreywacke composition (Fig. 5-4) taken from Sawyer (1986). In comparison to that of the metapelite, Fig. 5-4 is dominated by higher variance equilibria defining large fields in *P*–*T*. The relationship between the multivariant equilibria In Fig. 5-4 and the key

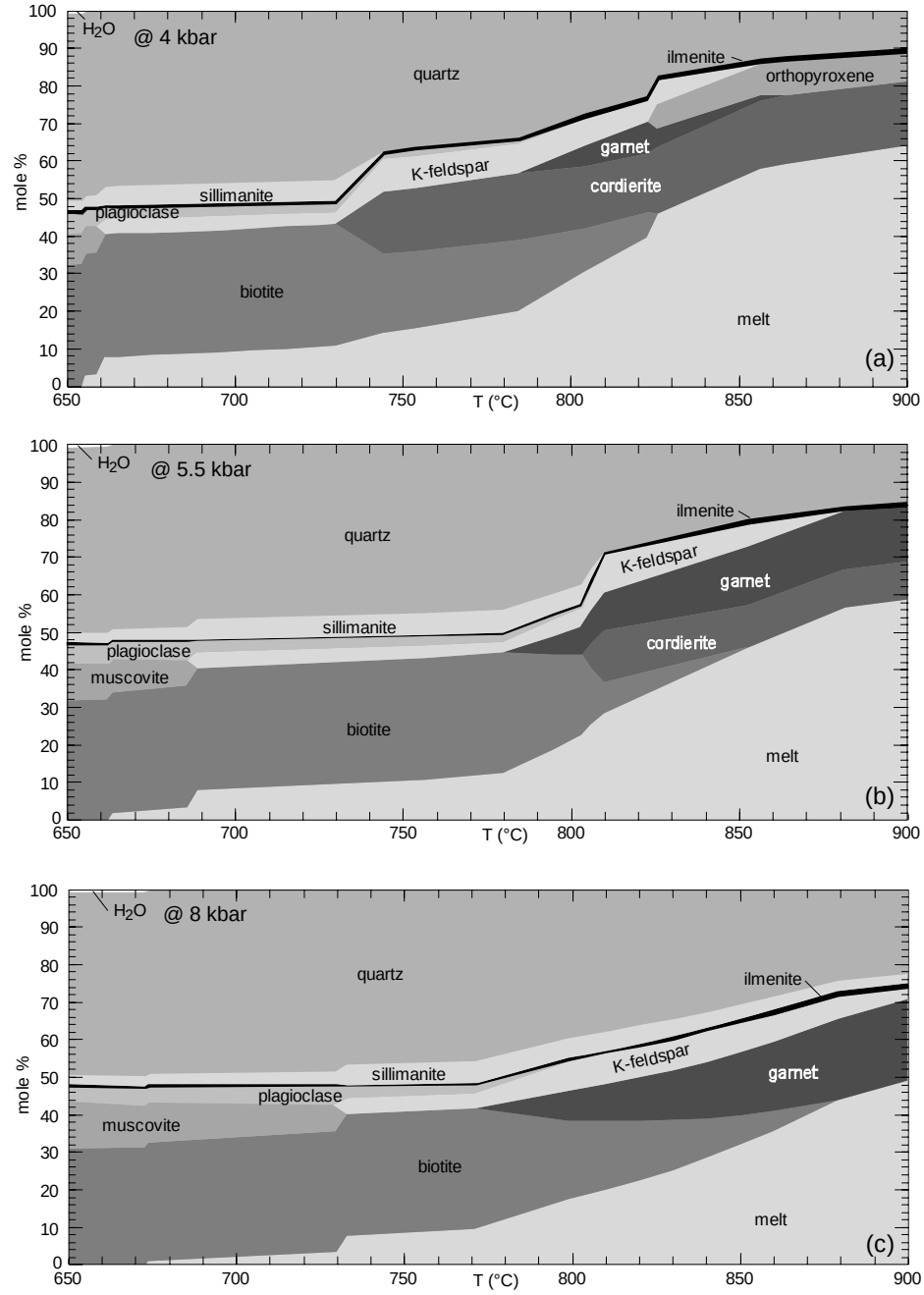

FIG. 5-3. Isobaric temperature versus mineral mole percent plots calculated at 4 kbar (a), 5.5 kbar (b) and 8 kbar (c) based on the composition used for Fig. 2. The plots show the relationship between the production of melt and changes in mineral assemblages and mineral proportions.

univariant equilibria in Fig. 1 is less clear, largely due to the absence of K-feldspar, sillimanite and muscovite from all or much of Fig. 5-4. The production of melt in the metagreywacke composition as a function of *T* is considerably different from that in Fig. 5-2. In particular, little melt is produced at temperatures below about 800°C. The dominance of high variance equilibria and the absence of the key KFMASH melting reactions results in a more regular melt production as a function of *T* and a lack of sharp kinks in the melt mole percent contours. Overall, the proportion of melt produced in the metagreywacke is considerably less than that of the model metapelite.

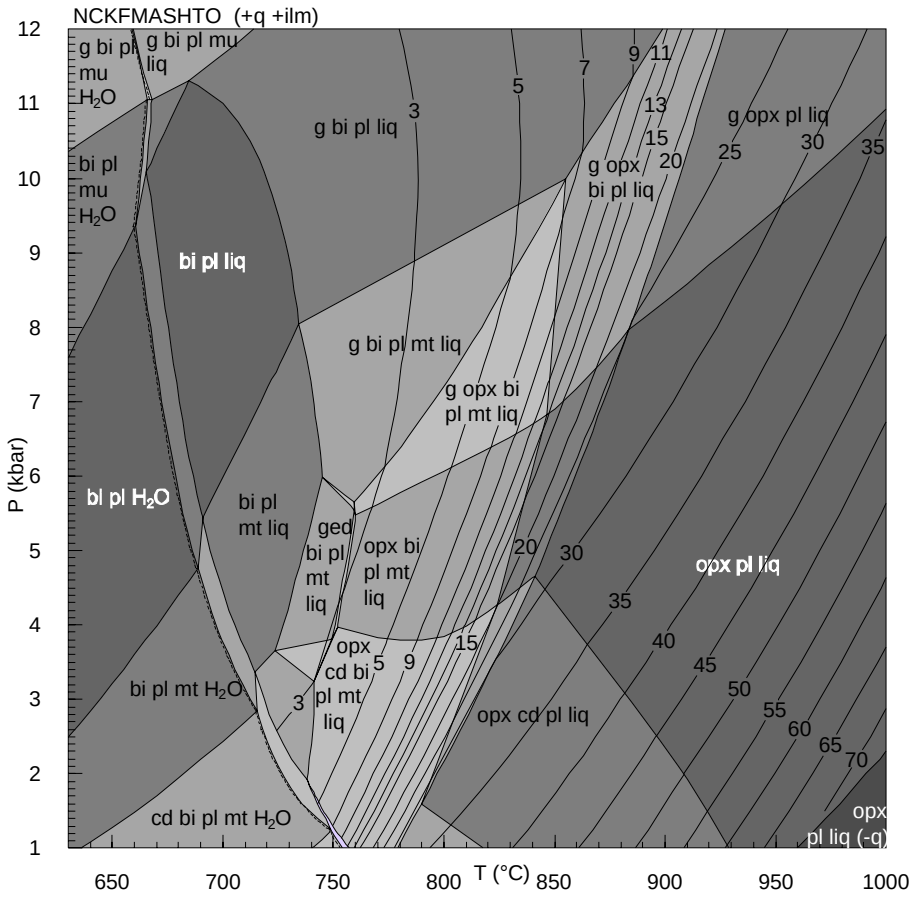

FIG. 5-4. Calculated pseudosection for a metagreywacke composition (ES36) from Sawyer (1986). Contours shown are mole percent melt.

The differences in the mineral assemblage evolution and melt production between the metagreywacke and the metapelite can be seen by comparing Fig. 5-3b and Fig. 5-5. In the greywacke composition the melt content reaches a maximum of about 35% at 900°C in comparison to almost 60% in the metapelite. Furthermore, the melt content in the metagreywacke does not exceed 10% until a temperature of close to 820°C compared with 750°C for the metapelite.

In metabasic rocks the minimum chemical system in which to consider partial melting reactions and high-grade mineral assemblages is NCFMASH. Currently, partial melting calculations cannot be undertaken in metabasic rocks with the existing melt models as they are restricted to relatively haplogranitic melts. However, the small number of phases commonly preserved in metabasic migmatites is consistent with their partial melting histories being dominated by high variance equilibria.

Modeling melt loss

The loss of melt from migmatites is now a well-established and generally accepted feature (*e.g.,* Fyfe 1973, Sawyer 1998, Kriegsman 2001, White & Powell 2002, Brown 2002, 2007, Guernina & Sawyer 2003). Melt loss at any stage in a rock's history, be it at prograde, peak or retrograde conditions, influences the subsequent mineral assemblage development (*e.g.,* White & Powell 2002). Here, the loss of melt can simply refer to melt migrating outside the volume of equilibration in which it formed (possibly producing a rock with both melt-depleted and melt-enriched parts), or the loss of melt from the rock as a whole (producing an overall melt-depleted rock). However, the mineral equilibria modeling of melt loss is scale-independent, although the application of such models does require the scale of melt loss to be considered.

Melt loss on the prograde path affects profoundly the total amount of melt that can be

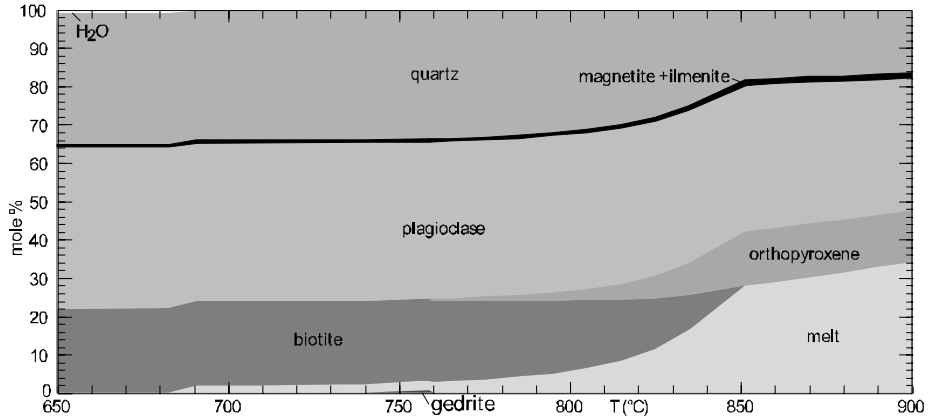

FIG. 5-5. Isobaric temperature *versus* mineral mol.% plots calculated at 5.5 kbar (based on the composition used for Fig. 5-4. The plots show the relationship between the production of melt and changes in mineral assemblages and proportions.

produced in a given rock. As melt gets less hydrous with increasing *T*, the loss of melt at lower-*T* retards the higher-*T* melting process, especially that which occurs beyond the stability of hydrous phases. This effect can be seen in comparing Fig. 5-2 with a pseudosection of the same rock with all the melt (≈ 30 mol.%) removed at 850°C and 8 kbar (Fig. 5-6a). The most notable feature of Fig. 5-6a is the elevation of the solidus to $T > 800$°C and the persistence of granulite-facies assemblages to lower *T*. In addition, the loss of melt extends the stability of K-feldspar to higher *T* and retards further melt production due to the reduced water content of the modified rock composition. Melt loss at even higher *T* (Fig. 5-6b) results in an even more profound change to the resulting pseudosection with the solidus shifted to $T > 900$°C at $P < 6$ kbar and a greater shift in the K-feldspar-out boundary. In both Figs. 5-6a and 6b the solidus at pressures above 6–7 kbar is the low-*T* boundary of the bi–sill–g–ksp–q–liq field, the main difference being the proportions of the minerals involved, with Fig. 5-6a having more biotite and less garnet at the solidus. At lower *P*, the two diagrams differ substantially. In Fig. 5-6b the low-*P* fields are biotite-absent and the solidus is controlled by the appearance of cordierite. Here, the appearance of cordierite is largely pressure-controlled such that the solidus takes a sub-isobaric dogleg up to $T > 950$. In contrast, the solidus in Fig. 5-6a remains nearly isothermal (800–850°C) and involves the production of biotite over the pressure range considered.

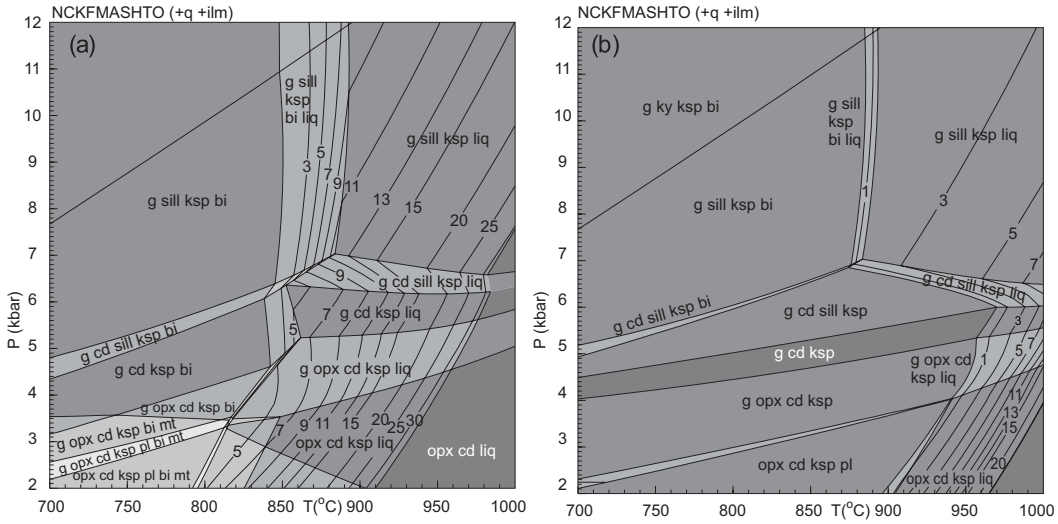

FIG. 5-6. *P-T* pseudosections constructed for melt depleted (relative to Fig. 5-1) bulk rock compositions. **a)** Pseudosection drawn for complete melt loss at 850°C and 8 kbar. **b)** Pseudosection drawn for near-complete melt loss at 900°C and 8 kbar.

Considerations in modeling migmatites

There are several features of migmatites that are problematic to model, especially regarding volumes of equilibration and open system processes. A number of lines of geochemical and mineral equilibria evidence are consistent with most migmatites and granulites in general having lost some to virtually all of their melt during metamorphism (*e.g.,* Brown 2002, 2007, White & Powell 2002, Guernina & Sawyer 2003), and thus the rocks preserved differ compositionally from their protoliths. This inherently makes the forward modeling of melting processes in most migmatites difficult. It is possible in many examples effectively to reintegrate melt back into residual rocks to create an approximate protolith composition (*e.g.,* White *et al*. 2004). However, such estimated protoliths should be treated with some caution as they require an estimate of the *P–T* path and melt-loss history. Regardless of the potential problems this method may involve it is likely that the general disposition of mineral-assemblage fields dominated by the key reactions between the ferromagnesian minerals is close to that of the protolith as melt produced at these conditions contains relatively little total FeO + MgO. In contrast, field boundaries involving the loss or gain of K-feldspar, plagioclase or quartz in melt-reintegrated compositions are considerably less certain and should not be interpreted too literally.

The interpretation of likely volumes of equilibration is a problem common to all metamorphic rocks. However, the ability of melt to segregate on a centimetre to decimetre scale makes the interpretation of likely volumes of equilibration and the likely composition of such volumes more difficult and somewhat more critical in migmatites. At the core of this problem is understanding the relative scales on which physical and chemical/ diffusive processes may operate. For example, if physical segregation occurs on a scale greater than the scale at which diffusion can operate effectively, then a given volume of rock is composed of a number of equilibration volumes. In contrast, if diffusion distances are greater than the scale of physical segregation then what may appear to be different volumes of equilibration represent just a heterogeneous distribution of phases. In reality, it is likely a combination of both the above relationships occurs with the diffusion distances of some elements greater than the scale of physical melt segregation and others smaller.

Melt can interact chemically with the solid phases in two ways, one by direct contact and reaction with them, and the other by a less direct diffusive process (*e.g.,* White *et al*. 2004, 2008, Baldwin *et al*. 2005). In the first mechanism, the physical migration of melt to reaction sites is required unless the reaction is restricted to the contacts between melt segregations and the host rock. This movement will be driven by pressure gradients developed in the rock during reaction and deformation. In the second mechanism, reaction between melt and minerals occurs via the diffusion of components through the melt to sites of reaction, down chemical potential gradients. This second mechanism does not require the physical movement of melt, though it may require melt-saturated grain boundaries to operate effectively over a cm scale. It is likely that in most migmatites both processes operate simultaneously, however, their relative importance to the final rock may vary.

There are consequences resulting from which of the above processes is dominant in a particular migmatite, and how understanding the evolution of the rocks can be undertaken using mineral equilibria modeling. The first mechanism can be modeled in an orthodox way via $P–X_{melt}$, $T–X_{melt}$ pseudosections, or a series of *P–T* pseudosections reflecting different residuum:melt ratios. In contrast, the establishment of chemical potential gradients makes a classical composition-based mineral equilibria approach such as pseudosections difficult, especially if such gradients are not transient features.

The issue of equilibration in the second mechanism is substantially complicated by the fact that different elements have different diffusivities. For example, in a migmatite there may be relatively little diffusion of, say, Al_2O_3 between residuum and leucosome such that chemical potential gradients in Al_2O_3 cannot be flattened, whereas diffusion of H_2O may be sufficiently fast such that both the leucosome and residuum maintain the same chemical potential of H_2O. Where such issues are of importance or interest, the common "composition-" based diagrams such as pseudosections may be of limited use. Here, diagrams explicitly dealing with the compositional conjugate variable (μ) may be required to understand the diffusive process (*e.g.,* White *et al*. 2004, Powell *et al*. 2005, White *et al*. 2008). Phase diagrams in which chemical potential is explicitly considered, such as $\mu–\mu$ diagrams, allow quantitative mineral equilibria methods to be utilized. Although, such methods are still in their infancy (*e.g.,* White *et al*. 2008), their application

has the potential to improve our understanding of the mineral assemblage and textural evolution of migmatites substantially. In particular, a chemical potential-based approach will allow the identification of diffusion-controlled features in migmatites, which may be more common than currently realized.

MINERAL ASSEMBLAGE EVOLUTION AND REACTION TEXTURES IN MIGMATITES

Partial melting in rocks occurs via multivariant reactions that largely involve solid reactants and products. The mineral assemblages and textures developed in migmatites typically reflect, at least to some degree, the progress of these reactions. Such textures are commonly used to delineate *P–T* paths for rocks (*e.g.,* White *et al*. 2002, Zeh *et al*. 2004, Kelsey *et al*. 2003, Johnson & Brown 2004, Halpin *et al*. 2007). Many textures in migmatites, especially those in leucosomes, are clearly related to the formation or, more commonly, the crystallization of melt. Textures in the residuum, such as interstitial quartz and feldspar, are also commonly the direct result of melt crystallization (*e.g.,* Sawyer 1999). However, many other textures not obviously directly related to the crystallization of melt, especially in the residuum, must also be related to the formation or crystallization of melt as they are part of the main melt producing/consuming reactions (*e.g.,* Kriegsman 2001, White & Powell 2002).

Melt-producing reactions and related textures

Due to the impact of deformation, recrystallization and continued metamorphism to higher *T*, metamorphic textures related to the prograde melting process and in particular the reactions involved are commonly not well preserved in migmatites. However, there are a number of exceptions from both contact metamorphic environments and regional metamorphic terrains. In addition, textural relationships commonly used for interpreting the *P–T* evolution may in addition be interpreted within the context of melt production.

The most obvious examples of the relationship between textural evolution of high-grade rocks and melt formation occur where leucosomes occur as pools surrounding large (porphyroblastic) reactant or peritectic product minerals of melting reactions. In these examples it appears that the melting process was, for at least part of the rock's history, spatially focused on a particular reactant or product phase.

Spectacular examples of partial melting reactions being spatially focused on a reactant mineral occur in the Mt. Stafford area of the Arunta Block in central Australia. This area preserves a profound metamorphic field gradient that goes from the upper greenschist facies into the granulite facies and has been the focus of a number of studies (*e.g.,* Vernon *et al*. 1990, Greenfield *et al*. 1996, 1998, White *et al*. 2003). In this area, melt-producing reaction between biotite, sillimanite and quartz was focused on sparsely distributed sillimanite pseudomorphs of andalusite. The migmatite structure is illustrated in Fig. 5-7a where extensive leucosome exists in aluminosilicate-rich portions of the rock. In the less aluminosilicate-rich parts, individual aluminosilicate porphyroblasts have a discrete leucosome surrounding them (Fig. 5-7a). Parts of the rock that now lack aluminosilicate may contain leucosome-hosted symplectite of spinel and cordierite that define a rectangular shape (Fig. 5-7b), consistent with them having replaced aluminosilicate. Other aluminosilicate-absent domains may lack this symplectite, consistent with them either having been aluminosilicate-poor or absent at the onset of this reaction.

The aluminosilicate replacement textures show a complex spatial arrangement with a layer of spinel–cordierite symplectite adjacent to the aluminosilicate and an outer cordierite rim. The texture typically lacks quartz even though the rocks are typically quartz-bearing overall. The layered structure of the texture is consistent with chemical potential gradients having been developed between the aluminosilicate porphyroblasts and the matrix biotite and quartz. Initially, aluminosilicate, biotite and quartz would have been in mutual contact allowing reaction to proceed at the aluminosilicate edge. As reaction proceeded, local sources of biotite became consumed and, as a result of relatively low rates of Al_2O_3 diffusion, cordierite moats replacing the aluminosilicate developed. Thus, as a consequence, reaction between aluminosilicate, biotite and quartz would have been diffusion-controlled and required progressively greater diffusion distances as the texture evolved and the reactants became separated by greater distances. As reaction was spatially focused around the aluminosilicate porphyroblasts, so too was the production of melt.

Similar or identical textures have been described by Johnson *et al*. (2004) from the aureole of the Bushveld Complex, again reflecting reaction between biotite and aluminosilicate during heating

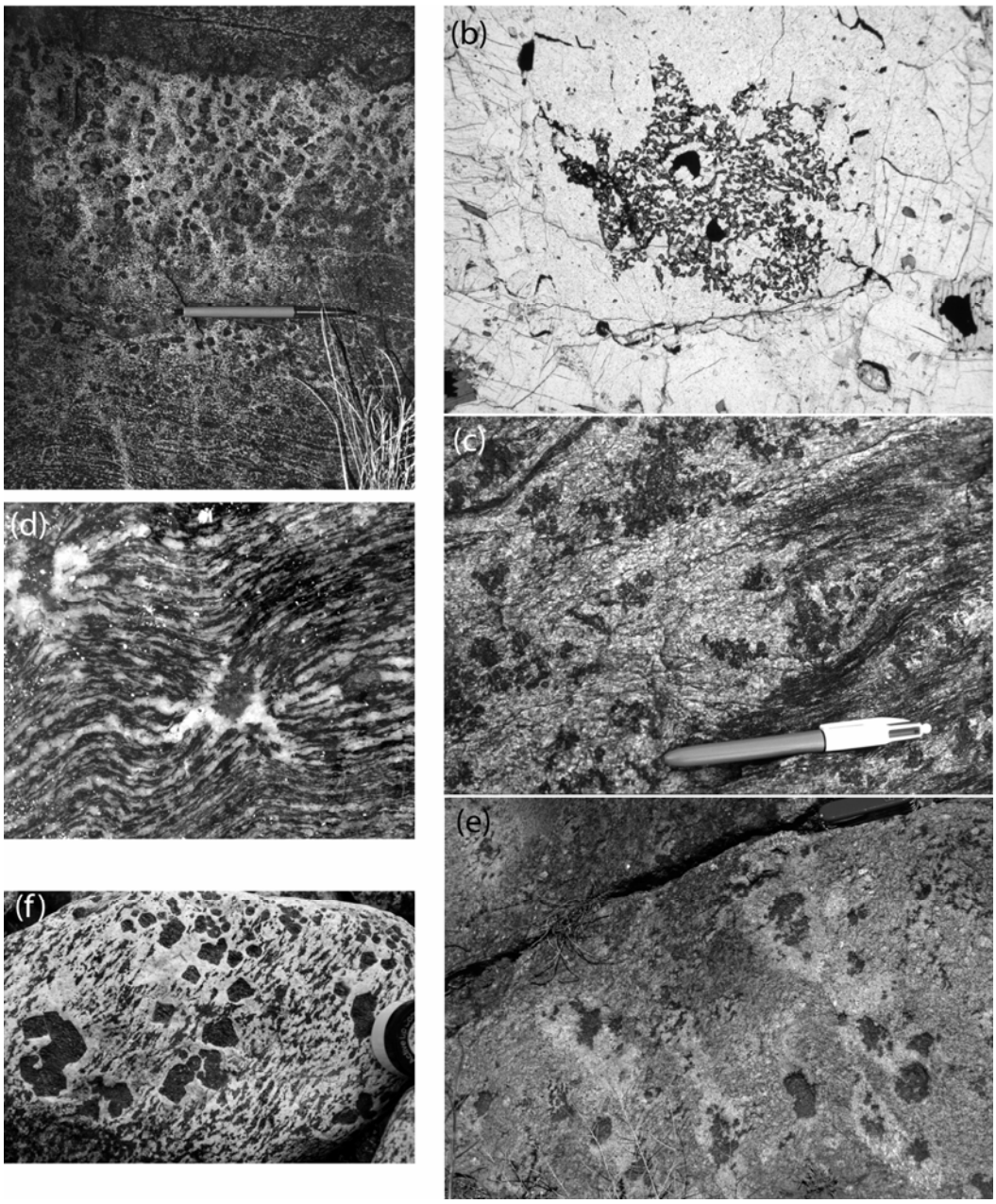

FIG. 5-7. Field photographs and photomicrographs of textures related to prograde partial melting reactions. **a)** Photograph of a graded bed from Mt Stafford. The bed grades from more psammitic at the base (lacking aluminosilicate porphyroblasts) to more pelitic at the top (rich in aluminosilicate porphyroblasts) prior to a sharp contact with an overlying psammitic layer. **b)** Photomicrograph of a structured aluminosilicate replacement texture composed of a symplectite of cordierite and spinel in the core and a surrounding cordierite mantle. Plane-polarized light, long axis of photo = 6mm **c)** Garnet-bearing leucosomes from Round Hill in the Broken Hill Block of Australia. The garnet forms large poikiloblasts around which the melting reactions were spatially focused. **d)** leucosome-hosted cordierite porphyroblasts in inter-boudin partitions in a metapelite from southern Brittany. The porphyroblast/leucosome shows the intimate relation between mineral growth and deformation structures with both enhanced cordierite stability and melt collection in the dilatant site. **e)** Large leucosome-hosted garnet porphyroblasts in metamorphosed granite from Broken Hill. The leucosomes form an interconnected network that links the individual spatially-focused melt production sites. **f)** Subhedral to euhedral garnet porphyroblasts in leucosome from dioritic gneiss in the Pembroke Valley in Fiordland, New Zealand.

followed by decompression to allow preservation of the textures.

Spatial focusing of reaction may also occur around a product (or peritectic) mineral of a partial melting reaction. In particular, leucosomes in metapelitic or metagranitic rocks concentrated around porphyroblasts of garnet (*e.g.,* Waters & Whales 1984, Waters 1988, Stüwe & Powell 1989, Powell & Downes 1990, Hand & Dirks 1992, White *et al*. 2004, Clarke *et al*. 2007, Fig. 5-7c, e), cordierite (*e.g.,* Fitzsimons 1996, Carson *et al*. 1997, Barbey *et al*. 1999, Johnson & Brown 2004, Fig. 5-7d) or orthopyroxene (Waters 1988, Stüwe & Powell 1989, Sawyer *et al*. 1999, Clarke *et al*. 2007) appear to be common features. Leucosomes hosting large peritectic minerals have also been recorded from migmatite in mafic rocks (*e.g.,* Clarke *et al*. 2005, Fig. 5-7f).

The growth of porphyroblasts involves diffusion on a scale considerably greater than the grain scale of the matrix (*e.g.,* Carlson 1989, 2002, White *et al*. 2008). This diffusion is a consequence of the chemical potential gradients set up between the sparsely distributed porphyroblast nuclei and the matrix, commonly as a consequence of a small overstep of the porphyroblast-forming reaction (*e.g.,* Carlson 1989, White *et al*. 2008). Wherever chemical potential gradients exist in a rock there is the potential to produce a layered structure (*e.g.,* Korzhinskii 1959, Joesten 1977, Foster 1986, Ashworth & Birdi 1990, White *et al*. 2004, 2008), and where these gradients are between a porphyroblastic mineral and the matrix, these zones will be concentric around the porphyroblast (*e.g.,* White *et al*. 2004, 2008). In addition, any reaction that involves this porphyroblast will allow diffusion between the porphyroblast and the matrix minerals to proceed, with the rates of diffusion becoming the rate-limiting step and the reaction being spatially focused.

The common presence of leucosome-hosted peritectic porphyroblasts in migmatite terrains is consistent with a strong diffusional control on melting in these rocks. An excellent example of this phenomenon occurs in the granulite-facies aluminous metapelitic rocks at Round Hill in the Broken Hill Block of Australia (Powell & Downes 1990, White *et al*. 2004). The metapelite at Round Hill contains numerous 1–15 cm diameter poikiloblastic garnet grains that occur in leucosomes. Garnet present in the matrix is typically much finer-grained (0.5–2 cm), and either lacks or has a weakly developed leucosome mantle.

White *et al*. (2004) proposed a model for these rocks in which the poor nucleation of garnet led to melt production being spatially focused around individual garnet grains. This occurred during reaction between biotite-sillimanite and quartz to produce garnet and eventually garnet and cordierite. The continued growth of the garnet porphyroblasts was achieved via diffusion between the porphyroblast and the matrix, driven by transient chemical potential gradients in the rock. Using qualitative μ–μ diagrams, White *et al*. (2004) showed that a consequence of this diffusive process was the development of a melt-rich layer separating the garnet from the matrix. The development of this layer is shown in a series of μ–μ diagrams (Fig. 5-8), and discussed in detail in White *et al*. (2004). In μ–μ space, the melt-rich layer separates the garnet–melt contact from a matrix of biotite–melt or biotite–cordierite–melt (with quartz and K-feldspar and sillimanite in excess). In addition, K-feldspar is also concentrated in this melt-rich layer (see White *et al*. 2004 for further discussion).

The melt formed around the garnet may migrate during deformation, leading to the formation of an interconnected network of leucosome. The lack of retrogression of the granulite-facies assemblage is consistent with considerable melt loss from the rocks overall, with the remaining leucosomes being largely composed of garnet and peritectic K-feldspar.

An excellent example of the scale on which the textures in a migmatite may evolve with changing conditions is provided by the migmatites in the Wuluma Hills (Sawyer *et al*., 1999; Clarke *et al*., 2007). Some of these rocks experienced two distinct periods of melt production both related to major low variance changes in mineral assemblages and mineral proportions (Clarke *et al*., 2007). The first period involved reaction between biotite, sillimanite and quartz to produce garnet, cordierite, K-feldspar and melt. This melting reaction was spatially focused around sparse garnet nuclei, resulting in leucosome-hosted garnet porphyroblasts in which the porphyroblasts were separated from any part of the host rock by up to ten centimetres. The second period of melt production was related to the growth of orthopyroxene that occurred via reaction between garnet and biotite (Fig. 5-9). This reaction resulted in orthopyroxene forming in both the leucosome (replacing garnet) and in the residuum or host rock (replacing biotite). The orthopyroxene in both domains has the same composition. Due to the pre-existing garnet porphyroblast texture, reaction

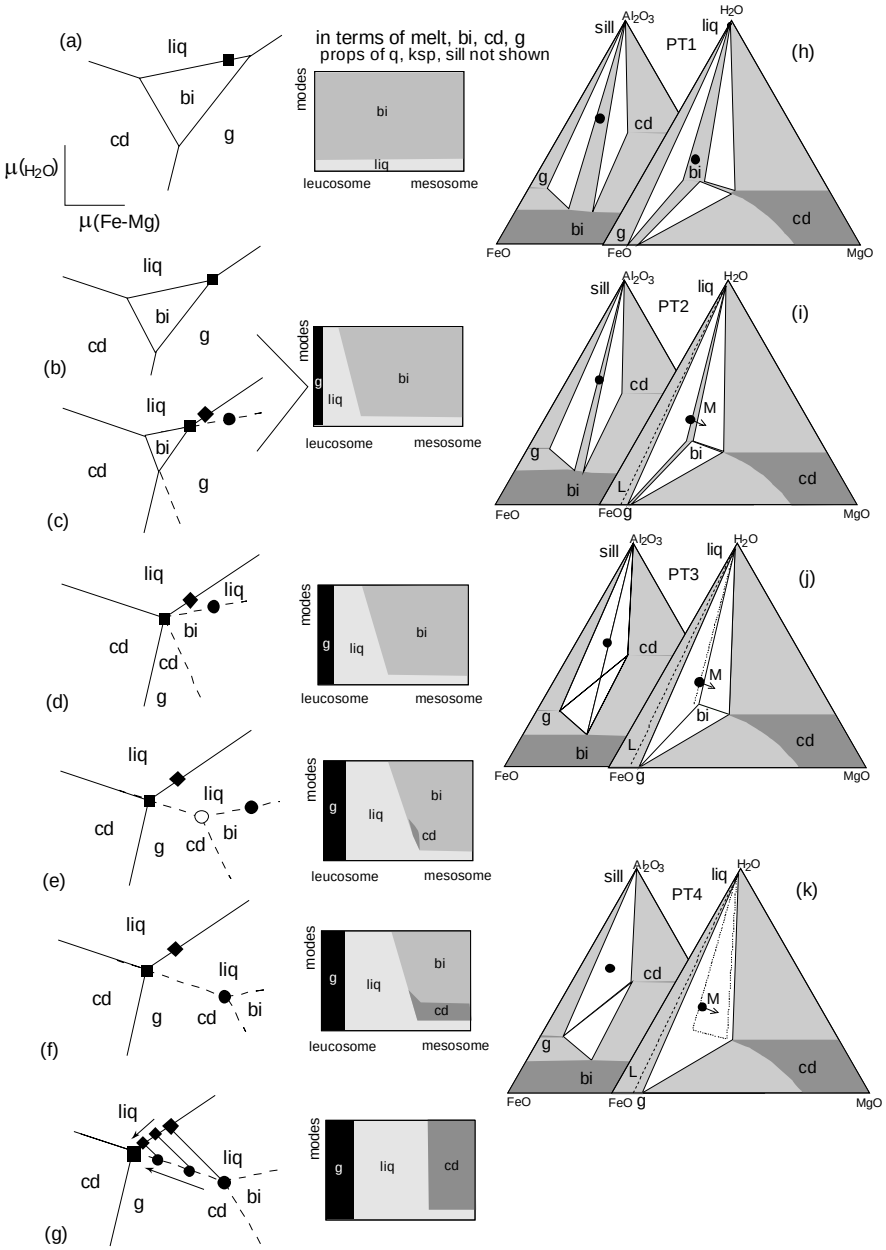

FIG. 5-8. Qualitative μ(FeO-MgO)–μ(H_2O) diagrams taken from White et al. (2004), with sillimanite present, showing the stable (solid lines) and metastable (dashed lines) relationships (Fig. 8a-g). In the μ(FeO-MgO)–μ(H_2O) diagrams, the filled square denotes the stable whole rock mineral assemblage. The filled diamonds represent the garnet leucosome and the filled and open circles represent the metastable, garnet-absent mesosome assemblage. The mode boxes to the right of the μ(FeO-MgO)–μ(H_2O) diagrams show the approximate mineral modes for the different mineral assemblage zones in the leucosome-mesosome structures corresponding to the adjacent μ(FeO-MgO)–μ(H_2O) diagram. The Al_2O_3-FeO-MgO (AFM) and H_2O-FeO-MgO (HFM) compatibility triangles (Fig. 8h-k) show the compositions of stable (solid lines) and metastable (dotted lines) equilibria along a prograde path. The filled circle in each of the AFM and HFM diagrams is the projected bulk-rock composition for sample RH011. The arrow, labeled "M", emanating from this point shows the compositional evolution trend of the mesosome away from the bulk rock composition with diffusion. The leucosome composition lies on the garnet liquid tie-line in the g-bi-liq or the g-cd-liq tie triangles in HFM, or to the left of this line (dashed line labeled "L") depending on the degree of compositional partitioning that has taken part. The position of the leucosome on the dashed line depends on the ratio of garnet to liquid. The loss of melt from the leucosome will drive the leucosome composition along the dashed line away from the liquid composition.

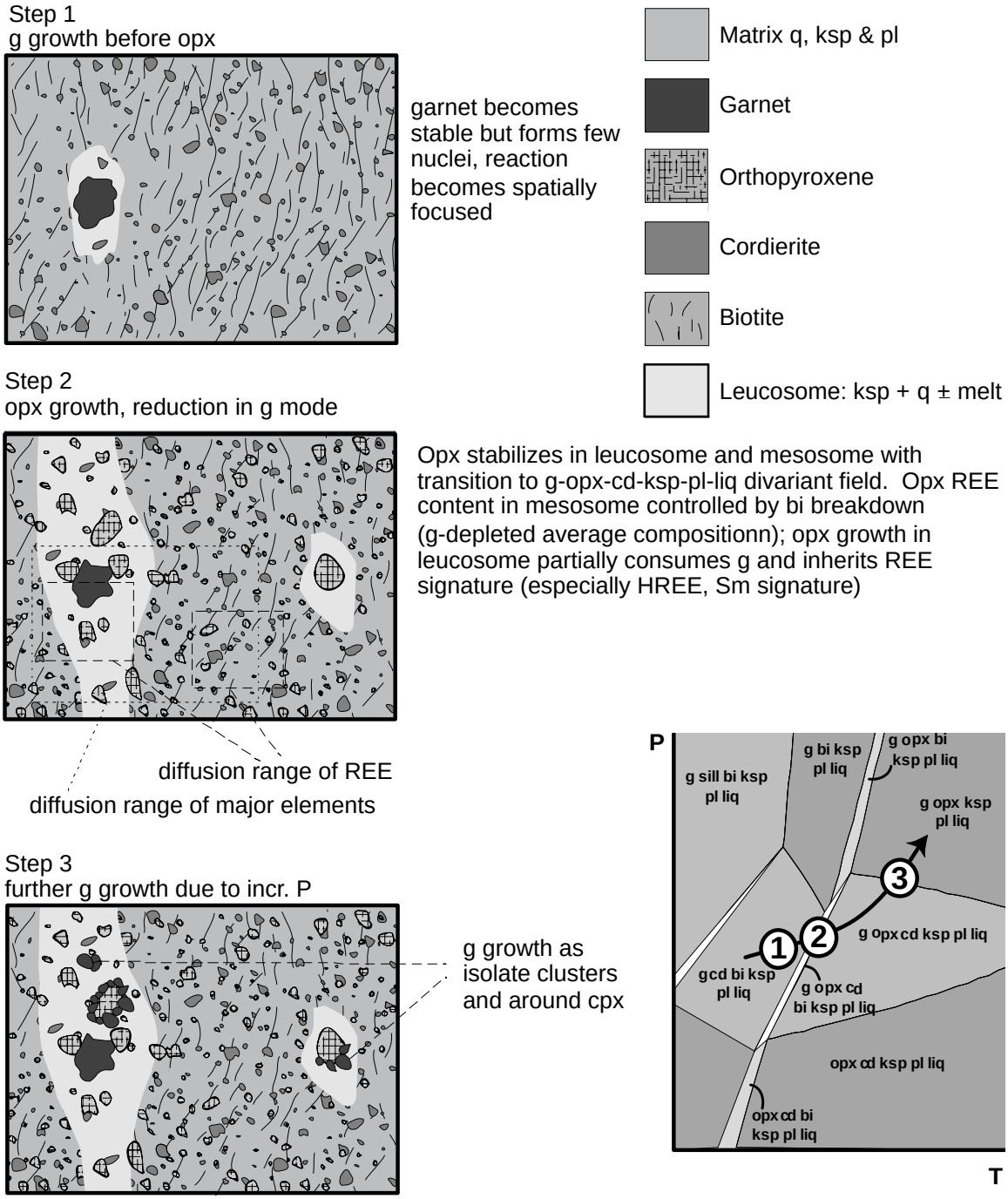

FIG. 5-9. Cartoon modified from Clarke *et al*. (2007) illustrating the textural and mineral assemblage evolution and the effect on REE partitioning during spatially-focused partial melting involving garnet occurring before orthopyroxene crystallizes.

between garnet and biotite required diffusion, particularly of FeO and MgO, on a scale of half the inter-porphyroblast distance (typically 3–20 cm). The lack of major element compositional variation in the orthopyroxene is consistent with the major elements equilibrating over that distance. However, the rock preserves distinct REE patterns in orthopyroxene between the leucosome and the residuum (Clarke *et al*. 2007). In rocks that lack garnet, leucosomes are concentrated on orthopyroxene porphyroblasts. Here, both the orthopyroxene in the leucosome and that in the host rock have a

similar REE pattern.

In the example from the Wuluma Hills, garnet porphyroblasts spatially control the main melting reactions, both initially as a product of a melting reaction and later as a reactant of a melting reaction. While the spatial focusing of melt production in rocks seems to be a moderately common phenomenon, it would be incorrect simply to assume the presence of porphyroblastic grains sitting in leucosome is *a priori* evidence of spatially focused melting. It is rather common for ferromagnesian minerals in leucosome to have a larger grain size than those in the matrix, probably due to the lack of solid-state deformation in the melt-rich segregations. However several criteria are indicative of spatially focused melting. For example, the absence of the porphyroblastic mineral outside the leucosome, or evidence that grains of this mineral in the matrix grew later than those in the leucosome is indicative of a link between the mineral and partial melting. However, the presence of a given mineral both as porphyroblasts in leucosome and in the matrix cannot necessarily be used as a criterion against spatially focused melting as this feature may segregations. However several criteria are indicative of spatially focused melting. For example, the absence of the porphyroblastic mineral outside the leucosome, or evidence that grains of this mineral in the matrix grew later than those in the leucosome is indicative of a link between the mineral and partial simply reflect subtly different nucleation times (*e.g.,* White *et al*. 2004). The use of phase diagrams such as pseudosections, combined with careful petrography and analysis of major and trace element compositions, may allow the inference of spatially focused melting to be strengthened.

Textures related to cooling and melt crystallization

Migmatites commonly preserve textures consistent with crystallization from melt. Typically these textures involve the main products of melt crystallization – quartz, plagioclase and K-feldspar. However, the crystallization of these phases in a migmatite is intimately entwined with changes in the common matrix/residuum minerals. A fairly obvious link between the crystallization of melt and changes to the residual or matrix assemblage is the development of melanosome-like, biotite-rich, mafic selvedges in granulite-facies migmatites (*e.g.,* Kriegsman 2001, Fig. 5-10a). Whereas biotite-rich melanosomes may form in lower grade migmatites as the result of muscovite-consuming melting reactions where they are product or residual phases, at higher grades they are typically reactants (*e.g.,* Grant 1985, Kriegsman 2001, White *et al*. 2001, White & Powell 2002). Thus, biotite-rich selvedges in granulite-facies migmatites most likely represent reaction between the melt and the high grade anhydrous assemblages in the residuum, the selvedge structure reflecting the original contact between leucosome and the residual rock (Kriegsman 2001, White & Powell 2002).

More subtle features in the residuum may also reflect cooling and the crystallization of melt. High temperature retrograde reaction textures such as partial pseudomorphs, symplectite structures and coronas are also a common feature of many migmatites and granulites in general. These textures are critical to deriving *P–T* paths for terrains. The most obvious replacement textures that may relate to melt crystallization involve the growth of biotite, muscovite or cordierite in metapelitic rocks and amphibole and biotite in intermediate to mafic rocks, as typically melt will be the source of the water required for these minerals to grow (*e.g.,* Powell 1983, Cenki *et al*. 2002, White & Powell 2002, White *et al*. 2005).

An important feature in the development, or lack of development, of retrograde reaction textures in metamorphic rocks is the role of melt loss from the rocks. The location of the solidus is strongly controlled by the amount of melt loss, coupled with the non-linear nature of melt crystallization as a function of *P–T*, which is controlled by the reactions between solid and liquid phases (Fig. 5-6). The distribution of melt within a rock will likely also be a controlling variable in the nature and distribution of melt-related retrogression. If retrograde reaction textures are considered only in simple systems (*e.g.,* FMAS), where the role of a melt phase is explicitly ignored, or even in larger systems (*e.g.,* KFMASH) if a melt phase is considered to be in excess, the role of melt in the mineral assemblage evolution is obscured.

A key feature of reaction textures is the apparent incomplete consumption of some of the reactant phases. Slow reaction kinetics during the retrograde evolution has in the past been invoked as the main cause of the incomplete consumption of reactants, and has led to the idea that such textures must represent a grossly disequilibrated state. However, recent studies in which the melt phase and melt loss from rocks is explicitly considered provide an alternative explanation for the apparent incomplete consumption of reactants in many of

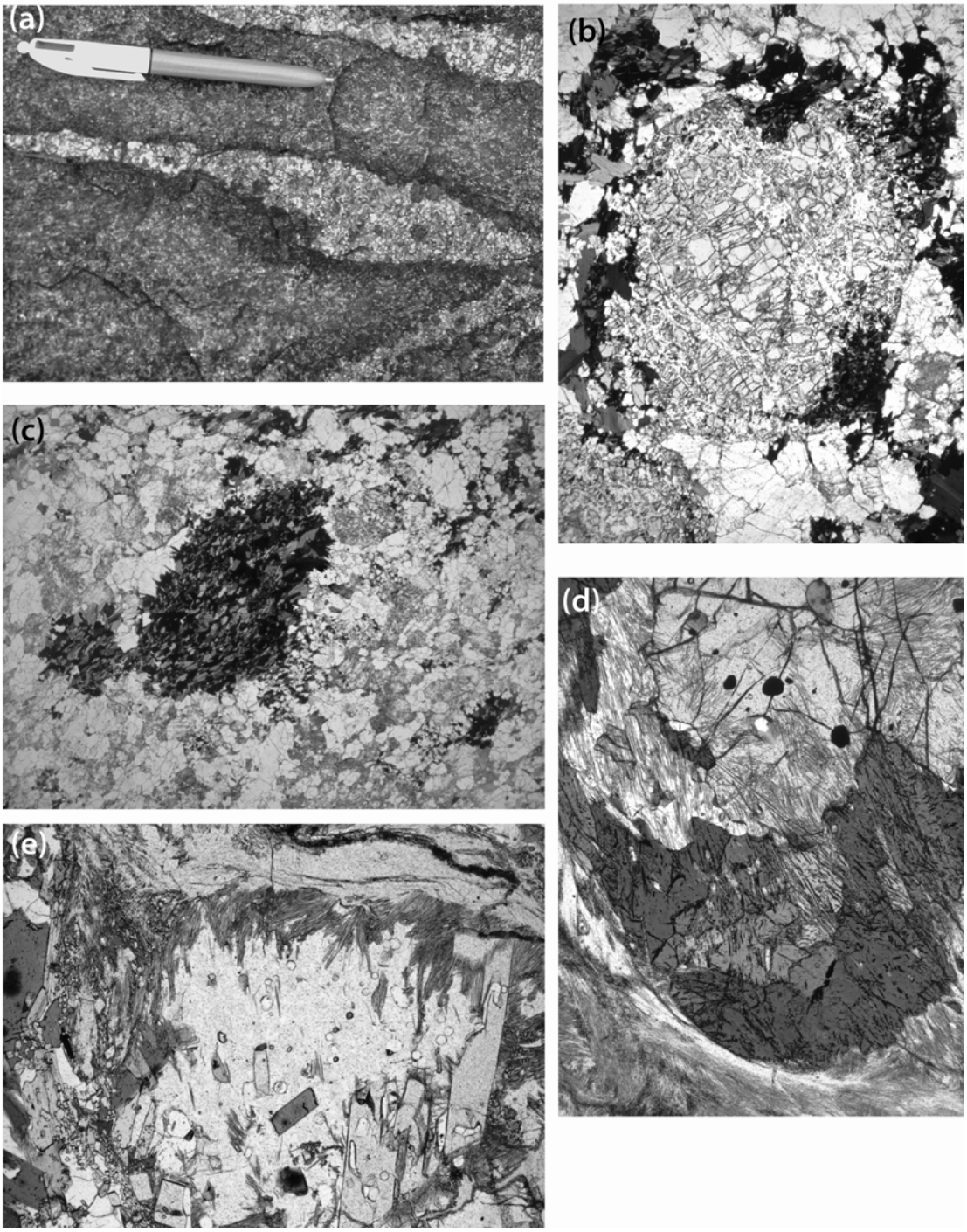

FIG. 5-10. Field photographs and photomicrographs of textures related to retrograde melt crystallization reactions. **a)** narrow melanosome-like biotite-rich selvedges separating leucosome from the residuum in metapsammitic gneiss from Round Hill, Broken Hill, Australia. **b)** Incipient replacement of garnet by biotite in an upper amphibolite-facies migmatite from Broken Hill. The garnet is also partially replaced by plagioclase and quartz along small fractures. Plane-polarized light, long axis of photo = 11.7 mm. **c)** Cluster of randomly oriented biotite that has completely pseudomorphed a garnet porphyroblast. Plane-polarized light, long axis of photo = 13 mm. **d)** Garnet rich in sillimanite inclusions partially replaced by biotite. Plane-polarized light, long axis of photo = 2.25 mm. **e)** Cordierite grain with prismatic sillimanite inclusions and partially replaced by fibrous sillimanite and minor biotite. Plane-polarized light, long axis of photo = 2.25 mm

these textures (*e.g.*, Brown 2002, White & Powell 2002, White *et al*. 2002, Johnson *et al*. 2004, Kelsey *et al*. 2003). An important consequence of the loss of melt from migmatites is that retrograde melt-consuming reactions will generally result in melt being the reactant completely consumed, not one of the solid minerals. Hence, the consumption of the solid reactants will cease, not for kinetic reasons but because the reaction has effectively gone to completion by consuming all the available melt. Once melt has been lost, further textural modification will likely be retarded by the lack of an intergranular medium (melt or fluid) through which diffusion can occur. However, many reaction textures in migmatites, especially those involving multiply layered coronas, may represent disequilibrium across the structure, but for many simple partial replacement textures disequilibrium need not be invoked. The effect of melt loss on the survival of peak minerals can be seen by considering an isobaric cooling path or an isothermal decompression path emanating from the g–sill–ksp–liq field in Fig. 5-6b. Both the cooling and the decompression paths result in the presence of the peak minerals (*i.e.*, excluding melt) with one additional phase (cordierite or biotite) being stable below the solidus as an equilibrium assemblage.

An example of variable degrees of intergranular retrogression can be seen in the partial to complete replacement of garnet by biotite in the felsic migmatites outlined in White *et al*. (2005). Here, a transition from metatexite to diatexite is preserved, a process driven by water-assisted melting. In the metatexites, which are characterized by melt segregation, garnet ranges from unretrogressed/weakly retrogressed (Fig. 5-10b) to completely pseudomorphed by randomly oriented clusters of biotite (Fig. 5-10c). The degree of replacement is likely related to the distribution of melt during the final stages of melt crystallization.

Retrograde reactions in high-grade rocks commonly manifest in texturally and compositionally complex ways, with individual textures requiring the addition or loss of elements. That is, individual textures cannot always be chemically balanced. For example, during cooling in the migmatites from Round Hill in the Broken Hill Block in Australia, retrograde reaction occurs between garnet, cordierite, K-feldspar and melt to produce biotite, sillimanite and quartz. Due to the pre-existing coarse-grained texture, and likely poor diffusivity of Al_2O_3, the textures developed are complex. In these rocks, biotite growth (along with minor sillimanite) is largely concentrated on matrix garnet (Fig. 5-10d), requiring the diffusion of MgO, H_2O, and K_2O into the site of biotite growth. In contrast, the replacement of cordierite is dominated by sillimanite (Fig. 5-10e), requiring the diffusion of FeO and MgO out of the site of sillimanite growth. Importantly, this melt crystallization reaction would appear to be the reaction responsible for the final crystallization of the melt (White *et al*. 2004). This textural evolution is akin to that described by Carmichael (1969) with the overall reaction being completed via a series of local partial reactions. Thus, the role of melt crystallization in individual reaction textures can be easily overlooked if such textures are considered in isolation.

Typical decompression-dominated *P–T* paths commonly produce cordierite in reaction textures. Such textures have mostly been interpreted only in terms of changes in *P–T* conditions and commonly in simple systems such as FMAS where the role of a melt phase is explicitly ignored. However, high-grade reaction textures involving the growth of cordierite will generally involve melt unless the cordierite is anhydrous, or another hydrous mineral is involved. Baldwin *et al*. (2005) interpreted cordierite coronas separating orthopyroxene from sillimanite in UHT granulites from Brazil, as not reflecting decompression, but as a result of changing a_{H2O} induced by a nearby influx of melt.

CONCLUSIONS

Mineral equilibria modeling provides important constraints on the formation and evolution of migmatites, not only allowing individual migmatites to be modeled, but as a mechanism to test hypotheses. However, it does not provide a magical solution to unraveling the myriad of processes that occur in migmatites, as many of these cannot be modeled using this method. Instead, mineral equilibria modeling provides a sound theoretical framework in which to consider the mineral assemblage evolution and partial melting processes in rocks. The correct use of such methods to interpret migmatites is concomitant with careful field observation and petrography and mineral equilibria methods should be used to support observations and not the other way round (Vernon *et al*. 2008).

Despite the numerous caveats in the application of mineral equilibria to rocks, it has proven useful in understanding metamorphic processes in general and, particularly in recent times, metamorphic processes in partially melted rocks. It has provided

a predictive framework in which to test ideas and to constrain quantitatively the consequences of various processes (*e.g.,* White *et al*. 2001, White & Powell 2002, Johnson *et al*. 2004). In terms of application to rocks, mineral equilibria methods are particularly useful for relating the *P–T* evolution of rocks, determined via the interpretation of metamorphic textures, with the production and crystallization of melt (*e.g.,* White *et al*. 2003, 2004, 2005, Johnson *et al*. 2004). However, such methods and the thermodynamic framework in which they are constructed are being constantly improved such that increasingly sophisticated modeling may be undertaken in future.

ACKNOWLEDGEMENTS

Ed Sawyer is thanked for the opportunity to present this contribution. Roger Powell is thanked for numerous discussions on phase diagrams and migmatites and for his part in many of the ideas proffered in this chapter. Geoff Clarke is also thanked for numerous discussions, providing several photographs and for introducing me to migmatites in the first place.

REFERENCES

ASHWORTH, J.R. & BIRDI, J.J. (1990): Diffusion modeling of coronae around olivine in an open system. *Geochim. et Cosmochim. Acta* **54**, 2389–2401.

BALDWIN, J. A., POWELL, R., BROWN, M., MORAES, R. & FUCK, R.A. (2005): Modeling of mineral equilibria in ultrahigh-temperature metamorphic rocks from the Anápolis–Itauçu Complex, central Brazil. *J. Metamorphic Geol.* **23**, 511–531.

BARBEY, P., MARIGNAC, J.M., MONTEL, J.M., MACAUDIÉRE, J., GASQUET, D. & JABBORI, J. (1999): Cordierite growth textures and the conditions of genesis and emplacement of crustal granite magmas: the Velay Granite complex (Massif Central, France). *J. Petrol.* **40**, 1425–1441.

BERMAN, R.G. (1988): Internally consistent thermodynamic data for minerals in the system Na_2O–K_2O–CaO–MgO–FeO–Fe_2O_3–Al_2O_3–SiO_2–TiO_2–H_2O–CO_2. *J. Petrol.* **29**, 445–522.

BROWN, M. (2002): Retrograde processes in migmatites and granulites revisited. *J. Metamorphic Geol.* **20**, 25–40

BROWN, M. (2007): Crustal melting and melt extraction, ascent and emplacement in orogens: mechanisms and consequences. *J. Geol. Soc., London* **164**, 709–730.

CARLSON, W.D. (1989): The significance of intergranular diffusion to the mechanisms and kinetics of porphyroblast crystallization. *Contrib. Mineral. Petrol.*, **103**, 1–24.

CARLSON, W.D. (2002): Scales of disequilibrium and rates of equilibration during metamorphism. *Am. Mineral.* **87**, 185–204.

CARMICHAEL, D.M. (1969): On the mechanism of prograde metamorphic reactions in quartz-bearing pelitic rocks. *Contrib. Mineral. Petrol.* **20**, 244–267.

CARRINGTON, D.P. & HARLEY, S.L. (1995): Partial melting and phase relations in high-grade metapelites: an experimental petrogenetic grid in KFMASH system. *Contrib. Mineral. Petrol.* **120**, 270–291.

CARSON, C.J., POWELL, R., WILSON, C.J.L & DIRKS, P.H.G.M. (1997): Partial melting during tectonic exhumation of a granulite terrane: an example from the Larsemann Hills, east Antarctica. *J. Metamorphic Geol.* **15**, 105–126.

CENKI, B., KRIEGSMAN, L.M. & BRAUN, I. (2002): Melt-producing and melt-consuming reactions in the Achankovil cordierite gneisses, South India. *J. Metamorphic Geol.* **20**, 543–561.

CLARKE, G.L., POWELL, R. & GUIRAUD, M. (1989): Low pressure granulite facies metapelitic assemblages and corona textures from MacRobertson Land, East Antarctica: the importance of Fe_2O_3 and TiO_2 in accounting for spinel-bearing assemblages. *J. Metamorphic Geol.* **7**, 323–335.

CLARKE, G.L., DACZKO, N.R., KLEPEIS, K.A. & RUSHMER, T. (2005): Roles for fluid and/or melt advection in forming high-P mafic migmatites, Fiordland, New Zealand. *J. Metamorphic Geol.* **23**, 557–567.

CLARKE, G.L., WHITE, R.W. LUI, S. FITZHERBERT, J.A. & PEARSON, N.J. (2007): Contrasting behaviour of rare earth and major elements during partial melting in granulite facies migmatites, Wuluma Hills, Arunta Block, central Australia. *J. Metamorphic Geol.* **25**, 1–18.

CONNOLLY, J.A.D. (1990): Calculation of multivariable phase diagrams: an algorithm based on generalised thermodynamics. *Am. J. Sci.* **290**, 666–718

DASGUPTA, S., SENGUPTA, P., EHL, J., RAITH, M. & BARDHAN, S. (1995): Reaction textures in a suite of spinel granulites from the Eastern Ghats Belt, India: evidence for polymetamorphism, a partial petrogenetic grid in KFMASH and the roles of ZnO and Fe_2O_3. *J. Petrol.* **36**, 435–461.

DIENER, J.F.A., POWELL, R., WHITE, R.W. & HOLLAND, T.J.B. (2007): A new thermodynamic model for clino- and orthoamphiboles in the system Na_2O–CaO–FeO–MgO–Al_2O_3–SiO_2–H_2O–O. *J. Metamorphic Geol.* **26**, 631–656.

FITZSIMONS, I.C.W. (1996): Metapelitic migmatites from Brattstrand Bluffs, east Antarctica – metamorphism melting and exhumation of the mid crust. *J. Petrol.* **37**, 395–414.

FOSTER, C.T. (1981): A thermodynamic model of mineral segregations in the lower sillimanite zone near Rangeley, Maine. *Am. Mineral.* **66**, 260–277.

FYFE, W. S., (1973): The granulite facies, partial melting and the Archaean crust. *Phil. Trans. Royal Soc. (London)*, **A273**, 457–461.

GRANT, J.A. (1985): Phase equilibria in partial melting of pelitic rocks. *In* Ashworth, J.R. (ed.). *Migmatites*. Blackie, London, 86–144.

GRANT, J.A. & FROST B.R. (1990): Contact metamorphism and partial-melting of pelitic rocks in the aureole of the Laramie Complex, Morton Pass, Wyoming. *Am. J. Sci.* **290**, 425–472.

GREENFIELD, J.E., CLARKE, G.L., BLAND, M. & CLARK, D.C. (1996): *In situ* migmatite and hybrid diatexite at Mt Stafford, central Australia. *J. Metamorphic Geol.* **14**, 363–378.

GREENFIELD, J.E., CLARKE, G.L., & WHITE, R.W. (1998): A sequence of partial melting reactions at Mt Stafford, central Australia. *J. Metamorphic Geol.* **16**, 363–378.

GUERNINA, S. & SAWYER, E.W., (2003). Large-scale melt-depletion in granulite terrains: an example from the Archean Ashuanipi sub-province of Quebec. *J. Metamorphic Geol.* **21**, 181–201.

HALPIN, J.A, CLARKE, G.L., WHITE, R.W. & KELSEY, D.E. (2007): Contrasting *P–T–t* paths for Neoproterozoic metamorphism in MacRobertson and Kemp Lands, east Antarctica. *J. Metamorphic Geol.* **25**, 683–701.

HAND, M. & DIRKS, P.H.G.M. (1992): The influence of deformation on the formation of axial-planar leucosomes and the segregation of small melt bodies within the migmatitic Napperby Gneiss, central Australia. *J. Structural Geol.* **14**, 591–604.

HENSEN, B.J. (1971): Theoretical phase relations involving garnet and cordierite in the system FeO–MgO–Al_2O_3–SiO_2. *Contrib. Mineral. Petrol.* **33**, 191–214

HOLLAND, T.J.B., & POWELL, R. (1985): An internally consistent thermodynamic dataset with uncertainties and correlations: 2: Data and results. *J. Metamorphic Geol.* **3**, 343–370.

HOLLAND, T.J.B., & POWELL, R. (1990): An enlarged and updated internally consistent thermodynamic dataset with uncertainties and correlations: the system K2O–Na_2O–CaO–MgO–MnO–FeO–Fe_2O_3–Al_2O_3–TiO_2–SiO_2–C–H_2–O_2. *J. Metamorphic Geol.* **8**, 89–124.

HOLLAND, T.J.B., & POWELL, R. (1996a): Thermodynamics of order–disorder in minerals. 1: symmetric formalism applied to minerals of fixed composition. *Am. Mineral.* **81**, 1413–1424.

HOLLAND, T.J.B., & POWELL, R. (1996b): Thermodynamics of order–disorder in minerals. 2: symmetric formalism applied to solid solutions. *Am. Mineral.* **81**, 1425–1437.

HOLLAND, T.J.B., & POWELL, R. (1998): An internally consistent thermodynamic dataset for phases of petrological interest. *J. Metamorphic Geol.* **16**, 309–343.

HOLLAND, T.J.B. & POWELL, R. (2001): Calculation of phase relations involving haplogranitic melts using an internally consistent dataset, *J. Petrol.* **42**, 673–683.

JOESTEN, R. (1977): Evolution of mineral assemblage zoning in diffusion metasomatism. *Geochim. Cosmochim. Acta* **47**, 283–294.

JOHNSON, T. & BROWN, M. (2004): Quantitative constraints on metamorphism in the Variscides of southern Brittany – a complementary pseudo-section approach. *J. Petrol.* **45**, 1237–1259.

JOHNSON, T.E., BROWN, M., GIBSON, R. L. & WING, B. (2004): Spinel–cordierite symplectites replacing andalusite: evidence for melt assisted diapirism in the Bushveld Complex, South Africa. *J. Metamorphic Geol.* **22**, 529–545.

KELSEY, D.E, WHITE, R.W. & POWELL, R. (2003): Orthopyroxene–sillimanite–quartz assemblages: distribution, petrology, *P–T–X* constraints and *P–T* paths. *J. Metamorphic Geol.* **21**, 439–453.

KORZHINSKII, D.S. (1959): *Physicochemical basis of the analysis of the paragenesis of minerals*. Consultants Bureau, New York. 142pp.

KRIEGSMAN, L.M. 2001. Partial melting, partial melt extraction and partial back reaction in anatectic migmatites. *Lithos* **56**, 75–96.

POWELL, R. (1983): Processes in granulite facies metamorphism. *In* Migmatites, melting and metamorphism, eds. M.P. Atherton & C.D. Gribble, pp 127–139; London, Shiva.

POWELL, R., & DOWNES, J. (1990): Garnet porphyroblast-bearing leucosomes in metapelites: mechanisms and an example from Broken Hill, Australia. *In* Ashworth, J.R., and Brown, M. (eds) High temperature metamorphism and crustal anatexis. Unwin Hyman, London, 105–123.

POWELL, R. GUIRAUD, M. & WHITE, R.W. (2005): Truth and beauty in metamorphic phase equilibria: conjugate variables and phase diagrams. *Can. Mineral.* **43**, 21–33

POWELL, R., & HOLLAND, T.J.B. (1988): An internally consistent thermodynamic dataset with uncertainties and correlations: 3. Application, methods, worked examples and a computer program. *J. Metamorphic Geol.* **6**, 173–204.

POWELL, R. & HOLLAND, T. (1990): Calculated mineral equilibria in the pelite system, KFMASH (K_2O–FeO–MgO–Al_2O_3–SiO_2–H_2O). *Am. Miner.* **75**, 367–380.

POWELL, R., & HOLLAND, T.J.B., 1993. On the formulation of simple mixing models for complex phases. *Am. Mineral.* **78**, 1174–1180.

POWELL, R., & HOLLAND, T.J.B., (1999): Relating formulations of the thermodynamics of mineral solid solutions: activity modeling of pyroxenes, amphiboles and micas. *Am. Mineral.* **84**, 1–14.

SAWYER, E.W. (1986): The influence of source rock type, chemical weathering and sorting on the geochemistry of clastic sediments from the Quetico metasedimentary belt, Superior Province, Canada. *Chem. Geol.* **55**, 77–95.

SAWYER, E.W. (1998): The formation and evolution of granite magmas during crustal reworking: the significance of diatexites. *J. Petrol.* **39**, 1147–1167.

SAWYER, E.W. (1999): Criteria for the recognition of partial melting. *Phys. Chem. Earth, Part A, Solid Earth and Geodesy* **24**, 269–279.

SAWYER, E.W., DOMBROWSKI, C. & COLLINS, W.J. (1999): Movement of melt during synchronous regional deformation and granulite-facies anatexis, an example from the Wuluma Hills, central Australia. *In* Castro, A., Fernandez, C. & Vigneresse, J.L. (eds) Understanding Granites: Integrating New and Classical Techniques. *Geol. Soc. London Sp. Publ.* **168**, 221–237.

STÜWE, K. & POWELL, R. (1989): Metamorphic segregations associated with garnet and orthopyroxene porphyroblast growth: two examples from the Larsemann Hills, east Antarctica. *Contrib. Mineral. Petrol.* **103**, 523–530.

THOMPSON, J.B., (1957): The graphical analysis of mineral assemblages in pelitic schists. *Am. Mineral.* **42**, 842–858.

VERNON, R.H., CLARKE, G.L. & COLLINS, W.J. (1990): Local, mid-crustal granulite facies metamorphism and melting: an example in the Mount Stafford area, central Australia. *In* Ashworth, J.R. & Brown, M. (eds). High temperature metamorphism and crustal anatexis. *Mineral. Soc. sp. publ.* Unwin Hyman, London, 272–319.

VERNON, R.H., WHITE, R.W. & CLARKE, G.L. (2008): Using microstructural evidence and *P–T* data to infer metamorphic non-events. *J. Metamorphic Geol.*, **26**, in press.

WATERS, D. J. 1988. Partial melting and formation of granulite facies assemblages in Namaqualand, South Africa. *J. Metamorphic Geol.* 6, 387–404.

WATERS, D.J. & WHALES, C.J. (1984): Dehydration melting and the granulite transition in metapelites from southern Namaqualand, S. Africa. *Contrib. Mineral. Petrol.* **88**, 269–275.

WHITE, R.W. & POWELL, R. (2002): Melt loss and the preservation of granulite facies mineral assemblages. *J. Metamorphic Geol.* **20**, 621–632.

WHITE, R.W., POWELL, R. & HOLLAND, T.J.B. (2001): Calculation of partial melting equilibria in the system Na_2O–CaO–K_2O–FeO–MgO–Al_2O_3–SiO_2–H_2O (NCKFMASH). *J. Metamorphic Geol.* **19**, 139–153.

WHITE, R.W., POWELL, R. & CLARKE, G.L. (2002): The Interpretation of reaction textures in Fe-rich metapelitic granulites of the Musgrave Block, central Australia: Constraints from mineral equilibria calculations in the system K_2O–FeO–MgO–Al_2O_3–SiO_2–H_2O–TiO_2–Fe_2O_3. *J. Metamorphic Geol.* **20**, 41–55.

WHITE, R. W., POWELL, R. & CLARKE, G. L. (2003): Prograde metamorphic assemblage evolution during partial melting of metasedimentary rocks at low pressures: migmatites from Mt Stafford, central Australia. *J. Petrol.* **44**, 1937–1960.

WHITE, R.W., POWELL, R. & HALPIN, J.A. (2004): Spatially focused melt formation in aluminous metapelites from Broken Hill, Australia. *J. Metamorphic Geol.* **22**, 825–845.

WHITE, R.W., POMROY, N.E. & POWELL, R. (2005): An *in situ* metatexite–diatexite transition in upper amphibolite facies rocks from Broken Hill, Australia. *J. Metamorphic Geol.* **23**, 579–602.

WHITE, R. W., POWELL, R. & HOLLAND, T. J. B. (2007): Progress relating to calculation of partial melting equilibria for metapelites and felsic gneisses. *J. Metamorphic Geol.* **25**, 511–527.

WHITE, R.W., POWELL, R. & BALDWIN, J.A., (2008): Calculated phase equilibria involving chemical potentials to investigate the textural evolution of metamorphic rocks. *Journal of Metamorphic Geology*, **26**, in press.

ZEH, A., KLEMD, R., BUHLMANN, S. & BARTON, J.M. (2004): Pro- and retrograde *P–T* evolution of granulites of the Beit Bridge Complex (Limpopo Belt, South Africa): constraints from quantitative phase diagrams and geotectonic implications. *J. Metamorphic Geol.* **22**, 79–95.

CHAPTER 6: GRANITES, MIGMATITES AND RESIDUAL GRANULITES: RELATIONSHIPS AND PROCESSES

Michael Brown
Laboratory for Crustal Petrology, Department of Geology,
University of Maryland,
College Park, MD 20742-4211, USA
E-mail: mbrown@umd.edu

INTRODUCTION

In this chapter, I address the relationship between (leuco-) granites, migmatites and residual granulites – the former recording magma ascent and pluton emplacement in the middle to upper crust and the latter recording evidence of pervasive melting, melt loss from and melt transfer through the middle to lower crust. The history of the origins of migmatite and granite, the relationships between migmatite and granite, and the origin of granulites is long and controversial. For historical background and different views of this debate the reader is referred to the books by Sederholm (1967, which contains his four classic papers on these topics among the seven chapters, *viz.* 1907, 1923, 1926, 1934), Gilluly (1948), Read (1957) and Mehnert (1968). For more modern views the reader is referred to reviews by Atherton (1993), Brown (1994, 2001a, b, 2007b), and Petford *et al.* (2000), the first four chapters on crustal evolution in the book by Vielzeuf & Vidal (1990) and the last six chapters in the book by Brown & Rushmer (2006).

What are the issues?

Crustal differentiation is mainly achieved through partial melting processes and segregation of more felsic melt from more mafic residue, which means that a compositionally layered crust is an inevitable result regardless of any additional complexity introduced by mantle inputs and hybridization processes (*e.g.*, Clemens 1990, Brown & Rushmer 2006, Kemp *et al.* 2006, 2007a, Hawkesworth & Kemp 2006). Magmas that crystallize after migration to shallower levels contribute to a more evolved upper crust, whereas the deeper crust becomes more refractory. Convergent plate margin processes (subduction and collision) transport fertile materials to depth in continental margin accretionary orogenic systems and subduction–to–collision orogenic systems, and bury fertile materials by thickening in backarcs and orogenic hinterlands. These fertile materials are the fuel for granite magmatism, which may be boosted by additions of mass and heat from mantle-derived magmas. These plate margin processes have operated since at least the Neoarchean (*e.g.*, Brown 2006, Gerya *et al.* 2008).

Common crustal rocks melt at temperatures as low as 700°C if an aqueous fluid phase is present. However, the deep continental crust is 'dry' (*e.g.*, Yardley & Valley 1997, Wannamaker *et al.* 2000) and under this condition major melt production generally occurs at temperatures above 800°C, and temperatures need to be greater than 900°C if hornblende-bearing protoliths are involved (*e.g.*, Clemens 2006). Meeting these thermal requirements may require input from extra-crustal heat sources. In circumstances where heat is advected with mafic to intermediate composition magmas the possibility exists for additions of mass to the source, and involvement of these magmas in the generation of more mafic S-type granites (*e.g.*, Vernon 2007) or even hornblende-bearing I-type granites from common metasedimentary protoliths (*e.g.*, Kemp *et al.* 2007a). The melt-depleted, residual crust might be similar to the composite section through mafic granulite, residual granulite and migmatite, tonalite and granodiorite that comprises the lower crust in the Hidaka metamorphic belt in Japan (*e.g.*, Vernon 2007, Kemp *et al.* 2007b).

Some ultrahigh pressure metamorphic (UHPM) terranes show extensive development of migmatite or other evidence of partial melting during exhumation from UHPM conditions. In these terranes, indications of partial melting have been a matter of debate rather than universally agreed as such. For example, features inferred to record melting have been documented in the Dabie Shan of China (Faure *et al.* 1999, Zhong *et al.* 2001), the Western Gneiss region of Norway (Labrousse *et al.* 2002) and the northeast Greenland Caledonides (Lang & Gilotti 2007). However, the debate may be over. Recent

Mineralogical Association of Canada Short Course 38, Quebec City, Quebec, p. 97-144

experimental results for fluid-present melting under UHPM conditions (*e.g.*, Hermann & Spandler 2008) and fluid-undersaturated melting during exhumation (decompression) from UHPM conditions (*e.g.*, Auzanneau *et al.* 2006) support the inference of melting derived from field and petrographic studies of UHPM rocks.

Melting occurs at distributed multiphase grain boundaries in a source (<mm^3) during a metamorphic cycle that may take several to several tens of Ma, whereas a pluton represents a large volume of magma (10^3–10^4 km^3 or more) that accumulated in multiple batches (each perhaps 10^{-1}–10^2 km^3) at a sink and crystallized within tens of ka to several Ma. Melt extraction, from segregation to emplacement, is a process with a length scale that spans more than seven orders of magnitude, or a volume concentration factor that exceeds 10^{21}, and a time scale of ~10^{12}–10^{14}s (Brown 2004).

The height from the anatectic front – the upper surface or roof of the volume of melting crust, a dynamic feature during orogenesis (Brown & Solar 1999) – to the level of emplacement varies according to the degree of orogenic thickening and amount of syn-collision extension or orogenic collapse. Only rarely is this distance going to be more than 30 km and commonly it will be (much) less (Fig. 6-1). The thickness of the source is unlikely to be more than 20 km. Since the number of feeders to an individual intrusion varies from one to several (Cruden 2006), and the footprint of the source drained for any single intrusion is unlikely to be smaller than the lateral extent of the granite (Fig. 6-2), the principal issue becomes one of focusing the melt (achieving the volume concentration from grain boundaries to plutons).

The spacing of intrusions in continental arcs and subduction to collision orogens (Bons & Elburg 2001, Cruden 2006) suggests focusing of melt during extraction and ascent and indicates extraction of melt from sources of similar footprint and presumably similar volume in any one setting. To a first approximation, the volume of granite emplaced in the middle to upper crust equals the volume of melt extracted from the middle to lower crust. Therefore, there is no space problem at the crustal scale. However, the ascent mechanisms that link melt extraction from the source to magma emplacement in a pluton remain contentious.

Numerical and analog modeling has led to the suggestion that melt extraction is a self-organized critical phenomenon (Vigneresse & Burg 2000, Bons & Elburg 2001, Bons & van Milligen 2001, Soesoo *et al.* 2004), similar to that proposed for volcanoes (Shaw & Chouet 1991) and basalt melt flow through the shallow mantle beneath ocean spreading centers as recorded by dunite-filled conduits (Braun & Kelemen 2002). A universal feature of self-organized critical phenomena is that they are driven systems that involve 'avalanches' with a fractal (power law) frequency–size distribution (Turcotte 1999, 2001). If this is true for melt extraction, we might expect the distribution of melt batch sizes and/or widths of melt flow channels to follow power law distributions.

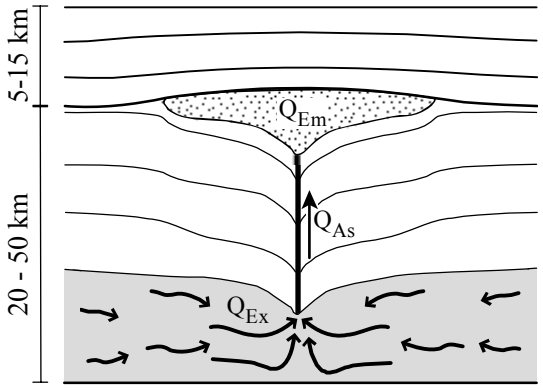

FIG. 6-1. A simple model of melt extraction, ascent and emplacement, in which the rates of melt production, extraction, ascent and emplacement are likely to be balanced at the crustal scale (from Brown, 2007, © 2007 Geological Society, with permission of the Geological Society Publishing House). The rate of melt production (Q_{Me}) is controlled by heat flow, and is not shown explicitly in the figure. Volume fluxes for melt extraction (Q_{Ex}), melt ascent (Q_{As}) and melt emplacement (Q_{Em}) are shown schematically (after Cruden 1998). The depths shown on the left-hand side of the figure are a general indication of the likely range in orogenic environments.

Results to date are ambiguous for migmatite leucosomes (Tanner 1999, Marchildon & Brown 2003, Bons *et al.* 2008), but widths of granite dikes measured in multiple studies do exhibit power law distributions (Kruhl 1994, Bons *et al.* 2004, Brown 2005, Urtson & Soesoo 2007). The ambiguity for leucosome widths may relate to the anisotropic fabrics in the protoliths, may relate to conflating leucosomes with small dikes, or may relate to drawdown during stagnation of melt flow networks and freezing of remaining melt. Melt extraction may be an example of the inverse cascade model for self-similar growth of clusters (Turcotte *et al.* 1999, 2002, Gabrielov *et al.* 1999), as implied by the model of Bons *et al.* (2004, 2008), but this remains to be demonstrated in nature.

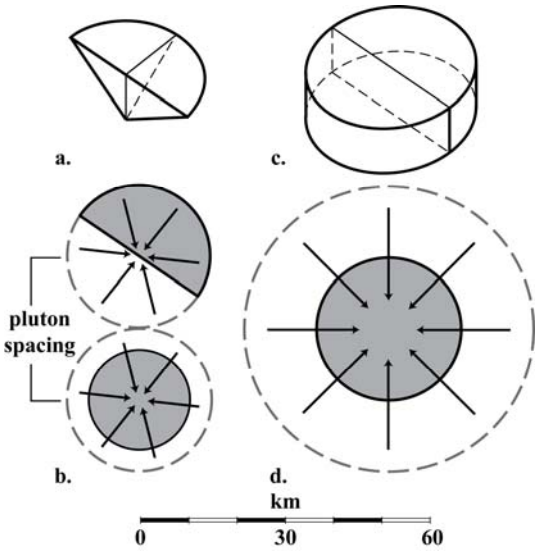

FIG. 6-2. A simple model to illustrate pluton–source relations in orogens (from Brown, 2007, © 2007 Geological Society, with permission of the Geological Society Publishing House). **a**, Perspective view of horizontal semi-circular half-cone-shaped pluton of diameter about 30 km and half-height about 5 km. **b,** Plan view of a horizontal semi-circular half-cone-shaped pluton of diameter about 30 km and a horizontal circular cone-shaped pluton of diameter about 21 km in relation to the footprint for a source of sufficient volume to fill the pluton (for a source about 30 km diameter, based on an assumed thickness of 15 km and 20 vol.% melting with 20 vol.% fractional crystallization of the melt during transport through the source). One implication of this model for the assumptions made is that plutons will be spaced at least 30 km apart. **c**, Perspective view of a horizontal tabular intrusion of diameter about 30 km and thickness about 10 km, which is four times greater volume than the plutons discussed in (b). **d,** Plan view of a horizontal tabular intrusion of diameter about 30 km in relation to the footprint for a source of sufficient volume to fill the intrusion (for a source about 60 km diameter, based on an assumed thickness of 15 km and 20 vol.% melting with 20 vol.% fractional crystallization of the melt during transport through the source). One implication of this model for the assumptions made is that intrusions will be spaced at least 60 km apart. A more sophisticated view of pluton–source shape and volume, and melt extraction and accommodation is given in Cruden & McCaffrey (2001) and Cruden (2006).

What are the volumes of melt generated?

According to one estimate from an area of 1.5 x 10^5 km^2 in the Lachlan Fold Belt of southeastern Australia – an accretionary orogenic belt that developed above a subducting ocean plate – about 10^3 plutons with a volume greater than 1 km^3 were emplaced during Siluro-Devonian orogenic events giving a total volume around 1.5 x 10^5 km^3 (Bons & Elburg 2001). This distribution is consistent with an average melt loss of ~10 vol.% from a source ~10 km thick (*e.g.*, Zen 1992); such an estimate ignores mass input due to melting in the mantle wedge and interaction with lower crustal melt. In contrast, another estimate from three successive highly focused, linear plutonic suites in an area of about 10^4 km^2 in the Cretaceous central Sierra Nevada Batholith in California, which also developed above a subducting ocean plate, yields magma volumes per unit area that are up to four times larger that those in the Lachlan Fold Belt (Cruden 2006). The difference may reflect a higher proportion of mass additions from the mantle and/or a higher degree of crustal melting in the formation of the central Sierra Nevada Batholith, which in turn may relate to plate kinematics and/or rates of subduction.

In contrast to these continental margin orogenic systems, in one study from the Ashuanipi subprovince of the Neoarchean Superior Province in Canada about 30 vol.% melt is inferred to have been extracted on average from residual granulite derived from greywacke protoliths (Guernina & Sawyer 2003). Extrapolation to the Ashuanipi subprovince as a whole suggests that around 6.5 x 10^5 km^3 of melt could have been extracted from granulite-facies lower crust; this would represent an equivalent 'layer' of granite some 7 km thick (Guernina & Sawyer 2003). An alternative calculation for the whole of the Superior Province, based on the map distribution of plutons that form the late Neoarchean pan-Superior granodiorite–granite suite, yields an average estimate for the province of 2–6 x 10^6 km^3 of melt generated, which would represent a 'layer' of granite 'only' 1–3 km thick (Cruden 2006). There is a larger area (proxy for volume) of granodiorite–granite suite plutons exposed in the Ashuanipi subprovince in comparison with the Superior Province as a whole, which may indicate generation of a larger amount of melt by higher degrees of melting in the source. Such an interpretation is consistent with the strongly depleted nature of the associated residual granulites exposed at the surface in the Ashuanipi subprovince (Guernina & Sawyer 2003). These melt volumes are huge and reflect massive differentiation of the continental crust during Neoarchean cratonization.

According to Cruden (2006), the focused nature of magmatic events in the central Sierra Nevada

Batholith and the predominantly tabular form of the plutons suggests higher degrees of melting and larger magma fluxes. In contrast, he argued that the defocused nature of the granodiorite–granite magmatism in the Superior Province and the predominantly wedge-shaped form of the plutons are more consistent with generally moderate degrees of melting. These differences may reflect the continental margin setting of the central Sierra Nevada Batholith, where mantle wedge-derived magmas advect heat continuously into the lower crust promoting overall higher degrees of melting (Cruden 2006). In addition, mass addition by mantle wedge-derived magmatism promotes hybridization with lower crustal melts contributing to the larger volume of middle to upper crustal plutons in continental arcs (Kemp *et al.* 2007a).

From partial melting to pluton emplacement – a brief overview

In 1907, Sederholm published his paper "Om granit och gneis deras uppkomst, uppträdande och utbredning inom urberget i Fennoskandia " in the "*Bulletin de la Commision géologique de Finlande.*" This article is now available in translation in "Selected Works: Granites and Migmatites" as the first chapter "On granite and gneiss, their origin, relations and occurrence in the pre-Cambrian complex of Fenno-Scandia" (Sederholm 1967), beginning a debate about crustal melting processes and what migmatite complexes represent that continues to the present day.

Figure 6-3 is a copy of the map of the eastern part of Spikarna Island (more correctly, the easternmost skerry of Spikarna) from Sederholm's 1907 paper. This map illustrates some of the ambiguities of melt generation at this crustal level, perhaps recorded by the thinner, sometimes folded leucosomes, *versus* magma frozen during transfer through this crustal level, perhaps recorded by the thin discordant dikes in the west and the thicker dike east of center that connect to leucosome networks throughout the outcrop. For a description of the outcrops mapped by Sederholm, the interested reader is referred to pp. 19–22 in Sederholm (1967).

In the anatectic zone – that portion of the crust thermally above the solidus (but generally structurally deep) – melt segregates from solid residue and migrates, forming magma as the melt entrains residual, peritectic or early crystallized solids. Leucosome may occur anywhere in the anatectic zone due to trapping of magma or the early crystallized products from migrating magma during extraction and ascent. Leucosome provides evidence of the melt extraction pathways and linkages to the magma ascent conduits. The magma also may freeze as granite during ascent as the rate of flow declines or batches of the magma may reach a level of emplacement and contribute to pluton growth before crystallizing (*e.g.*, Powell 1983, Brown 1994, 2004, 2007b, Brown & Solar 1999, Weinberg 1999, Olsen *et al.* 2004, Slagstad *et al.* 2005). Thus, any predominantly two-dimensional outcrop represents a map slice through the integrated crustal record of these processes (see Brown & Solar 1998b, 1999). The study of outcrops that represent different depth slices through the crust provides information about the third dimension (see example in final section of this chapter), as, indeed, does modeling of any gravity anomaly, and application of accessory phase dating techniques to components within each of these outcrops enables us to unravel the fourth dimension of time.

Crustal melting and granite magmatism represents an integrated process modulated by feedback relations, although for convenience we generally describe this process in four stages as follows: melting, melt segregation and extraction, magma ascent, and magma emplacement. There is no *a priori* reason to suppose that the process or these stages are fundamentally different in continental margin accretionary orogenic systems or in the hinterland of subduction to collision orogenic systems. However, the proportion of mass input from the mantle may vary from significant to insignificant and the proportion of fractionation of hybrid magmas *versus* melting of the crust may be different from continental margins to collisional hinterlands.

Regional scale crustal melting is a process that occurs in response to crustal thickening and/or exhumation, or due to the infusion of heat. Heat generally will be the principal rate control at the crustal scale, whereas deformation due to regional stress will be the mechanism enabling segregation and extraction (Brown 1994, 2007b). Likely, ~90% of melt generated is extractable with ~10% remaining on grain boundaries.

Segregation by intragranular porous flow probably occurs on a similar time scale to melting, but migration of segregated melt by channel flow in veins is faster. Gravity-driven and/or shear-enhanced compaction of the solid matrix is likely to be rate controlling at the outcrop scale (Rutter 1997,

FIG. 6-3. Copy of Sederholm's petrological sketch map of the eastern part of Spikarna Island (more correctly, the easternmost skerry of Spikarna) in the skargaard of Tvärminne, east of Hango, from his 1907 paper (reproduced from Sederholm, 1967, originally published in the *Bull. Comm. geol. Finl.* **23**, © 1907 Geological Survey of Finland, with permission of the Geological Survey of Finland).

Rutter & Mecklenburg 2006). Rates of ascent vary according to the mechanism of ascent, but there is consensus that some form conduit flow is likely the dominant mechanism and that the time scale for ascent is short (Brown 2007b). Emplacement of individual melt batches occurs on a similar time scale to ascent – hundreds to thousands of years – whereas pluton construction may take hundreds of thousands to several millions of years.

It is useful to consider qualitatively the processes involved in granite magmatism in terms of volume fluxes (Fig. 6-1; Q_{Me}, melting; Q_{Ex}, extraction; Q_{As}, ascent; and, Q_{Em}, emplacement) over distinct time intervals (*e.g.,* Thompson 1999, Brown 2001a, b, 2004). Relationships between pairs of these quantities may allow assessment of the relative efficiencies and magnitudes of melt flow mechanisms. Thus, if $Q_{Ex} = Q_{As}$ and $Q_{As} = Q_{Em}$, then $Q_{Me} = Q_{Ex} = Q_{As} = Q_{Em}$ and no focusing was necessary – the system potentially may be described by pervasive flow (*e.g.*, Hasalová *et al.* 2008a, b). However, if $Q_{Me} > Q_{Ex}$ (and Q_{As} is not rate-limiting), then fracturing potentially occurs near the source, and Q_{Ex} is increased by channeled flow (*e.g.*, Bea *et al.* 2007); on the other hand, if $Q_{Em} > Q_{Ex}$ (and Q_{As} is not rate-limiting), episodic extraction is necessary (*e.g.*, Handy *et al.* 2001), or the melt flux is rapidly exhausted. Finally, if $Q_{Me} < Q_{Ex}$, the source may be drained rapidly.

It is also useful to consider pluton emplacement style and the source residue characteristics that result from these volume fluxes (Brown 2007b). Comparing volume fluxes (Fig. 6-1) for ascent (Q_{As}) *versus* emplacement (Q_{Em}), if $Q_{As} = Q_{Em}$ then magma is likely to be emplaced into horizontal wedge or tabular plutons, whereas if $Q_{As} > Q_{Em}$ then magma is likely to be trapped in the ascent conduit, where it may promote lateral growth of weaknesses – thermal or mechanical – in the walls of the ascent conduit to form blobby plutons or it may simply freeze *in situ* to form vertical lozenge plutons. Comparing volume fluxes (Fig. 6-1) for extraction from the source (Q_{Ex}) *versus* emplacement, if $Q_{Ex} = Q_{Em}$ then residual granulite will be left in the source, and magma is likely to be emplaced into horizontal wedge or tabular plutons, whereas if $Q_{Ex} > Q_{Em}$ then blobby or vertical lozenge plutons may form during ascent and magma may be left in the source to crystallize as leucosome. Comparing volume fluxes (Fig. 6-1) for extraction *versus* ascent, if $Q_{Ex} = Q_{As}$ then residual granulite will be left in the source, whereas if $Q_{Ex} > Q_{As}$ then accumulated melt will be stuck in the source where it may crystallize as granite within residual granulite.

What is the source of the heat for melting?

The source of the enhanced heat to drive melting is elusive in many circumstances. Numerical models of thickened orogens generally do not produce temperatures necessary for extensive melting (*e.g.*, Connolly & Thompson 1989, Jamieson *et al.* 1998, 2004). Under 'dry' conditions, some crustal compositions will melt where peak temperatures reach 800°C (*e.g.,* mica-rich metapelite), as may be achieved in these models, but there is a thermal deficiency of up to 250°C to achieve 40 vol.% melting in comparison with experiments for melting of greywacke, felsic igneous rocks and amphibolite (Clemens 2006). In general, temperatures in the lower to middle crust are buffered around the transition from granulite facies to ultrahigh temperature metamorphic conditions (~900°C), as reflected in retrieved peak *P–T* conditions from many granulite terranes worldwide (Pattison *et al.* 2003, Brown 2007a). These temperatures are consistent with predominant mica-breakdown and subordinate amphibole-breakdown melting of the continental crust, but not sufficient if melt volumes on the order of 40 vol.% are required from common crustal protoliths.

Radiogenic heating is important and may be sufficient if initial thickening is by a factor approaching three and sufficient time is available (*e.g.*, McKenzie & Priestley 2008), although this may depend upon the distribution of the heat-producing elements (U, Th, K; see Sandiford & McLaren 2002), and whether decompression occurs during exhumation (Thompson 1999). In some circumstances, melting may result from a 'hot' geotherm due to an increased concentration of heat-producing elements (*e.g.,* Andreoli *et al.* 2006, McLaren *et al.* 2006). However, the timescale for radiogenic heating generally is long in comparison with other mechanisms (perhaps a minimum of several 10^7 years), whereas the timescale for metamorphism in some orogens is short (perhaps only several 10^6 years and in some cases much less) indicating that other sources of heat are important in many metamorphic belts.

The role of viscous dissipation (shear heating) during deformation is controversial but appears to have been undervalued. It is a contributory factor in the early stages of heating in thickening orogens driven by fast rates of convergence and may be more significant than realized previously (Leloup &

Kienast 1993, Kincaid & Silver 1996, Stüwe 1998, Harrison *et al.* 1998, Burg & Gerya 2005, Stüwe 2007, Hartz & Podladchikov 2008). Shear heating with lithospheric thickening at high integrated strength may be the solution for the enigmatic source of additional heat in many metamorphic belts formed by subduction to collision orogenesis. However, the mechanism is self-limiting and self-regulating because increasing the temperature reduces the strength and thus the rate of heat production (Burg & Gerya 2005, Hartz & Podladchikov 2008).

Heat advection by pervasive intracrustal melt flow, by ascent and emplacement of leucogranite magma, or by intracrustal convection may be important in some circumstances, but the volume of additional melt generated by these mechanisms is likely to be limited (Brown & Solar 1999, Weinberg 1999, Babeyko *et al.* 2002, Leitch & Weinberg 2002, Annen *et al.* 2006b, Hasalová *et al.* 2008a, b). Alternatively, tectonic processes such as thinning the continental lithosphere to raise the convecting asthenosphere during extension or delamination of the mantle lithosphere during tectonic shortening and arc-related magmatism or delamination of continental lithosphere after thickening in subduction to collision orogenesis have been invoked to cause an enhanced mantle heat flow (*e.g.,* Loosveld & Etheridge 1990, Sandiford & Powell 1991, Babeyko *et al.* 2002). Thickening of thin lithosphere characterized by higher intrinsic basal heat flow from the mantle, for example as occurs in backarcs (Currie & Hyndman 2006), also may generate large hot orogens (*e.g.,* Hyndman *et al.* 2005).

Nonetheless, in many cases, additional heat from an external source is necessary. This heat may be advected with mafic magma (*e.g.*, Patchett 1980, Huppert & Sparks 1988, Bergantz 1989, Vielzeuf *et al.* 1990, Finger & Clemens 1995, Grunder 1995, Patiño-Douce 1999, Thompson 1999, Bodorkos *et al.* 2002, Clemens 2003, Dufek & Bergantz 2005, Annen *et al.* 2006a, Vernon 2007, Depine *et al.* 2008), which is likely to be important in continental margin accretionary orogenic systems. Heat from mantle-derived magma emplaced at the base of the crust has been argued to be very effective during lithosphere extension (*e.g.,* Bergantz 1989, Bea *et al.* 2007). However, this relationship commonly has proven to be ambiguous for exposed levels of the deep crust (Barboza *et al.* 1999, Peressini *et al.* 2007) and demonstrating mafic magmatism synchronous with UHT metamorphism has proven elusive (*e.g.,* Baldwin & Brown 2008), leaving the role of mantle-derived magma as attractive but cryptic or enigmatic.

MELTING

> *"It might . . . appear somewhat strange to combine a . . . review of migmatites and their rather complex origin with the so-called 'granite-problem' . . . however, many problems are shared by both groups, and a close inspection of the one encompasses some insight into the other . . . since migmatites . . . illustrate the origin of granite . . .* in statu nascendi *. . . it is possible to give a detailed account of the geochemical balance involved in the origin of granite . . ."*
>
> K.R. Mehnert (1968)

> *"In rocks with the right composition . . . major amounts of granitic melt will be formed by fluid-absent reactions . . . many of these melts will rise in the crust until crystallization and/or structural factors cause them to stop . . . granulite-facies metamorphism should be considered as the main mechanism . . . by which the crust becomes internally differentiated . . . the deep crust must contain a substantial component of granulitic restite . . ."*
>
> J.D. Clemens (1990)

Under equilibrium conditions in an isotropic crust, melting begins at multiphase grain junctions that include quartz and feldspar, and a hydrate phase. However, the earth's crust is anisotropic and in a state of stress, and variations in bulk composition and grain size influence the sites at which melting begins. Thus, differential stress varies within any particular volume of crust and variations in differential stress give rise to pressure gradients throughout this volume of crust. It follows that equilibrium conditions cannot be modeled using hydrostatic thermodynamics. In hydrostatic thermodynamics, we assume the mean stress to be the main contributor to the internal energy of a phase, and we assume effects due to strain or differential stress are small and may be neglected. Various authors have shown that this assumption is unwise, including Kamb (1961), Patterson (1973), Robin (1974), Green (1980) and Bayley (1985). Interactions among mechanical and chemical processes are likely to be a fertile area for research in the years to come.

Melting may begin at sites of lower or higher resolved normal stress, once the initial thermal

overstep is close to that required to overcome the activation energy for the particular melting reaction. For wet melting (solidus with negative dP/dT), the start of reaction is more likely at sites of higher resolved normal stress, whereas for hydrate-breakdown melting (solidus with positive dP/dT), the start of reaction is more likely at sites of lower resolved normal stress (Brown & Solar 1998a, pp. 212–213). Deformation leads to dissipation of energy as heat, which may be significant in determining possible sites of initial melting but has not been investigated (*cf.* Hobbs *et al.* 2007). Once melting begins, melt connects in all common crustal protoliths in both non-deforming and deforming environments (Laporte *et al.* 1997).

As melting begins, so permeability develops, leading to gradients in melt pressure and melt flow. This implies non-equal melt pressure and confining stress and differences in melt–solid (lower stress) and solid–solid (higher stress) interfaces. The implications of these stress differences in relation to melting have not been investigated; to do so requires the theory of non-hydrostatic thermodynamics (see above). In non-hydrostatic thermodynamics the chemical potentials are controlled by the local resolved normal stress at an interface or surface, which will lead to important feedbacks as melting begins at sites of higher or lower resolved normal stress as discussed above.

Wet melting

At a regional scale, there is only a small amount of free water in the middle and lower crust (<1 vol.%) near the solidus. Local introduction of water may occur in the inner zone of contact aureoles around granitic and mafic intrusions (Pattison & Harte 1988, Symmes & Ferry 1995, Johnson *et al.* 2003). In addition, water may infiltrate from adjacent units that have a higher solidus or along shear zones or regionally (Selbekk *et al.* 2000, Johnson *et al.* 2001b, Slagstad *et al.* 2005, White *et al.* 2005, Berger *et al.* 2008, Florian *et al.* 2008). Given the limited porosity of high-grade subsolidus crust, deformation-enhanced dynamic permeability is likely required to facilitate fluid infiltration; zones of regional scale transpressive deformation may be particularly appropriate to promote fluid-enhanced melting (*e.g.*, the St. Malo migmatite belt – see Brown 1995, Milord *et al.* 2001). Inconsistency between the observed volumes of (apparently) locally derived leucosome and that expected for the calculated peak P–T conditions may be indicative of fluid infiltration and wet melting.

Once fluid-consuming melting reactions have used up the available water, further melting must proceed by fluid-conserving (hydrate-breakdown) melting reactions, which leads to progressively more water-undersaturated melt with increasing temperature. However, since dissolved water and temperature have opposite effects on viscosity, the viscosity of the melt remains around $10^{4–5}$ Pa, depending on composition (Clemens & Petford 1999).

Two generalized examples of fluid-consuming reactions for metapelite are:

$$\text{Ms + Pl (+/– Kfs) + Qtz + } H_2O = \text{L}$$

and

$$\text{Ms + Bt + Pl + Qtz + } H_2O = \text{L}$$

[mineral abbreviations are from Kretz (1983), plus L for melt]. The negative slope of the solidus for wet melting limits vertical migration of the melt (it will crystallize during limited decompression to the solidus) whereas this is not the case for water-undersaturated melting (because hydrate-breakdown melting reactions have positive slopes in P–T space at crustal pressures).

Hydrate-breakdown melting

Hydrate-breakdown melting occurs over a range of temperature after an initial insignificant wet melting step that generates minimal melt from the small amount of free water (<1 vol.%) at the water-saturated solidus. With increasing temperature, the crust progressively encounters muscovite and biotite breakdown in metasedimentary and (leuco-) granite protoliths, biotite with or without hornblende breakdown in quartzofeldspathic (*e.g.*, calc-alkaline) plutonic rocks and hornblende breakdown in amphibolite, respectively (*e.g.*, White *et al.* 2004, Clemens 2006). Generalized examples of hydrate-breakdown melting reactions are

$$\text{Ms + Pl + Qtz = Als + Kfs + L,}$$

$$\text{Bt + Als + Qtz = Grt/Crd + Kfs + L,}$$

$$\text{Bt + Pl}_1 \text{ + Als + Qtz = Grt/Crd + Pl}_2 \text{ (+/– Kfs) + L}$$

$$\text{Bt + Pl + Qtz = Opx (+/– Cpx +/– Grt) + L}$$

and

$$\text{Hbl + Qtz = Pl + Opx + Cpx (+/– Grt) + L.}$$

The volume of melt will vary as a function of P, T, t and hydrate mode in the protolith, but common rock types (metapelite and metagrey-

wacke, and some calc-alkaline plutonic rocks and amphibolite) may yield 10–50 vol.% of water-undersaturated melt at attainable crustal temperatures (Vielzeuf & Vidal 1990, Brown & Rushmer 2006). The compositions of the melts may range from leucogranite to trondhjemite and granodiorite to tonalite, depending on the chemistry and mineralogy of the source rocks and the temperature of melting. In general, the solid products of hydrate-breakdown reactions (*e.g.*, Opx, Grt and Crd in metasedimentary protoliths and Pxe in basaltic protoliths) have difficulty nucleating. Thus, it is energetically favorable for diffusion-controlled melting to continue at initially established sites and for the solid products to continue to grow at these sites (Waters 1988, Powell & Downes 1990, Brown 1994, 2004, Brown & Dallmeyer 1996, White *et al.* 2004).

Peraluminous (leuco-) granite is the common product of crustal melting in collisional orogenic systems and in experiments on melting crustal protoliths (*e.g.*, Patiño-Douce 1999). However, the chemistry of many granites *sensu lato*, particularly the more mafic 'S-type' granite bodies, is not matched by experimental melt compositions and dissolution of entrained residue or peritectic products of melting is required to match their chemistry (*e.g.*, Sawyer 1996, Stevens *et al.* 2007).

The common occurrence of pristine to only weakly retrogressed residual granulite suggests melt has been lost from the lower crust, taking the dissolved water with it, consistent with the widespread occurrence of (leuco-) granite bodies in the upper crust (*e.g.*, White & Powell 2002, Guernina & Sawyer 2003) and partitioning of water into the melt. In a closed system, cooling potentially will lead to retrogression by reaction between melt and/or exsolved water and residue, unless segregation has separated them sufficiently (Brown 2002).

Hydrate-breakdown melting has been investigated by experiments on natural and synthetic samples, reviewed by Clemens (2006), and by phase equilibria modeling, as discussed by White *et al.* (2001, 2004) and White & Powell (2002). White discusses the melting process further in Chapter 5 (White 2008).

Mantle input to crustal melting in continental arcs

Many granite bodies in continental arcs appear to have crystallized from hybrid magmas (Grunder 1995, Davidson *et al.* 2005, 2007, Dufek & Bergantz 2005) – magmas formed by interaction between basaltic melt and melt derived from pre-existing crust – and hybridization has been argued as the general case based on experimental datasets (Patiño-Douce 1995, 1999). The pressure–temperature–time path followed by ascending hybrid magmas dictates the phase assemblage that crystallizes and as a result, the composition of liquid fractionates.

Recently, Kemp *et al.* (2007a) have used Hf and O isotope compositions retrieved from zoned zircon crystals to reinvestigate the petrogenesis of the classic hornblende-bearing (I-type) granites of southeastern Australia. The Hf and O isotope compositions correlate with each other over the full range of compositions from those characteristic of the mantle to those characteristic of the putative metasedimentary protoliths (*cf.* Collins 1996, Keay *et al.* 1997). Kemp *et al.* (2007a) argued that the correlation demonstrates that these granites formed by reworking of metasedimentary protoliths by mantle-derived magmas and not by melting of lower crustal igneous protoliths as previously proposed (*e.g.*, Chappell *et al.* 2004 and references therein). Although the mass of mantle-derived material incorporated into the hybrid magma that forms I-type upper crustal plutons is minor, this new petrogenetic model suggests that I-type granite magmatism is an important driver of the coupled growth and differentiation of continental crust in continental arcs (*e.g.*, Davidson & Arculus 2006, Kemp *et al.* 2006, Hawkesworth & Kemp 2006).

Accessory phases and the chemistry of anatectic melts

How granites image their sources (Chappell 1979) may need reassessment in light of our better understanding of melting reactions and the behavior of accessory minerals during melting, and the influence that both rock-forming and accessory minerals may exert on the elemental and isotope chemistry of melts. Indeed, at the extreme of rapid melting, extraction and ascent we may expect that accessory phases do not dissolve fast enough to saturate melt and that effective partition coefficients converge to one (*e.g.*, Bea *et al.* 2007).

Accessory phases (*e.g.*, Ap, Mnz, Xen and Zrn) are significant repositories of trace elements under subsolidus conditions. Therefore, understanding the behavior of the accessory phases during melting is important to understanding trace element and isotope compositions of the resulting melts. Crustal anatexis does not necessarily lead to saturation of the melt and depletion of the residue for elements

sequestered in the accessory phases (Reid 1990, Fraser *et al.* 1997, Villaseca *et al.* 2003, 2007). First, there is a tendency for residual accessory phase grains to occur as inclusions in peritectic phases. Second, peritectic phases commonly preferentially accommodate those elements liberated by accessory phase dissolution. For example, dissolution of phosphate minerals in melt (*e.g.*, Xen) leads to partitioning of highly compatible Y and HREE into peritectic garnet (*e.g.*, Pyle & Spear 1999, Pyle *et al.* 2001), whereas the LREE–Eu budget is controlled by feldspar (*e.g.*, Villaseca *et al.* 2007). Third, the kinetics of accessory phase dissolution may lead to disequilibrium.

These features have implications for melt composition (Brown 2007b). Non-equilibrium effects may control initial isotope compositions (Hogan & Sinha 1991, Zeng *et al.* 2005a, b) and the chemical composition of accessory phases during crystallization (*e.g.*, Wark & Miller 1993). Unintended consequences include affecting rates of melt extraction calculated using Mnz dissolution (Ayres *et al.* 1997), and melt temperatures calculated using Zr and LREE concentrations and Zrn and Mnz solubility (*e.g.*, Miller *et al.* 2003, Chappell *et al.* 2004). However, disequilibrium can also be used to advantage to place maxima on rates of processes (*e.g.*, Bea *et al.* 2007).

As much as one third of the subsolidus whole rock Zr may be present in rutile and garnet, and suprasolidus breakdown of garnet to cordierite releases Zr that commonly forms new zircon as inclusions in cordierite (*e.g.*, Fraser *et al.* 1997, Degeling *et al.* 2001). However, at the transition to UHT metamorphic conditions (T >900˚C), although garnet may contain more than double the Zr concentration common in ordinary metapelitic granulites, the Zr released by garnet breakdown tends to be accommodated in the product phases preventing growth of new metamorphic zircon (Degeling *et al.* 2001), making dating close to peak metamorphism difficult in UHTM granulites. Low-Zr concentrations in granites may reflect P–T evolution rather than low-T melting (Villaseca *et al.* 2007) or the rate of segregation (Sawyer 1991).

The flux of trace elements into the melt during dissolution of accessory phases is a function of radial diffusion-controlled dissolution rate and surface area, which are correlated with grain size, and the degree of under-saturation of the melt with respect to the element(s) concerned (Watson 1996). Mnz and Zrn populations commonly have different average grain size, and grain sizes that vary from protolith to protolith within a source terrane (Nemchin & Bodorkos 2000). These features lead to relative differences in LREE and Zr concentrations among small volume melt batches.

In hydrate-breakdown melting, low melt fraction melt pockets may be isolated along the hydrate grain boundaries. In this case, equilibrium may be achieved for trace elements concentrated in accessory phases located along hydrate grain boundaries or sequestered in the hydrate. In contrast, in wet melting, low melt fraction melt pockets form at quartz–feldspar grain junctions, which limits the opportunity for melt to equilibrate with trace elements in accessory phases associated with hydrate grain boundaries or sequestered in hydrate phases. Syn-anatectic deformation is likely to be important in determining whether equilibrium is achieved (Walte *et al.* 2005). For example, granular flow (diffusion-accommodated grain boundary sliding) allows melt migration along grain boundaries, which potentially enables interaction between accessory mineral grains and the interstitial melt, whereas diffusion creep by dissolution-precipitation favors equilibration of grain surface compositions with the interstitial melt, potentially inhibiting melt interaction with distributed accessory phases.

The initial Pb isotope composition of batches of melt is sensitive to the age(s) and abundance of Zrn in the source and the amount of radiogenic Pb incorporated in the melt through dissolution of Zrn (Hogan & Sinha 1991). Similarly, Sm/Nd ratios and Nd isotopic compositions of individual batches of melt depend on the amount of Ap and Mnz dissolved in the melt (Zeng *et al.* 2005a, b). In contrast, mica and feldspar control the Rb content of melt and the Rb/Sr ratio, and fractionation during non-modal melting will yield liquid with a distinct isotope signature (Zeng *et al.* 2005a, b, c). Although mixing during accumulation and extraction may homogenize melt batches, heterogeneity in the initial isotopic composition of granites is inherited from the source and preserved as a result of incremental construction from multiple batches of melt (*e.g.*, Deniel *et al.* 1987, Hogan & Sinha 1991, Pressley & Brown 1999, Glazner *et al.* 2004, Matzel *et al.* 2005, 2006, Tomascak *et al.* 2005).

Because of the issues discussed in this section, inverting the trace element and isotope chemistry of granites to link them to source terranes is not a simple task. Use of these data to link or deny links between middle to upper crustal granites and middle to lower crustal sources requires care.

MELT EXTRACTION

"The small islands . . . of Spikarna . . . are localities where the mixed rocks can be studied particularly well . . . and consist . . . of an augen gneiss-like rock type, in which there occur several zones of a veined gneiss-like rock 10 to 30 metres broad . . . The veins are generally parallel to the main directions of the zones, but a close inspection shows veins with a perpendicular position . . . The smaller veins intersect the hornblende schist as a fairly regular network . . . This network structure obviously depends on incipient melting. If it had proceeded a little farther, the different fragments would have been more widely separated from each other and become bent and twisted in a way that is very characteristic of this type of gneiss . . . there are locations where the refusion is more advanced . . . we find fragments of hornblende schist, some of which are rather well preserved, others so strongly melted that for the most part only a skeleton of mica remains . . .

. . . we can state with regard to all these folded (crinkled) gneisses mixed with granitic veins, that their structure is dependent on movements in a mass of rock which as a whole was on the verge of melting."

J.J. Sederholm (1967).

The composition of granite in middle to upper crustal plutons requires that 10–25 vol.% of melt be extracted from the source, implying that melt was derived from a source volume of four to ten times the granite volume (Fig. 6-2; Brown 2004). By the time a lower to middle crustal source exhumes melt will have drained away, although leucosome commonly marks the drainage network. Leucosome is evidence of former melt-filled veins (or veins filled with mixtures of melt and peritectic and/or early crystallized minerals) that once supplied melt to an ascent conduit but now trapped because connectivity to the conduit failed. However, in some residual granulites there is only minimal evidence of leucosome and most of the melt has drained away without leaving behind much early crystallized quartzofeldspathic leucosome. Compaction of (most of) the remaining melt-filled porosity and collapse of any vein networks leaves a melt-depleted residual granulite.

For flow, melt must form an interconnected network at some scale, the host must be permeable at some scale and the solid residue must compact; these scales are the grain-to-vein and the vein-to-conduit scales, and there must be sufficient connectivity within a source volume to feed an ascent column. Fractional crystallization may occur during flow, producing compositional zoning in leucosomes (Sawyer 1987), and contamination with xenocrysts during flow has been demonstrated (Sawyer 1999, Sawyer *et al.* 1999, Vernon & Johnson 2000, Vernon *et al.* 2003). We may infer flow at some scale if the bulk rock composition for anatectic rock is residual in comparison with a probable protolith composition, and if the difference is consistent with net melt loss (*e.g.*, Solar & Brown 2001a). However, any estimate of volume of melt lost can only be a minimum, since flow through the crustal level of investigation means that the process of melt flow and melt loss is open system (Brown 2004).

Melt extraction is driven by variations in stress that generate gradients in melt pressure. The local rate of melt segregation may be controlled by the proportion of melt generated (a function of heat input) and the rate of matrix compaction (Rutter 1997, Rutter & Mecklenburg 2006). The strain field controls the local- and crustal-scale form of melt migration pathways (Brown *et al.* 1995a, b, Brown & Solar 1998a, b, 1999, Guernina & Sawyer 2003, Sawyer 1994, 2000, 2001, Sawyer *et al.* 1999, Solar & Brown 2001 a, b). If the proportion of melt increases at a rate faster than the rate at which it may be segregated, the melt may become overpressured (with respect to the local confining stress) and generate escape pathways. Melt migrates down local gradients in pressure to sites of lower pressure (Rutter 1997, Rutter & Mecklenburg 2006), where it may accumulate or where it may again become overpressured, and migrate to larger ascent conduits. This deformation-enhanced extraction process generally produces metatexite migmatites – rocks with residual compositions and remnant, commonly cumulate leucosome (*e.g.,* Solar & Brown 2001a). For further discussion of nomenclature in relation to processes, see Chapter 1 (Sawyer 2008).

If melt accumulates in the lower to middle crustal source or if there is an influx of hydrous fluid into the source, the increased volume of melt may promote loss of cohesion in the melt-bearing protoliths. The loss of cohesion allows bulk flow to form a diatexite or in interlayered protoliths with different fertility a schollen migmatite (Brown 1973, 1979, 1994, 1995, Wickham 1987a, b, Sawyer 1994, 1996, 1998, 2001, Brown & Rushmer

1997, Brown & Solar 1999, Greenfield *et al.* 1996, Milord *et al.* 2001, Solar & Brown 2001a, b, Vernon *et al.* 2001, 2003, Milord & Sawyer 2003, Guernina & Sawyer 2003, White *et al.* 2005, Berger *et al.* 2008, Weinberg & Mark 2008). In flowing diatexite magma, segregation of melt from solid commonly takes place, giving rise to schlieren structure (Sawyer 1998, Milord & Sawyer 2003). In addition, segregation is efficient in the formation of leucodiatexite by progressive separation of ferromagnesian phases from melt (Brown 1979, Sawyer 1998, Sawyer *et al.* 1999, Milord *et al.* 2001, Vernon *et al.* 2003). In the innermost zone of the migmatitic aureole of the Huntly Gabbro in northeast Scotland, orthopyroxene-bearing and orthopyroxene-free diatexite both have residual compositions and both represent residue-enriched crystal–liquid mushes left after extraction of up to 55 vol.% melt; the orthopyroxene-bearing diatexite is interpreted to record higher melt losses (Droop *et al.* 2003).

Sawyer (1996) and Stevens *et al.* (2007) have suggested that entrainment of residue in melt may be required to form granite with 'S-type' chemistry. Such a model is consistent with the observation of peritectic garnet enclosed in leucosome in stromatic migmatite (Brown *et al.* 1999), but which likely demands rapid rates of ascent consistent with transport in dikes at the crustal scale (Clemens *et al.* 1997). Sawyer (2008) discusses types of diatexite and their origins further in Chapter 1.

Microstructural criteria indicative of former melt

Although high-grade rocks exposed at the surface do not preserve well transient features present at the ambient metamorphic conditions in the crust, careful petrographic studies of microstructures in natural anatectic systems has provided evidence of the former presence of melt at the grain scale (Figs. 6-4 a and b; *e.g.*, Brown *et al* 1999, Sawyer 1999, 2001, Brown 2001a, b). We may infer the former presence of melt using the following criteria: mineral pseudomorphs after grain-boundary melt films and pockets [in contact migmatites (*e.g.*, Rosenberg & Riller 2000, Marchildon & Brown 2001, 2002), in regional migmatites (*e.g.*, Brown *et al.* 1999, Marchildon & Brown 2003) and in granulite (*e.g.*, Sawyer 1999, 2001, Brown 2002, Guernina & Sawyer 2003)]; magmatic rims on subsolidus cores of grains [*e.g.*, rational faces, overgrowths of different compositions (*e.g.*, Marchildon & Brown 2001, 2002, Sawyer 2001, Hasalová *et al.* 2008a)] or magmatic microstructures in leucosomes (*e.g.*, Vernon & Collins 1988, Brown 2002); spatial distribution of like and unlike phases [*i.e.,* mineral phase distribution (Ashworth & McLellan 1985, Hasalová *et al.* 2008a)]; sub-parallel intra-granular fractures [*e.g.*, feldspar-filled fractures in quartz (Rosenberg & Riller 2000); quartz–albite-filled fractures in K-feldspar (Závada *et al.* 2007)]; and, annealed microfractures (*e.g.*, in quartz; Watt *et al.*

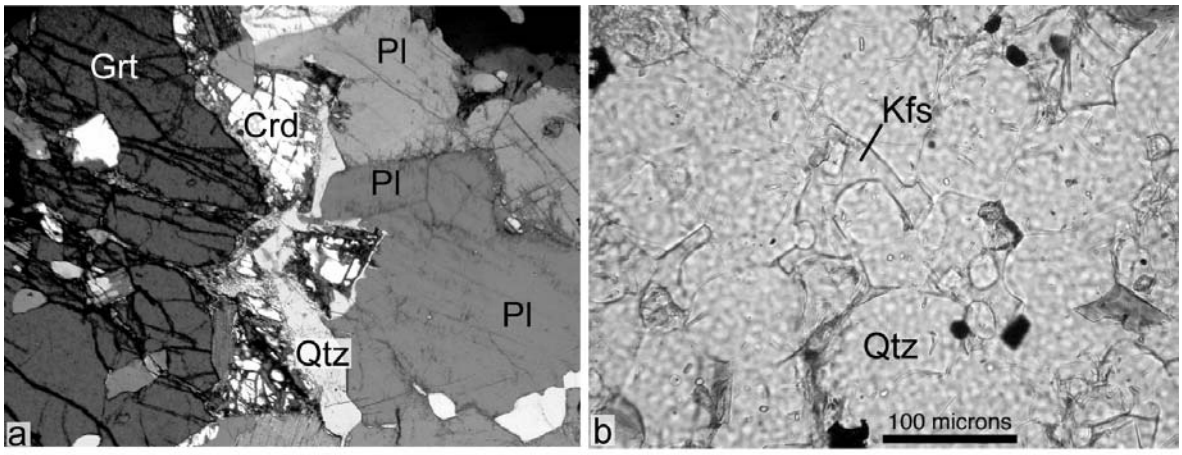

FIG. 6-4. **a**, Photomicrograph of residual diatexite, Crouesty, Morbihan, southern Brittany metamorphic belt, France, to show euhedral feldspar (Pl) in interstitial quartz (Qtz) inferred to mimic melt pocket (upper-centre of field of view); long dimension of field of view is 6.67 mm. For additional details of these rocks see Brown & Dallmeyer (1996).
b, Photomicrographs of cuspate interstitial K-feldspar (Kfs) pocket in contact with subequant quartz (Qtz) grains showing rounded outlines. Note small, subhedral quartz grains partially or completely included within K-feldspar (plane polarized light). From layer-parallel leucosome in migmatite of the Onawa contact aureole, Maine (see Marchildon & Brown, 2002, for additional details of these rocks).

2000, Marchildon & Brown 2001, 2002). Detailed observations by Sawyer (2001) and Závada *et al.* (2007) have shown that initial segregation of melt occurs by opening microfractures along grain boundaries or as accumulations adjacent to hydrate phases. In addition, Závada *et al.* (2007) suggested that cavitation may be an important process in the deformation of melt-bearing lower crust, which has also be shown to occur in deformation experiments on feldspar aggregates (Rybacki *et al.* 2008). For further information about microstructures in formerly melt-bearing rocks see Chapter 4 of this volume (Holness 2008).

Mesoscale structures in migmatites and residual granulites

Movement of melt within and out of melt-bearing source rocks is generally considered to be a response to deformation, whether imposed by the far-field stress or induced by the melting process itself (Hollister & Crawford 1986, Clemens & Mawer 1992, Brown 1994, 2004, 2005, Davidson *et al.* 1994, Sawyer 1994, 2001, Brown & Rushmer 1997, Rutter 1997, Sawyer *et al.* 1999, Petford *et al.* 2000, Marchildon & Brown 2001, 2002, 2003, Rosenberg 2001, Rushmer 2001, Vigneresse & Burg 2005). Melt extraction occurs at a melt fraction around 7 vol.% – the 'melt connectivity transition' (MCT) – and is most likely a discontinuous process as melt volume increases then decreases during melt build-up and melt loss events (Sawyer 1994, Brown *et al.* 1995b, Vigneresse *et al.* 1996, Brown & Solar 1999, Brown 2004, Rosenberg & Handy 2005, Vigneresse & Burg 2005). Below this melt fraction melt may not segregate because melt pockets may not be sufficiently connected and significantly above this melt fraction the rock becomes too weak to permit melt segregation as the proportion of melt-bearing grain boundaries increases rapidly.

For metasedimentary and gneissose protoliths at suprasolidus conditions, it has been shown in many studies that the scale of compositional layering, the fabric anisotropy and the strain field control sites of early melt concentration (Fig. 6-5) (*e.g.,* van der Molen 1985a, b, McLellan 1988, D'Lemos *et al.* 1992, Maaløe 1992, Brown 1995, 2004, Collins & Sawyer 1996, Sawyer 1994, 1999, Brown *et al.* 1995a, b, 1999, Williams *et al.* 1995, Brown & Rushmer 1997, Brown & Solar 1998a,

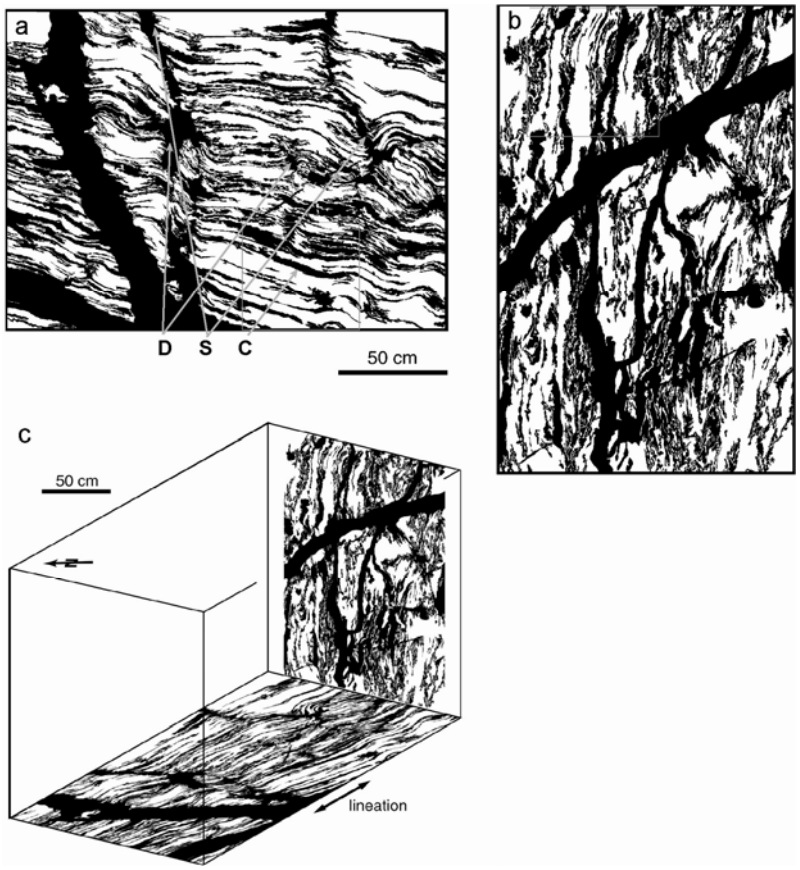

FIG. 6-5. Binary maps of inferred melt-bearing structures in **a)** subhorizontal (D – dilation band, S – shear band and C – compaction band) and **b)** subvertical exposures, and **c)** to show the three-dimensional relationship and prolate topology of the leucosome, Petit Mont, Morbihan, southern Brittany metamorphic belt, France. Reprinted from *Tectonophys*. **364**, Marchildon, N. & Brown, M., Spatial distribution of melt-bearing structures in anatectic rocks from Southern Brittany: Implications for melt transfer at grain- to orogen-scale, 215-235. © 2003 Elsevier, with permission from Elsevier.. For additional details of these outcrops see Marchildon & Brown (2003).

Guernina & Sawyer 2003, Marchildon & Brown 2003). At one extreme, the processes driving melt segregation and the formation of stromatic migmatites with leucosomes generally parallel to strongly foliated mesosomes reflect the mechanical anisotropy of the melting rock at low melt fraction, whether melt fraction is increasing to or has dropped below the MCT, and any control by the state of stress is a minimum. However, with increasing melting migmatites become mechanically more isotropic allowing arrays of interconnected melt-filled fractures or deformation bands to form (Fig. 6-6a). Melt is expressed from compaction (generally fabric-parallel) bands into shear (oblique to fabric) and dilation (generally fabric-normal) bands (Fig. 6-7). These vein networks represent fast drainage pathways ultimately feeding dikes to transport magma to shallower crustal levels.

Incongruent melting that involves biotite or hornblende breakdown may result in leucosome concentration around the peritectic product minerals (Powell & Downes 1990), although this is not always the case (*e.g.*, Guernina & Sawyer 2003). I infer that in some circumstances the peritectic minerals control sites of early melt concentration (Powell & Downes 1990, Hand & Dirks 1992, Brown 2004, White *et al.* 2004). With increasing temperature, an increase in melt fraction leads to progressive weakening, which may lead to formation of a network of deformation bands

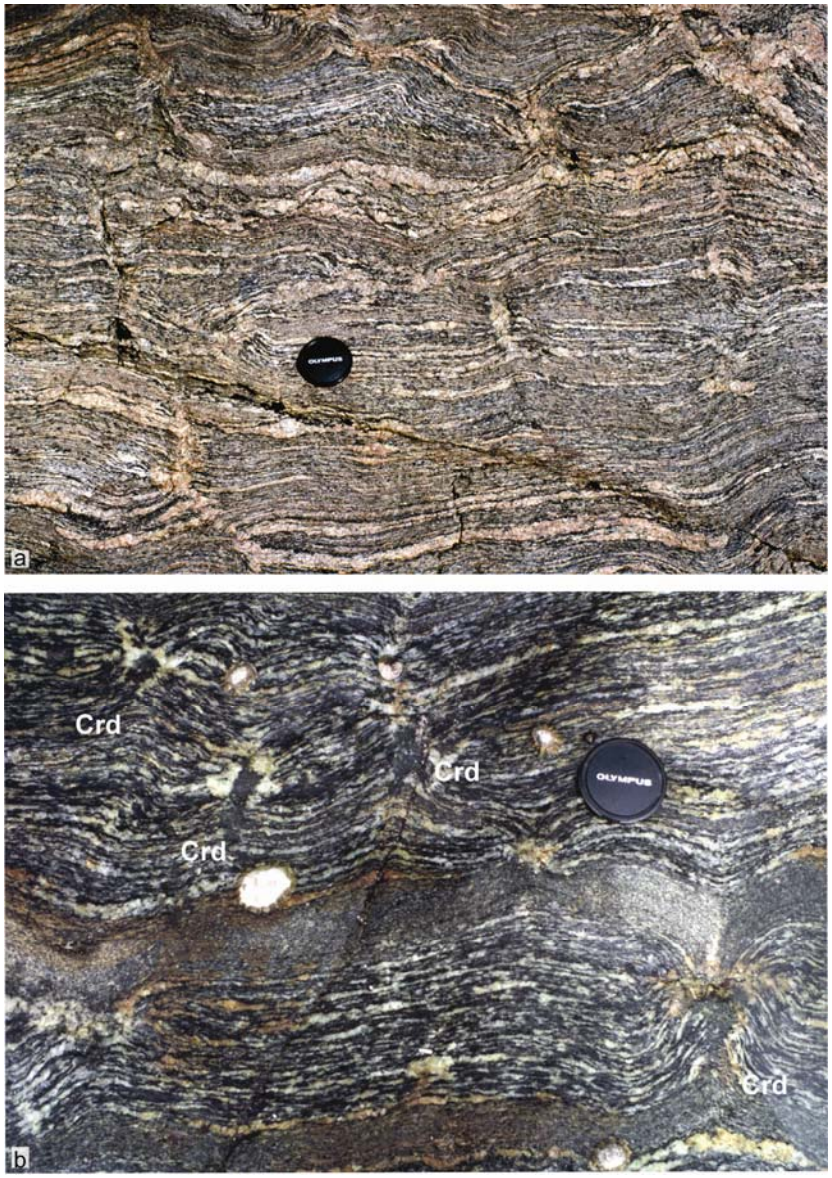

FIG. 6-6. **a,** Stromatic migmatite with layer-parallel leucosome stromata, transverse leucosomes and leucosome in shear bands (Port Navalo Plage, Morbihan, southern Brittany metamorphic belt, France).

b, Cordierite in transverse structures either is associated with minimal leucosome (*e.g.*, upper left) or appears to be independent of any residual leucosome (*e.g.*, bottom right), suggesting melt loss from these stromatic migmatites (Port Navalo, Morbihan, S. Brittany, France).

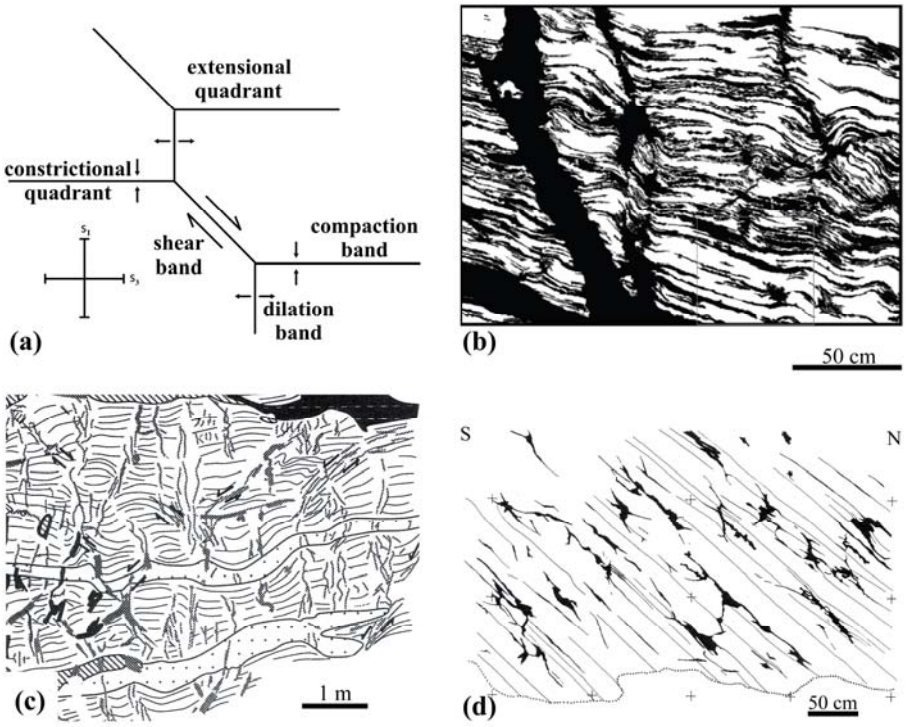

Fig. 6-7. Relationship between idealized deformation band networks and networks of leucosome stromata in residual migmatites. From Brown (2006), with permission. **a,** Idealized diagram (modified after Du Bernard *et al.*, 2002) to show the coexistence of shear, compaction and dilation bands (S1 and S3 are greatest and least far-field principal stresses, respectively). **b,** Binary image of subhorizontal surface perpendicular to foliation and parallel to lineation to show patterning of leucosomes, Petit Mont, Arzon, S. Brittany (reprinted from *Tectonophys*. **364**, Marchildon, N. & Brown, M., Spatial distribution of melt-bearing structures in anatectic rocks from Southern Brittany: Implications for a melt transfer at grain-to-orogen scale, 215-235. © 2003 Elsevier, with permission from Elsevier). **c,** Detail from outcrop map to show the inter-relationships between stromatic leucosomes parallel to fabric and transverse leucosomes in apparent inter-boudin partitions and shear bands (reprinted from Oliver & Barr, 1997, The geometry and evolution of magma pathways through migmatites of the Halls Creek Orogen, Western Australia, *Mineral. Mag*. **61**, 3-14, with permission of the Mineralogical Society). **d,** Outcrop map (vertical face, parallel to the stretching lineation) to show the distribution of leucosomes in a strongly melt-depleted metagreywacke. Thin, continuous leucosomes are oriented parallel to the layering and wider discordant leucosomes occur in shear bands and apparent inter-boudin partitions to form a net-like array of melt channels in the outcrop (reprinted from Guernina & Sawyer, 2003, Large-scale melt-depletion in granulite terranes: An example from the Archean Ashuanipi Subprovince of Quebec, *J. Metamorphic Geol*. **21**, 181-201, © 2008 Blackwell Publishing Ltd., with permission of Wiley-Blackwell).

nucleated on the local concentrations of melt (Fig. 6-6b; *cf.* Grujic & Mancktelow 1998). As a result, the peritectic minerals occur preferentially in deformation bands (Fig. 6-6b; *e.g.,* Brown 2004) and in leucosomes in stromatic migmatites (Fig. 6-8; *e.g.,* Jones & Brown 1990, Brown & Dallmeyer 1996, White *et al.* 2004). This occurs in spite of a homogeneous distribution of reactant phases in the matrix, which supports the inference that deformation is localized by the concentration of melt at these sites. This contrasts with the study by Hand & Dirks (1992), where pre-existing crenulation structures apparently controlled the sites of initial incongruent melting; in general, this seems to be less common.

Evidence of concentration of leucosome and (leuco-) granite in fold hinge zones and shear zones is common (Ashworth 1976, Barr 1985, McLellan 1988, Mogk 1990, Allibone & Norris 1992, Brown & Solar 1998a, Sawyer *et al.* 1999, Marchildon & Brown 2003, Weinberg & Mark 2008), which implies preferential melt flow to these sites. Several generations of melt may accumulate in such low-pressure sites, and the resultant granite may show evidence of *in situ* crystallization and fractionation to more evolved magmatic compositions than those of leucosomes that record the melt flow networks (Sawyer *et al.* 1999). Furthermore, Weinberg &

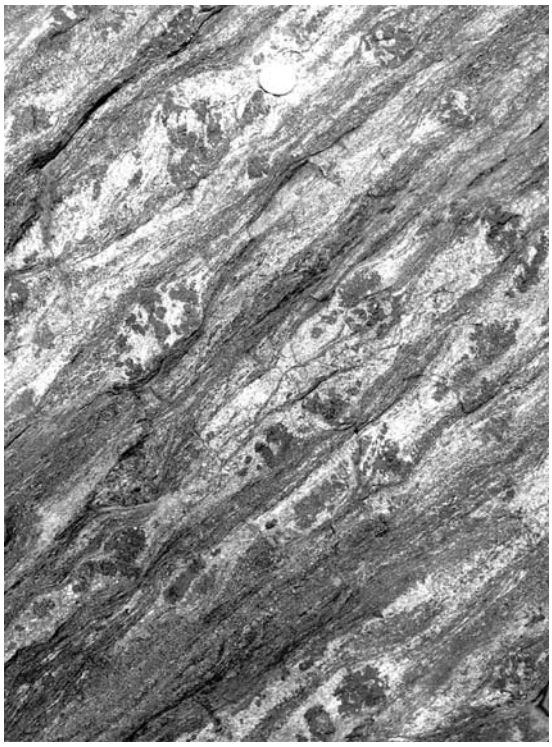

FIG. 6-8. Foliation-parallel stromatic leucosomes composed of peritectic garnet poikiloblasts in a medium-grained K-feldspar–quartz-rich matrix contained within strongly foliated cordierite–sillimanite–biotite-rich host record melt loss pathways through the residual migmatites, from Round Hill, Broken Hill, southeastern Australia (see White *et al.*, 2004 for detailed discussion).

Mark (2008) have argued that the presence of melt along foliation planes parallel to fold axial surfaces will assist in tightening and stretching folding rocks, which in turn may lead to disruption and the local formation of diatexite magmas.

There are multiple lines of evidence for melt loss from migmatites and granulites. First, leucosome networks appear to represent melt extraction pathways (for a contrary view see Bons *et al.* 2008). In general, leucosomes are not melt accumulation sites, as demonstrated by their composition, which commonly consist of early crystallized minerals, implying that fractionated melt has been lost from these rocks (Brown *et al.* 1995b, Solar & Brown 2001a, b, Brown 2004). Second, there is only limited retrogression of peritectic minerals, such as Opx, Grt and Crd, which demands melt loss, the melt taking dissolved water necessary for retrogression with it out of the source (Ellis & Obata 1992, Brown 2002, White & Powell 2002). For example, pristine peritectic minerals occur in leucosomes at granulite facies, such as coarse-grained garnet in migmatites in central Massachusetts, northern Appalachians (Tracy & Robinson 1983) and at Broken Hill, Australia (White *et al.* 2004), and in leucosome-poor layers at granulite facies, such as the coarse-grained orthopyroxene-rich layers in granulites of the Wuluma Hills, central Australia (Sawyer *et al.* 1999). Third, melt loss is indicated by depleted bulk rock compositions, which are demonstrated qualitatively by an abundance of peritectic minerals (Opx, Grt, Crd) in granulites with insufficient leucosome to account for these abundances (Sawyer *et al.* 1999) and demonstrated quantitatively by comparative geochemistry (*e.g.*, Solar & Brown 2001a, White *et al.* 2004). Overall, the evidence suggests efficient removal of melt from residue at low melt fractions.

Ultimately, melt drains from the source via discrete planar or cylindrical conduits to form plutons (*e.g.*, D'Lemos *et al.* 1992, Brown 1994, 2001a, b, 2004, 2005, Collins & Sawyer 1996, Brown & Solar 1999, Solar & Brown 2001a, Marchildon & Brown 2003); how such conduits form is not agreed (see next section). Multiple studies have provided general descriptions of the structural control over pervasive melt flow and the relationship between mesoscale structures and ascent conduits (*e.g.*, D'Lemos *et al.* 1992, Brown 1994, 2001a, b, 2004, 2005, Collins & Sawyer 1996, Brown & Solar 1998a, b, 1999, Solar & Brown 2001a, Marchildon & Brown 2003, Hasalová *et al.* 2008a). The thermal effects of pervasive melt migration have been qualitatively investigated by Brown & Solar (1999) and Weinberg (1999), and modeled by Leitch & Weinberg (2002), whereas the chemical effects of pervasive melt migration have been described and modeled by Hasalová *et al.* (2008b).

Overall, the evidence suggests that the three main modes of fluid flow through solids (intergranular porous flow, conduit flow in vein networks and channel flow in ascent conduits) were occurring synchronously. Synchronicities of these flow modes may be explained by granular behavior, where there is a melt film present between grains and between aggregates of grains in melt-bearing rock that reduces the large cohesive forces that characterize a solid medium (*cf.* Nicolas & Poliakov 2001). Melt migration through the anatectic zone will depend on the size of the aggregates, particularly the

lozenges of melt-depleted or low-melt fraction rock between vein networks in many migmatites (Brown 2004, Olsen *et al.* 2004, Rutter & Mecklenburg 2006). Melt flow evolves in time and space from intergranular porous flow to channel flow in vein networks to channel flow in larger conduits as the dimension of the aggregates increases (*cf.* Olsen *et al.* 2004). Nicolas & Poliakov (2001) use a physical experiment on pressurized air circulation through a granular medium to illustrate these synchronous flow modes (Fig. 6-9), but the rates of flow for crustal systems will be somewhat slower than those they calculate for mafic systems due to the slightly higher viscosity of the melt (one to three orders of magnitude higher).

The mechanics of melt extraction from the anatectic zone

Open system deformation of melting rock involves compaction or dilation of the matrix of solid grains to expel or suck in melt locally. In compactive deformation, the solid grains forming the matrix may deform permanently, with the possibility of complete melt expulsion (Rutter & Mecklenburg 2006). In dilatant deformation, infiltration-driven decompaction may lead to formation of diatexite.

Rutter & Mecklenburg (2006) represented the yield surface for a melting rock on a diagram of differential stress (σ_1–σ_3) *versus* effective mean stress (σ–ρ, where $\sigma = [\sigma_1+\sigma_2+\sigma_3]/3$, and ρ = the pore pressure) (Fig. 6-10). The yield surface forms a closed loop that separates instantaneous stress states that lead to permanent deformation from those that may not (stress states inside the yield surface). The yield surface is a dynamic entity that may expand or contract with changes in pore pressure during progressive deformation of melting rock; for example, it shrinks in size as melt pressure increases from curve A to curve B in Fig. 6-10. For stress states along the abscissa, melting rock may undergo hydrostatic compaction involving melt expulsion, which increases the effective mean stress as the melt pressure decreases, expanding the yield surface as the melting rock strengthens due to melt loss (Fig. 6-10).

For effective mean stress states to the left of the projection of the critical state line in Fig. 6-10, deformation of melting rock is dilatant. Dilatant

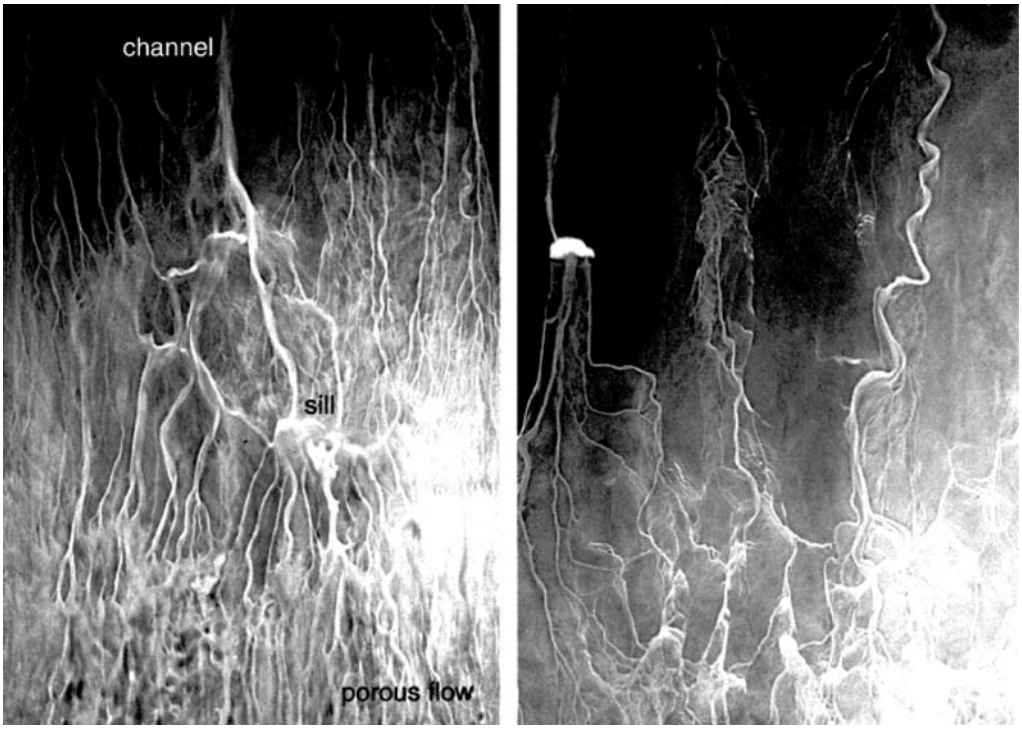

FIG. 6-9. Images to show pressured air migration through a box filled with fine glass beads illustrating the simultaneous occurrence of intergranular porous flow, macroscopic porous flow in vein networks and channel flow. Source: Exhibition 'braided stream' in San Francisco Exploratorium (http://www.exploratorium.edu/cmp/exhibits/b/braided_stream.html). See Nicolas & Poliakov (2001) for more details.

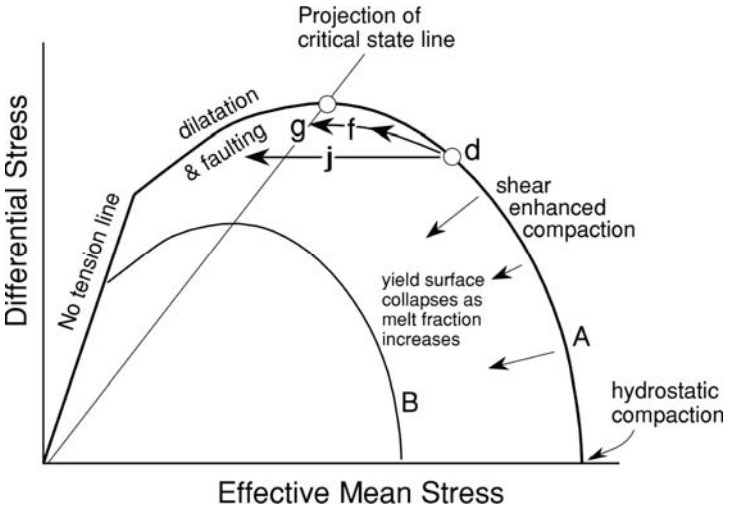

FIG. 6-10. Schematic representation of the yield surface for a melting rock. From Rutter & Mecklenburg (2006): The extraction of melt from crustal protoliths and the flow behavior of partially molten crustal rocks: an experimental perspective. *In* Evolution and Differentiation of the Continental Crust (M. Brown & T. Rushmer, eds). Cambridge University Press (384-429). © 2006 Cambridge University Press. Reproduced by permission of Cambridge University Press. The projection of the critical state line is the projection of the crest of successive yield loops (*e.g.*, small circle at intersection with crest of loop A) at different porosities. To the left of this line the deformation is dilatant, and to the right it is compactive. See text for discussion.

deformation is accommodated by strain localization and formation of dilatant shear bands. Melt is redistributed into the shear bands, which reduces melt pressure in the matrix and increases the effective mean stress supported by the matrix. As melt pressure decreases in the matrix with deformation so the yield surface expands, requiring higher differential stress and/or higher melt pressure for deformation to continue due to dilatancy hardening.

For effective mean stress states to the right of the projection of the critical state line in Fig. 6-10, the deformation of melting rock is compactive. Compactive deformation is accommodated by macroscopic ductile flow and expulsion of melt, which reduces melt pressure and increases the effective mean stress supported by the melting rock. As melt pressure decreases with deformation so the yield surface expands, requiring higher differential stress and/or higher melt pressure for deformation to continue due to strain hardening.

Increases in pore pressure induced by deformation modify the effective mean stress with consequent effects on the mechanical behavior. For example, in Fig. 6-10, consider a deformation path from the small circle labeled d on the yield surface to the small circle labeled g. Compactive deformation occurs as differential stress and melt pressure increase. Assuming that insufficient melt is expelled to decrease melt pressure and drive up the effective mean stress, progressive compactive deformation leads to a decrease in effective mean stress until isovolumetric failure is achieved at g. Alternatively, consider the increase in melt volume with progressive melting and limited melt expulsion. An increase in melt pressure (Fig. 6-10, path j) at constant differential stress displaces the stress state to the left until dilatant deformation occurs with failure at the yield surface.

Variations in melt pressure due to periodic melt build-up and melt loss are likely to maintain the ambient volume of melt around the 'melt connectivity transition' of Rosenberg & Handy (2005). This provides an understanding of why melt extraction is most likely a discontinuous process (Sawyer 1994, Brown *et al.* 1995b, Vigneresse *et al.* 1996, Brown & Solar 1999, Brown 2004, Rosenberg & Handy 2005, Vigneresse & Burg 2005).

Thermally activated creep causes the effective size of the yield surface to vary with strain rate, becoming very small for low strain rates. Thus, time-dependent isotropic compaction may occur under very small effective stresses of <1 MPa. Local variations of shear stress must be of the same order, which is a measure of the contribution that tectonic stresses make to the driving force for melt migration (Rutter & Mecklenburg 2006). In contrast, gravity-induced melt pressure gradients are ~0.003 MPa m^{-1}, which is a measure of the contribution that gravity-induced stresses make to the driving force for melt migration (Rutter & Mecklenburg 2006). If the flow strength of melting rock is ~1 MPa, tectonic stress differences driving melt migration will be of the same order. Thus, a pressure gradient of 1 MPa over 1–10 metres represents a substantial enhancement relative to gravity-induced pressure gradients. In contrast, a pressure gradient of 1 MPa over 1 km or more reduces the influence of tectonic stress as a driving force for melt migration to less than gravity-induced

pressure gradients.

There are three principal contributors to the driving force for melt extraction (Brown *et al.* 1995b): gravity, causing compaction of the solid matrix and upward drainage of melt; volume change associated with melting, causing expansion-contraction convection; and, differential stress, causing deformation-enhanced melt segregation and expulsion or influx, as discussed above. The rate of supply of heat to drive the endothermic melting reactions limits the maximum rate of melt production. There is no requirement for a steady state to be established.

Hydrate-breakdown melting causes a net volume expansion of the system, so that the excess melt volume must dilate the rock mass creating spaces between grains or forming mesoscopic crack arrays, including opening of any existing foliation surfaces. In contrast, wet melting results in net volume decrease, requiring compaction by permanent deformation of the framework of solid grains. Petrographically distinct layers or volumes will respond differently to these forces, leading to the potential for local segregations by expansion-contraction convection.

If the solidus surface or 'roof' of a suprasolidus source does not fail by fracture and if lateral drainage pathways are impermeable, melt volume will increase until limited by heat supply. In this undrained state the rock will be weak and pressure gradients will be insignificant, but the rock mass will be able to respond in a very ductile fashion to small regional stresses and may be a very effective detachment horizon in the lower crust (Rutter & Mecklenburg 2006). If the 'roof' or sides of a suprasolidus rock mass are breached, this source may supply a large amount of magma to shallower crustal levels very rapidly.

In contrast, if drainage is permitted concurrently with melt production – assuming intergranular porous flow to deformation bands and channel flow along the bands – the melt volume and vein aperture dimensions, and the pressure drop in each part of the system will spontaneously adjust by inflation with melt or compaction of the solid framework. This adjustment continues until the volume-averaged melt flux is the same everywhere in the system.

Consider an isotropic quartz–feldspar dominated source heated from below under the influence of gravity alone. Rutter & Mecklenburg (2006) compute the time required to extract 10 vol.% melt by intergranular porous flow for a grain size of 5 mm (Fig. 6-11; upper solid curves, labeled with melt water contents of 0.1, 1.0 and 3.0 wt.%) or by channel flow through a network of 5 cm wide veins 1 m apart (Fig. 6-11; lower dashed curves for same range of melt water contents), with other assumptions as stated by them. The effective permeability of the rock mass for channel flow in veins is ~10^6 greater than for intergranular porous flow, which accounts for the much faster rate of drainage. In the absence of tectonic deformation, it is clear that porous flow alone is too slow to extract melt in geologically realistic times (<10^7 years, Wickham 1987b, Brown *et al.* 1995b), except for 'wet' melt (>3 wt.% water). Once the melt collects into a network of veins, the times for extraction become realistic, even with intergranular porous flow as the mechanism to move melt to the veins in

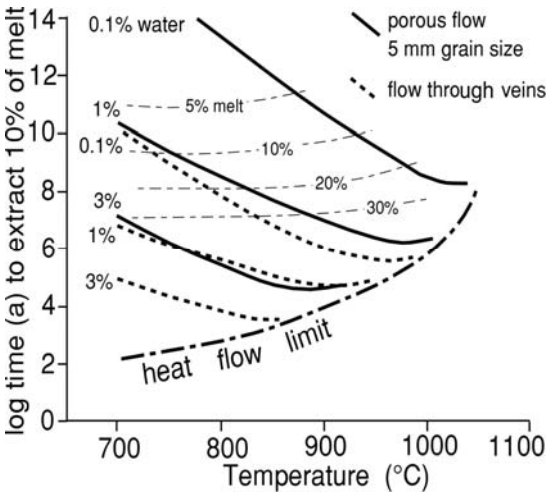

FIG. 6-11. Comparison of the time required to extract 10% of the volume of a granitic rock as melt (under gravity alone) according to: **a,** the porous intergranular flow model for a mean grain size of 5 mm (upper solid curves, labeled with melt water contents of 0.1, 1.0 and 3.0 wt.%); and, **b,** the macroscopic porous flow model applied to a network of veins of volume fraction 5% (lower dashed curves for same range of melt water contents). An upper limit to extraction rate is set by the rate that the latent heat of fusion may be supplied to the material (heat flow limit curve). Contours of melt vol.% are also shown applying to the curves for porous flow. From Rutter & Mecklenburg (2006): The extraction of melt from crustal protoliths and the flow behavior of partially molten crustal rocks: an experimental perspective. *In* Evolution and Differentiation of the Continental Crust (M. Brown & T. Rushmer, eds). Cambridge University Press (384-429). For more details see Rutter & Mecklenburg (2006).

the first place. Gravity-induced melt pressure gradients of ~0.003 MPa m^{-1} are too small to drive this initial flow of melt to veins and tectonic deformation, as discussed above, is necessary.

Melting rock is composed of lozenges of low melt fraction (melt-depleted or less melted) rock surrounded by interconnected veins of high melt fraction magma (*cf.* Olsen *et al.* 2004). Differential load is transmitted to the lozenges via a contiguous network of contact surfaces, but the whole mass is drained of melt by the veins (Rutter & Mecklenburg 2006). The stress gradient driving melt into the veins is approximately the far-field differential stress (~1 MPa) divided by the vein separation (~1 m). Hence, the smaller the melt fraction and the stronger the rock mass, the greater is the momentum that the stress may impart to the melt. The enhancing effect of a higher strength at lower melt fraction is partially offset by the lower permeability at lower melt fraction. For realistic variations of melt fraction and viscosity with temperature and water content, increasing temperature always increases the rate of deformation-enhanced melt extraction (Rutter & Mecklenburg 2006).

Figure 6-12 shows graphically how the time required to extract 10 vol.% of melt by shear-enhanced compaction from a hypothetical quartzo-feldspathic protolith of mean grain size of 5 mm, containing 0.1, 0.3, and 1.0 wt.% water, varies with temperature at a constant differential stress of 1 MPa. Melt is assumed to accumulate in veins separated by 1 m that inflate until they are sufficiently permeable for melt to drain upwards by virtue of the density contrast between melt and solids. For 'dry' melts combined with low temperatures, melt extraction times may be reduced proportionally if the differential stress and hence the distortional strain rate is increased. Thus, a combination of melt extraction by shear-enhanced compaction and gravity driven flow through veins allows melt extraction in geologically realistic times (Rutter & Mecklenburg 2006).

Figure 6-13 shows the expected average thickness of veins with spacing of 1 m in a protolith of mean grain size of 5 mm, containing 0.1, 0.3, 1.0 and 3.0 wt.% water, where the rate of density-driven flow through the veins equals the rate of supply of melt to the veins by shear-enhanced compaction. The first case (Fig. 6-13a) is for a constant compaction rate of 10^{-13} s^{-1}, which corresponds to 10 vol.% melt loss from a source in 30,000 years. The second case (Fig. 6-13b) is for a constant applied differential stress of 1 MPa. The range of vein thicknesses and separations predicted and timescales are reasonable when compared with natural examples.

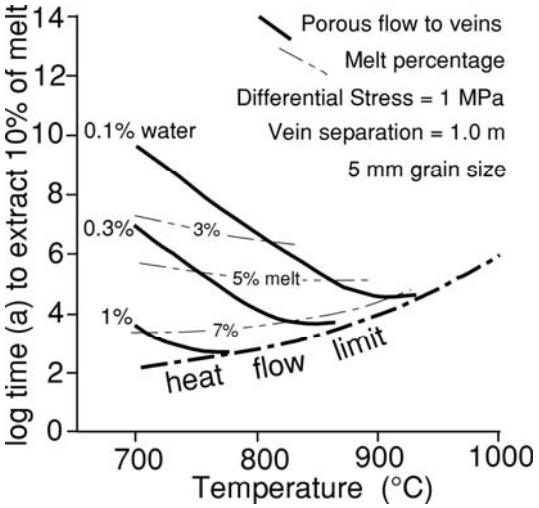

FIG. 6-12. Computed time to extract 10 vol. % of melt by shear-enhanced compaction from a hypothetical quartzo-feldspathic protolith of mean grain diameter 5 mm, containing 0.1, 0.3, and 1.0 wt.% water. Melt is assumed to accumulate in veins separated by 1 m that inflate until they are sufficiently permeable to drain melt upwards by virtue of the density contrast between melt and solids. At short timescales, extraction rate is limited by heat flow. Applied differential stress is assumed to be 1 MPa. Contours shown are for melt vol.%. Melt viscosity follows the Hess & Dingwell (1996) description. From Rutter & Mecklenburg (2006): The extraction of melt from crustal protoliths and the flow behavior of partially molten crustal rocks: an experimental perspective. *In* Evolution and Differentiation of the Continental Crust (M. Brown & T. Rushmer, eds). Cambridge University Press (384-429). © 2006 Cambridge University Press. Reproduced by permission of Cambridge University Press. For more details see Rutter & Mecklenburg (2006).

MAGMA ASCENT

In the previous section, we have seen that there is abundant evidence in exposures of the deep crust for vein networks preserved in migmatites and residual granulites and that melt extraction from such vein networks is realistic. We may infer that melt segregates and accumulates in these networks until a drainage event occurs. In addition, we have seen that coherency is destroyed in melt-bearing rocks as melt fraction increases or by ongoing deformation, leading to the formation of diatexite. Local ponding of melt or magma is implied by mesoscale bodies of leucosome or diatexite in migmatites and residual granulites (*e.g.*, southern

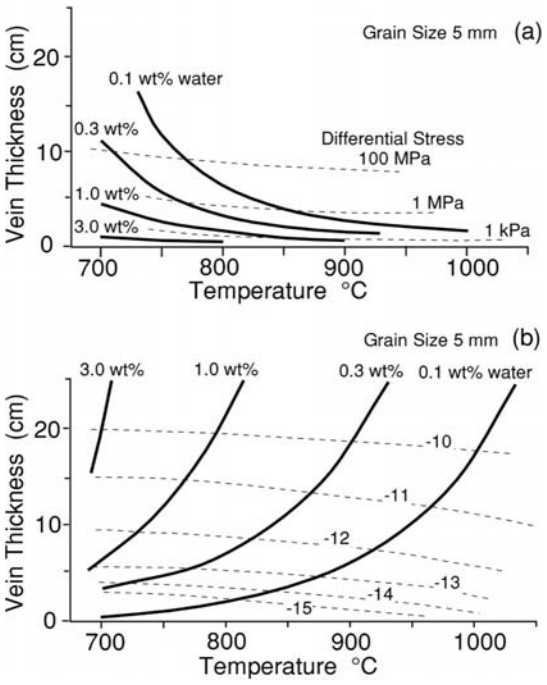

FIG. 6-13. Graphs showing the expected average thickness of veins in a network of average spacing 1 m in a protolith of mean grain size 5 mm for the water contents indicated, such that the rate of density driven flow through the veins equals the rate of supply of melt to the veins by shear-enhanced compaction. **a,** Graph for a constant compaction rate of 10^{-13} s^{-1}, which corresponds to 10% volume loss from the protolith in 30,000 years. Contours (dashed lines) are of constant differential stress. **b,** Graph for a constant applied differential stress of 1 MPa. Contours (dashed lines) are of constant log compactive strain rate. From Rutter & Mecklenburg (2006): The extraction of melt from crustal protoliths and the flow behavior of partially molten crustal rocks: an experimental perspective. *In* Evolution and Differentiation of the Continental Crust (M. Brown & T. Rushmer, eds). Cambridge University Press (384-429). © 2006 Cambridge University Press. Reproduced by permission of Cambridge University Press. For more details see Rutter & Mecklenburg (2006).

Brittany, France, Jones & Brown 1990; Antarctica, Allibone & Norris 1992; Western Australia, Oliver & Barr 1997; Opatica Subprovince, Canada, Sawyer 1998; Arunta Inlier, central Australia, Sawyer *et al.* 1999; Cooma Complex, Australia, Vernon *et al.* 2003; the Karakoram Shear Zone, north-west India, Weinberg & Mark 2008). It is these vein networks and ponded melt and magma that feed drainage channels to transport melt/magma to shallower levels in the orogenic crust to form plutons (Brown 1994, Sawyer 1998, Brown 2004, 2006).

Extraction and emplacement are complementary processes between which there is a feedback relation, modulated by processes in the ascent conduit. A critical point is reached at some combination of melt fraction and distribution in the source that enables the periodic formation of conduits of a size that allows melt to flow out of sub-volumes in the source (*i.e.,* the volume in the source from which melt is drained to form an individual upper-crustal pluton). For this to occur, it is likely that the melt volume generally in the source will be in the range 7–10 vol.% and that a vein network will be interconnected within at least part of each source sub-volume. Such a conclusion is consistent with general estimates of the melt fraction in the crust beneath the Central Andes and the Tibetan Plateau (Schilling & Partzsch 2001) and the general spacing of plutons in orogens (Cruden 2006).

Whether each drainage channel represents a single melt-draining event from its collection zone or whether there is build-up of melt pressure before periodic activation of a draining conduit in a cyclic fashion (*e.g.*, Handy *et al.* 2001), must be determined on a case-by-case basis. However, there is increasing evidence of common ascent conduits for multiple batches of melt (*e.g.*, Brown & Solar 1999; Solar & Brown 2001a, Sawyer & Bonnay 2003). Some sheeted plutons may represent staging levels in the transfer of melt to shallower levels, evidence of which is now eroded away (*e.g.*, the Pangong injection complex, Indian Karakoram, Weinberg & Searle 1998; the McDoogle pluton, Sierra Nevada, Mahan *et al.* 2003).

Magma ascent mechanisms

There are four main mechanisms proposed for magma ascent, as follows: diking by hydrofracture or ductile fracture; mesoscale porous to channel flow; compaction-generated flow instabilities; and, diapirism.

Diking by hydrofracture or ductile fracture. In the hydrofracture model for magma ascent, it is proposed that small melt-filled fractures propagate, coalesce and drain into larger developing crustal scale features. These features in turn propagate as brittle cracks to the upper crust, draining the source and transporting a large volume of magma through a small number of individual dikes (*e.g.,* Rubin 1995). This view is based on linear elastic fracture mechanics. In this model, inelastic deformation associated with breaking bonds by intergranular and

transgranular fracture in a small process zone ahead of the fracture tip (Fig. 6-14a, upper diagram), with or without chemical weakening (subcritical brittle fracture or brittle fracture, respectively), is driven by the magnified stresses at the macroscopic fracture tip (*e.g.*, Eichhubl 2004).

Hydrofracturing assumes an isotropic protolith, pervasive interconnected melt-filled porosity, initial fracturing due to melt-enhanced embrittlement and gradients in fluid pressure sufficient to drive melt from interconnected pores to hydrofractures (Bons *et al.* 2001). Steep fluid-filled fractures may become unstable if they exceed a critical crack length (Weertman 1971, Secor & Pollard 1975, Spence *et al.* 1987, Takada 1990) and move together with their fluid content (Dahm 2000, Bons 2001, Bons *et al.* 2001), although this is disputed by Rubin (1998). Transport of melt is postulated to occur via stepwise and discontinuous aggregation of mobile hydrofractures, increasing the accumulated volume of melt at each step to promote ascent. In principle, the result is a highly dynamic self-organized system in which intermittent, local events of fracture propagation will cause avalanches of instabilities and merging of hydrofractures (Bons *et al.* 2004, 2008).

A major problem in the hydrofracturing model is the transition from pervasive processes exploiting existing porosity to segregated flow in self-propagating melt-filled cracks. Rubin (1998) has argued that the critical crack length is too long to permit cracks to initiate spontaneously from a matrix in which melt is pervasively distributed. An intermediate mechanism capable of bridging the extremes between pervasive and segregated flow is required, at least to explain the initial stages of melt segregation into hydrofractures, but the zipper effect of migrating mobile hydrofractures may not leave much evidence of this intermediate mechanism or of the early stage of melt transport through the deep crust.

In addition, in the deep crust below the brittle to ductile transition, thermally activated flow processes will lead to extensive inelastic deformation and blunting of crack tips. Thus, process similar to those in creep failure of ceramics at high homologous temperature under low rates of loading, such as nucleation, growth and coalescence of pores by predominantly diffusive deformation mechanisms and side lobe damage (Fig. 6-14a, lower diagram), seem more relevant to failure in the anatectic zone. There is support for growth and coalescence of melt-filled pores from microstructures in natural low melt fraction rocks (*e.g.*, Sawyer 2001, Marchildon & Brown 2002), experiments (*e.g.*, Wark & Watson 2002) and theory (*e.g.*, Sleep 1988). Consequently large aperture and ductile fracture are expected to be the

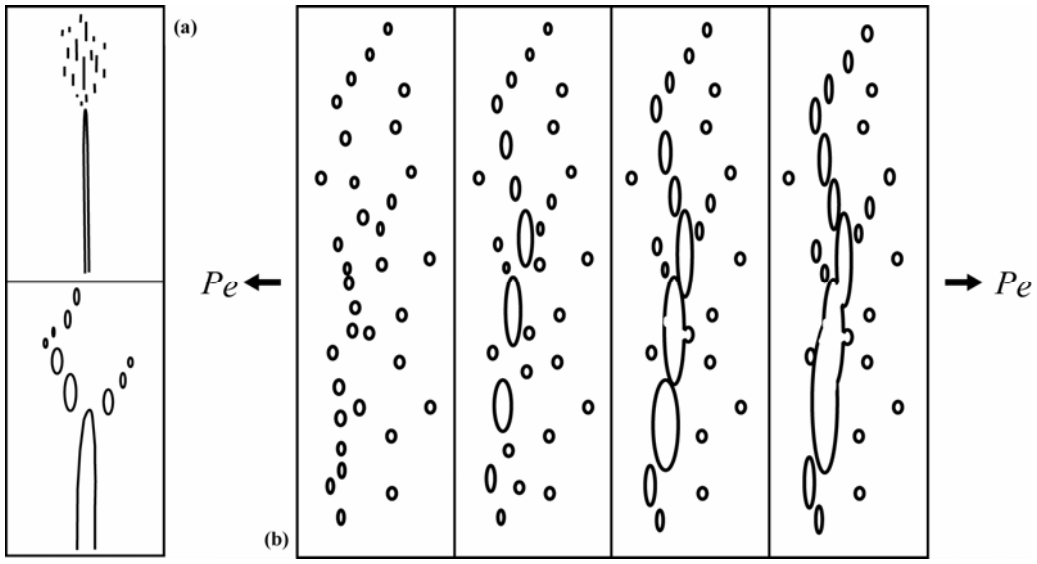

FIG. 6-14. **a,** Damage distribution at fracture tips (P_e = effective pressure, or σ_3 - P_{melt}); upper figure shows frontal damage typical of brittle fracture and lower figure shows side-lobe damage typical of ductile fracture (modified after Eichhubl, 2004). **b,** Sequence of formation of ductile fracture by growth of melt pockets and coalescence of melt pockets; fractures are inferred to grow with the long axis perpendicular to the least principal compressive stress, as modified by P_{melt} (modified after Eichhubl, 2004).

modes of failure in suprasolidus crust (Brown 2004, *cf.* Eichhubl 2004). Fracture propagation most likely takes place by development and coalescence of melt-filled pores ahead of a fracture tip, with fracture opening involving extensive inelastic deformation and diffusive mass transfer (*cf.*, Eichhubl *et al.* 2001, Eichhubl & Aydin 2003, Eichhubl 2004).

Figure 6-15 is a map of homologous temperature *versus* normalized stress, which shows the thermal and stress conditions under which ductile fracture occurs before those appropriate for subcritical or critical brittle fracture can be reached. In melting rock, the differential stress and effective mean stress are low, and the cohesive strength is low (relative to the strength of the grains) at melt fractions greater than about 7–8 vol.%. The loading rate varies with tectonic setting, but where loading rates are low, the prevailing conditions in the anatectic zone are generally appropriate for ductile fracture (Eichhubl 2004, Brown 2006).

Melt flow in self-generated melt-induced deformation band networks and ductile opening mode fracture systems has been inferred from observations of residual high-grade metamorphic complexes (*e.g.*, Brown & Marchildon 2003, Brown 2004, 2005). Linking among shear bands (Antonellini *et al.* 1994), compaction bands (Mollema & Antonellini 1996) and dilation bands (Du Bernard *et al.* 2002) potentially creates a reservoir for melt storage and a mechanism for deformation-assisted melt movement. Deformation band networks connect to dikes, which transport magma to shallower levels in the crust. These dikes represent structures analogous to large scale dilation bands or ductile opening mode fractures. They form by opening mode failure along zones of localized porosity increase or by pore growth and coalescence (Fig. 6-14), and may propagate from shear bands (Fig. 6-16a and b) (Regenauer-Lieb 1999, Eichhubl *et al.* 2001, Simakin & Talbot 2001, Du Bernard *et al.* 2002, Eichhubl & Aydin 2003, Brown 2004, 2005). The ductile structures will grow until they reach a critical length, at which point brittle fracture processes take over to allow magma transport through the subsolidus crust. Thus, the particular circumstances for high-flux flow of overpressured melt from deformation band networks to ductile opening mode fractures are generally short-lived and are terminated by the formation of a through-going dike that drains the local source.

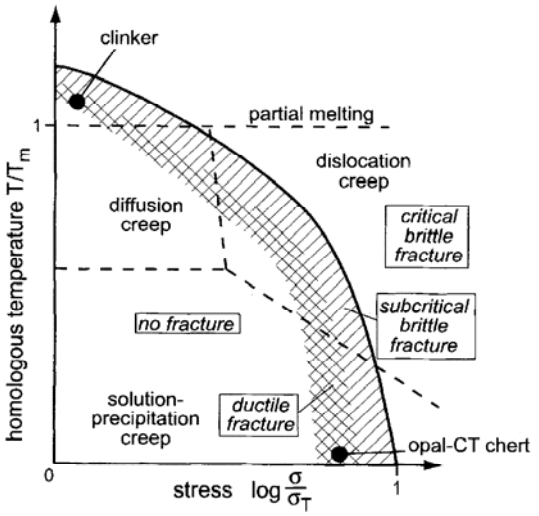

FIG. 6-15. Fracture mechanism map in space defined by normalized stress σ/σ_T (where σ_T is the uniaxial tensile strength for critical brittle failure at room temperature) *versus* homologous temperature T/T_M (where T_M is the melting temperature). Reprinted from Eichhubl, 2004, © 2007 Geological Society, with permission of the Geological Society Publishing House). For further details see Eichhubl (2004).

In former suprasolidus crust now represented by migmatite, smaller dikes have blunt fracture tips and zigzag geometry close to the tips. These features contrast with the straight geometry of larger dikes. Although the dikes are discordant (Fig. 6-16c), commonly the granite in them displays petrographic continuity with leucosome in the host migmatite (Fig. 6-17). This relationship suggests that dikes transporting magma through a particular crustal level do suck in melt from the local environment as they rise through the suprasolidus crust. Thus, at any particular crustal level we may find dikes frozen during birth, small dikes that have not transported magma far and larger dikes that have transported magma from deeper in the anatectic zone.

Although a strong intrinsic anisotropy of permeability allows melt focusing and flow down gradients in pressure to transecting dikes, to extract melt from the source requires sustained transient near-lithostatic to supra-magmastatic melt pore pressure in the melt flow network. This high melt pore pressure limits drawdown and decreasing transport rates, and prevents collapse of the storage network.

If diking is the ascent mechanism, it is likely that a ductile to brittle fracture process is the mechanism by which the dykes initiate and propagate. Dike interaction may focus magma flow into a smaller number of more widely spaced dikes during ascent (*e.g.*, Ito & Martel 2002).

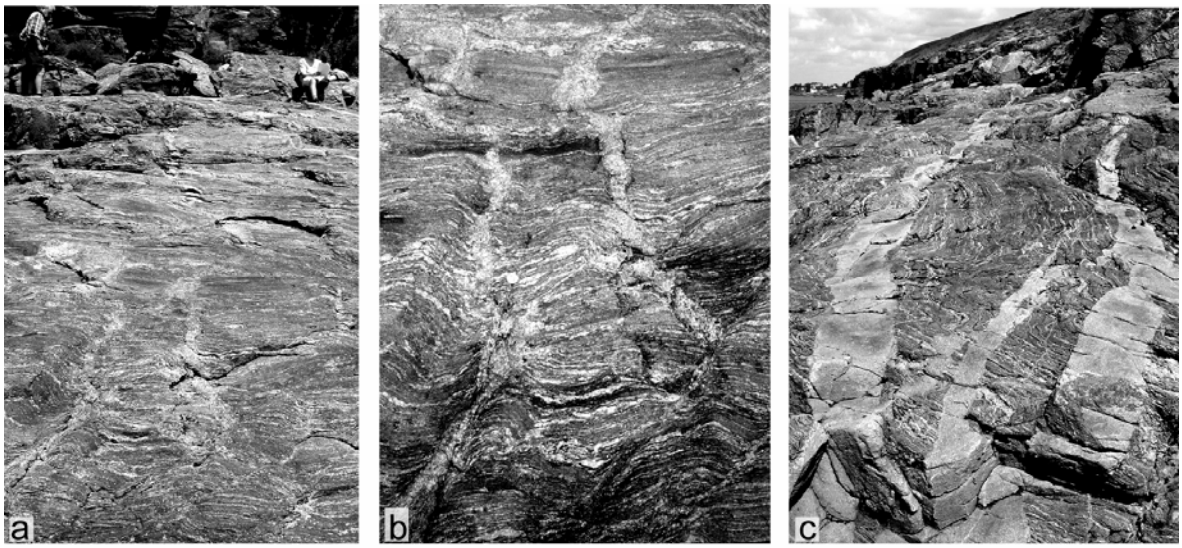

FIG. 6-16. **a,** Centimetric discordant dikes of granite with zigzag form at tips (bottom of image; Petit Mont, Arzon, S. Brittany, France). **b,** Close up of zigzag form at tips; for further details of this outcrop see Brown (2004). **c,** View approximately NW of 0.5 m wide dikes of granite in stromatic migmatite (Petit Mont, Arzon, S. Brittany, France). For further details of this outcrop see Brown (2005).

Mesoscale porous to channel flow. Exhumed anatectic crust exhibits a range of grain- to outcrop-scale structures that support an inference of inter-granular porous flow of melt to veins and channel flow of melt in veins to larger scale structurally controlled ascent conduits (*e.g.*, D'Lemos *et al.* 1992, Brown 1994, Collins & Sawyer 1996, Brown & Rushmer 1997, Brown & Solar 1998a, Sawyer *et al.* 1999, Weinberg 1999, Hasalová *et al.* 2008a, b). In mesoscale porous to channel flow, melt flow is driven by deformation from one scale to the next. This mechanism may avoid the problems associated with the transition from pervasive processes to segregated flow inherent in hydrofracturing.

Within the eastern part of the Gföhl Unit in the Moldanubian domain of the Bohemian Massif, Hasalová *et al.* (2008a, b) have demonstrated a gradual transition from high-grade solid state orthogneiss through stromatic and schlieren migmatite into irregular bodies of granite conformable with a foliation that records crustal scale channel flow of melt-bearing crust (Schulmann *et al.* 2008). The orthogneiss to granite sequence is characterized by progressive changes in mineralogy, mineral chemistry and microstructure consistent with increasing grain-scale equilibration between melt infiltrating from a deeper source and the host orthogneiss during exhumation from 790°C at 8.5–6 kbar to 690°C at 5–4 kbar. Overall, the variations require a large volume of melt to have passed through and interacted with the orthogneiss.

In the Acadian belt in the northern Appalachians, the form of leucosomes in host migmatites and granite in ascent conduits mimics the apparent strain ellipsoid recorded by the host rock fabrics (Brown & Solar 1999, Solar & Brown 2001a). Concordant tabular granite bodies occur in zones of apparent flattening strain (S > L; Fig. 6-18a), whereas concordant rod-like granite bodies occur in zones of apparent constrictional strain (L > S; Fig. 6-18b). In Mesoproterozoic aluminous metapelite from Broken Hill, Australia, White *et al.* (2004) described spatially focused melt formation where the resulting pathways for melt escape, as recorded by leucosome, are parallel to foliation defined by highly depleted melanosomes (Fig. 6-8; see also Figs. 3, 4 and 5 in White *et al.* 2004). In contrast, in the Mt. Hay area of the eastern Arunta Inlier, central Australia, magma is inferred to have migrated through Paleoproterozoic lower crust via a network of narrow, structurally controlled pathways parallel to the moderate to steeply plunging regional elongation direction, defined by leucosome associated with coaxial folds and a strong mineral elongation lineation (Fig. 6-19; see also Collins & Sawyer 1996).

Weinberg has argued that pervasive migration may lead to formation of magma 'sheets' preferentially emplaced parallel to high permeability zones, including fold axial surfaces

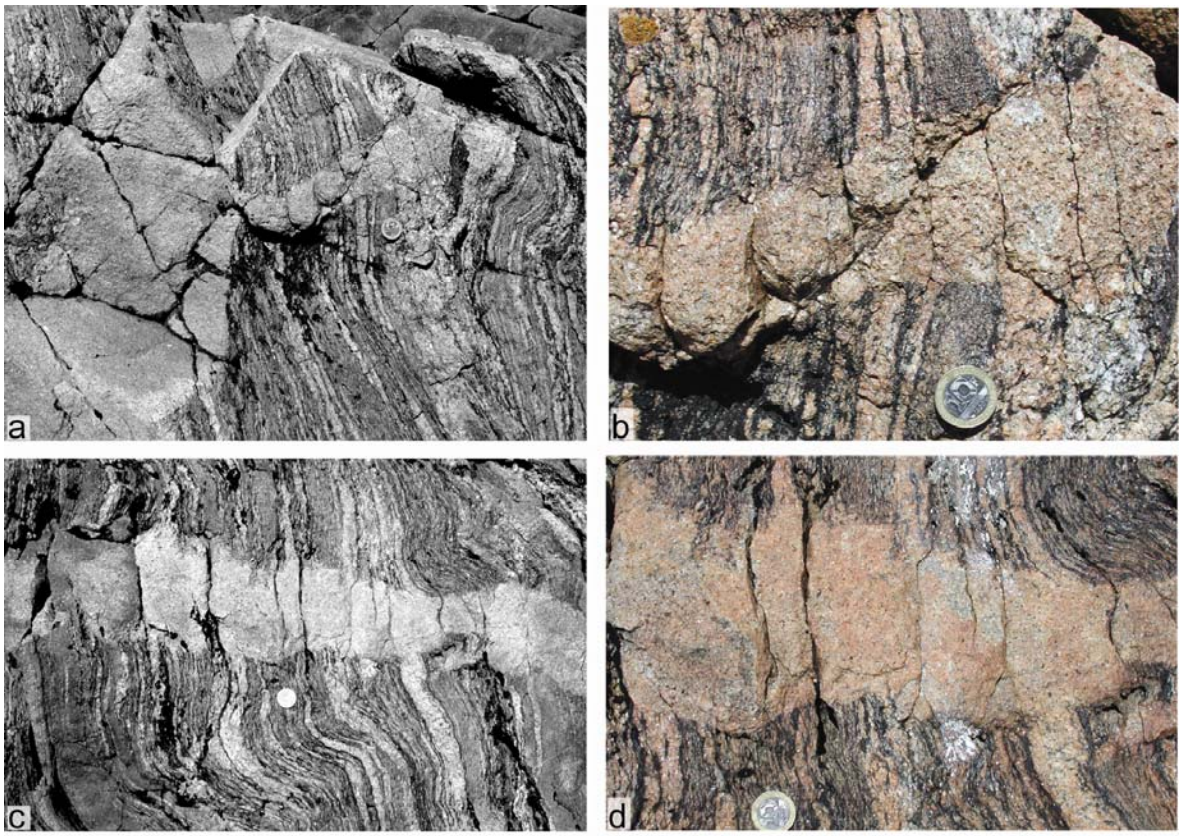

FIG. 6-17. **a,** Highly discordant centimetric dike of granite showing petrographic continuity (mineralogy, mode, grain size and microstructure) with the layer-parallel leucosomes it cross cuts (Petit Mont, Arzon, S. Brittany, France). **b,** Close-up view of area above coin in **a**. **c,** Discordant centimetric dike of granite that exhibits petrographic continuity (mineralogy, mode, grain size and microstructure) with leucosome in stromatic migmatite (Petit Mont, Arzon, S. Brittany, France). **d,** Close-up view of area above coin in **c**. For further details of these dikes see Marchildon & Brown (2003) and Brown (2004, 2005).

(Weinberg 1999, Weinberg & Mark 2008). Although pervasive migration of melt must be restricted to suprasolidus crust to avoid freezing, advection of heat with migrating melt may expand the suprasolidus domain allowing migration of melt to shallower depths (Brown & Solar 1999, Weinberg 1999). This feedback relation between migration of melt and heating allows successive batches of melt to reach increasingly shallower levels (Leitch & Weinberg 2002, Jackson *et al.* 2003). Such a process may result in an injection complex several kilometres thick, consisting of about half magma and half crust.

Compaction-generated flow instabilities. The anatectic zone is an over-pressured system with near-lithostatic to supra-magmastatic melt pore pressures and spatial and temporal variations in rheology and permeability. Connolly & Podladchikov (1998, 2007) have shown that rheological asymmetry between compaction and decompaction in viscous materials may lead to formation of mechanical flow channeling instabilities (porosity waves) that nucleate from small perturbations to an initially uniform porosity. These instabilities grow by drawing melt from the surrounding matrix, offering a mechanism both for collecting small amounts of melt and for disaggregating the matrix to form a magmatic suspension. Since flow is enhanced where porosity is higher, more melt drains to the instabilities from the background porosity further enhancing the flow, which induces additional influx of melt to grow the developing porosity waves. This coupling between flow and porosity leads to melt accumulation and transport in the form of upward migrating high porosity zones (Podladchikov & Connolly 2001), which may develop channelized flow in the core

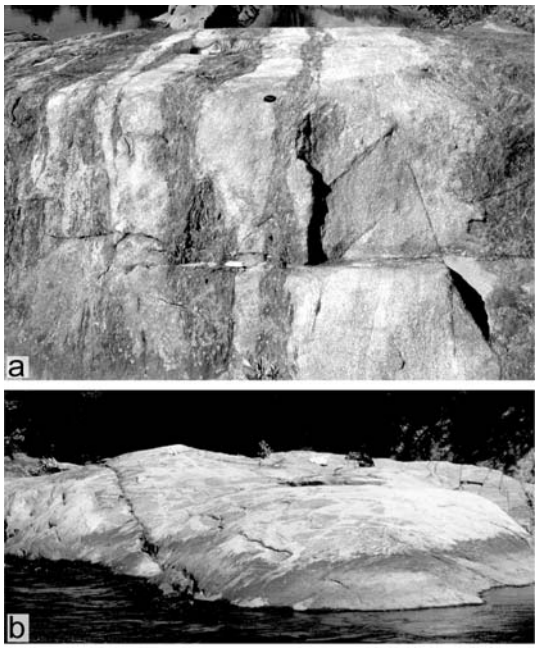

FIG. 6-18. **a,** view to the NNE of subhorizontal and subvertical surfaces through concordant sheets of granite in residual stromatic migmatite within a regional-scale zone of apparent flattening strain (S > L) in the Acadian orogen of west-central Maine, USA (Swift River, Roxbury, Maine; lens cap for scale). Further details are available in Brown & Solar (1998a, 1999) and Solar & Brown (2001a). **b,** Concordant, broadly cylindrical-shaped body of granite in diatexite from a regional-scale zone of apparent constrictional strain (L > S) in the Acadian orogen of west-central Maine, USA (Swift River, south of Roxbury). At this locality, leucosome and the granite plunge parallel to the regional mineral elongation lineation. Further details are available in Brown & Solar (1998a, 1999) and Solar & Brown (2001a).

FIG. 6-19. Granite in cylindrical body that is inferred to record magma migration through Paleoproterozoic lower crust via structurally-controlled pathways parallel to the moderate-to-steeply plunging regional elongation direction, from Mt. Hay, eastern Arunta Inlier, central Australia (for more details see Collins & Sawyer, 1996).

(Richardson *et al.* 1996, Connolly & Podladchikov 2007). Thus, porosity waves represent an intermediate mechanism bridging the extremes of pervasive and segregated flow. Connolly & Podladchikov (2007) speculated that the decrease in temperature and increase in local viscous compaction length with decreasing depth may cause channelized flows to anastomose upward. This may be an effective mechanism to transport melt through the anatectic zone under suprasolidus conditions, particularly in isotropic lithologies. However, what happens at the anatectic front?

The mechanism of melt transfer into subsolidus crust may involve melt-enhanced embrittlement, since the solidus represents the boundary to the anatectic zone with its interconnected melt-filled porosity. Compaction within the anatectic zone may generate strong variations in pressure near the solidus, which may enable deformation at the solidus to be essentially elastic in character. Under this condition, melt may be transported into the subsolidus (zero porosity) crust by an elastic shock, which may be expressed by the formation of dikes. However, the anatectic front is an unstable interface so that amplification of flow instabilities across the solidus by ductile processes is an alternative mechanism to form ascent conduits in some circumstances (Connolly & Podladchikov 1998). Experiments by Whitehead & Helfrich (1991) showed that flow instabilities develop increasing resistance as they advance into cooler regions across an interface and the number of advancing fingers rapidly decreases with time to one as the flow becomes focused. In the crustal environment, thermal softening will displace the solidus farther up in the crust localizing the zone in which ascent of melt will preferentially occur. This style of transport is consistent with models developed from field observations by Brown & Solar (1999) and Weinberg (1999), in which the magma transport and

style of pluton construction are controlled by the rate of ascent *versus* the rate of crystallization of the accumulated melt and the eventual decay of the thermal structure.

Diapirism. Diapirism may be possible in the lower crust, particularly perhaps during the formation of gneiss domes (*e.g.*, Teyssier & Whitney 2002, Whitney *et al.* 2004). Intracrustal convection has been argued to be important in some circumstances (Babeyko *et al.* 2002), and diapiric ascent may be the mechanism by which some granites are emplaced in the deep crust in continental arcs (*e.g.*, Miller & Patterson 1999). However, whether diapirism is a viable ascent process for upper crustal plutons remains a matter about which opinions differ (Emerman & Marrett 1990, Clemens & Mawer 1992, Rubin 1993, Weinberg & Podladchikov 1994, Burov *et al.* 2003). Diapirism involves decompaction and ascent of melt plus residue, implies partial convective overturn and may be limited by the brittle–ductile transition zone; it is argued to be an important process in the Archean (*e.g.*, Chardon *et al.* 1998, Collins *et al.* 1998, Peschler *et al.* 2004, Sandiford *et al.* 2004). A structural analogy is sometimes drawn between granite and salt diapirs, but it is clear that regional extension is the trigger for salt diapirism (*e.g.*, Jackson & Vendeville 1994) and the same has been proposed for the formation of gneiss domes (*e.g.*, Teyssier & Whitney 2002, Brown 2005). The formation of country rock diapirs that have ascended into the upper levels of the layered mafic and ultramafic rocks of the Bushveld complex demonstrates that diapirism is a viable process in the right circumstances (*e.g.*, Uken & Watkeys 1997, Johnson *et al.* 2004).

MAGMA EMPLACEMENT

Melt extraction, magma ascent and pluton emplacement represent a significant heat and mass transfer from lower to upper continental crust. The size, shape and spatial distribution of plutons likely reflect aspects of melting in the lower crust, and extraction and emplacement are complementary processes between which there is a feedback relation, modulated by processes in the ascent conduit (Brown 2007b). Superimposed on this intrinsic control are space-making processes due to regional deformation.

The perception that emplacement occurs at a 'level of neutral buoyancy' is inconsistent with the density of granite liquid (~2,440 kg/m^3 at 1 GPa, 800°C) and the range of emplacement depths observed in nature. Further, the generalization that emplacement is controlled primarily by structural interactions between ascending magma and anisotropies in upper crust is only a partial explanation of what happens at best. In transcurrent terranes, in the shallow crust pluton emplacement may occur in intra-jog regions between overlapping faults, which are low mean stress sites appropriate for magma accumulation and pluton construction (*cf.* Connolly & Cosgrove, 1999), whereas in deeper crust plutons may be located at the shoulders of shear zones in low mean stress sites that arise due to strain incompatibilities caused by regional variations in rheological properties (Weinberg *et al.* 2004). Pluton construction may be accommodated by magma expansion into evolving structural traps or by multiple material transfer processes acting locally (Patterson & Fowler 1993), but these mechanisms also represent only partial explanations of what happens in general. There is a systematic variation in three dimensional shape with depth, from horizontal wedge or tabular to blobby to vertical lozenge (*e.g.*, Brown 2001a, b), which suggests that emplacement occurs by two principal mechanisms, according to host rock behavior (a function of thermal gradient, strain rate, *etc.*). These are: in the brittle regime, vertical inflation (lifting the roof/depressing the floor, accommodation mechanism(s) unspecified) after horizontal flow in a fracture or pre-existing anisotropy; and, in the ductile regime, lateral expansion (swelling out like a balloon, accommodation mechanism(s) unspecified) localized by some instability.

In the brittle regime, magma ascent may be arrested by a structure or 'crack stopper', some instability or thermal death. Emplacement occurs when mainly vertical flow switches to predominantly horizontal flow. Analysis of the length *vs.* thickness of horizontal tabular plutons suggests they inflate according to a power law relationship, interpreted to mean that vertical thickening only occurs after magma has traveled horizontally some critical minimum distance (McCaffrey & Petford 1997, Cruden & McCaffrey 2001, 2002, McCaffrey & Cruden 2002, 2003). Inflation is accommodated by depression of the floor and/or lifting of the roof (Cruden 1998). Although sagging of the floor may occur because magma has been extracted at depth, there is no simple relationship since the volume of melt in the pluton is likely to have been extracted from a source up to order of magnitude larger in volume (Cruden

2006). To lift the roof, P_{melt} must overcome the lithostatic load and the tectonic overpressure.

In the ductile regime, amplification of naturally occurring instabilities in the system likely causes the switch from ascent to emplacement. Instabilities may be internal to the ascent column, such as fluctuations in permeability or magma flow rate (or changes in cross-sectional shape), or external to the ascent column, such as variations in strength or state of stress in host rock (Brown 2001a, b). They are not mutually exclusive, and feedback relations are similar whatever the initial instability.

Consider an ascent column with zones of higher permeability, these are conduits of higher magma flux, but higher flux increases permeability, and also heats and weakens the host rock surrounding the conduits, which in turn increases the strain rate, and so on. Magma in the preferred ascent conduit will exploit the weakening and may expand into the host rock, switching ascent to emplacement and forming a vertical lozenge pluton. A similar phenomenon occurs if the instability is due to differences in the strength of the host rock or the stress field around the ascent column. Magma exploits the weaker/lower stress sectors, swelling out of the ascent column into those sites, heating and weakening the host rocks, which enables further lateral expansion, forming a blobby pluton.

Above the anatectic zone, differences in flow rate or cross-sectional shape of the ascent conduit may lead to fluctuations around the critical width for flow without freezing. If freezing occurs in the slower/narrower parts of the conduit, flow will focus in the faster/wider parts. Heating of the host rock will cause weakening that will facilitate swelling of the conduit. The switch to emplacement may lead to formation of a pluton with a horizontal tabular head, formed by inflation of a sub-horizontal magma fracture, and a hemi-ellipsoidal root that passes down into a migmatite zone through which magma was transferred (*e.g.*, Brown & Solar 1999).

In circumstances where plutons are constructed from multiple batches of magma intruded at a similar level in the crust an injection complex or a sheeted granite may be the result according to the depth at which magma is emplaced. The Pangong injection complex of the Indian Karakoram (Weinberg & Searle 1998) and the Wuluma Granite of the Arunta Inlier in central Australia (Lafrance *et al.* 1995) may represent examples of injection complexes located close to the source. In contrast, the McDoogle pluton in the Sierra Nevada (Mahan *et al.* 2003) and the Galway granite in western Ireland (Leake 2006) on the one hand, and the Qôrqut granite complex of southern West Greenland (Brown *et al.* 1981) on the other hand (Fig. 6-20), may represent intermediate depth examples of sub-vertically sheeted and sub-horizontally sheeted plutons, respectively. These injection complexes and sheeted granites record pluton growth by multiple emplacements of many small magma batches (perhaps 10^3–10^5 batches).

This chapter is primarily concerned with links between middle to lower crustal sources and middle to upper crustal granites rather than with the process of magma emplacement and pluton growth *per see*. The reader interested in more information about pluton emplacement mechanics is referred to the following sources: Brown (2007b), Cruden (1998, 2006), Cruden & McCaffrey (2001, 2002), McCaffrey & Cruden (2002, 2003), McCaffrey & Petford (1997) and Miller & Patterson (1999).

GRANULITE–MIGMATITE–GRANITE SYSTEMS

"Thus, from observations in different localities, we come to the conclusion that the coastal granites and the larger gneissose rock-masses are formed by the refusion of older rocks. During the process of refusion . . . a considerable part has remained in an unmelted or semi-molten state, and after the consolidation of the granite it appears as large and small fragments 'swimming' in the granite . . . I have no further doubts that the zone described has been completely in a stage of melting, that is, partly molten, partly semi-molten and partly solid . . ."

J.J. Sederholm (1967)

"Migmatite terrains may well be complex as their location corresponds to some important intersection . . . for a period during the evolution of the terrain. Thus a given migmatite location will not only correspond to where first major melting occurs but also to where melts produced at a deeper level ascend."

R. Powell (1983)

In assessing the potential relationships among migmatites and granite, integrated multidisciplinary studies are essential, as the examples below demonstrate, and consistent evidence from field relations and/or geochemistry and/or geochronology normally is required. Based on such multi-disciplinary datasets, high-level granite without any

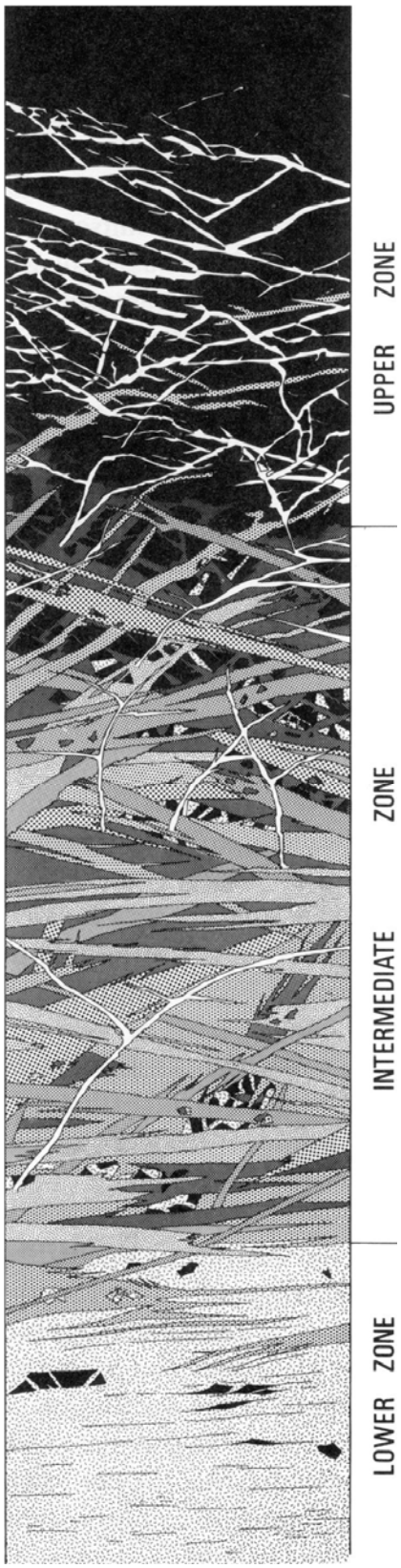

FIG. 6-20. Vertical section through approximately 2,000 m of the Qôrqut granite complex to demonstrate the components of each of the three zones within the complex. Jackstraws (bottom part) = leucocratic granite; various stipples = grey biotite granite; white = composite granite; and, black = country rock. Section prepared from field photographs. Reprinted from Friend *et al*. 1985, The geology of the Qôrqut Granite Complex north of Qôrqut, Godthåbsfjord, southern West Greenland, *Bull. Grønlands Geol. Undersøgelse* **151**, 43p., © 1985 Geological Survey of Denmark and Greenland, with permission of GEUS.

apparent connection to deeper migmatites and residual granulite and outcrop-scale granite within migmatite complexes have been inferred to be related to each other, or to the apparent source rocks or to both each other and the apparent source rocks.

Examples are provided by studies of: the late Svecofennian granite–migmatite complex of southern Finland (Sederholm 1967, Johannes *et al.* 2003, Stalfors & Ehlers 2006); the Black Forest, Germany (Mehnert 1968); the St. Malo migmatite belt and the Cadomian granites of north-east Brittany, France (Brown 1979, 1995, Brown & D'Lemos 1991, D'Lemos & Brown 1993, Power 1993); the Trios Seigneurs Massif in the Pyrenees (Wickham 1987a); leucogranite microplutons in migmatites of the Taylor Valley, Antarctica (Allibone & Norris 1992); Carboniferous and Cretaceous polyphase granites and migmatites of the Fosdick Mountains in Marie Byrd Land, west Antarctica (Korhonen *et al.* 2007, Saito *et al.* 2007); the leucogranite of central and southern Brittany and the southern Brittany migmatite belt, France (Brown & Dallmeyer 1996, Marchildon & Brown 2003, Brown 2005); the Acadian migmatites and granite of the northern Appalachians of New Hampshire and Maine, USA (Brown & Solar 1998a, b, Solar *et al.* 1998, Brown and Pressley 1999, Brown *et al.* 1999, Pressley & Brown 1999, Solar & Brown 2001a, Tomascak *et al.* 2005); the Cooma complex and the Murrumbidgee Batholith, southeastern Australia (Ellis & Obata 1992, Vernon *et al.* 2001, 2003, Richards & Collins 2002, Healy *et al.* 2004); granulite and granite in the Wuluma Hills, central Australia (Collins *et al.* 1989, Lafrance *et al.* 1995, Sawyer *et al.* 1999, Clarke *et al.* 2007); the Caledonian granite and the Krummendal supracrustal sequence of East Greenland (Kalsbeek *et al.* 2001); the Inzie Head gneisses and the Grampian granite of north-east Scotland (Johnson *et al.* 2001a, b, 2004); the Harney Peak leucogranite and its source rocks in

the Black Hills of South Dakota, USA (Nabelek & Bartlett 1998, Nabelek *et al.* 1992); the Superior Province, Canada (Cruden 2006), particularly the Opatica (Sawyer 1998) and Ashuanipi (Guernina & Sawyer 2003) subprovinces; and, the Ladybird granite and Monashee complex, southeastern British Columbia, Canada (Hinchey *et al.* 2006, Hinchey & Carr 2006).

Whether migmatites and residual granulites are sources of magma for high-level granite in general remains controversial. Although contemporary mafic magmatism is not a common feature of migmatite terranes it does occur (see below), and contemporary mafic granulites are common, if enigmatic, in many granulite and ultrahigh-temperature metamorphic terranes (Barboza *et al.* 1999, Baldwin & Brown 2008). Also, there is increasing geochemical evidence of interaction between mantle wedge-derived magmas and anatectic melts derived from metasedimentary sources in continental margin accretionary orogenic systems (*e.g.,* Kemp *et al.* 2007a).

An additional consideration comes from melt compositions in melting experiments in comparison with natural S-type granites. Such a comparison has led Stevens *et al.* (2007) to argue that the large-scale major-element geochemical trends defined by S-type granites are the product of garnet addition to melts of different composition, with the most mafic compositions representing addition of up to 20 wt.% of the peritectic products of biotite-breakdown melting. This is consistent with observations from outcrop, where the peritectic products of biotite-breakdown melting are infinitely associated with leucosome (Brown & Dallmeyer 1996, White *et al.* 2004), as proposed by Sawyer (1996), and 3-D studies of stromatic migmatite (Brown *et al.* 1999).

Contemporaneous mafic to intermediate magma is associated with some migmatite complexes, particularly in contact aureoles of mafic plutons in arc-related terranes. Barnes *et al.* (2002) document anatexis and hybridization related to the dioritic Velfjord plutons emplaced at mid-crustal levels into regional-scale migmatitic metapelitic and metacarbonate rocks in the Bindal Batholith, Norway. In a second example, Droop *et al.* (2003) give a detailed account of the Huntly Gabbro and its associated contact metamorphic rocks. They argue for a variety of processes operating during contact anatexis and subsequent melt segregation and extraction that may be similar to those occurring at much larger scales in the deeper crust during high-grade regional metamorphism involving generation of granite magma. This study shows that crustal melting and magma production may occur without extensive chemical interaction among the mantle-derived mafic magma that input heat and the crustal melts themselves.

The Hidaka metamorphic belt of northern Japan represents a tilted crustal section through about two-thirds of a magmatic arc (Osanai *et al.* 1991, 1992). The lower part of the exposed section consists mainly of mafic rocks with thin intercalations of high-grade migmatitic pelite and psammite, whereas the upper part consists of medium- to low-grade metasedimentary rocks. The highest metamorphic grades reached are granulite facies, and syn-metamorphic granitic rocks are widely distributed in this metamorphic terrane (Shimura *et al.* 2004). The granite bodies are mainly tonalitic and granodioritic in composition, and are classified into dominant peraluminous S-types and subordinate metaluminous I-types. S-type granites in the lower part of the section are Opx–Grt–Bt tonalite in the granulite zone, Grt–Crd–Bt tonalite in the amphibolite zone and Crd–Bt–Ms tonalite in the Bt–Mus gneiss zone. The mineralogical and chemical nature of this strongly peraluminous tonalite is consistent with derivation from crustal melts of pelitic source rocks in the deeper unexposed arc crust (Osanai *et al.* 1992, Shimura *et al.* 1992, 2004). Another regional scale example is the Delamerian orogen of south-east Australia, where there are several well characterized examples of granite–migmatite complexes that show evidence of interactions with mafic melts, including the Glenelg river complex (*e.g.*, Kemp 2003, 2004) and the metatexite migmatites and diatexites of Kangaroo Island (*e.g.*, Foden *et al.* 2002). Vernon (2007) and Kemp *et al.* (2007a) consider the wider implications of these regional relationships.

The common association of regional scale middle crustal migmatites with outcrop-scale granites suggests that regional scale migmatite terrains display an integrated record of both melt generation and magma transfer. These regional scale migmatite terrains are inferred to represent the upper levels of the anatectic zone through which magma is fed from deeper, granulite-facies levels of the anatectic zone to granites emplaced in shallower subsolidus middle to upper crust (*e.g.*, Brown & Solar 1999, Brown 2004, Olsen *et al.* 2004, Slagstad *et al.* 2005). Melt from deeper levels in the anatectic zone that pervasively intrudes through a regional scale migmatite terrain will be superheated

and is unlikely to freeze at the ambient temperature (Leitch & Weinberg 2002). As a result, interactions may occur between magma in the process of transferring to a shallower crustal level and the host migmatites. Examples include additional melting or renewed melting and/or partial crystallization and/or residue segregation. These interactions could lead to modification of the magma towards a more evolved composition (*e.g.*, Sawyer 1987, 1996, Stevens *et al.* 2007). The petrographic continuity observed between dikes and leucosomes in the residual migmatites they cut in the southern Brittany migmatite belt is consistent with such interactions (Brown 2004, 2005, 2007b).

AN EXAMPLE OF 3-D INTERPRETATION OF MIGMATITE–GRANITE RELATIONS FROM WESTERN MAINE–EASTERN NEW HAMPSHIRE, NE APPALACHIANS, USA

Based on observations from western Maine–eastern New Hampshire, Brown & Solar (1998a, b, 1999) proposed a model for melt ascent and emplacement that may have general applicability to obliquely convergent (transpressive) orogens. At map scale in western Maine–eastern New Hampshire, granite plutons in low-grade terranes have discrete contact metamorphic aureoles (Fig. 6-21; and elsewhere, see the summary in Pattison & Tracy 1991) and high-grade regional metamorphic zones are spatially related to granites (Fig. 6-21; and elsewhere, see the summary in Pattison & Tracy 1991).

A map is a projection of the surface geology onto an arbitrary horizontal plane. Thus, granites may vary in size and in their relations with regional scale tectonic structures as determined by differences in crustal level exposed. For example, in western Maine–eastern New Hampshire, smaller plutons commonly are conformable with regional scale structures, such as the Phillips pluton in a zone of apparent constrictional strain, whereas larger plutons commonly cut across regional structures, such as the Lexington pluton, which cuts across both zones of apparent flattening strain and apparent constrictional strain (Fig. 6-21). Relative barometry between the aureole of the Lexington pluton and the metamorphism around the Phillips pluton reveals a difference of up to 1 kbar (Brown

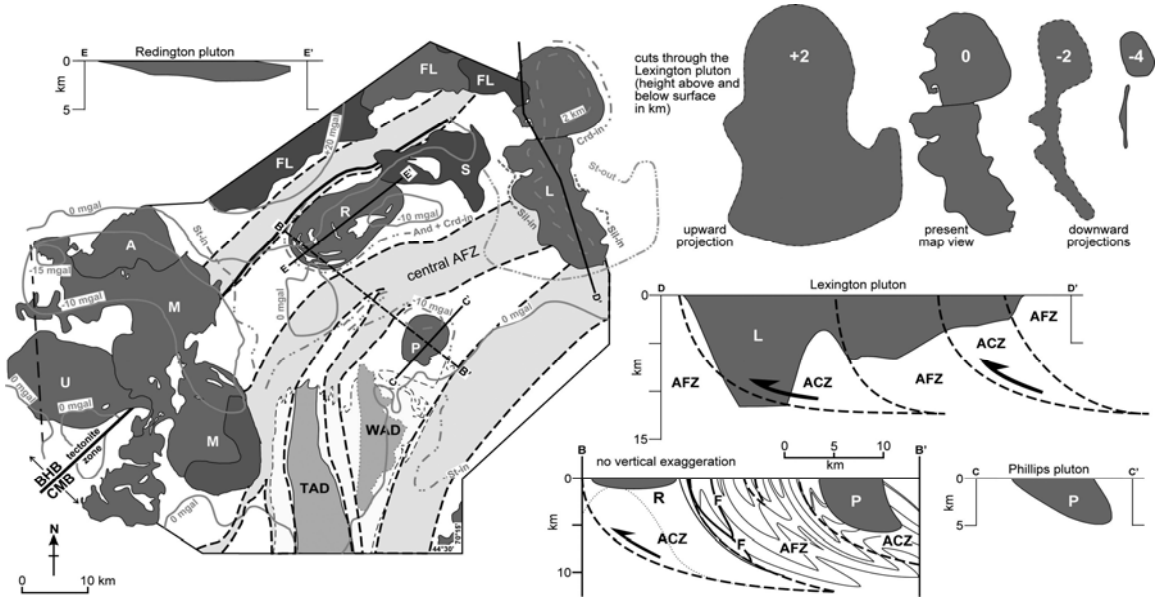

FIG. 6-21. Map to show the relationship between granite plutons and the Central Maine belt shear zone system (modified after Brown & Solar, 1998b, 1999). AFZ denotes a zone of apparent flattening strain and ACZ denotes a zone of apparent constrictional strain; migmatite domains are shown in pale yellow and orange, whereas plutons are indicated in blue (diorite *sensu lato*) and red (granite *sensu lato*). An indication of the extent of the metamorphic aureole surrounding each pluton is given by an appropriate isograd (see Brown & Solar, 1998b for details). B–B′ and C–C′ are lines of true-scale sections that cross the Phillips pluton. The N–S longitudinal section (D–D′) and horizontal slices through the Lexington pluton are based on models in Unger *et al.* (1989). A is the Adamstown pluton, FL is the Flagstaff Lake pluton, L is the Lexington pluton, M is the Mooselookmeguntic pluton, P is the Phillips pluton, R is the Redington pluton, S is the Sugarloaf pluton and U is the Umbagog pluton; TAD is the Tumbledown anatectic domain and WAD is the Weld anatectic domain.

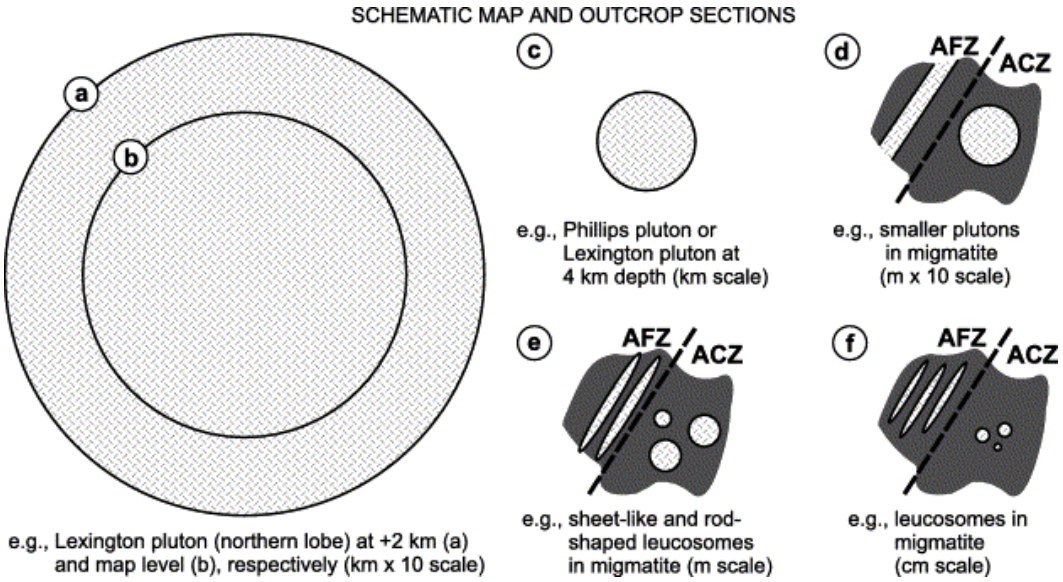

FIG. 6-22. Summary of observations using schematic map (horizontal) sections through plutons and outcrop (horizontal or oblique) sections through migmatites (see text for further discussion). From Brown & Solar (1999): The mechanism of ascent and emplacement of granite magma during transpression: a syntectonic granite paradigm. Reprinted from *Tectonophys.* **312**, Brown & Solar, The mechanism of ascent and emplacement of granite magma during transpression: A syntectonic granite paradigm, 1-33, © 2003 Elsevier, with permission from Elsevier.

& Solar 1998b). Removing an additional ~4 km of crust from the site of the Lexington pluton yields a map pattern similar to that of the Phillips pluton (Fig. 6-21), consistent with the difference in recorded pressure.

Brown & Solar (1998b, 1999) interpret the smaller granites, such as the Phillips pluton, to represent more deeply eroded bodies than the larger granites, such as the Lexington pluton. The smaller plutons correspond to cuts through root zones, which are interpreted from gravity data also to be present beneath the laterally extensive larger plutons (Fig. 6-22). These structures are inferred to have been feeder channels by which new batches of magma became part of the pluton; the feeder channels connect the main body or tabular head of the pluton to the source of the melts. However, based on the absence of migmatite immediately around the exposed cut through the Phillips pluton combined with the fact that it continues for several km at depth, as interpreted from the gravity anomaly, Brown & Solar (1998b, 1999) inferred that the map pattern is a 'middle cut' through the feeder channel to a once larger pluton. Whatever volume of magma might have passed through this feeder channel, at the level of erosion there was insufficient heat advected with the magma to raise the adjacent wall rocks above the solidus for wet granite to generate migmatite. In contrast, larger plutons associated with discrete contact metamorphic aureoles represent cuts through bodies at shallower levels in the crust closer to the tops of these plutons (Fig. 6-22).

Brown & Solar (1998b, 1999) observed decametric to metric bodies of granite at the outcrop scale associated with migmatites where the form of the granite bodies was controlled by the tectonic structures (Fig. 6-22). Thus, in zones of apparent flattening strain stromatic migmatite is associated with generally concordant planar sheet-like bodies of granite (*e.g.*, Fig. 6-18a), whereas in zones of apparent constrictional strain inhomogeneous migmatite is associated with rod-shaped leucosomes and cylindrical bodies of granite (*e.g.*, Fig. 6-18b). Within individual outcrops in migmatite the form of the leucosomes reflects the shape of the apparent tectonic strain ellipsoid recorded by fabrics in the host rock. Although the planar leucosomes and sheet-like granites of the zones of apparent flattening strain exploit the mechanical anisotropy, pinch-and-swell structures and absence of solid-state fabrics suggest that deformation and emplacement were synchronous.

Brown & Solar (1999) inferred that the 3-D form of melt-escape paths in transpressive orogens is controlled by the contemporaneous deformation and is governed by strain partitioning. Magma ascent in obliquely convergent (transpressive)

orogens is a syntectonic process, and pluton construction is a syntectonic process when viewed at the crustal scale, in spite of the local discordances between pluton contacts and regional scale structures (Brown and Solar 1998b, 1999) – *quod erat demonstrandum*!

The Weld anatectic domain to the southwest of the Phillips pluton is poorly exposed, but Brown & Solar (1998b, see also Pressley & Brown 1999) interpreted it to be composed of stromatic migmatite and inhomogeneous migmatite with lenses of schlieric granite. Given the ubiquitous moderate to steeply NE-plunging mineral elongation lineation, it is implicit that rocks similar to these stromatic migmatites and inhomogeneous migmatites with lenses of schlieric granite exposed immediately south of the Phillips pluton plunge underneath the pluton. Geochemical data reported from the Phillips pluton support evidence from field relations of its composite nature, particularly the isotopic composition of Nd that suggests the pluton is composed of multiple batches of melt (Pressley & Brown 1999, Brown & Pressley 1999). Furthermore, these authors showed that the leucogranite comprising most of the pluton was derived from a source with similar isotopic composition to the surrounding Central Maine Belt rocks, although minor granodiorite has an isotopic composition compatible with derivation from the underlying crust. These data are consistent with an inference that the deepest part of the Phillips pluton is close to or transitional into residual migmatites that was the source of the common leucogranite in the exposed pluton.

Brown & Solar (1998b, 1999) also postulated that migmatites occur immediately beneath the northern lobe of the Lexington pluton, at a depth of ~12 km, given the depth of the northern lobe as modeled by Unger *et al.* (1989). For any enhanced geotherm appropriate to this high-temperature, low-pressure metamorphic belt, it is reasonable to expect upper amphibolite-facies metamorphic conditions at a depth appropriate to the inferred bottom of the northern lobe of the Lexington pluton. Both the northern lobe of the Lexington pluton and the Phillips pluton are found in zones of apparent constriction, and Brown & Solar (1998a, b, 1999) argued that melt accumulated preferentially in these zones and was driven out of the zones of apparent flattening by enhanced deformation.

Brown & Solar (1999) postulated that at the peak of the thermal evolution, the solidus for granite melt is at the shallowest level in the crust within the core of an actively deforming orogenic belt. Thus, melt transferring through the orogenic crust in foliation-parallel and lineation-parallel conduits may reach shallow levels without freezing. The melt will be superheated, so if the melt has accumulated into large enough batches it may be transported into the unmelted crust and ascend some distance before arrest at the site of a future pluton. The mechanism of this transfer might involve melt-enhanced embrittlement or amplification of flow instabilities across the anatectic front. In the zones of apparent constrictional strain, amplification of flow instabilities across the anatectic front to generate pipe-like structures may be the mechanism of melt ascent.

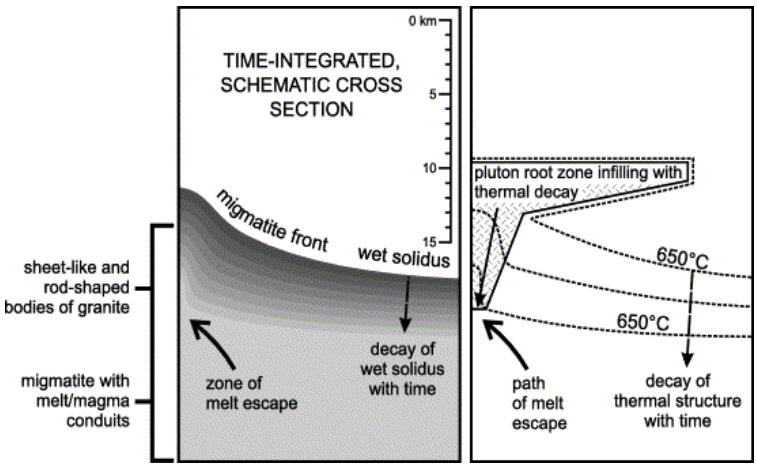

FIG. 6-23. Time-integrated, schematic cross-section through orogenic crust to illustrate the relations between the thermal evolution of the anatectic zone and the construction of a pluton composed of a tabular head and a root zone that extends down to migmatites of the anatectic zone. The cross-section is vertical in a plane parallel to the mineral elongation lineation. From Brown & Solar (1999): The mechanism of ascent and emplacement of granite magma during transpression: a syntectonic granite paradigm. Reprinted from *Tectonophys.* **312**, Brown & Solar, The mechanism of ascent and emplacement of granite magma during transpression: A syntectonic granite paradigm, 1-33, © 2003 Elsevier, with permission from Elsevier.

Brown & Solar (1998b) argued that the exposed level of the Lexington pluton likely was emplaced around the brittle–ductile transition and the exposed level of the Phillips pluton likely was emplaced below the brittle–ductile transition. For a geotherm consistent with these inferences, the northern lobe of the Lexington pluton and the Phillips pluton may pass gradationally into residual inhomogeneous migmatite at depth beneath the present erosion surface. As orogenic deformation wanes, so the thermal structure decays, the height to which any batch of melt can ascend moves downward in the crust, and the periods between arrivals of melt batches into the magma feeder channel at the base of the pluton may become longer. In this circumstance, individual batches of magma may freeze before the arrival of subsequent batches, which will construct a downward-growing composite root zone that progressively occupies the magma feeder channel beneath a large pluton (Figs. 6-22 and 6-23). Thus, pluton construction is terminated by downward congelation of granite melt in the magma feeder channel during the waning stages of orogeny. Although this is one alternative among a range of possible scenarios, it is a reasonable interpretation of the data in western Maine–eastern New Hampshire and may have application elsewhere in transpressive orogens.

In producing a model that relates generation of melt to ascent and emplacement, it is necessary to project relationships observed at the erosion surface to depth. A general model of granite ascent and emplacement is shown in Fig. 6-24 (Brown & Solar 1999). At shallower contemporary levels in the crust, we may expect to see the maximum areal extent of granite plutons. With each successively deeper slice, the pluton becomes smaller, and the pluton may be more likely to be composite structure, as opposed to homogeneous in structure, in passing from the main tabular body to the root zone. Ultimately, the pluton passes downward into the source region represented by residual migmatites that preserve outcrop-scale melt-escape structures.

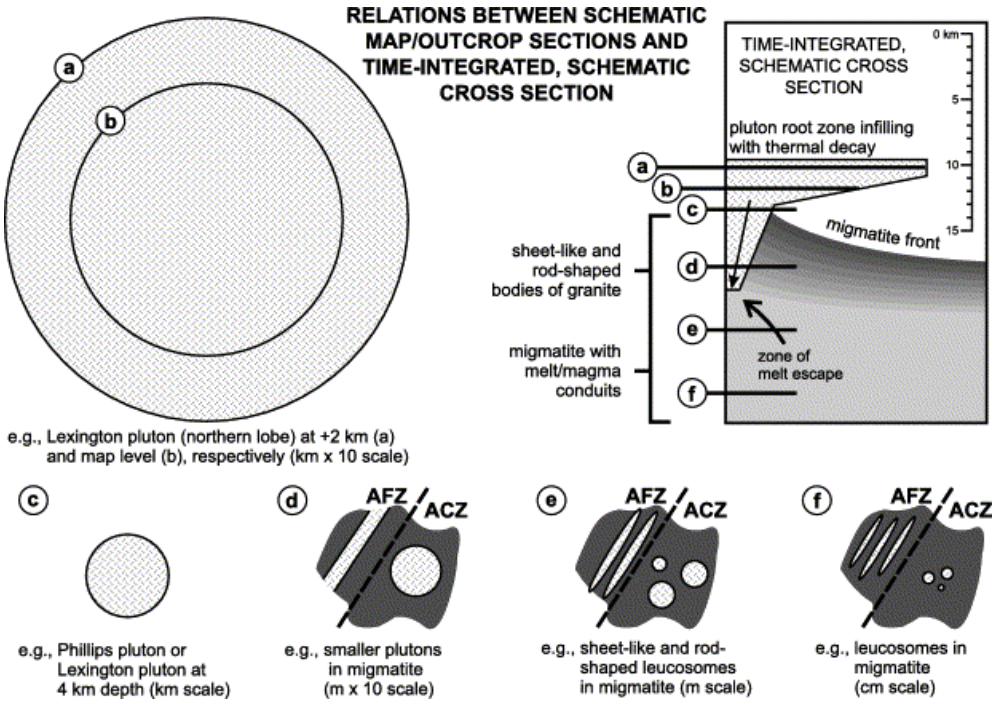

FIG. 6-24. Relations between schematic map and outcrop sections and the time-integrated, schematic cross-section through orogenic crust, based on relationships in western Maine–eastern New Hampshire, from which a general model of granite ascent and emplacement was developed by Brown & Solar (1999). From Brown & Solar (1999): The mechanism of ascent and emplacement of granite magma during transpression: a syntectonic granite paradigm. Reprinted from *Tectonophys.* **312**, Brown & Solar, The mechanism of ascent and emplacement of granite magma during transpression: A syntectonic granite paradigm, 1-33, © 2003 Elsevier, with permission from Elsevier.

ACKNOWLEDGEMENTS

We have come far in our understanding of migmatites and granites, but much remains to do. I hope that this Chapter represents another step on the path to a better understanding. I have tried to represent the literature fairly within the constraints of reasonable length, and I acknowledge that my understanding, such as it is, owes as much to the many discussions, both indoors and in the field, that I have had with colleagues and students as to my own investigations and contributions. Nonetheless, I am responsible for any misrepresentations or infelicities that may persist. I thank Barry Reno for help with figures, Fawna Korhonen and Ed Sawyer for review comments that materially improved this Chapter, and the US National Science Foundation and the University of Maryland for supporting my research into melt extraction from anatectic rocks.

REFERENCES

ALLIBONE, A.H. & NORRIS, R.J. (1992): Segregation of leucogranite microplutons during syn-anatectic deformation – an example from the Taylor Valley, Antarctic. *J. Metamorphic Geol.* **10**, 589-600.

ANDREOLI, M.A., HART, R.J., ASHWAL, L.D. & COETZEE, H. (2006): Correlations between U, Th content and metamorphic grade in the western Namaqualand Belt, South Africa, with implications for radioactive heating of the crust. *J. Petrol.* **47,** 1095-1118.

ANNEN, C., BLUNDY, J.D. & SPARKS, R.S.J. (2006a): The genesis of intermediate and silicic magmas in deep crustal hot zones. *J. Petrol.* **47**, 71-95.

ANNEN, C., SCAILLET, B. & SPARKS, R.S.J. (2006b): Thermal constraints on the emplacement rate of a large intrusive complex: the Manaslu leuco-granite, Nepal Himalaya. *J. Petrol.* **47**, 71-95.

ANTONELLINI, M.A., AYDIN, A. & POLLARD, D.D. (1994): Microstructure of deformation bands in porous sandstones at Arches National Park, Utah. *J. Struct. Geol.* **16**, 941-959.

ASHWORTH, J.R. (1976): Petrogenesis of migmatites in the Huntly-Portsoy area, north-east Scotland. *Mineral. Mag.* **40**, 661-682.

ASHWORTH, J.R. & MCLELLAN, E.L. (1985): Textures. *In* Migmatites (J.R. Ashworth, ed). Blackie & Son Ltd., Glasgow (180-203).

ATHERTON, M.P. (1993): Granite magmatism. *J. Geol. Soc. London* **150**, 1009-1023.

AUZANNEAU, E., VIELZEU, D. & SCHMID, M.W. (2006): Experimental evidence of decompression melting during exhumation of subducted continental crust. *Contrib. Mineral. Petrol.* **152**, 125–148.

AYRES, M., HARRIS, N. & VANCE, D. (1997): Possible constraints on anatectic melt residence times from accessory mineral dissolution rates: an example from Himalayan leucogranites. *Mineral. Mag.* **61**, 29-36.

BABEYKO, A. YU., SOBOLEV, S.V., TRUMBULL, R.B., ONCKEN, O. & LAVIER, L.L. (2002): Numerical models of crustal scale convection and partial melting beneath the Altiplano–Puna plateau. *Earth Planet. Sci. Lett.***199**, 373-388.

BALDWIN, J.A. & BROWN M. (2008): Age and duration of ultrahigh-temperature metamorphism in the Anápolis-Itauçu Complex, southern Brasília Belt, Central Brazil – constraints from U–Pb geochronology, mineral rare earth element chemistry and trace-element thermometry. *J. Metamorphic Geol.* **26**, 213-233.

BARBOZA, S.A., BERGANTZ, G.W. & BROWN, M. (1999): Regional granulite facies metamorphism in the Ivrea zone: Is the Mafic Complex the smoking gun or a red herring? *Geology* **27**, 447-450.

BARNES, C.G., YOSHINOBU, A.S., PRESTVIK, T., NORDGULEN, O., KARLSSON, H.R. & SUNDVOLL, B. (2002): Mafic magma intraplating: anatexis and hybridization in arc crust, Bindal Batholith, Norway. *J. Petrol.* **43**, 2171-2190.

BARR, D. (1985): Migmatites in the Moines. *In* Migmatites (J.R. Ashworth ed). Blackie, Glasgow, (225-264).

BAYLEY, B. (1985): Deformation with simultaneous chemical change: The thermodynamic basis. *In* Metamorphic reactions: Kinetics, textures, and deformation (A.B. Thompson & D.C. Rubie, eds) Springer-Verlag, New York, 269-277.

BEA, F., MONTERO, P., GONZÁLEZ-LODEIRO, F. & TALAVERA, C. (2007): Ziron inheritance reveals exceptionally fast crustal magma generation processes in Central Iberia during the Cambro-Ordovician. *J. Petrol.* **48**, 2327-2339.

BERGANTZ, G.W. (1989): Underplating and partial melting. Implications for melt generation and extraction. *Science* **33**, 267-309.

BERGER, A., BURRI, T., ALT-EPPING, P. & ENGI, M. (2008): Tectonically controlled fluid flow and

water-assisted melting in the middle crust: An example from the Central Alps. *Lithos*, doi: 10.1016/j.lithos.2007.07.027

BODORKOS, S., SANDIFORD, M., OLIVER, N.H.S. & CAWOOD, P.A. (2002): High-T, low-P metamorphism in the Palaeoproterozoic Halls Creek orogen, northern Australia: the middle crustal response to a mantle-related thermal pulse. *J. Metamorphic Geol.* **20**, 217-237.

BONS, P.D. (2001): The formation of large quartz veins by rapid ascent of fluids in mobile hydrofractures. *Tectonophys.* **336**, 1-17.

BONS, P.D. & ELBURG, M.A. (2001): Fractal size distribution of plutons: An example from the Lachlan Fold Belt, Australia. *In* S-type granites and related rocks (B.W. Chappell & P.D. Fleming, eds). *Australian Geol. Surv. Org. Record* 2001/2, 21-22.

BONS, P.D. & VAN MILLIGEN, B.P. (2001): New experiment to model self-organized critical transport and accumulation of melt and hydrocarbons from their source rocks. *Geology* **29**, 919-922.

BONS, P.D., DOUGHERTY-PAGE, J. & ELBURG, M.A. (2001): Stepwise accumulation and ascent of magmas. *J. Metamorphic Geol.* **19**, 627-633.

BONS, P.D., ARNOLD, J., ELBURG, M.A., KALDA, J., SOESOO, A. & VAN MILLIGEN, B.P. (2004): Melt extraction and accumulation from partially molten rocks. *Lithos* **78**, 25-42.

BONS, P.D., BECKER, J.K., ELBURG, M.A. & URTSON, K. (2008): Granite formation: Stepwise accumulation of melt or connected networks. *Trans. Royal Soc. Edinburgh: Earth Sci*, in press.

BRAUN, M.G. & KELEMEN, P.B. (2002): Dunite distribution in the Omanman ophiolite: Implications for melt flux through porous dunite conduits. *Geochem., Geophys, Geosys.* **3**, Article #8603.

BROWN, M. (1973): The Definition of Metatexis, Diatexis and Migmatite. *Proc. Geol. Assoc.* **84**, 371-382.

BROWN, M. (1979): The petrogenesis of the St. Malo migmatite belt, Armorican Massif, France, with particular reference to the diatexites. *Neues Jahrb. Mineral Abh.* **135**, 48-74.

BROWN, M. (1994): The generation, segregation, ascent and emplacement of granite magma: The migmatite-to-crustally-derived granite connection in thickened orogens. *Earth Sci. Rev.* **36**, 83-130.

BROWN, M. (1995): The late-Precambrian geodynamic evolution of the Armorican segment of the Cadomian belt (France): Distortion of an active continental margin during south-west directed convergence and subduction of a bathymetric high. *Géologie de la France*, **3**, 3-22.

BROWN, M. (2001a): Crustal melting and granite magmatism: key issues. *Phys & Chem, Earth (A)* **26**, 201-212.

BROWN, M. (2001b): Orogeny, migmatites and leucogranites: a review. *Proc. Indian Acad. Sci.* **110**, 313-336.

BROWN, M., (2002): Prograde and Retrograde Processes in Migmatites Revisited. *J. Metamorphic Geol.* **20**, 25-40.

BROWN, M. (2004): Melt extraction from lower continental crust. *Trans. Royal Soc. Edinburgh: Earth Sciences*, **95**, 35-48

BROWN, M. (2005): Invited comments on Clemens's 'Granites and granitic magmas'. *Proc. Geol. Assoc.* **116**, 9-16.

BROWN, M. (2006): Melt extraction from lower continental crust of orogens: the field evidence. *In* Evolution and Differentiation of the Continental Crust (M. Brown & T. Rushmer (eds). Cambridge University Press (331-383).

BROWN, M. (2007a): Metamorphic conditions in orogenic belts: A record of secular change. *Internat. Geol. Review*, **49**, 193-234.

BROWN, M. (2007b): Crustal melting and melt extraction, ascent and emplacement in orogens: Mechanisms and consequences. *J. Geol. Soc. London* **163**, 709-730.

BROWN, M. & DALLMEYER, R.D. (1996): Rapid Variscan exhumation and role of magma in core complex formation: Southern Brittany metamorphic belt, France. *J. Metamorphic Geol.* **14**, 361-379.

BROWN, M. & D'LEMOS, R.S. (1991): The Cadomian granites of Mancellia, north-east Armorican Massif of France: relationship to the St. Malo migmatite belt, petrogenesis and tectonic setting. *In* Precambrian Granitoids - Petrogenesis, Geochemistry and Metallogeny (I. Haapala & K.C. Condie, eds). *Precamb. Res.* **51**, 393-427.

BROWN, M. & MARCHILDON, N. (2003): The mechanism of melt extraction from lower crust. *Geophys. Res. Abstracts,* **5**, 01312

BROWN, M. & PRESSLEY, R.A. (1999): Crustal melting in nature: Prosecuting source processes. *Phys & Chem, Earth (A)* **24**, 3, 305-316.

BROWN, M. & RUSHMER, T. (1997): The role of deformation in the movement of granite melt: views from the laboratory and the field. *In* Deformation-enhanced Fluid Transport in the Earth's Crust and Mantle (M.B. Holness, ed). The Mineralogical Society Series: 8. Chapman and Hall, London (111-144).

BROWN, M. & RUSHMER, T. (2006): Evolution and Differentiation of the Continental Crust. Cambridge University Press, 553 pp.

BROWN, M. & SOLAR, G.S. (1998a): Shear zone systems and melts: Feedback relations and self-organization in orogenic belts. *J. Struct. Geol.* **20**, 211-227.

BROWN, M. & SOLAR, G.S. (1998b): Granite ascent and emplacement during contractional deformation in convergent orogens. *J. Struct. Geol.* **20**, 1,365-1,393.

BROWN, M. & SOLAR, G.S. (1999): The mechanism of ascent and emplacement of granite magma during transpression: a syntectonic granite paradigm. *Tectonophys.* **312**, 1-33.

BROWN, M., FRIEND, C.R.L., MCGREGOR, V.R. & PERKINS, W.T. (1981): The late-Archaean Qôrqut granite complex of southern West Greenland. *J. Geophys. Res.* **86**, 10,617-10,632.

BROWN, M., RUSHMER, T. & SAWYER, E.W. (1995a): Introduction to Special Section: Mechanisms and consequences of melt segregation from crustal protoliths. *J. Geophys. Res.* **100**, 15,551-15,563.

BROWN, M., AVERKIN, Y.A., MCLELLAN, E.L. & SAWYER, E.W. (1995b): Melt segregation in migmatites. *J. Geophys. Res.* **100**, 15,655-15,679.

BROWN, M.A., BROWN, M., CARLSON, W.D. & DENISON, C. (1999): Topology of syntectonic melt flow networks in the deep crust: inferences from three-dimensional images of leucosome geometry in migmatites. *Am. Mineral.* **84**, 1793-1818.

BURG, J.-P. & GERYA, T.V. (2005): The role of viscous heating in Barrovian metamorphism of collisional orogens: thermomechanical models and application to the Lepontine Dome in the Central Alps. *J. Metamorphic Geol.* **23**, 75-95.

BUROV, E., JAUPART, C. & GUILLOU-FROTTIER, L. (2003): Ascent and emplacement of buoyant magma bodies in brittle-ductile upper crust. *J. Geophys. Res. – Solid Earth*, **108**, 2177.

CHAPPELL, B.W. (1979): Granites as images of their source rocks. *Geol. Soc. Am., Abstr. with Prog.* **11**, 400.

CHAPPELL, B.W., WHITE, A.J.R., WILLIAMS, I.S. & WYBORN, D. (2004): Low- and high-temperature granites. *Trans. Royal Soc. Edinburgh: Earth Sci.* **95**, 125-140.

CHARDON, D., CHOUKROUNE, P. & JAYANANDA, M. (1998): Sinking of the Dharwar Basin (South India): implications for Archaean tectonics. *Precamb. Res.* **91**, 15-39.

CLARKE, G.L., WHITE, R.W., LIU, S., FITZHERBERT, J.A. & PEARSON, N.J. (2007): Contrasting behavior of rare earth and major elements during partial melting in granulite facies migmatites, Wuluma Hills, Arunta Block, central Australia. *J. Metamorphic Geol.* **25**, 1-18.

CLEMENS, J.D. (1990): The granulite - granite connexion. *In* Granulites and Crustal Evolution (D. Vielzeuf & Ph. Vidal, eds). Kluwer Academic Publishing, Dordrecht (25-36).

CLEMENS, J. D. (2003): S-type granitic magmas – petrogenetic issues, models and evidence. *Earth Sci. Rev.* **61**, 1-18.

CLEMENS, J.D. (2006): Melting of the continental crust: fluid regimes, melting reactions, and source-rock fertility. *In* Evolution and Differentiation of the Continental Crust (M. Brown & T. Rushmer, eds). Cambridge University Press (297-331).

CLEMENS, J.D. & MAWER, C.K. (1992): Granitic magma transport by fracture propagation. *Tectonophys.* **204**, 339-360.

CLEMENS, J.D. & PETFORD, N. (1999): Granitic melt viscosity and silicic magma dynamics in contrasting tectonic settings. *J. Geol. Soc.* **156**, 1057-1060.

CLEMENS, J.D., PETFORD, N. & MAWER, C.K. (1997): Ascent mechanisms of granitic magmas: causes and consequences. *In* Deformation-enhanced Fluid Transport in the Earth's Crust and Mantle (M.B. Holness, ed). *Mineral. Soc. Series, 8, London*, Chapman and Hall (145-172).

COLLINS, W.J. (1996): Lachlan Fold Belt granitoids: products of three-component mixing. *Trans. Royal Soc. Edinburgh: Earth Sci.* **87**, 171-81.

COLLINS, W.J. & SAWYER, E.W. (1996): Pervasive magma transfer through the lower-middle crust during non-coaxial compressional deformation: An alternative to diking. *J. Metamorphic Geol.* **14**, 565-579.

COLLINS, W.J., FLOOD, R.H., VERNON, R.H. & SHAW, S.E. (1989): The Wuluma granite, Arunta block, central Australia - an example of insitu, near isochemical granite formation in a granulite-facies terrane. *Lithos* **23**, 63-83.

COLLINS, W.J., VAN KRANENDONK, M.J. & TEYSSIER C. (1998): Partial convective overturn of Archaean crust in the east Pilbara Craton, Western Australia: driving mechanisms and tectonic implications. *J. Struct. Geol.* **20**, 1405-1424.

CONNOLLY, J.A.D. & PODLADCHIKOV, Y.Y. (1998): Compaction-driven fluid flow in viscoelastic rock. *Geodinamica Acta*, **11**, 55-84.

CONNOLLY, J.A.D. & PODLADCHIKOV, Y.Y. (2007): Decompaction weakening and channeling instability in ductile porous media: Implications for asthenospheric melt segregation. *J. Geophys. Res. – Solid Earth* **112**, Article Number: B10205.

CONNOLLY, J.A.D. & THOMPSON, A.B. (1989): Fluid and enthalpy production during regional metamorphism. *Contrib. Mineral. Petrol.* **102**, 346-366.

CONNOLLY, P. & COSGROVE, J. (1999): Prediction of fracture-induced permeability and fluid flow in the crust using experimental stress data. *AAPG Bull.* **83**, 757-777.

CRUDEN, A.R. (1998): On the emplacement of tabular granites. *J. Geol. Soc. London* **155**, 853-862.

CRUDEN, A.R. (2006): Emplacement and growth of plutons: implications for rates of melting and mass transfer in continental crust. *In* Evolution and Differentiation of the Continental Crust (M. Brown & T. Rushmer eds). Cambridge University Press (455-519).

CRUDEN, A.R. & MCCAFFREY, K.J.W. (2001): Growth of plutons by floor subsidence: Implications for rates of emplacement, intrusion spacing and melt-extraction mechanisms. *Phys. Chem. Earth, A* **26**, 303-315.

CRUDEN, A.R. & MCCAFFREY, K.J.W. (2002): Different scaling laws for sills, laccoliths and plutons: Mechanical thresholds on roof lifting and floor depression. *In* First International Workshop: Physical Geology of Subvolcanic Systems – Laccoliths, Sills and Dykes (LASI) (C. Breitkreuz, A. Mock & N. Petford, eds). *Wissenschaftliche Mitteilung Institute für Geologiei Technische Universität Bergakademie Freiberg*, **20/2002**, 15-17.

CURRIE C.A. & HYNDMAN, R.D. (2006): The thermal structure of subduction zone back arcs. *J. Geophys. Res.* **111**, B08404, doi:10.1029/2005JB004024.

DAHM, T. (2000): On the shape and velocity of fluid-filled fractures in the earth. *Geophys. J. Internat.* **142**, 181-192.

DAVIDSON, J.P. & ARCULUS, R.J. (2006): The significance of Phanerozoic arc magmatism in generating continental crust. *In* Evolution and Differentiation of the Continental Crust (M. Brown & T. Rushmer, eds). Cambridge University Press (135-172).

DAVIDSON, C., SCHMID, S.M. & HOLLISTER, L.S. (1994): Role of melt during deformation in the deep crust. *Terra Nova* **6**, 133-142.

DAVIDSON, J.P., HORA, J.M., GARRISON, J.M. & DUNGAN, M.A. (2005): Crustal forensics in arc magmas. *J. Volcan. Geotherm. Res.* **140**, 157-170.

DAVIDSON, J., TURNER, S., HANDLEY, H., MACPHERSON, C. & DOSSETO, A. (2007): Amphibole "sponge" in arc crust? *Geology* **35**, 787-790. DOI: 10.1130/G23637A.1

DEGELING, H., EGGINS, S. & ELLIS, D.J. (2001): Zr budgets for metamorphic reactions, and the formation of zircon from garnet breakdown. *Mineral. Mag.* **65**, 749-758.

DENIEL, C., VIDAL, P., FERNANDEZ, A., LEFORT, P. & PEUCAT, J.J. (1987): Isotopic study of the Manaslu Granite (Himalaya, Nepal) – inferences on the age and source of Himalayan leucogranites. *Contrib. Mineral. Petrol.* **96,** 78-92.

DEPINE, G.V., ANDRONICOS, C.L. & PHIPPS-MORGAN, J. (2008): Near isothermal conditions in the middle and lower crust induced by melt migration. *Nature* **452**, 80-83. doi: 10.1038/nature06689

D'LEMOS, R.S. & BROWN, M. (1993): Sm-Nd isotope characteristics of late Cadomian granite magmatism in northern France and the Channel Islands. *Geol. Mag.* **130**, 797-804.

D'LEMOS, R.S., BROWN, M. & STRACHAN, R.A. (1992): Granite magma generation, ascent and emplacement within a transpressional orogen. *J. Geol. Soc. London* **149**, 487-490.

DROOP, G.T.R., CLEMENS, J.D. & DALRYMPLE, D.J. (2003): Processes and conditions during contact anatexis, melt escape and restite formation: The Huntly Gabbro Complex, N.E. Scotland. *J. Petrol.* **44**, 995-1029.

DU BERNARD, X., EICHHUBL, P. & AYDIN, A. (2002): Dilation bands: A new form of localized failure in granular media. *Geophys. Res. Lett.* **29**, doi:10.1029/2002GL015966.

DUFEK, J. & BERGANTZ, G.W. (2005): Lower crustal magma genesis and preservation: a stochastic framework for the evaluation of basalt–crust interaction. *J. Petrol.* **46**, 2167-2195.

EICHHUBL, P. (2004). Growth of ductile opening-mode fractures in geomaterials. *In* The Initiation, Propagation, and Arrest of Joints and Other Fractures (J.W. Cosgrove & T. Engelder, eds). *Geol. Soc. London, Sp. Pub.* **231**, 11-24.

EICHHUBL, P. & AYDIN, A. (2003): Ductile opening-mode fracture by pore growth and coalescence during combustion alteration of siliceous mudstone. *J. Struct. Geol.* **25**, 121-134.

EICHHUBL, P., AYDIN, A. & LORE, J. (2001): Opening-mode fracture in siliceous mudstone at high homologous temperature – effective of surface forces. *Geophys. Res. Lett.* **28**, 1299-1302.

ELLIS, D.J. & OBATA, M. (1992): Migmatite and melt segregation at Cooma, New South Wales. *Trans. Royal Soc. Edinburgh: Earth Sci.* **83**, 95-106.

EMERMAN, S.H. & MARRETT, R. (1990): Why dikes? *Geology* **18**, 231-233.

FAURE, M., LIN, W., SHU, L.S., SUN, Y. & SCHARER, U. (1999): Tectonics of the Dabieshan (eastern China) and possible exhumation mechanism of ultra high-pressure rocks. *Terra Nova* **11**, 251-258.

FINGER, F. & CLEMENS, J.D. (1995): Migmatization and "secondary" granitic magmas: effects of emplacement of "primary" granitoids in Southern Bohemia, Austria. *Contrib. Mineral. Petrol.* **120**, 311-326.

FLORIAN, G., BUSSY, F., EPARD, J-L & BAUMGARTNER, L. (2008): Water-assisted migmatization of metagraywackes in a Variscan shear zone, Aiguilles-Rouges massif, western Alps. *Lithos* doi:10.1016/j.lithos.2007.07.024.

FODEN, J.D., ELBURG, M.A., TURNER, S.P., SANDIFORD, M.A., O'CALLAGHAN, J. & MITCHELL, S. (2002): Granite production in the Delamerian orogen, South Australia. *J. Geol. Soc. London* **159**, 557-575.

FRASER, G., ELLIS, D. & EGGINS, S. (1997): Zirconium abundance in granulite-facies minerals, with implications for zircon geochronology in high-grade rocks. *Geology* **25**, 607-610.

FRIEND, C.R.L., BROWN, M., PERKINS, W.T. & BURWELL, A.D.M. (1985): The geology of the Qôrqut granite complex north of Qôrqut, Godthåbsfjord, southern West Greenland. *Bulletin Grønlands Geologiske Undersøgelse*, **151**, 43p. plus 1:50,000 scale geological map of the Qôrqut area.

GABRIELOV, A., NEWMAN, W.I. & TURCOTTE, D.L. (1999): Exactly soluble hierarchical clustering model: Inverse cascades, self-similarity, and scaling. *Physical Rev. E*, **60**, 5293-5300.

GERYA, T.V., CONNOLLY, J.A.D. & YUEN, D.A. (2008): Why is terrestrial subduction one-sided? *Geology* **36**, 43-46.

GILLULY, J. (1948): Origin of granite. *Geol. Soc. Am.* **Memoir 28**, 139 pp..

GLAZNER, A.F., BARTLEY, J.M., COLEMAN, D.S., GRAY, W. & TAYLOR, R.Z. (2004): Are plutons assembled over millions of years by amalgamation from small magma chambers? *GSA Today* **14,** 4-11.

GREEN, H.W., II (1980): On the thermodynamics of nonhydrostatically stressed solids. *Philosoph. Mag.* **41**, 637-647.

GREENFIELD, J.E., CLARKE, G.L., BLAND, M. & CLARK, D.J. (1996): In-situ migmatite and hybrid diatexite at Mt Stafford, central Australia. *J. Metamorphic Geol.* **14**, 413-426.

GRUJIC, D. & MANCKTELOW, N.S. (1998): Melt-bearing shear zones: Analogue experiments and comparison with examples from southern Madagascar. *J. Struct. Geol.* **20**, 673-680.

GRUNDER, A.L. (1995): Material and thermal roles of basalt in crustal magmatism: Case study from eastern Nevada. *Geology* **23**, 952-956.

GUERNINA, S. & SAWYER, E.W. (2003): Large-scale melt-depletion in granulite terranes: An example from the Archean Ashuanipi Subprovince of

Quebec. *J. Metamorphic Geol.* **21**, 181-201.

HAND, M. & DIRKS, P.H.G.M. (1992): The influence of deformation on the formation of axial-planar leucosomes and the segregation of small melt bodies within the migmatitic Napperby Gneiss, central Australia. *J. Struct. Geol.* **14**, 591-604.

HANDY, M.R., MULCH, A., ROSENAU, N. & ROSENBERG, C.L. (2001): The role of fault zones and melts as agents of weakening, hardening and differentiation of the continental crust: a synthesis. *In* The nature and tectonic significance of fault zone weakening (R.E. Holdsworth, J. Magloughlin, R.J. Knipe, R.A. Strachan & R.C. Searle, eds). *Geol. Soc. Spec. Pub.* **186**, 305-332.

HARRISON, T.M., GROVE, M., LOVERA, O.M. & CATLOS, E.J. (1998): A model for the origin of Himalayan anatexis and inverted metamorphism. *J. Geophys. Res. - Solid Earth*, **103**: 27017-27032.

HARTZ, E.H. & PODLADCHIKOV, Y.Y. (2008): Toasting the jelly sandwich: The effect of shear heating on lithospheric geotherms and strength. *Geology* **36**, 331-334.

HASALOVÁ, P., SCHULMANN, K., LEXA, O., ŠTÍPSLÁ, P., HROUDA, F., ULRICH, S., HALODA, J. & TYCOVA, P. (2008a): Origin of migmatites by deformation enhanced melt infiltration of orthogneiss: a new model based on quantitative microstructural analysis. *J. Metamorphic Geol.* **25**, 29-53.

HASALOVÁ, P., ŠTÍPSLÁ, P, POWELL, R., SCHULMANN, K., JANOUŠEK, V. & LEXA, O. (2008b): Transforming mylonitic metagranite by open-system interactions during melt flow. *J. Metamorphic Geol.* **25**: 55-80.

HAWKESWORTH, C.J. & KEMP, A.I.S. (2006): Evolution of the continental crust. *Nature* **443** (7113), 811-817.

HEALY, B., COLLINS, W.J. & RICHARDS, S.W. (2004): A hybrid origin for Lachlan S-type granites: the Murrumbidgee Batholith example. *Lithos* **78**, 197-216.

HERMANN, J.& SPANDLER, C.J. (2008): Sediment melts at sub-arc depths: an experimental study. *J. Petrol.* **49**, 717-740.

HINCHEY, A.M. & CARR, S.D. (2006): The S-type Ladybird leucogranite suite of southeastern British Columbia: Geochemical and isotopic evidence for a genetic link with migmatite formation in the North American basement gneisses of the Monashee complex. *Lithos* **90**, 223-248.

HOBBS, B., REGENAUER-LIEB, K. & ORD, A. (2007): Thermodynamics of folding in the middle to lower crust. *Geology* **35**, 175-178.

HOGAN, J.P. & SINHA, A.K. (1991): The effect of accessory minerals on the redistribution of lead isotopes during crustal anatexis: a model. *Geochim. Cosmochim. Acta* **55**, 335-348.

HOLLISTER, L.S. & CRAWFORD, M.L. (1986): Melt-enhanced deformation: A major tectonic process. *Geology* **14**, 558-561.

HOLNESS, M.B. (2008): Decoding migmatite microstructures. *In* Working with Migmatites (E.W. Sawyer & M. Brown, eds.). *Mineral. Assoc. Canada, Short Course* **38**, x-x+22.

HUPPERT, H.E. & SPARKS, R.S.J. (1988): The generation of granitic magmas by intrusion of basalt into continental crust. *J. Petrol.* **29**, 599-624.

HYNDMAN, R. D., CURRIE, C. A. & MAZZOTTI, S. P. (2005): Subduction zone backarcs, mobile belts, and orogenic heat. *GSA Today* **15**, 4-10.

ITO, G. & MARTEL, S.J. (2002): Focusing of magma in the upper mantle through dike interaction. *J. Geophys. Res.* **107**, B10, 2223, doi:10.1029/2001JB000251

JACKSON, M.P.A. & VENDEVILLE, B.C. (1994): Regional extension as a geologic trigger for diapirism. *Geol. Soc. Am. Bull.* **106**, 57-73.

JACKSON, M.D., CHEADLE, M.J. & ATHERTON, M.P. (2003): Quantitative modeling of granitic melt generation and segregation in the continental crust. *J. Geophys. Res. - Solid Earth*, **108**, Art. No. 2332.

JAMIESON, R.A., BEAUMONT, C., FULLSACK, P. & LEE, B. (1998): Barrovian regional metamorphism: Where's the heat? *In* What Drives Metamorphism and Metamorphic Reactions? (P.J. Trealor & P.J. O'Brien, eds). *Geol. Soc. London, Spec. Pub.* 23-45.

JAMIESON, R. A., BEAUMONT, C., MEDVEDEV, S. & NGUYEN, M. H. (2004): Crustal channel flows: Numerical models with implications for metamorphism in the Himalayan-Tibetan orogen. *J. Geophys. Res.* **109**: B06407, doi:10.1029/2003JB002811.

JOHANNES, W., EHLERS, C., KRIEGSMAN, L.A. & MENGEL, K. (2003): The link between migmatites

and S-type granites in the Turku area, southern Finland. *Lithos* **68**, 69-90.

JOHNSON, T.E., HUDSON, N.F.C. & DROOP, G.T.R. (2001a): Partial melting in the Inzie Head gneisses: the role of water and a petrogenetic grid in KFMASH applicable to anatectic pelitic migmatites. *J. Metamorphic Geol.* **19**, 99-118.

JOHNSON, T.E., HUDSON, N.F.C., DROOP, G.T.R. (2001b): Melt segregation structures within the Inzie Head gneisses of the northeastern Dalradian. *Scot. J. Geol.* **37**, 59-72.

JOHNSON, T.E., HUDSON, N.F.C. & DROOP, G.T.R. (2003): Evidence for a genetic granite-migmatite link in the Dalradian of NE Scotland. *J. Geol. Soc.* **160**, 447-457.

JOHNSON, T., BROWN, M., GIBSON, R. & WING, B. (2004): Spinel-cordierite symplectites replacing andalusite: Evidence for melt-assisted diapirism in the Bushveld Complex, South Africa. *J. Metamorphic Geol.* **22**, 529-545; doi:10.1111/ j.1525-1314.2004.00531.x.

JONES, K.A. & BROWN, M. (1990): High temperature 'clockwise' P-T paths and melting in the development of regional migmatites: an example from southern Brittany, France. *J. Metamorphic Geol.* **8**, 551-578.

KALSBEEK F, JEPSEN H.F. & NUTMAN, A.P. (2001): From source migmatites to plutons: tracking the origin of ca.435 Ma S-type granites in the East Greenland Caledonian orogen. *Lithos* **57**, 1-21.

KAMB, W.B. (1961): The thermodynamic theory of nonhydrostatically stressed solids. *J. Geophys. Res.* **66**, 259-271.

KEAY, S., COLLINS, W. J. & MCCULLOCH, M.T. (1997): A three-component Sr-Nd isotopic mixing model for granitoid genesis, Lachlan fold belt, eastern Australia. *Geology* **25**, 307-310.

KEMP, A.I.S. (2003): Plutonic boninite-like rocks in an anatectic setting: Tectonic implications for the Dalamerian orogen in southeastern Australia. *Geology* **31**, 371-374.

KEMP, A.I.S. (2004): Petrology of high-Mg, low-Ti igneous rocks of the Glenelg River Complex (SE Australia) and the nature of their interaction with crustal melts. *Lithos* **78**, 119-156.

KEMP, A.I.S., HAWKESWORTH, C.J., PATERSON, B.A. & KINNY, P.D. (2006): Episodic growth of the Gondwana supercontinent from hafnium and oxygen isotopes in zircon. *Nature* **439/2**, doi:10.1038/nature04505.

KEMP, A.I.S., HAWKESWORTH, C.J., FOSTER, G.L., PATERSON, B.A., WOODHEAD, J.D., HERGT, J.M., GRAY, C.M. & WHITEHOUSE, M.J. (2007a): Magmatic and crustal differentiation history of granitic rocks from Hf-O isotopes in zircon. *Science* **315**, 980-983.

KEMP, A.I.S., SHIMURA, T., HAWKESWORTH, C. J. & EIMF (2007b): Linking granulites, silicic magmatism, and crustal growth in arcs: Ion microprobe (zircon) U-Pb ages from the Hidaka metamorphic belt, Japan. *Geology* **35**, 807–810. DOI: 10.1130/G23586A.1

KINCAID, C. & SILVER, P. (1996): The role of viscous dissipation in the orogenic process. *Earth Planet. Sci. Lett.***142**, 271-288.

KORHONEN, F. BROWN, M. & SIDDOWAY, C.S. (2007): Petrologic and geochronological constraints on the polymetamorphic evolution of the Fosdick migmatite dome, Marie Byrd Land, West Antarctica. U.S. Geological Survey and the National Academies; USGS of-2007-1047, Extended Abstract 049.

KRETZ, R. (1983): Symbols for rock-forming minerals. *Am. Mineral.* **68**, 277-279.

KRUHL, J.H. (1994): The formation of extensional veins: an application of the cantor-dust model. *In* Fractals and dynamic systems in geoscience (J.H. Kruhl, ed.). Springer Verlag, Berlin (95-104).

LABROUSSE, L., JOLIVET, L., AGARD, P., HÉBERT, R. & ANDERSEN, T.B. (2002): Crustal-scale boudinage and migmatization of gneiss during their exhumation in the UHP province of Western Norway. *Terra Nova* **14**, 263–270.

LAFRANCE, B., CLARKE, G.L., COLLINS, W.J. & WILLIAMS, I.S. (1995): The emplacement of the Wuluma granite–melt generation and migration along steeply dipping extensional fractures at the close of the Late Strangeways Orogenic Event, Arunta Block, Central Australia. *Precamb. Res.* **72**, 43-67.

LANG, H.M. & GILOTTI, J.A. (2007): Partial melting of metapelites at ultrahigh-pressure conditions, Greenland Caledonides. *J. Metamorphic Geol.* **25**, 129–147 doi:10.1111/j.1525-1314.2006. 00687.x

LAPORTE, D., RAPAILLE, C. & PROVOST, A. (1997): Wetting angles, equilibrium melt geometry, and the permeability threshold of partially molten crustal protoliths. *In* Granite: From segregation of melt to emplacement fabrics (J.L. Bouchez,

D.H.W. Hutton & W.E. Stephens, eds.). Kluwer Academic Publishers, The Netherlands (31-54).

LEAKE B.E. (2006): Mechanism of emplacement and crystallization of the northern margin and center of the Galway granite, western Ireland. *Trans. Royal Soc. Edinburgh: Earth Sci.* **97**, 1-23.

LEITCH, A.M. & WEINBERG, R.F. (2002): Modelling granite migration by mesoscale pervasive flow. *Earth Planet. Sci. Lett.***200**, 131-146.

LELOUP, P.H. & KIENAST, J.R. (1993): High-temperature metamorphism in a major strike-slip shear zone - The Ailao Shan – Red River, Peoples Republic of China. *Earth Planet. Sci. Lett.***118,** 213-234.

LOOSVELD, R.J.H. & ETHERIDGE, M.A. (1990): A model for low-pressure facies metamorphism during crustal thickening. *J. Metamorphic Geol.* **8**, 257-267.

MAALØE, S. (1992): Melting and diffusion processes in closed-system migmatization. *J. Metamorphic Geol.* **10**, 503-516.

MAHAN, K.H., BARTLEY, J.M., COLEMAN, D.S., GLAZNER, A.F. & CARL, B.S. (2003): Sheeted intrusion of the synkinematic McDoogle pluton, Sierra Nevada, California. *Geol. Soc. Am. Bull.* **115**, 1570-1582.

MARCHILDON, N. & BROWN, M. (2001): Melt segregation in late syn-tectonic anatectic migmatites: an example from the Onawa Contact Aureole, Maine, U.S.A. *Phys & Chem, Earth (A)* **26**, 225-229.

MARCHILDON, N. & BROWN, M. (2002): Grain-scale melt distribution in two contact aureole rocks: Implication for controls on melt localization and deformation. *J. Metamorphic Geol.* **20**, 381-396.

MARCHILDON, N. & BROWN, M. (2003): Spatial distribution of melt-bearing structures in anatectic rocks from Southern Brittany: implications for melt-transfer at grain- to orogen-scale. *Tectonophys.* **364**, 215-235.

MATZEL, J., MUNDIL, R., PATERSON, S., RENNE, P. & NOMADE, S. (2005): Evaluating pluton growth models using high resolution geochronology: Tuolumne intrusive suite, Sierra Nevada, CA. *Geol. Soc. Am., Abstr. with Prog.* **37**, 6, 131.

MATZEL, J.E.P., BOWRING, S.A. & MILLER, R.B. (2006): Time scales of pluton construction at differing crustal levels: Examples from the Mount Stuart and Tenpeak intrusions, North Cascades, Washington. *Geol. Soc. Am. Bull.* **118**, 1412-1430.

MCCAFFREY, K.J.W. & CRUDEN, A. (2002): Dimensional data and growth models for intrusions. *In* First International Workshop: Physical Geology of Subvolcanic Systems - Laccoliths, Sills and Dykes (LASI (C. Breitkreuz, A. Mock & N. Petford, eds). Wissenschaftliche Mitteilung Instute für Geologie Technische Universität Bergakademie Freiberg, 20/2002, 37-39.

MCCAFFREY, K.J.W. & CRUDEN, A. (2003): Dimensional data and growth models for intrusions. *Geophys. Res. Abstr.* **5**, 09697.

MCCAFFREY, K.J.W. & PETFORD, N. (1997): Are granitic intrusions scale invariant? *J. Geol. Soc. London* **154**, 1-4.

MCKENZIE, D. & PRIESTLEY, K. (2008): The influence of lithospheric thickness variations on continental evolution. *Lithos* doi:10.1016/j.lithos.2007.05.005

MCLAREN, S., SANDIFORD, M, POWELL, R., NEUMANN, N. & WOODHEAD, J. (2006): Palaeozoic intraplate crustal anatexis in the Mount Painter province, South Australia: timing, thermal budgets and the role of crustal heat production. *J. Petrol.* **47**, 2281-2302.

MCLELLAN, E.L. (1988): Migmatite structures in the Central Gneiss Complex, Boca de Quadra, Alaska. *J. Metamorphic Geol.* **6**, 517-542.

MEHNERT, K.R. (1968): Migmatites and the Origin of Granitic Rocks. Amsterdam: Elsevier.

MILLER, C.F., MCDOWELL, S.M. & MAPES, R.W. (2003): Hot and cold granites? Implications of zircon saturation temperatures and preservation of inheritance. *Geology* **31**, 529-532.

MILLER, R.B. & PATTERSON, S.R. (1999): In defense of magmatic diapirs. *J. Struct. Geol.* **21**, 1161-1173.

MILORD, I. & SAWYER, E.W. (2003): Schlieren formation in diatexite migmatite: examples from the St Malo migmatite terrane, France. *J. Metamorphic Geol.* **21**, 347-362.

MILORD, I., SAWYER, E.W. & BROWN, M. (2001): Formation of diatexite migmatite and granite magma during anatexis of semi-pelitic metasedimentary rocks: an example from St Malo, France. *J. Petrol.* **42**, 487-505.

MOGK, D.W. (1990): A model for the granulite-migmatite association in the Archean basement of southwestern Montana. *In* Granulites and Crustal

Evolution (D. Vielzeuf & P. Vidal, eds). Kluwer, Amsterdam (133-155).

MOLLEMA, P.N. & ANTONELLINI, M.A. (1996): Compaction bands; a structural analog for anti-mode I cracks in Aeolian sandstone. *Tectonophys.* **267**, 209-228.

NABELEK, P.I. & BARTLETT, C.D. (1998): Petrologic and geochemical links between the post-collisional Proterozoic Harney Peak leucogranite, South Dakota, USA, and its source rocks. *Lithos* **45**, 71-85.

NABELEK, P.I, RUSS-NABELEK, C. & DENISON, J.R. (1992): The generation and crystallization conditions of the Proterozoic Harney Peak leucogranite, Black Hills, South Dakota, USA – Petrologic and geochemical constraints. *Contrib. Mineral. Petrol.* **110**, 173-191.

NEMCHIN, A. & BODORKOS, S. (2000): Zr and LREE concentrations in anatectic melt as a function of crystal size distributions of zircon and monazite in the source region. *Geol. Soc. Am., Prog. & Abstr*. **32**, 398.

NICOLAS, A. & POLIAKOV, A. (2001): Melt migration and mechanical state in the lower crust of oceanic ridges. *Terra Nova* **13**, 64-69.

OLIVER, N.H.S. & BARR, T.D. (1997): The geometry and evolution of magma pathways through migmatites of the Halls Creek Orogen, Western Australia. *Mineral. Mag.* **61**, 3-14.

OLSEN, S.N., MARSH, B.D.& BAUMGARTNER, L.P. (2004): Modelling mid-crustal migmatite terrains as feeder zones for granite plutons: the competing dynamics of melt transfer by bulk *versus* porous flow. *Trans. Royal Soc. Edinburgh: Earth Sci.* **95**, 49-58.

OSANAI, Y., KOMATSU, M. & OWADA, M. (1991): Metamorphism and granite genesis in the Hidaka Metamorphic Belt, Hokkaido, Japan. *J. Metamorphic Geol.* **9**, 111-124.

OSANAI, Y., OWADA, M. & KAWASAKI, T. (1992): Tertiary deep crustal ultrametamorphism in the Hidaka Metamorphic Belt, northern Japan. *J. Metamorphic Geol.* **10**, 401-414.

PATCHETT, P.J. (1980): Thermal effects of basalt on continental crust and crustal contamination. *Nature* **283**, 559-561.

PATIÑO-DOUCE, A.E. (1995): Experimental generation of hybrid silicic melts by reaction of high-Al basalt with metamorphic rocks. *J. Geophys. Res.* **B100**, 15623-15639.

PATIÑO-DOUCE, A.E. (1999): What do experiments tell us about the relative contributions of crust and mantle to the origin of granitic magmas? *In* Understanding Granites; Integrating New and Classical Techniques (A. Castro, C. Fernández & J.-L. Vigneresse, eds). *Geol. Soc. London, Spec. Publ.* **168**, 55-75.

PATTERSON, M.S. (1973): Nonhydrostatic thermodynamics and its geologic applications. *Rev. Geophys. & Space Phys.* **11**, 355-389.

PATTERSON, S.R. & FOWLER, K., JR. (1993): Reexamining pluton emplacement processes. *J. Struct. Geol*. **15**, 191-206.

PATTISON, D.R.M. & HARTE, B. (1988): Evolution of structurally contrasting migmatites in the 3-kbar Ballachulish aureole, Scotland. *J. Metamorphic Geol.* **6**, 475-494.

PATTISON, D.R.M. & TRACY, R.J. (1991): Phase equilibria and thermobarometry of metapelites. *In* Contact Metamorphism (D.M. Kerrick, ed). *Rev. in Mineral.* **26**, Mineralogical Society of America, Washington, DC, (105-206).

PATTISON, D.R.M., CHACKO, T., FARQUHAR, J. & MCFARLANE, C.R.M. (2003): Temperatures of granulite-facies metamorphism: Constraints from experimental phase equilibria and thermo-barometry corrected for retrograde exchange. *J. Petrol.* **44**, 867-900.

PERESSINI, G., QUICK, J.E., SINIGOI, S., HOFMANN, A.W.& FANNING, M. (2007): Duration of a large mafic intrusion and heat transfer in the lower crust: a SHRIMP U-Pb zircon study in the Ivrea–Verbano Zone (Western Alps, Italy). *J. Petrol.* **48**, 1185-1218.

PESCHLER, A.P., BENN, K. & ROEST, W.R. (2004): Insights on Archean continental geodynamics from gravity modelling of granite-greenstone terranes. *J. Geodynamics,* **38**, 185-207.

PETFORD, N., CRUDEN, A.R., MCCAFFREY, K.J.W. & VIGNERESSE, J.L. (2000): Granite magma formation, transport and emplacement in the Earth's crust. *Nature* **408**, 669-673.

PODLADCHIKOV, YU.YU. & CONNOLLY, J.A.D. (2001): The transition from pervasive to segregated melt flow in ductile rock. *EUG X1*, *J. Conference Abstracts*, 813.

POWELL, R. (1983): Processes in granulite-facies metamorphism. *In* Migmatites, Melting and Metamorphism (M.P. Atherton & C.D. Gribble, eds). Shiva, Nantwich (127-139).

POWELL, R. & DOWNES, J. (1990): Garnet porphyroblast-bearing leucosomes in metapelites: Mechanisms, phase diagrams and an example from Broken Hill. *In* High temperature metamorphism and crustal anatexis (J.R. Ashworth & M. Brown, eds). Unwin Hyman, London (105-123).

POWER, G.M. (1993): Geochemical differences between the Cadomian granites of Mancellia and the St. Malo migmatites, Armorican Massif, France. *J. Geol. Soc.* **150**, 465-468.

PRESSLEY, R.A. & BROWN, M. (1999): The Phillips Pluton, Maine, USA: Evidence of heterogeneous crustal sources, and implications for granite ascent and emplacement mechanisms in convergent orogens. *Lithos* **46**, 335-366.

PYLE, J.M. & SPEAR, F.S. (1999): Yttrium zoning in garnet; coupling of major and accessory phases during metamorphic reactions. *Geol. Materials Res.* **1**, 49 pp.

PYLE, J.M., SPEAR, F.S., RUDNICK, R.L. & MCDONOUGH, W.F. (2001): Monazite-xenotime-garnet equilibrium in metapelites and the new monazite-garnet thermometer. *J. Petrol.* **42**, 2083-2107.

READ, H.H. (1957): The Granite Controversy. Thomas Murby & Co., London, 430 pp.

REGENAUER-LIEB, K. (1999): Dilatant plasticity applied to Alpine collision: Ductile void growth in the intraplate area beneath the Eifel volcanic field. *J. Geodynamics* **27**, 1-21.

REID, M.R. (1990): Ionprobe investigation of rare Earth element distributions and partial melting of metasedimentary granulite. *In* Granulites and crustal evolution (D. Vielzeuf & P. Vidal, eds). *NATO ASI Series. Series C: Math. & Phys. Sci.* **311**, 507-522.

RICHARDS, S.W. & COLLINS, W.J. (2002): The Cooma Metamorphic Complex, a low-P high-T (LPHT) regional aureole beneath the Murrumbidgee Batholith. *J. Metamorphic Geol.* **20**, 119-134.

RICHARDSON, C.N., LISTER, J.R. & MCKENZIE, D. (1996): Melt conduits in a viscous porous matrix. *J. Geophys. Res.* **101**, 20,423-20,432.

ROBIN, P.Y. (1974): Thermodynamic equilibrium across a coherent interface in a stressed crystal. *Am. Mineral.* **59**, 1286-1298.

ROSENBERG, C.L. (2001): Deformation of partially molten granite: a review and comparison of experimental and natural case studies. *Internat. J. Earth Sci. (Geol. Rundschau)* **90**, 60-76.

ROSENBERG, C.L. & HANDY, M.R. (2005): Experimental deformation of partially melted granite revisited: Implications for the continental crust. *J. Metamorphic Geol.* **23**, 19-28.

ROSENBERG, C.L. & RILLER, U. (2000): Partial-melt topology in statically and dynamically recrystallized granite. *Geology* **28**, 7-10.

RUBIN, A.M. (1993): Dikes vs. diapirs in visco-elastic rock. *Earth Planet. Sci. Lett.***117**, 653-670.

RUBIN, A.M. (1995): Propagation of magma-filled cracks. *Ann. Rev. Earth Planet. Sci.* **23**, 287-336.

RUBIN, A.M. (1998): Dike ascent in partially molten rock. *J. Geophys. Res.* **103**, 20,901-20,919.

RUSHMER, T. (2001): Volume change during partial melting reactions: implications for melt extraction, melt geochemistry and crustal rheology. *Tectonophys.* **342**, 389-405.

RUTTER, E.H. (1997): The influence of deformation on the extraction of crustal melts: A consideration of the role of melt-assisted granular flow. *In* Deformation-enhanced fluid transport in the Earth's crust and mantle (M.B. Holness, ed). Chapman & Hall, London (82-110.)

RUTTER, E.H. & MECKLENBURG, J. (2006): The extraction of melt from crustal protoliths and the flow behavior of partially molten crustal rocks: an experimental perspective. *In* Evolution and Differentiation of the Continental Crust (M. Brown & T. Rushmer, eds). Cambridge University Press (384-429).

RYBACKI, E., WIRTH, R. & DRESEN, G. (2008): High-strain creep of feldspar rocks: Implications for cavitation and ductile failure in the lower crust. *Geophys. Res. Lett.* **35**, L04304, doi:10.1029/2007GL032478.

SAITO, S., KORHONEN, F., BROWN, M. & SIDDOWAY, C.S. (2007): Petrogenesis of granites in the Fosdick migmatite dome, Marie Byrd Land, West Antarctica. U.S. Geological Survey and The National Academies, USGS OF-2007-1047, Extended Abstract 105.

SANDIFORD, M. & MCLAREN, S. (2002): Tectonic feedback and the ordering of heat producing elements within the continental lithosphere. *Earth Planet. Sci. Lett.***204**, 133-150.

SANDIFORD, M. & POWELL, R. (1991): Some remarks on high-temperature–low-pressure metamorphism in convergent orogens. *J.*

Metamorphic Geol. **9**, 333-340.

SANDIFORD, M., VAN KRANENDONK, M.J. & BODORKOS, S. (2004): Conductive incubation and the origin of dome-and-keel structure in Archean granite-greenstone terrains: A model based on the eastern Pilbara Craton, Western Australia. *Tectonics* **23**, Art. No. TC1009.

SAWYER, E.W. (1987): The role of partial melting and fractional crystallization in determining discordant migmatite leucosome compositions. *J. Petrol.* **28**, 445-473.

SAWYER, E.W. (1991): Disequilibrium melting and the rate of melt-residuum separation during migmatization of mafic rocks from the Grenville front, Quebec. *J. Petrol.* **32**, 701-738.

SAWYER, E.W. (1994): Melt segregation in the continental crust. *Geology* **22**, 1019-1022.

SAWYER, E.W. (1996): Melt segregation and magma flow in migmatites: implications for the generation of granite magmas. *Trans. Royal Soc. Edinburgh: Earth Sci.* **87**, 85-94.

SAWYER, E.W. (1998): Formation and evolution of granite magmas during crustal reworking: the significance of diatexites. *J. Petrol.* **39**, 1147-1167.

SAWYER, E.W. (1999): Criteria for the recognition of partial melting. *Phys. Chem. Earth, (A)*, **24**, 269-279.

SAWYER, E.W. (2000): Melt distribution and movement in anatectic rocks. *Geophys. Res. Abstr.* **2**.

SAWYER, E.W. (2001): Melt segregation in the continental crust: Distribution and movement of melt in anatectic rocks. *J. Metamorphic Geol.* **18**, 291-309.

SAWYER, E.W. (2008): Working with migmatites: Nomenclature for the constituent parts. *In* Working with Migmatites (E.W. Sawyer & M. Brown, eds.). *Mineral. Assoc. Canada, Short Course* **38**, 1-28.

SAWYER, E.W. & BONNAY, M. (2003): Melt segregation and magma movement in the crust. *Geophys. Res. Abstr.* **5**, 02458.

SAWYER, E.W., DOMBROWSKI, C. & COLLINS, W.J. (1999): Movement of melt during synchronous regional deformation and granulite-facies anatexis, an example from the Wuluma Hills, central Australia. *In* Understanding granites: integrating new and classical techniques (A. Castro, C. Fernandez & J.-C. Vigneresse, eds). *Geol. Soc., Spec. Pub.* **168**, 221-237.

SCHILLING, F.R. & PARTZSCH, G.N. (2001): Quantifying partial melt fraction in the crust beneath the central Andes and the Tibetan Plateau. *Phys. Chem. Earth, A,* **26**, 239-246.

SCHULMANN, K., LEXA, O., ŠTÍPSKÁ, P., RACEK, M., TAJČMANOVÁ, L., KONOPÁSEK, J., EDEL, J.-B., PESCHLER, A., & LEHMANN, J. (2008). Vertical extrusion and horizontal channel flow of orogenic lower crust: key exhumation mechanisms in large hot orogens? *J. Metamorphic Geol.* **26**, 000-000. doi:10.1111/j.1525-1314.2007.00755.x.

SECOR, D.T. & POLLARD, D.D. (1975): On the stability of open hydraulic fractures in the Earth's crust. *Geophys. Res. Lett.* **2**, 510-513.

SEDERHOLM, J.J. (1967): SELECTED WORKS: GRANITES AND MIGMATITES. Oliver and Boyd, Edinburgh.

SELBEKK, R.S. SKJERLIE, K.P. & PEDERSEN, R.B. (2000): Generation of anorthositic magma by H2O-fluxed anatexis of silica-undersaturated gabbro: an example from the north Norwegian Caledonides. *Geol. Mag.* **137**, 609-621.

SHAW, H.R. & CHOUET, B.A. (1991): Fractal hierarchies of magma transport in Hawaii and critical self-organization of tremor. *J. Geophys. Res.* **96**, 10,191-10,207.

SHIMURA, T., KOMATSU, M. & IIYAMA, J.T. (1992): Genesis of the lower crustal garnet orthopyroxene tonalites (S-type) of the Hidaka Metamorphic belt, northern Japan. *Trans. Royal Society Edinburgh – Earth Sci.* **83**, 259-268.

SHIMURA, T., OWADA, M., OSANAI, Y., KOMATSU, M. & KAGAMI, H. (2004): Variety and genesis of the pyroxene-bearing S- and I-type granitoids from the Hidaka Metamorphic Belt, Hokkaido, northern Japan. *Transactions of the Royal Society of Edinburgh–Earth Sciences*, **95**, 161-179.

SIMAKIN, A. & TALBOT, C. (2001): Transfer of melt between microscopic pores and macroscopic veins in migmatites. *Phys. Chem. Earth, A* **26**, 363-367.

SLAGSTAD, T. JAMIESON, R.A. & CULSHAW, N.G. (2005): Formation, crystallization, and migration of melt in the mid-orogenic crust: Muskoka domain migmatites, Grenville Province, Ontario. *J. Petrol.* **46**, 893-919.

SLEEP, N.H. (1988): Tapping of melt by veins and dikes. *J. Geophys. Res.* **93**, 10,255-10,272.

SOESOO, A., KALDA, J., BONS, P., URTSON, K. & KALM, V. (2004): Fractality in geology: a possible use of fractals in the studies of partial melting processes. *Proc. Estonian Acad. Sci., Geology*, **53**, 13-27.

SOLAR, G.S. & BROWN, M. (2001a): Petrogenesis of Migmatites in Maine, USA: Possible Source of Peraluminous Leucogranite in Plutons. *J. Petrol.* **42**, 789-823.

SOLAR, G.S. & BROWN, M. (2001b): Deformation partitioning during transpression in response to Early Devonian oblique convergence, Northern Appalachian orogen, USA. *J. Struct. Geol.* **23**, 1043-1065.

SOLAR, G.S., PRESSLEY, R.A., BROWN, M. & TUCKER, R.D. (1998): Granite ascent in convergent orogenic belts: testing a model. *Geology* **26**, 711-714.

SPENCE, D.A., SHARP, P. & TURCOTTE, D.L. (1987): Buoyancy-driven crack propagation: A mechanism for magma migration. *J. Fluid Mechanics* **17** 135-153.

STALFORS, T. & EHLERS, C. (2006): Emplacement mechanisms of late-orogenic granites: structural and geochemical evidence from southern Finland. *Internat. J. Earth Sci.* **95**, 557-568.

STEVENS, G. VILLAROS, A. & MOYEN, J.F. (2007): Selective peritectic garnet entrainment as the origin of geochemical diversity in S-type granites. *Geology* **35**, 9-12.

STÜWE, K. (1998): Heat sources of Cretaceous metamorphism in the Eastern Alps - a discussion. *Tectonophys.* **287,** 251-269.

STÜWE, K. (2007): *Geodynamics Of The Lithosphere.* Springer, 504 pp.

SYMMES, G.H. & FERRY, J.M. (1995): Metamorphism, fluid-flow and partial melting in pelitic rocks from the Onawa contact aureole, Central Maine, USA. *J. Petrol.* **36**, 587-612.

TAKADA, A. (1990): Experimental study on propagation of liquid-filled crack in gelatin: shape and velocity in hydrostatic stress conditions. *J. Geophys. Res.* **95**, 8471-8481.

TANNER, D.C. (1999): The scale-invariant nature of migmatites from the Oberpfalz, NE Bavaria and its significance for melt transport. *Tectonophys.* **302**, 297-305.

TEYSSIER, C. & WHITNEY, D.L. (2002): Gneiss domes and orogeny. *Geology* **30**, 1139-1142.

THOMPSON, A.B. (1999): Some time–space relationships for crustal melting and granitic intrusion at various depths. *In* Understanding Granites: Integrating New and Classical Techniques (A. Castro, C. Fernãndez & J.L. Vigneresse, eds). *Geol. Soc. Spec. Pub.* **168**, 7-25.

TOMASCAK, P.B., BROWN, M., SOLAR, G.S., BECKER, H.J., CENTORBI, T.L. & TIAN, J. (2005): Source contributions to Devonian granite magmatism near the Laurentian Border, New Hampshire and Western Maine, USA. *Lithos* **80,** 75-99.

TRACY, R. J. & ROBINSON, P. (1983): Acadian migmatite types in pelitic rocks of central Massachusetts. *In* Migmatites, Melting and Metamorphism (M.P. Atherton & C.D. Gribble, eds). Shiva, Nantwich. (163-173).

TURCOTTE, D.L. (1999): Self-organized criticality. *Reports on Progress in Physics* **62**, 1377-1429.

TURCOTTE, D.L. (2001): Self-organized criticality: Does it have anything to do with criticality and is it useful? *Nonlinear Processes in Geophysics*, **8,** 193-196.

TURCOTTE, D.L., MALAMUD, B.D., MOREIN, G. & NEWMAN, W.I. (1999): An inverse-cascade model for self-organized critical behavior. *Physica A*, **268**, 629-643.

TURCOTTE, D.L., MALAMUD, B.D., GUZZETTI, F. & REICHENBACH, P. (2002): Self-organization, the cascade model, and natural hazards. *Proc. National Acad. Sci.* **99**, 2530-2537.

UKEN, R. & WATKEYS, M. K. (1997): Diapirism initiated by the Bushveld Complex, South Africa. *Geology* **25**, 723-726.

UNGER, J.D., LIBERTY, L.M., PHILLIPS, J.D., WRIGHT, B.E. (1989): Creating a 3-dimensional transect of the earth's crust from craton to ocean basin across the N. Appalachian Orogen. *In* 3-Dimensional Applications in Geographical Information Systems (J. Raper, ed). Taylor and Francis, London, (137-148).

URTSON, K. & SOESOO, A. (2007): An analogue model of melt segregation and accumulation processes in the Earth's crust. *Estonian J. Earth Sci.* **56**, 3-10.

VAN DER MOLEN, I. (1985a): Interlayer material transport during layer-normal shortening, I, the model. *Tectonophys.* **115**, 275-295.

VAN DER MOLEN, I.. (1985b): Interlayer material transport during layer-normal shortening, II, boudinage, pinch-and-swell and migmatite at Søndre Strømfjord Airport, west Greenland. *Tectonophys.* **115**, 275-295.

VERNON, R.H. (2007): Problems in identifying restite in S-type granites of southeastern Australia, with speculations on sources of magma and enclaves. *Can. Mineral.* **45**, 147-178.

VERNON, R.H. & COLLINS, W.J. (1988): Igneous microstructures in migmatites. *Geology* **16**, 1126-1129.

VERNON, R.H. & JOHNSON, S.E. (2000): Transition from gneiss to migmatite and the relationship of leucosome to peraluminous granite in the Cooma Complex, SE Australia. *In* Stress, Strain and Structure. A volume in Honour of W.D. Means (M.W. Jessell & J.L. Urai, eds). *J. Virtual Explorer* **2** (print & CD).

VERNON, R.H., RICHARDS, S.W. & COLLINS, W.J. (2001): Migmatite-granite relationships: Origin of the Cooma Granodiorite magma, Lachlan Fold Belt, Australia. *Phys. Chem. Earth* **26**, 267-271.

VERNON, R.H., COLLINS, W.J. & RICHARDS, S.W. (2003): Contrasting magmas in metapelitic and metapsammitic migmatites in the Cooma Complex, Australia. *Visual Geosci.* **8**, 45-54.

VIELZEUF, D. & VIDAL, PH. (1990): *Granulites and Crustal Evolution*. Kluwer Academic Publishers, 585 pp.

VIELZEUF, D., CLEMENS, J.D., PIN, C. & MOINET, E. (1990): Granites, granulites and crustal differentiation. *In* Granites and Crustal Evolution (D. Vielzeuf & P. Vidal, eds). Kluwer, Dordecht (59-85).

VIGNERESSE, J.L. & BURG, J.P. (2000): Continuous vs. discontinuous melt segregation in migmatites: Insights from a cellular automaton model. *Terra Nova* **12**, 188-192.

VIGNERESSE, J.L. & BURG, J.P. (2005): Simulation of crustal melt segregation through cellular automata: Insight on steady and non-steady state effects under deformation. *Pure & Applied Geophys.* **162**, 987-1011.

VIGNERESSE, J.L., BARBEY, P. & CUNEY, M. (1996): Rheological transitions during partial melting and crystallization with application to felsic magma segregation and transfer. *J. Petrol.* **37**, 1579-1600.

VILLASECA, C., MARTÍN ROMERA, C., DE LA ROSA, J. & BARBERP, L. (2003): Residence and redistribution of REE, Y, Zr, Th and U during granulite-facies metamorphism: behaviour of accessory and major phases in peraluminous granulites of central Spain. *Chem. Geol.* **200,** 293-323.

VILLASECA, C., OREJANA, D. & PATERSON, B.A. (2007): Zr–LREE rich minerals in residual peraluminous granulites, another factor in the origin of low Zr–LREE granitic melts? *Lithos* **96,** 375-386.

WALTE, N.P., BONS, P.D. & PASSCHIER, C.W. (2005): Deformation of melt-bearing systems – insight from in situ grain-scale analogue experiments. *J. Struct. Geol.* **27**, 1666-1679.

WANNAMAKER, P.E., YARDLEY, B.W.D. & VALLEY, J.W. (2000): Enriched: the petrologic case for a dry lower crust; discussion and reply. *J. Geophys. Res.* **105**, 6,057-6,068.

WARK, D.A. & MILLER, C.F. (1993): Accessory mineral behavior during differentiation of a granite suite: Monazite, xenotime and zircon in the Sweetwater Wash pluton, southeastern California, USA. *Chem. Geol.* **110**, 49-67.

WARK, D.A. & WATSON, E.B. (2002): Grain-scale channelization of pores due to gradients in temperature or composition of intergranular fluid or melt. *J. Geophys. Res.* **107**, B2, 2040, DOI:10.1029/2001JB000365.

WATERS, D.J. (1988): Partial melting and the formation of granulite facies assemblages in Namaqualand, South Africa. *J. Metamorphic Geol.* **6,** 387-404.

WATSON, E.B. (1996): Dissolution, growth and survival of zircons during crustal fusion: Kinetic principles, geological models and implications for isotopic inheritance. *Trans. Royal Soc. Edinburgh - Earth Sci.* **87**, 43-56.

WATT, G.R., OLIVER, N.H.S. & GRIFFIN, B.J. (2000): Evidence for reaction-induced microfracturing in granulite facies pelitic migmatites. *Geology* **28**, 331-334.

WEERTMAN, J. (1971): Theory of water-filled crevices in glaciers applied to vertical magma transport beneath ocean ridges. *J. Geophys. Res.* **76**, 1171-1183.

WEINBERG, R.F. (1999): Mesoscale pervasive felsic magma migration: alternatives to dyking. *Lithos* **46**, 393-410.

WEINBERG, R.F. & MARK, G. (2008): Magma migration, folding and disaggregation of migmatites in the Karakoram Shear Zone. *Geol. Soc. Am. Bull.*, in press.

WEINBERG., R.F. & PODLADCHIKOV, Y. (1994): Diapiric ascent of magmas through power-law crust and mantle. *J. Geophys. Res. - Solid Earth* **99**, 9543-9559.

WEINBERG, R.F. & SEARLE, M.P. (1998): The Pangong injection complex, Indian Karakoram: A case of pervasive granite flow through hot viscous crust. *J. Geol. Soc.* **155**, 883-891.

WEINBERG, R.F., SIAL, A.N. & MARIANO, G. (2004): Close spatial relationship between plutons and shear zones. *Geology* **32**, 377-380.

WHITE, R.W. (2008): Insights gained from the petrological modeling of migmatites: Particular reference to mineral assemblages and common replacement textures. *In* Working with Migmatites (E.W. Sawyer & M. Brown, eds.). *Mineral. Assoc. Canada, Short Course* **38**, x-x.

WHITE, R.W. & POWELL, R. (2002): Melt loss and the preservation of granulite facies mineral assemblages. *J. Metamorphic Geol.* **20**, 621-632.

WHITE, R.W., POWELL, R. & HOLLAND, T.J.B. (2001): Calculation of partial melting equilibria in the system Na_2O-CaO-K_2O-FeO-MgO-Al_2O_3-SiO_2-H_2O (NCKFMASH). *J. Metamorphic Geol.* **19**, 139-153.

WHITE, R.W., POWELL, R. & HALPIN, J.A. (2004): Spatially-focused melt formation in aluminous metapelites from Broken Hill, Australia. *J. Metamorphic Geol.* **22**, 825-845.

WHITE, R.W., POMROY, N.E. & POWELL, R. (2005): An in situ metatexite–diatexite transition in upper amphibolite facies rocks from Broken Hill, Australia. *J. Metamorphic Geol.* **23**, 579-602.

WHITEHEAD, J.A. & HELFRICH, K.R. (1991): Instability of flow with temperature-dependent viscosity: A model of magma dynamics. *J. Geophys. Res.* **96**, 4145-4155.

WHITNEY, D.L., TEYSSIER, C. & VANDERHAEGHE, O. (2004): Gneiss domes and crustal flow. *In* Gneiss Domes in Orogeny (D.L. Whitney, C.T. Teyssier & C. Siddoway, eds). *Geol. Soc. Am. Spec. Paper* **380**, 15-33, Boulder, Colorado.

WICKHAM, S.M. (1987a): Crustal anatexis and granite petrogenesis during low-pressure regional metamorphism: the Trios Seigneurs Massif, Pyrenees, France. *J. Petrol.* **28**, 127-169.

WICKHAM, S.M. (1987b): The segregation and emplacement of granitic magmas. *J. Geol. Soc. London* **144**, 281-297.

WILLIAMS, M.L., HANMER, S., KOPF, C. & DARRACH, M. (1995): Syntectonic generation and segregation of tonalitic melts from amphibolite dikes in the lower crust, Striding-Athabasca mylonite zone, northern Saskatchewan. *J. Geophys. Res.* **B100**, 15717-15734.

YARDLEY, B.W.D. & VALLEY, J.W. (1997): The petrologic case for a dry lower crust. *J. Geophys. Res.* **102**, 12173-12185.

ZÁVADA P., SCHULMANN, K., KONOPÁSEK, J., ULRICH, S. & LEXA, O. (2007): Extreme ductility of feldspar aggregates – Melt-enhanced grain boundary sliding and creep failure: Rheological implications for felsic lower crust. *J. Geophys. Res.* **112**, B10210, doi:10.1029/2006JB004820.

ZEN, E-A. (1992): Using granite to image the thermal state of the source terrane. *Trans. Royal Soc. Edinburgh - Earth Sci.* **83**, 107-114.

ZENG, L., ASIMOW, P.D. & SALEEBY, J.B. (2005a): Coupling of anatectic reactions and dissolution of accessory phases and the Sr and Nd isotope systematics of anatectic melts from a metasedimentary source. *Geochim. Cosmochim. Acta* **69**, 3671-3682.

ZENG, L., SALEEBY, J.B. & ASIMOW, P. (2005b): Nd isotope disequilibrium during crustal anatexis; a record from the Goat Ranch migmatite complex, southern Sierra Nevada Batholith, California. *Geology* **33**, 53-56.

ZENG, L., SALEEBY, J.B. & DUCEA, M. (2005c): Geochemical characteristics of crustal anatexis during the formation of migmatite at the Southern Sierra Nevada, California. *Contrib. Mineral. Petrol.* **150**, 386-402, doi:10.1007/s00410-005-0010-2.

ZHONG, Z., ZHANG, H., SUO, S. & YOU, Z. (1999): Partial melting processes during exhumation of ultrahigh-pressure metamorphic rocks in Dabieshan, China. *J. China Univ. Geosciences* **10**, 194–199.

CHAPTER 7: THE INTERPLAY BETWEEN TECTONICS/STRUCTURE AND MIGMATITE MORPHOLOGY IN THE FIELD

Gary S. Solar
Laboratory for Orogenic Studies
Department of Earth Sciences
SUNY College at Buffalo,
1300 Elmwood Avenue
Buffalo, New York 14222
solargs@buffalostate.edu

INTRODUCTION

Migmatites in the field have for many been a source of confusion, and even frustration, regardless of the migmatites' petrogenesis and tectonic implications, due for the most part to the appearance of these rocks in outcrop. For those many, migmatites appear too complex to interpret, and have been described as "swirled-up soup" or dismissed as "failed" granites that need no more explanation because, by implication, the rocks would have formed without structural coherence and therefore there is no tectonic significance to the structure of the rock. Such rocks are considered by some to have formed their mineral and structural patterns as a fluid rather than by flow during solid-fluid interaction. I have to admit some of these same reactions when first confronted with these types of rocks. The good news, however, is that once the rocks are examined systematically in the field, and at the map scale, a structurally-coherent pattern does emerge, but in some cases it takes finding the right balance of scales in order to do so. In this chapter, methods and techniques that can and should be used at both the outcrop and map scales are described that will lead the field geologist toward accomplishing the task of documenting and then interpreting the structural geology and tectonic implications of migmatites and their associated smaller volume bodies of granite of any type and in every region. Many terms and rock names associated with migmatites are used in this chapter, and the reader is referred to other chapters in this volume for complete explanations of the various migmatite terms, types (Sawyer 2008: chapter 1) and textures (Holness 2008: chapter 4).

BEFORE GETTING STARTED WITH MIGMATITES

Understanding the protolith(s) of the migmatites

Before attempting to understand migmatites and related rocks, it is arguably the most central exercise to understand the non-migmatites in the same region. In particular, it is important to study the regional rocks that are interpreted to be the likely protolith to the migmatites. Without this information, one has little context of the migmatite development starting from the sub-solidus state, and therefore understanding what one is examining at outcrop and map scales is more challenging due to the lack of understanding of the variations in the pre-melting mineralogy and structure. So, in regard to the protoliths, the migmatite researcher is particularly interested in (1) the spatial distribution, overprinting relations and regional variation in the orientation of rock fabrics in it, as defined by metamorphic minerals, (2) outcrop-scale general geometry of the structure in the protolith (*e.g.*, compositional layers and folds of all structures), and (3) the map-scale variation of mineral composition, fabrics, other structures, and any stratigraphy in the region. With this information as a starting point, interpretations of the evolution of the composition, development of the fabrics, and the progression of the structures in the migmatites are all founded solidly. The investigation of the protolith does not stop there. During the course of the work on the migmatites themselves, it will become important to return to outcrops of presumed protoliths for further context. If feasible, it will be helpful to revisit the outcrops of protolith as more is learned from studying the migmatites.

Just as important is to investigate the location and nature of the migmatite front, or "melt-in"

Mineralogical Association of Canada Short Course 38, Quebec City, Quebec, p. 145–158

isograd, in the field. If the presumed protoliths are in relatively close proximity to the migmatites, investigating and understanding the nature of the "migmatite-in" isograd (*i.e.*, the solidus in the field) can be as informative as the same information garnered from both the migmatites and their protoliths. Once found, one can determine any variations in both the migmatites and protoliths as one traverses toward or away from the front. Are there field gradients in fabrics, percentage of leucosome, other granites, or the shapes of these? For example, with distance from the migmatite front in western Maine, Solar & Brown (2001b) reported an increase in the proportion of leucosome, and increasing disruption of pre- and post-partial melting structure in the migmatites (*e.g*, relict bedding, foliation and metatexite structure).

Other background information

As with any field study, understanding is aided by experiments (*e.g.*, Rushmer 1995), analog models (*e.g.*, Bons *et al.* 1991, Druguet & Carreras 2006) and by theoretical considerations (see Brown 2007). Beyond the scope of this chapter are several aspects of terminology and migmatite–granite connections. For these, the reader is referred to Mehnert (1968), Brown (1973) and Sawyer (1998, 2008), in addition to the other contributions in the present volume. Also beyond the scope of this chapter are topics at a smaller scale than outcrops, including microtextures in migmatites, but thorough discussions are found in Ashworth & McLellan (1985) and Vernon & Collins (1988), so the reader is referred to those contributions. The reader is also referred to Sawyer (1999) and Holness (2008) for an evaluation of melting textures. Also of importance to the study of migmatites, granite and the migmatite protoliths are *P–T* data (see Pattison & Tracy 1991), calculations using pseudosections in appropriate systems (*e.g.*, Johnson *et al.* 2003, White 2008), and studies reporting melting reactions of different composition rocks (*e.g.*, Thompson & Tracy 1976, Patiño Douce & Harris 1998). Further, the connection between granite at all scales and migmatite leucosomes has been established (*e.g.*, Sawyer 1998, Solar & Brown 2001b, Brown 2008); the methods and considerations in this chapter are built upon this relation. Of course, the reader is referred also to the other chapters in this contribution for a full discussion of information and theories important to the field study of migmatites and related rocks.

MIGMATITES AT THE OUTCROP SCALE

Outcrop scale investigation of migmatites, as it would for any rock investigation, is done in two stages. First, collect pertinent data, such as rock type, fabric intensity and orientation. Then use those data to look for systematic variations across the outcrop, or between closely spaced outcrops. The following are the major categories of information that should be considered at the outcrop, and between closely spaced outcrops.

Migmatite type and protolith

At the outset of investigation of any outcrop of migmatitic rocks, it is important:

1 to document the mineral content of all components (leucosome, melanosome, host rock),
2 to identify the migmatite type,
3 to document the structure of the migmatite, and
4 to evaluate the rocks for evidence of the protolith (*e.g.*, relict structures and textures).

For the first task, it is standard practice to document mineral compositions. Clearly, compositions of migmatite components vary a great deal owing to differences in protolith composition, and melt loss and/or gain (*in situ* leucosomes *vs*. injected melt *vs*. residual compositions due to melt removal from the rocks). Common observation of leucosomes in migmatites shows a general lack of K-feldspar that suggests melt removal from the system. The reader is referred to other chapters of this volume for a full description of these processes and their implications, but it is to be clear that interpretations made from migmatites in large part hinge on the documentation of mineral composition of the migmatite components. The importance cannot be overemphasized.

Classifying migmatite type is a separate issue. By this writing, much work has been done on classification of migmatites, the modern terminology propelled forward with the landmark contribution of Mehnert (1968) and continued by Brown (1979) and Sawyer (1998) among others (see Sawyer 2008). Of all the types known, two migmatitic rock types have emerged over the years of study as the most commonly found. Stromatic migmatites (Figs. 7-1a & 7-2b) are the most common metatexite migmatite (or deformed varieties of them, *e.g.*, "folded" or fold-structured migmatite). Stromatic migmatite leucosomes are found commonly in the plane of the paleosome foliation (hence the stromatic pattern) because melt collected along that weakest plane in the rocks, from which melt could escape once pooling reached

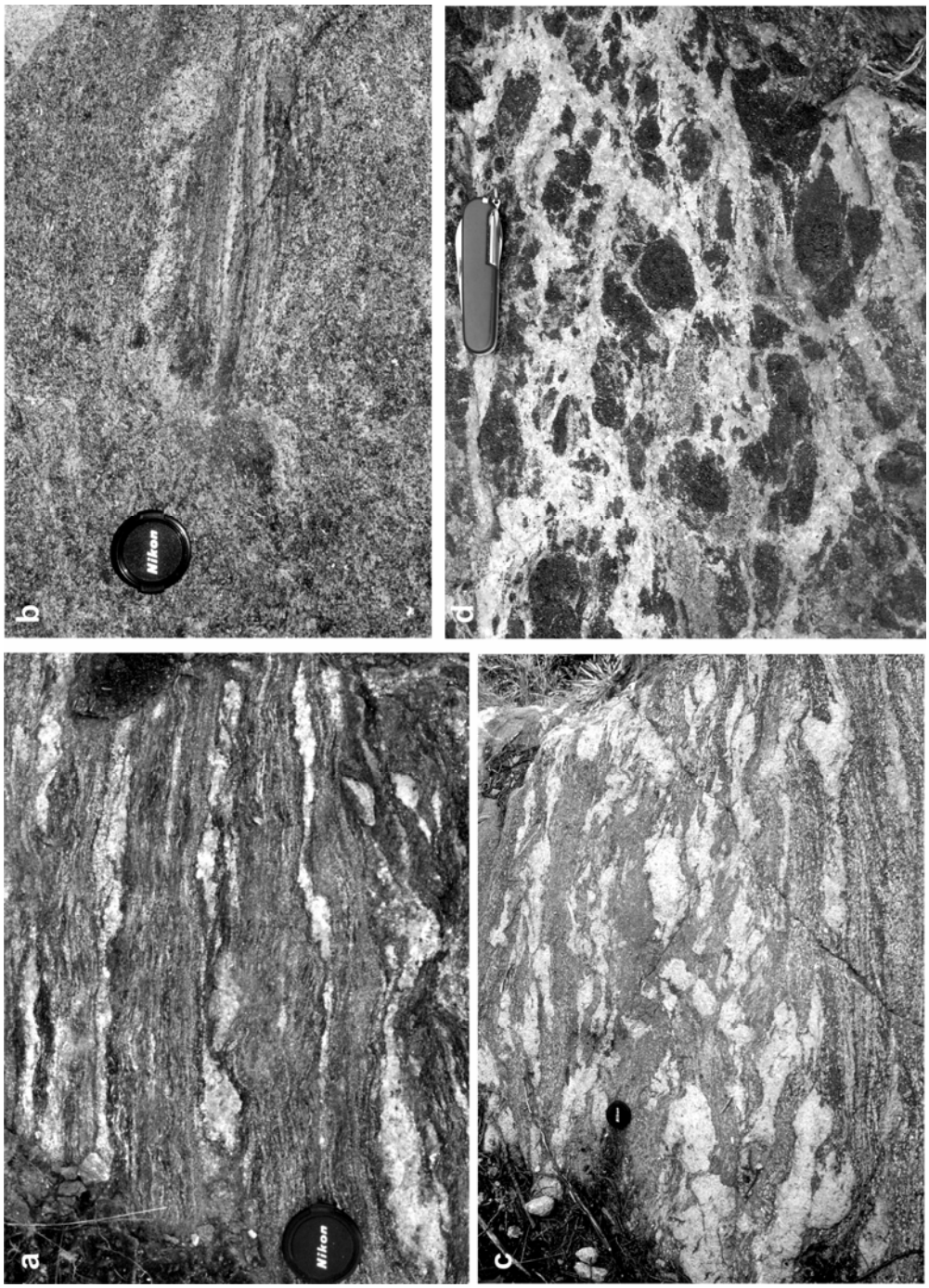

FIG. 7-1. Examples of migmatite types and associate rocks. **a,** Stromatic migmatite, southern Maine. Leucosomes are distinct from paleosome by Bt+Grt±Sil±Pl melanosomes defining a sub-concordant tripartite structure. **b,** Diatexite migmatite with pod-shaped schollen of metasedimentary rock with relict stratigraphy, western Maine. Leucosomes are texturally gradational with the matrix minerals. Protolith structure (if in existence at this scale) is not evident except for inside the schollen. **c,** Vein migmatite, western Maine. Leucosomes are pod-like, and the host rock is strongly residual in composition (Bt+Grt). **d,** Patch migmatite, central Adirondack Mountains, New York State. Patches are aggregates of diopside surrounded by a halo of Pl+Qtz. Quartzofeldspathic stromatic-style leucosome drapes and includes the aggregates.

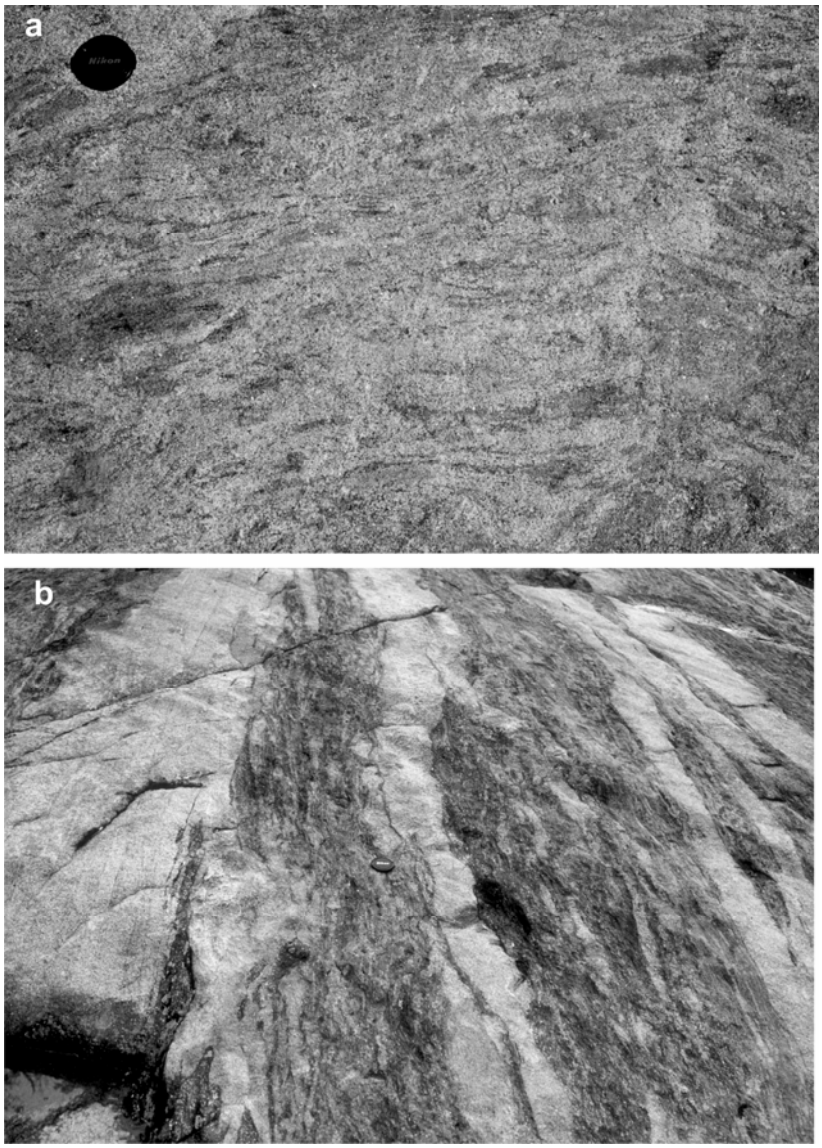

FIG. 7-2. **a,** Schlieric granite, western Maine. Structure is illustrative of formation during flow *en masse*.

b, Concordant sheets of granite in stromatic migmatite, western Maine.

a critical volume (Sawyer 2001). Perhaps just as prevalent in areas of stromatic migmatite is the related rock diatexite (Figs. 7-1b & 7-3), a rock interpreted to have undergone disruption of the metatexite structure during anatexis. Indeed, outcrops of diatexite locally have schollen of metatexite within them (Figs. 7-1b & 7-3a) suggesting the former developed from the latter. See Sawyer (2008) for a detailed description of these types of rocks. As one may expect, two other rock types are to be expected in migmatite terrains. These are residue-rich granitic rocks (*e.g.*, schlieric granite; Fig. 7-2a), and granitic rocks of various compositions and textures (Fig. 7-2b).

This is not to imply that other migmatitic rocks are not found or important, but rather, these other types may illustrate differences in protolith and/or prevailing differential stress during and after the formation of migmatites. For example, an important type is vein-structured migmatite (Fig. 7-1c), rocks that bear resemblance to stromatic migmatites, but leucosomes are in more discrete veins and pod-shaped forms. Migmatites that deformed in the subsolidus state are much more challenging to interpret from a standpoint of formation simply because these rocks have solid-state overprints on the migmatite structure (such as boudinage and folds of leucosome), and commonly the deformation will have effectively erased the evidence of the history of migmatite formation in the rock, when it was melting and/or melt-present. Although much less commonly studied, calc-silicate

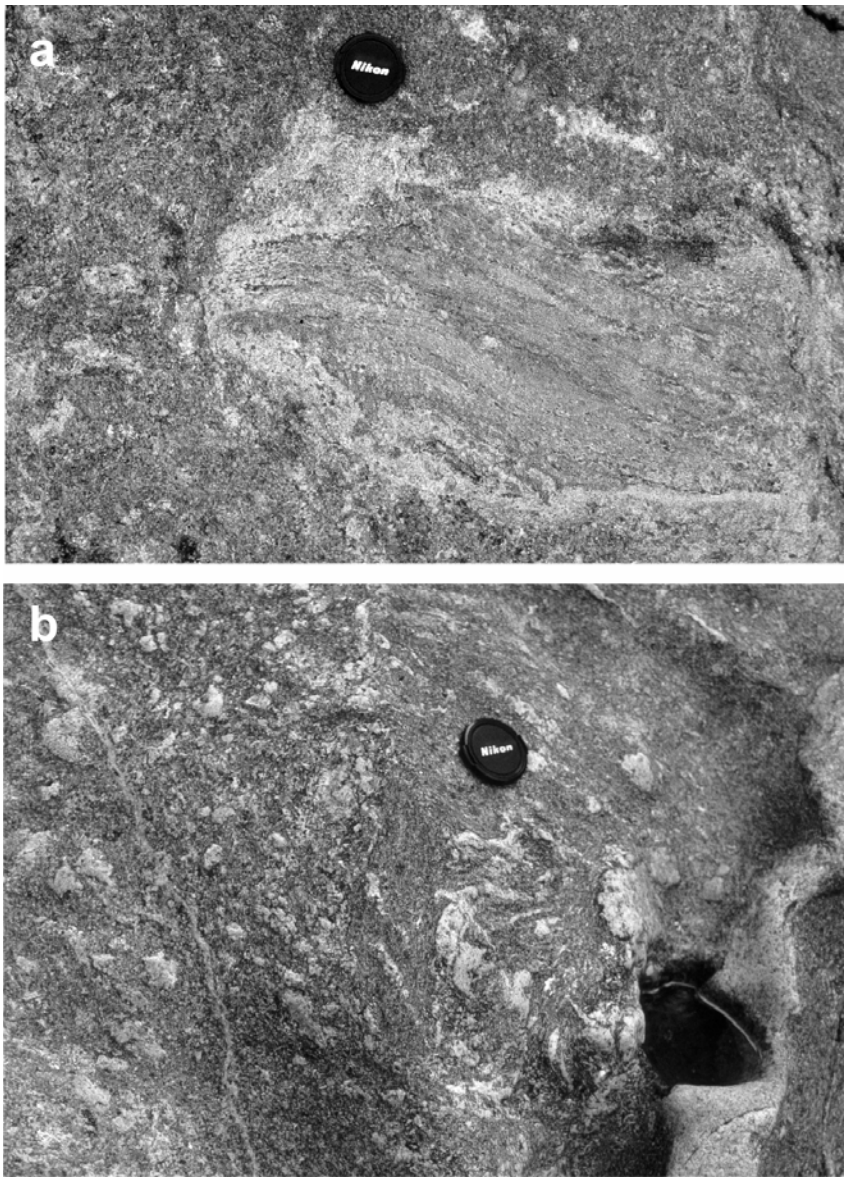

FIG. 7-3. Melt structures in diatexite, western Maine.

a, Leucosome halo around schollen of relict stratified calc-silicate-rich metasedimentary rock in diatexite.

b, Oblique view of rod-shaped (prolate) leucosomes in diatexite. The outcrop surface at the top right is along the long dimension of rod-shaped leucosomes that are moderately plunging to the right (north) in the field of view. The left part of the photograph is pavement outcrop oriented at a high angle to the rod-shaped leucosomes. In that view leucosomes are sub-circular.

migmatites are known with a common texture similar to patch migmatites that features distinctive clots of ferromagnesian minerals (usually pyroxene) mantled by quartzofeldspathic halo-like leucosomes that formed under low differential stress (Fig. 7-1d). Many interpret the patches to be "flecky" texture that formed at subsolidus conditions (*e.g.*, Ashworth 1985). However, these rocks typically have strong fabrics and stromatic-type leucosomes, and locally the fabrics and leucosomes drape the patches. Commonly the patches are found only in the areas of the rock that have leucosome, suggesting some connection between these two features.

Once a classification is made, however, it is important also to avoid associating the type of migmatite with any specific formation process or model without testing it thoroughly. There are, for example, many competing theories and models that explain the origin of the stroma during the formation of what are called stromatic migmatites. Furthermore, there is no reason to assume that all the stromatic migmatites in an area formed the same way; one should not forget that stromatic refers to morphology and not to process. It is essential not to fall into the trap of allowing models to drive field investigation.

Likewise, with the exception of diatexite, migmatitic rocks commonly preserve some relict structure of their sub-solidus protolith. This is particularly true of metasedimentary rock protoliths

where compositional layers at the centimetre and metre scales may be relict stratigraphy (*e.g.*, alternating pelitic and psammitic compositional layers; see the schollen in Figs. 7-1b and 7-3a). This aspect is powerful information about migmatites, particularly if the non-migmatitic protolith is represented by regional rocks as described above. In metatexite such structure is preserved very well across rocks where melting perhaps was at a lower percentage, melt escaped without necessity for a high melt fraction, and/or melting occurred preferentially in layers of appropriate composition, thus preserving the rock structure . Where increased melt fraction may have caused disruption of pre-existing structures and the formation of diatexite migmatites, relict structures can be preserved in pod-shaped schollen where compositional contrasts in the protolith hindered melting, hence making the rock locally resistant to flow. In metapelitic migmatitic rocks these pods are commonly rich in calc-silicate minerals as if a relict concretion in the protolith (Figs. 7-1b and 7-3a).

Fabric attitude, intensity and trajectory in and among migmatite outcrops

Naturally, it is standard practice to collect attitude data on foliations and lineations in any rocks in the field. There is no reasonable limit to collecting such data, and it is best to collect data systematically across exposures, both across and along strike, in the pursuit of any orderly variation in attitude. The collection of one or two measurements across large exposures of migmatites will not result in much documentation or understanding of fabric variation, or of any other data collected at the rock. There is no prescribed way of collecting these data, however, just that fabric measurements should be both systematic and representative without missing details (cm-scale folds may be missed if it is decided to measure attitudes using a grid at a 1 metre scale).

Other than orientation, determination of the intensity of mineral fabrics can be as important as the documentation of the migmatites themselves. Draping, textures of individual grains or aggregates, boudinage of leucosomes, and fabrics *vs*. folds all require documenting in order for a full analysis. Documenting fabric intensity begins with the usual qualitative evaluation of how ordered the foliation and lineation are in the rock, usually using "strong" and "weak," but also L- *vs*. S-tectonite as descriptors. If at all possible, a quantitative approach is preferred, but only as the next step in the analysis.

There are several techniques to document fabric shapes that can be used at the outcrop, on outcrop photographs or in thin section. One of the simpler techniques is the inverse SURFOR (surface orientation) wheel of Panozzo (1987), developed with the idea of documenting the strain ellipse in 2-D sections (and ultimately the strain ellipsoid using multiple sections). The method uses a grid of evenly spaced parallel lines inside a circle that is rotated about the center, and intersections of the grid lines with grain boundaries are tallied at each 10° of rotation. The orientation of the grid where the largest number of intersections occurred is interpreted to represent the orientation of the shortest axis of the grain shape ellipse (Fig. 7-4a), and this orientation is at a maximum angle to the longest axis, the orientation of which is therefore determined through the analysis. The orientation of the grid lines where the least intersections occurred, by definition, is consistent with the long aspect of the grain shape being in that direction (Fig. 7-4b). Further, the difference in intersections between these extremes is an approximation of the aspect ratio of the grain shape ellipse. In Fig. 7-4, the aspect ratio of long to short axes would calculate to 6.8 to 1 whereas the actual ratio of each object is 6.2 to 1. The technique therefore yields a reasonable quantification of the aspect ratio of the fabric ellipse in that section, but clearly determines the orient-

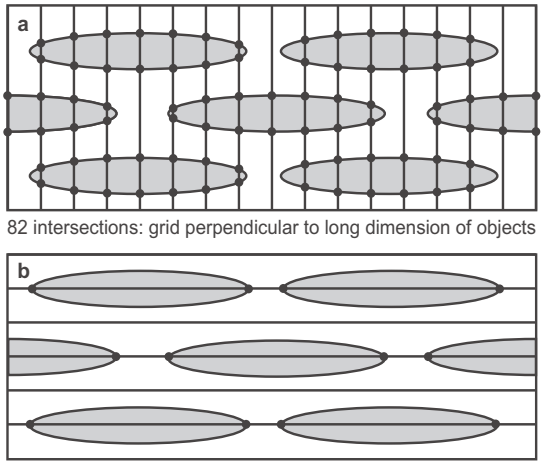

FIG. 7-4. Principle of analysis using the Inverse SURFOR (surface orientation) wheel of Panozzo (1987). (a) Maximum intersections of a parallel grid occur when the grid lines are perpendicular to the long aspect of objects (*e.g.*, grains and grain aggregates). (b) Minimum intersections of the same grid lines in (a) occur when the lines are parallel to the long aspect. See text for details.

ation of the ellipse axes. The method is excellent for any preferred orientation in 2-D because even ellipses with low aspect ratios will emerge after analysis. Three dimensional analysis is made possible by performing the analysis on mutually perpendicular sections. A pitfall of the method, however, is that as designed it presupposes that surfaces between grains are the same as those present prior to deformation so that the strain ellipse can be quantified. In migmatites, there is little doubt that mineral and structural surfaces are secondary, and therefore using them as a marker of the strain ellipse is not justified. However, the method as it is designed is powerful inasmuch as it can be used to document the shape of any fabric ellipsoid. If more than one fabric ellipse is defined by different minerals, the method can be used to document the differences between them in the same sections or surfaces. A suite of data across outcrops can prove invaluable in fabric analysis at many scales.

Once fabrics are documented for attitude and intensity across outcrops, these data are then used to document the fabric trajectory across large outcrops and between closely spaced outcrops. Whenever possible it is invaluable to produce a fabric form line map of exposures (see Fig. 7-5 for a regional scale version). The goal is to evaluate if fabrics are preferentially oriented, and at what scale, and to understand the variation of the fabric intensity as one traverses along and across the fabric trend. Patterns that can emerge are either systematic curvature of fabrics associated with high strain zone boundaries, or at the boundaries of migmatite zones, or both, that can be correlated with differences in 3-D shapes of fabrics. If so, the fabrics in the migmatites have recorded something significant about the regional structural geology.

Percent leucosome, melanosome and host rock (paleosome)

Part of any complete examination of migmatitic rocks is the documentation of percentages of the components, particularly the neosome parts (the leucosome and the melanosome) and the host rock (paleosome, or non-neosome), but also the smaller volume granite bodies. Such data can be used to determine melt loss or gain (*e.g.*, Kriegsman 2001) in the map area. The task of documenting percentages of these components is a simple one, yet one of the most tedious at the outcrop. One can perform 2-D area % calculation of components on more than one surface at different orientations in order to calculate volume %, however, 2-D data could be used as a proxy for volume % if the surface used is assumed to be representative of every surface orientation. This assumption may not be appropriate depending upon the 3-D geometry of migmatite components, so caution is warranted. For this analysis, data for leucosomes seem to have significant weight, but percent melanosome should not be overlooked. The interpretation that the melanosome is the residuum that segregated as melt accumulated to form leucosomes (see Sawyer 2008) carries with it the implication that percent melanosome leads to estimates of melt loss, giving melanosomes equal weight to leucosomes in this analysis.

To document percentages, assumptions must be made about how to measure them, and the job can be accomplished in a few different ways to different degrees of accuracy. First, traditional point-counting could be employed, using outcrop surfaces as one would thin sections. This method could give reasonable results, but the technique depends heavily upon grid line spacing; the finer the spacing, the more reliable the data for area %. Data may not be useful unless spacing is at the millimetre scale, but with the size of most migmatite components (centimetre scale or higher), time is a major factor when employing this technique.

Because many leucosomes are approximately elliptical in 2-D surfaces, even if irregularly shaped (see Figs. 7-1a & 7-1c), a more reasonable technique of measuring percentages is to section off surface areas of the outcrop and calculate the cumulative leucosome area assuming that leucosomes are ellipses. Under that assumption, measures of long and short axial dimensions of a leucosome permits calculation of its area using the formula for area of an ellipse. A sum of the leucosome areas in the study section gives total area leucosome on that surface, and area % is found by simply comparing total area leucosome to the total surface area of the data collection site. Naturally, this technique works for melanosomes, so calculated area % melanosome and leucosome reveals the area % neosome, and the remainder is area % host rock (paleosome). The area used for data collection depends upon the size of migmatite components, but a reasonable area may be $1m^2$.

However, a complication to any technique is that in practice it is challenging locally to determine the contacts of leucosomes with paleosome if leucosomes are millimetre thicknesses. This is commonly found in diatexite (see Fig. 7-1b) and in schlieric granites (Fig. 7-2a). Like any analyses, however, judgment calls need to be made.

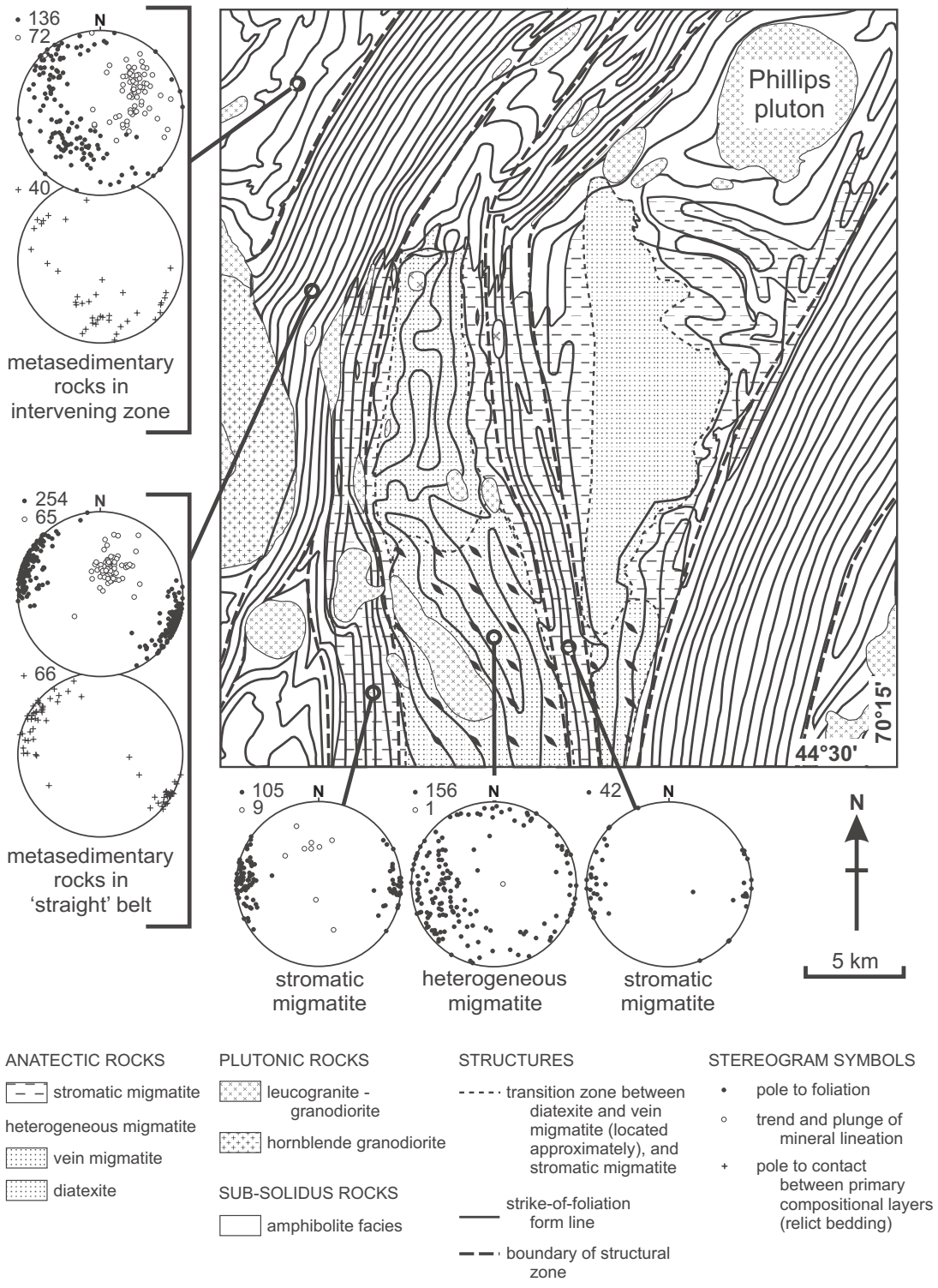

FIG. 7-5. Migmatite and structural map of part of western Maine, modified after Solar & Brown (2001a, b). The migmatite front is the bounding line between migmatites in the central, eastern and southern areas with sub-solidus rocks (presumed the protolith metasedimentary rocks, unornamented). Form lines are drawn along strikes of foliations, and spacing of the lines indicate general dip where closer spacing is steeper dips. Stereograms show all data, and separated by structural zone, by localized parts of zones and by rock type to illustrate differences and similarities across the region, and within zones.

Orientation, geometry and spatial relations of migmatite structures and granite bodies in migmatite outcrops.

The geometry of migmatite leucosomes and smaller volume granite bodies (generally metre-scale thickness; Fig. 7-2b) are interpreted to be the record of the melt flow network through the rock (*e.g.*, Sawyer 1998, 2001, Brown & Solar 1999) provided there has been no significant post-migmatite deformation. As noted by Solar & Brown (2001b), melt flow during deformation is suggested if outcrop scale leucosomes and other granite bodies are located in structurally controlled sites within the migmatites. Such sites at outcrop scale include inter-boudin partitions, strain shadows, extension fractures and shear surfaces, fold hinge zones, and around schollen (Fig. 7-3a). Many outcrops of migmatites have several different such sites within close proximity. In part, it is this complexity that has led many to misunderstand migmatites, interpreting them to be without preferred structure. In truth, migmatite structures are as varied as migmatitic rocks themselves, and in many cases may represent both local stress fields during development and regional tectonic stress fields during orogenesis. As described by Sawyer (2001), smaller volume leucosomes form preferentially along the foliation because melt would begin the segregation process by pooling along the weakest structures in the rock. Evacuation of that melt would occur via extension or shear fractures, among other structures. Brown & Solar (1998) and Solar & Brown (2001b) advocated for at least some melt flow along foliations as pulses during general shear and/or flattening of the rocks (see Fig. 7 in Brown & Solar 1998). Therefore documentation of the orientation, geometry and spatial relations of leucosomes and the other migmatite structures is fundamental to understanding both the melt segregation and flow history in migmatites, and the structure and tectonics that these aspects have recorded.

The first step in performing documentation of migmatite outcrops is simply to map them at the metre scale and below. The goal is to portray accurately in a map of an outcrop the spatial relations of all rock types (those can vary at the metre scale), and their general plan-view geometry, and geometry in vertical surfaces if available (*cf.* Fig. 7-2b for the former case and Fig. 6-18a of Brown (2008) showing the vertical exposure at the same outcrop). Unlike steeply dipping exposures, the plan-view mapping permits a larger scale of observation, a 'bird's-eye' view of outcrops (or closely spaced outcrops) that is not necessarily available for study standing at the outcrop itself. An effective method to produce such a detailed map is to use a grid system (*e.g.*, metre scale or lower) that facilitates manual documentation of the relation of rock type contacts to known points on the outcrop. More modern technology, such as a "total station" or high resolution GPS receivers, permits the collection of this information in much the same way, however, in the opinion of this author, the manual gridding technique forces one to examine the rocks more closely during the performance of the technique (and to place contacts more precisely). From the base mapping, the attitude of fabrics, and the attitude and geometry of leucosome and melanosome (and by extension the paleosome) can be overlain, properly located at the centimetre and metre scales, and integrated with the rock type information and any other data collected, either at the outcrop or in the laboratory using collected specimens.

The essential data to collect when studying leucosomes and the smaller volume granite bodies (see Figs. 7-1a, 7-3b & 7-2b for examples) are the 3-D shapes, sizes and styles (*e.g.*, tabular or 'pinch and swell' structures) using a series of differently oriented 2-D surfaces in order to investigate 3-D structural relations between them. Included in these data should be notes of whether shapes of these bodies are prolate, oblate, and any shape in between (see Fig. 7-3b for an example of prolate leucosomes). Are the shapes lenses, pod-like, sheet-like, or columnar? The trend and plunge of major axes of these shapes required recording. An effective data set will correlate shape, size and orientation data in order to evaluate any patterns (*e.g.*, Solar & Brown 2001b). The next scale up at the outcrop is to relate together all structures in the migmatitic rocks. What are the spatial relations of these structures (given by the map of the outcrop)? Do they define a distinctive pattern, or do they not? If not, there may be one at another scale of observation.

Beyond the importance to understanding migmatite outcrops and the magmatic flow history *vs.* the deformation in the rocks, the attitude and geometry of these structures in many cases help determine the timing of anatexis relative to deformation, be it syntectonic (fabrics and leucosomes are concordant, or nearly so), or tectonism occurred after anatexis (*e.g.*, fabrics transecting leucosomes, leucosome boudinage and

folds). Smaller volume granite bodies will also have attitudes and geometries important to this story (see Fig. 7-2b), but because the bodies are usually clearly intrusive to the migmatite, and are generally considered the result of larger scale magmatic flow through the crust, linking source to sink, they record the larger scale process. In some cases both leucosomes and smaller volume granite bodies (metre scale and lower) that occur in migmatite outcrops show 'pinch and swell'. In those cases, such structures are interpreted as having recorded either (or both) deformation or collapse of the melt conduits when the host rock was still hot enough to deform plastically, and that the melt was still mobile (liquid-dominated) at that time.

Fabrics *vs.* leucosomes and melanosomes (neosomes)

Data collected at the migmatite outcrop cannot be complete without a documentation of the relation between mineral and grain-aggregate fabrics with the migmatite structures. Are fabrics concordant with the shape and orientation of the leucosomes and melanosomes? Are fabrics continuous with the neosome, and do they transect and refract at the neosome contacts? Alternatively, are fabrics truncated at neosome contacts, or do the fabrics drape the neosome components? Do the paleosome fabrics appear distinct and separate from the neosome, or is there a gradation between them? Answers to each of these questions permit integration of fabric and migmatite component data as described above. However, just as it is with leucosome styles and shapes, such fabric–neosome relations can vary at the metre scale in the outcrop, and without outcrop-scale context, these variations may seem without pattern, but one likely exists at some scale, and is expected if these data are collected from cogenetic features.

MIGMATITES AT THE MAP SCALE

Of course, the logical next step with outcrop-scale data is the study of migmatites across the study area at the map scale. This can involve relating outcrops together or interpreting data across a region. In either case, without interpretation at the map scale, the outcrop data may not be useful beyond the outcrop at which they were collected. In addition to standard mapping of rock types (*e.g.*, looking for zones of migmatite types and structures defined by fabric ellipsoid types), the following are important techniques that need to be employed in the use of outcrop scale data.

Zones defined by migmatite types, and their relation to the regional structure

Once mapping is complete, patterns of migmatite types will likely emerge whether or not the migmatites are genetically related. In this analysis, zones of migmatites at map scale may be defined. At first, mapping of zones could be based on the types of migmatites as listed above, separating zones of stromatic *vs.* vein migmatite *vs.* diatexite, and so on. However, such zone patterns at map scale may have a level of complexity that does not permit an understanding of how these rocks have recorded the regional tectonic history, and it may be more illustrative to group types into lithotectonic units. Presented with just this situation, Solar & Brown (2001b) showed two types of zone of migmatites based upon grouping of types that are structurally related and upon the consistency of internal structures within them (*e.g.*, the orientation of components) that are consistent with the orientation of the zones and the regional structure (Fig. 7-5). These two types of zone alternate across strike, one zone defined by sub-parallel components in stromatic migmatite, and the other zone is a grouping of types whose components are much more variably oriented, composed of diatexite and vein migmatite dominantly. From this zoning, Solar & Brown (2001b) showed that the zones of stromatic migmatite are in zones where regional structures are consistently oriented and 3-D fabrics are consistently oblate to plane strain (S>L), consistent with the formation of stromatic migmatite according to the regional structure (concordant sub-tabular leucosomes and granites; Figs. 7-2b and 7-5). Likewise, the other zone of migmatites (the "heterogeneous migmatites" of Solar & Brown, 2001b) correlates at the map scale with regional structural zones where fabrics and other structures are much more variably oriented and where 3-D fabrics are consistently relatively prolate (L>S). Again, the larger variation of structures in these migmatites is consistent with the regional structure (concordant sub-cylindrical leucosomes and granites). From this zone pattern, one can interpret that the history of the formation of migmatites is linked to the regional structural story, either coevally, or by the morphology of the migmatite simply having followed the preexisting structure, or both. Brown & Solar (1999) used this information to suggest that the zones of heterogeneous migmatite are in structural positions at the regional scale where roots of plutons are found, as if such zones were where melt was focused, making these

zones melt ascent conduits in the structural system.

As indicated above when defining zones of migmatites, a powerful method in attempting to interpret migmatites in relation to regional structure and tectonic history is by using attitude data from outcrops overlain on a map of rock types that include the migmatite zones. A graphical representation of fabric attitudes is most useful in performing such analysis. Using the standard attitude symbols, form line maps of fabrics are the most convenient way of evaluating trends in attitude data. If a pattern emerges where fabrics are similarly oriented, it is useful to find ways of drawing form lines that illustrate dips as well. One way to do this can be spacing of form lines, wider spacing for shallower dips, and closer spacing for steeper dips (Fig. 7-5). When connected to the migmatite type information on such maps, a pattern may emerge where certain form lines can be correlated to certain types of migmatites. In western Maine, Solar & Brown (2001a, b) showed such a correlation where stromatic migmatites are found where form lines are straight, consistently oriented and closer spaced (steeper dips; Fig. 7-5), whereas heterogeneous migmatites (diatexite, vein migmatite and schlieric granite) map where form lines are much more variable. From their analysis of these data, Solar & Brown (2001b) made a map-scale connection between migmatite type and regional structure that was consistent with data at the outcrop scale, and suggested that the migmatite type that formed in a given area was controlled by the deformation of the rocks, making a direct connection between tectonics and migmatite development.

The next step in this methodology is to augment form-line maps by plotting structural data on standard diagrams (stereograms, rose diagrams) that will permit further interpretation of any zonation in the attitude data. If one exists, an evaluation of the map-view shapes of zones is accomplished by comparing together the map pattern of migmatite types, the form lines of fabrics and patterns of fabric attitudes on diagrams. Stereograms of fabric attitudes should first be a single plot of all data, but many have found it useful to separate data spatially. If zones are identified, plot stereograms for each zone as illustrated in Figure 7-5. Further, if more than one rock type is found in a zone, it may be useful to plot a stereogram for each rock type, or show rock type differences using distinctive ornament of the symbols on the same diagram (Fig. 7-5).

Map-scale relation to other rock types, particularly granite

Any relation between deformation, migmatites and granite bodies is dependent on the level of erosion and the scale of observation. It does not follow that discordant contacts locally at outcrop scale or regional scale preclude syntectonic ascent and emplacement when viewed in three dimensions at the crustal scale (Brown & Solar 1999, Solar & Brown 2001b). The same approach is necessary for the correct interpretation of syntectonic veins at the outcrop scale, which may be discordant to the rock fabric, but which nonetheless predate the later strain during progressive deformation.

So, interpreting map scale data of rock types and structures in migmatite zones usually also means interpreting the shapes and structural position and orientation of granite bodies. As stated above, at map scale, the position of heterogeneous migmatites have been correlated with where roots of plutons are found to suggest that those parts of the structural system were melt ascent conduits (Brown & Solar 1999). In regions where outcrop percentage is reasonably high, going from outcrop to map scale to determine the map-scale shape of granite bodies is clearly simpler than in regions where there is significant cover, and outcrop percent is low or with areas of the region with more cover than others. The latter is the case for much of the Grenville Province, and the Appalachians of the eastern USA and Canada. So interpreting how the granite bodies relate structurally at map scale to the migmatites and other rocks is challenging. A reasonable approach to this problem is to mimic shapes of the granite bodies at the map scale relative to the shapes of their equivalents in the migmatitic outcrops. If leucosomes and metre scale bodies of granite in outcrops or in a series of closely spaced outcrops are sheet-like, vertical and sub-concordant to structures and fabrics, a justifiable interpretation of kilometre-scale bodies would be that they follow this same pattern, just at the larger scale. In fact, justifying that granite bodies would do otherwise at map scale would be difficult or simply not justified because such an interpretation calls on the emplacement of granite at map scale to be fundamentally different to that of the emplacement of granite at outcrop scale. The granite sheets in Figure 7-2b could be smaller scale versions of kilometre-scale sheet-like plutons (see smaller plutons in Fig. 7-5). A clear exception to this,

however, would be granite bodies of tens of kilometres across in plan view. But, it is these larger bodies that can be then evaluated in relation to the map-scale structure as described above. Are the granite bodies situated in particular structural zones, and if so which ones? It is clearly useful as well to have geophysical data available in order to investigate the third dimension; however again one can use the relations at outcrop scale to help here as well. How far down (or up) these bodies extend is never a simple matter to determine. In fact, it would be unreasonable to expect a vertical sheet-like body of granite, like one of those in Figure 7-2b, to be so for extensive sections of crust due to issues of crustal strength that can be a major factor in granite ascent and emplacement (Brown & Solar 1999).

TECTONIC INTERPRETATION OF OUTCROP AND MAP DATA OF MIGMATITES

The formation of migmatites is typical in thickened orogens, where an enhanced thermal gradient is affected by granitic magmatism for which the intracrustal ascent and emplacement occurred during the orogenic deformation (*e.g.*, Brown & Solar 1999). In this context, interpretations regarding the timing of mineral growth, migmatite structures and the shapes of smaller volume granite bodies must take into account several factors, such as the partitioning of deformation at all scales, the effects of composition and rheology of the protolith on fabric and migmatite component development, and the episodic and diachronous nature of deformation and mineral growth (Solar & Brown 1999, 2001b). So, when attempting to use information on migmatites and their associated granites, it must be done under each of these guidelines in concert.

Outcrop-scale data provides the 'ground truth' for any study of migmatites. Clearly, when attempting to understand structural geology (and tectonic history) of a region that includes migmatites all structural data must be employed as each element has recorded some part of the story. In migmatites and their associated granites, the mineral fabrics, shapes of leucosomes and granite bodies are the record of the magma plumbing of orogens where the granite melt flow network is revealed. Caution is warranted, however, because it is unreasonable to assume that the plumbing record is complete, or even that each plumbing element (*e.g.*, leucosomes) is truly coeval. It is much more reasonable to assume that the data being collected at outcrop scale is a composite of information representing different stages of the same process. Taken together, the different stages reveal the picture. Patterns derived from these data are quite reasonably attributed to having been controlled by tectonic stresses prevailing during their development. Indeed, in regional migmatites, what other cause could have produced the common regularity of structures in, and defined by, migmatites and their associated granites?

To elaborate, it is illustrative and clarifying to relate together the 3-D shapes of the fabric ellipsoids in the migmatitic paleosomes with the 3-D shapes of leucosomes and smaller volume granites in the same outcrops. Solar & Brown (2001a, b) found that prolate leucosomes (Fig. 7-3b) that plot in the apparent constriction field of a Flinn diagram are within structural zones defined, in part, by fabric ellipsoids that also plot in that field. The long axes of both structures are similarly oriented (Fig. 7-5, stereograms). Likewise, in that same study, more oblate leucosomes (close to plane strain shapes; Fig. 7-1a) plot at the line of plane strain or into the apparent flattening field of a Flinn diagram. These are shown to be within structural zones defined, in part, by fabric ellipsoids that also plot in that field. Again, major ellipse axes of both structures are similarly oriented (Fig. 7-5, stereograms). Solar & Brown (2001a, b) concluded that this positive correlation is a record of how the migmatitic structures are controlled by the prevailing state of strain in the bulk rock, and that, consistent with conclusions in Sawyer (2001) of where melt pools during segregation, leucosomes take the shape of the bulk strain ellipsoid because melt segregation follows the fabric development. This also means that the strain ellipsoid defined by the fabrics was well developed by the time the rocks began to melt, and that the strain may have continued during melting if the smaller volume granites follow structural suit (Brown & Solar 1998). The importance of understanding the strain in the protolith rocks as expressed above is thereby verified.

Map-scale data of migmatitic terrains, like outcrop-scale data, are considered to be the best way of evaluating the record of tectonic activity during which the terrain developed. The difference, of course, is that the map-scale data are interpreted from the outcrop-scale data, therefore without a proper set of field data, the map interpretations are of no use. Assuming outcrop data are complete and

robust, regional maps made from them will illustrate the same relations as the outcrop-scale data, but at the next scale upward, and so map interpretations may not violate outcrop information. Just as important, the proper map scale interpretation gives meaningful context to the outcrop-scale relations. As many field researchers can relate, outcrop relations that were enigmatic at the time of study, suddenly make simple sense after looking at those relations at a bigger scale.

It is clear that all scales of observations are absolutely essential for understanding what those observations represent, and have recorded. A proposition that leucosomes and smaller volume granite bodies are evidence of melt flow through the crust, and a postulation that granite in plutons within and outside the migmatites represent evolved melt that escaped syntectonically from a similar source to the migmatites, carries with them important implications for field and map data. Each bit of information at all scales, and in concert with data collected using appropriate laboratory techniques (*e.g.*, microstructures, geochemistry and geochronology; *e.g.*, Solar *et al.* 1998), will reveal the mechanism and connection among these components, and ultimately the tectonics they record.

ACKNOWLEDGEMENTS

I wish to thank E.W. Sawyer and M. Brown for the organization of this volume, and for the invitation to contribute with this chapter. I also thank E.W. Sawyer for his review of an earlier version of this chapter. The ideas and techniques explained in this chapter are the end product of working with many individuals, including many students and professionals alike. However, any misconceptions and errors are my own.

REFERENCES

ASHWORTH, J.R. (1985): Introduction. In *Migmatites*, Ashworth, J.R. (ed.), pp 1-35. Blackie, Glasgow.

ASHWORTH, J.R. & MCLELLAN, E.L. (1985): Textures. In "*Migmatites*", Ashworth, J.R. (ed.), pp 180-203. Blackie, Glasgow.

BONS, P.D., ELBURG, M.A. & DOUGHERTY-PAGE, J. (2001): Analogue modeling of segregation and ascent of magma. *In* Animations in Geology, Ailleres, L. & Rawling, T. (eds.), *J. Virtual Explorer*, **4**, http://virtualexplorer.com.au/journal/2001/04/bons/index.html.

BROWN, M. (1973): The definition of metatexis, diatexis and migmatite. *Proc. Geol. Ass.* **84**, 371-382.

BROWN, M. (1979): The petrogenesis of the St. Malo migmatite belt, Armorican Massif, France, with particular reference to the diatexites. *Neues Jb. Miner. Abh.* **135**, 48-74.

BROWN, M. (2007): Crustal melting and melt extraction, ascent and emplacement in orogens: mechanisms and consequences. *J. Geol. Soc., London* **164**, 709-730.

BROWN, M. (2008): Granites, migmatites and residual granulites: relationships and processes. *In* Working with Migmatites (E.W. Sawyer & M. Brown, eds.). *Mineral. Assoc. Can., Short Course* **38**, 97-144.

BROWN, M. & SOLAR, G.S. (1998): Granite ascent and emplacement during contractional deformation in convergent orogens. *J. Struct. Geol.* **20**: 1365-1393.

BROWN, M. & SOLAR, G.S. (1999): The mechanism of ascent and emplacement of granite magma during transpression: a syntectonic granite paradigm. *Tectonophysics* **312**, 1-33.

DRUGUET, E. & CARRERAS, J. (2006): Analogue modeling of syntectonic leucosomes in migmatite schists. *J. Struct. Geol.* **28**, 1734-1747.

HOLNESS, M. (2008): Decoding migmatite microstructures. *In* Working with Migmatites (E.W. Sawyer & M. Brown, eds.). *Mineral. Assoc. Canada, Short Course* **38**, 57-76.

JOHNSON, T.E., BROWN, M. & SOLAR, G.S. (2003): Low-pressure subsolidus and suprasolidus phase equilibria in the MnNCKFMASH system. Constraints on conditions of regional metamorphism in western Maine, northern Appalachians. *Am. Mineral.* **88**, 624-638.

KRIEGSMAN, L.M. (2001): Quantitative field methods for estimating melt production and melt loss. *Phys. Chem. Earth, Part A: Solid Earth & Geodesy* **26**, 247-253.

MEHNERT, K.R. (1968): *Migmatites and the Origin of Granitic Rocks*. Elsevier, Amsterdam.

PANOZZO, R. (1987): two-dimensional strain determination by the inverse SURFOR wheel. *J. Struct. Geol.* **9**, 115-119.

PATIÑO DOUCE, A.E. & HARRIS, N. (1998): Experimental constraints on Himalayan anatexis. *J. Petrol.* **39**, 689-710.

PATTISON, D.R.M. & TRACY, R.J. (1991): Phase-equilibria and thermobarometry of metapelites. *Rev. in Mineral.* **26**, 105-206.

RUSHMER, T. (1995): An experimental deformation study of partially molten amphibolite: Application to low-melt fraction segregation. *J. Geophys. Res.* **100**, 15681-15695.

SAWYER, E.W. (1998): Formation and evolution of granite magmas during crustal reworking: the significance of diatexites. *J. Petrol.* **39**, 1147-1167.

SAWYER, E.W. (1999): Criteria for the recognition of partial melting. *Phys. Chem. Earth (A)* **24**, 269-279.

SAWYER, E.W. (2001): Melt segregation in the continental crust: distribution and movement of melt in anatectic rocks. *J. Metamorphic Geol.* **19**, 291-309.

SAWYER, E.W. (2008): Working with migmatites: nomenclature for the constituent parts. *In* Working with Migmatites (E.W. Sawyer & M. Brown, eds.). *Mineral. Assoc. Canada, Short Course* **38**, 1-28.

SOLAR, G.S. & BROWN, M. (2001a): Deformation partitioning during transpression in response to Early Devonian oblique convergence, northern Appalachian orogen, USA. *J. Struct. Geol.* **23**, 1043-1065.

SOLAR, G.S. & BROWN, M. (2001b): Petrogenesis of stromatic and inhomogeneous migmatite in Maine, USA: potential source of peraluminous granite? *J. Petrol.* **42**, 789-823.

SOLAR, G.S., PRESSLEY, R.A., BROWN, M. & TUCKER, R.D. (1998): Granite ascent in convergent orogenic belts: testing a model. *Geology* **26**: 711-714.

THOMPSON, A.B. & TRACY, R.J. (1976): Model systems for anatexis of pelitic rocks. II, facies series melting and reaction in the system CaO–$KAlO_2$–$NaAlO_2$–Al_2O_3–SiO_2–H_2O. *Contrib. Mineral. Petrol.* **70**, 429-438.

VERNON, R. H. AND COLLINS, W. J. (1988): Igneous microstructures in migmatites. *Geology* **16**, 1126-1129.

WHITE, R. (2008): Insights into crustal melting and the formation of migmatites gained from the petrological modeling of migmatites. *In* Working with Migmatites (E.W. Sawyer & M. Brown, eds.). *Mineral. Assoc. Canada, Short Course* **38**, 77-96.